

**ANAEROBIC DIGESTION OF LIGNOCELLULOSIC
BIOMASS AND POTENTIAL USE OF LOW-COST BIOMASS
RESIDUES FOR THE AD PROCESS OPTIMISATION**

**ANAEROBIC DIGESTION OF LIGNOCELLULOSIC
BIOMASS AND POTENTIAL USE OF LOW-COST BIOMASS
RESIDUES FOR THE AD PROCESS OPTIMISATION**

UCHENNA EGWU

A thesis submitted in partial fulfillment of the requirements of the
Newcastle University for the degree of Doctor of Philosophy

Research was undertaken in the Department of Civil Engineering and
Geosciences, School of Engineering, Newcastle University

September 2019

Abstract

This research investigated anaerobic digestion (AD) with various types of lignocellulosic biomass feedstocks from Nigeria, and the potential use of low-cost ash-extracts produced from agricultural biomass, such as empty palm bunch, cocoa pod, banana peel, for the enhancement of AD biogas production. Experiments investigated co-digestion mixtures, comprising several tropical grass silages and cassava processing wastes in CSTR under mesophilic and thermophilic temperatures, at an organic loading rate of $2.0 \text{ gVS.L}^{-1}.\text{d}^{-1}$ and 20 d HRT. Under each temperature regime, two pairs of 1 L CSTR were used – one pair as control, and the other pair supplemented with biomass ash-extracts. The experiment was run for three HRT, all reactors achieving steady-state operation during the third HRT cycle. At steady-state, the specific methane production (SMP) recorded in the thermophilic reactors, was 299.9 and 338.2 N mL $\text{CH}_4.\text{g}^{-1}\text{VS added. d}^{-1}$ for the control and the supplemented pairs of reactors, respectively, indicating that methane production had increased by 13% due to ash-extract supplementation. Similarly, for the mesophilic reactors, the SMP was 297.9 and 330 N mL $\text{CH}_4.\text{g}^{-1}\text{VS added. d}^{-1}$ for the control and ash-supplemented reactors respectively, signifying that ash-extracts improved mesophilic CH_4 production by 11%. Statistical comparison of CH_4 production in control and ash-supplemented reactors showed p-values ≤ 0.05 for both temperatures, which confirms that ash-extracts improved biomethane production significantly. Supplementing different feedstocks, such as gamba grass, guinea grass, elephant grass, rice straw and cassava processing wastes, with ash-extracts in both BMP batch assays and CSTR, also gave enhanced methane production. From the chemical analysis data and literature, it was possible to conclude that biomass ash-extracts appear to provide both alkalinity and/or trace metals for the enhancement of methane production when digesting agricultural wastes as both mono-substrates and co-digestion mixtures. The low cost of biomass ash-extracts compared to commercially available chemical additives, i.e. alkali and trace elements, make them economically feasible AD supplements for improving methane production from a wide range of grass biomass and other agricultural wastes in developed and developing countries.

Keywords: *Anaerobic digestion (AD), biomass-extracts, CSTR, Grass silage and cassava wastes, mesophilic, thermophilic, steady-state condition*

Dedication

I dedicate this thesis

To God

Who sits on His heavenly throne

Who rules and reigns from heaven above

The great I Am

The Alpha and Omega

The beginning and the end

The Wonderful God

The everlasting Father

Acknowledgments

I want to thank the almighty God who made it possible for me to start and finish this research. I sincerely appreciate the support of my loving wife, Beatrice Uchenna Egwu, and my sons, Fortunate and Jason, and my beautiful daughter Kindness, during my research. I am grateful to Dr. Paul Sallis, who did not only effectively supervise my research, who supported me and my family through difficult personal circumstances. I also want to thank my second supervisor, Prof. David Graham for his advice and questioning which helped me look critically at the effectiveness of ash supplements from different perspectives. I especially want to appreciate Apostle Bright Onoka and his family for their prayers, encouragement and support, and the entire leadership of City of God Christian Centre in Newcastle upon Tyne, for standing by me and my family always. I earnestly thank the laboratory technicians, especially David Race, David Earley, and Dr. Amy Bell for their support. I wish to acknowledge my colleagues, especially Peter Leary, who helped me with the Pipeline program to convert my sequence data to OTU tables, Burham Shamurad and Dr. Kishor Acharya for giving me guidance on how to analyze the data generated from sequencing the DNA extracts from my anaerobic CSTR samples. I also want to say a big 'thank you' to Dr. Carl Samuel for his supports. I sincerely want to thank Engr. Prof. O. I. Okoro, Prof. D. A. Okpara and Engr. Dr. Gregg Ezeokpube for their invaluable supports which reinforced my courage during difficult times. Finally, I offer my sincere thanks to the management of Michael Okpara University of Agriculture Umudike and TETFund Nigeria for financing this research. I am eternally grateful.

Table of Contents

Contents

Abstract.....	i
Dedication.....	ii
Acknowledgments	iii
Contents.....	v
List of Tables	xii
List of Figures.....	xiv
List and definition of Abbreviations	xx
Chapter 1 INTRODUCTION	1
1.1 The World energy consumption and the Nigerian experience	1
1.2 Definition of biomass	3
1.3 Energy demand and supply in Nigeria	3
1.4 Potential of agricultural wastes (biomass) as energy feedstocks.....	4
1.5 Status of AD technology in Nigeria	5
1.6 Challenges to bioenergy development in Nigeria	6
1.7 The potential use of biomass-derived supplement from ash for AD process optimization.....	7
1.8 Aim and objectives.....	7
1.8.1 Aim.....	7
1.8.2 Objectives	7

1.9	Structure of the thesis.....	8
Chapter 2	Literature Review.....	11
2.1	Anaerobic Digestion – An Overview.....	11
2.2	Advantages of Anaerobic digestion of biomass.....	12
2.2.1	Disadvantages of anaerobic digestion.....	13
2.3	The AD process degradation pathway.....	13
2.3.1	Disintegration and hydrolysis.....	14
2.3.2	Acidogenesis (fermentation).....	15
2.3.3	Acetogenesis.....	15
2.3.4	Methanogenesis.....	16
2.4	Potential biomass for biomethane production.....	16
2.4.1	Perennial Ryegrass (<i>Lolium perenne</i>).....	17
2.4.2	Cassava (<i>Manihot esculenta Crantz</i>) process wastes.....	17
2.4.3	Rice Straw (<i>Oryza spp</i>).....	19
2.4.4	Napier Grass (<i>Pennisetum purpureum Schum</i>).....	21
2.4.5	Gamba grass (<i>Andropogon gayanus</i>).....	22
2.4.6	Guinea grass (<i>Panicum maximum</i>).....	23
2.4.7	Speargrass (<i>Imperata cylindrica</i>).....	25
2.5	Factors that determine the biogas potential of feedstocks.....	26
2.6	Biomethane potential of feedstocks.....	27
2.6.1	Determination of the theoretical energy value of biomass feedstocks.....	28

2.6.2	Biochemical Methane Potential (BMP) Assay	30
2.7	Process parameters that affect the performance of anaerobic digestion	30
2.7.1	Temperature	30
2.7.2	pH.....	33
2.7.3	Alkalinity	34
2.7.4	Effect of mixing on the AD process	35
2.7.5	Solid residence time (SRT)	36
2.7.6	Organic loading rate	36
2.7.7	Redox Potential or Oxidation-Reduction Potential (ORP).....	37
2.7.8	Toxicity and inhibition	37
2.7.9	Volatile fatty acids	39
2.7.10	Aromatic, phenolic and chlorinated hydrocarbons.....	40
2.7.11	Sulfate and sulfide inhibition.....	40
2.7.12	Metal inhibition	41
2.8	Lignocellulosic biomass as AD substrate	41
2.8.1	Cellulose.....	42
2.8.2	Hemicellulose	42
2.8.3	Lignin.....	43
2.9	Pretreatment of lignocellulosic biomass	44
2.10	Mono-digestion and co-digestion of lignocellulosic biomass.....	46
2.11	Optimisation of the AD process using conventional supplements.....	47

2.12	Optimisation of the AD process using biomass-derived low-cost supplements...	47
Chapter 3	Materials and Methods.....	49
3.1	Biomass Feedstocks.....	49
3.2	Preparation of low-cost AD supplements	50
3.2.1	Elemental composition of selected biomass feedstocks	51
3.2.2	Determination of the abundance of the major chemical compounds in some selected crystals from biomass ash-extract.....	54
3.2.3	Analysis of carbon, nitrogen, oxygen, nitrogen and sulfur contents of selected biomass feedstocks	56
3.2.4	Estimation of cellulose, hemicellulose and lignin contents in biomass feedstocks	57
3.3	Seed sludge (reactor Inoculum)	63
3.4	Experimental Procedures	64
3.4.1	Batch Reactors – Biomethane Potential (BMP) Assay	64
3.4.2	GC method for Methane Analysis.....	65
3.4.3	Kinetic analysis of BMP data	68
3.5	Continuous stirred-tank reactors (CSTR).....	68
3.6	Stability of the AD process	71
3.6.1	Determination of Total volatile acid (FOS) and Total Alkalinity (TAC) ratio	71
3.7	Data analysis.....	72
Chapter 4	Effect of feeding interval, operating temperature, organic loading rate and pH on the SMP and VMP of CSTR fed with a grass silage mixture of perennial ryegrass, clover and Timothy grass as feedstock.....	73

4.1	Materials and methods.....	75
4.2	Results and discussion	77
4.2.1	Operational parameters	77
4.2.2	OLR and VS destruction	80
4.2.3	Variation of ammonium nitrogen, TKN nitrogen, and COD	81
4.2.4	Volatile fatty acid inhibition and alkalinity	86
4.2.5	Propionate-to-acetate ratio	90
4.3	Effect of temperature on biogas production	92
4.3.1	Overall biogas production (day 1 - 140)	92
4.3.2	Irregular daily feeding practice and a steady-state conditions.....	94
4.4	Conclusion.....	102
Chapter 5 Effect of low-cost biomass extracts on the performance of thermophilic and mesophilic AD reactors during the co-digestion of tropical grass silage and cassava processing waste		
		105
5.1	Materials and methods.....	106
5.1.1	Experimental set-up	107
5.1.2	Data analysis.....	109
5.2	Results and discussion	109
5.2.1	Solids composition, destruction and organic loading rate	109
5.2.2	pH of pilot scale CSTR	112
5.2.3	Variation in COD and ammonium-Nitrogen of pilot scale CSTRs.....	114

5.2.4	Specific methane production and cumulative methane production in CSTR under pseudo-steady-state conditions	116
5.3	Conclusion and recommendation	118
Chapter 6	Effect of 10 °C steps in operating temperature and increasing OLR on Specific Methane Production (SMP) during the AD of a mixed lignocellulosic feedstock.....	121
6.1	Materials and methods	123
6.1.1	Materials	123
6.1.2	Methods.....	123
6.2	Results and discussion.....	124
6.2.1	Temperature and pH.....	124
6.2.2	Effect of organic loading rate on volatile solids destruction in CSTR	126
6.2.3	Effect of HRT on the chemical oxygen demand (COD _T), total Kjeldahl N (TKN), and ammoniacal-N in the CSTR.....	128
6.2.4	Effects of volatile fatty acids (VFA) concentration on the CSTR	130
6.3	Specific and volumetric specific methane production.....	134
6.3.1	Overall methane content, specific methane production and volumetric methane production in the CSTR.....	134
6.3.2	Effect of increase in organic loading rate from 1.0 to 1.25 gVS. L ⁻¹ . d ⁻¹ on the specific and volumetric methane potential during 2 nd HRT in the CSTR	136
6.3.3	Effect of increase organic loading rate from 1.25 to 1.5 gVS. L ⁻¹ .d ⁻¹ on the specific and volumetric methane production during 3 rd HRT in the CSTR	138
6.4	Conclusion	140

Chapter 7	Assessing biomass ash extracts as sources of buffer and trace nutrients supplements for improved CH ₄ production during the anaerobic co-digestion of cassava wastes and cattle slurry.....	141
7.1	Materials and methods.....	142
7.1.1	Materials.....	142
7.1.2	Methods.....	144
7.2	Results and discussion	144
7.2.1	Characterization of the biomass feedstock and the carbon-to-nitrogen ratio	144
7.2.2	Organic loading rate and volatile solids destruction.....	146
7.2.3	Reactor concentrations of ammoniacal nitrogen (NH ₄ ⁺ -N), free ammonia (NH ₃), chemical oxygen demand (COD _T), total Kjeldahl nitrogen (TKN) and pH	147
7.3	Volatile fatty acid profile.....	151
7.3.1	Volatile fatty acid (VFA) profile for Pair 1 Reactors.....	151
7.3.2	Total volatile fatty acid (TVFA) from IC analysis	155
7.3.3	Stability checks for AD reactors.....	157
7.4	Methane production and composition.....	161
7.4.1	Performance of the reactors during pseudo-steady-state conditions.....	161
7.5	Conclusion.....	164
Chapter 8	Final remarks and recommendations for further research work.....	167
8.1	Final remarks.....	167
8.2	Recommendations	167
Chapter 9	Annex A.....	191

List of Tables

Table 2-1 Theoretical Biogas potentials of pure samples from selected substrate components	27
Table 2-2 Classification of anaerobic digesters by temperature	31
Table 2-3 Alkalinity equivalent weight ratios (Federation, 2007).....	35
Table 2-4 Oxidation-Reduction Potential (ORP) and bacterial activity in AD reactors.....	37
Table 2-5 Effect of ammonia nitrogen on anaerobic digestion at neutral pH.....	39
Table 3-1 Main characteristics of the biomass feedstocks.....	49
Table 3-2 Selected agricultural wastes used to produce low-cost AD supplements.....	50
Table 3-3 Elemental analysis of some selected biomass feedstocks for their metal composition.....	53
Table 3-4 Elemental analysis of biomass ash-extracts used as supplements for the AD process optimization	54
Table 3-5 Stoichiometric formula and TMP of various biomass feedstocks used for this study	57
Table 3-6 Procedure for the determination of the cellulose contents in biomass feedstock ...	59
Table 3-7 Results from the determination of cellulose, hemicellulose and lignin contents in Elephant grass, Guinea grass and Gamba grass	63
Table 3-8 Important parameters monitored during the anaerobic digestion processes in continuous reactors	70
Table 3-9 Ripley ratio, FOS:TAC ratio, intermediate alkalinity (IA) : partial alkalinity (PA) ratio or Volatile acids and alkalinity ratio (Andreoli <i>et al.</i> , 2007).....	72
Table 4-1 Summary of the materials and methods	75
Table 4-2 Characteristics o the biomass feedstock and inoculum	76
Table 4-3 Summary of CSTR operating conditions.....	76
Table 4-4 Comparison of the pH in the Pair 1, Pair 2 and Pair 3 reactors.....	78
Table 4-5 Solubility of ammonium bicarbonate at different temperatures (Engineers, 2008)	83

Table 4-6 Maximum concentrations of VFAs detected in the Pair 1, Pair 2 and Pair 3 reactors during the period of instability in the AD reactors (day 55 – 140)	88
Table 4-7 Minimum, maximum, mean and standard deviation of the SMP from Paired CSTR.	95
Table 4-8 Correlation tests and t-test statistics of paired mean SMP of the Pair 1, Pair 2 and Pair 3 CSTR at 95% confidence interval and significances of p-value (2-tailed).....	99
Table 5-1 Feedstock composition.....	106
Table 5-2 Characteristics o the feedstock and inoculum.....	107
Table 5-3 Names and operating conditions of the CSTR.....	108
Table 5-4 Elemental composition of the biomass feedstock components used to feed AD reactors.....	109
Table 5-5 Variations in mean ammonium-N concentration in AD reactors using Paired Sample Statistical Correlations and T-tests at 95% confidence interval.....	116
Table 6-1 Characteristics of the mixed biomass feedstock	123
Table 6-2 Operating conditions, Organic loading rates, hydraulic retention time (HRT) and dosing days	124
Table 7-1 Composition and properties of inoculum and cassava waste used for the study .	143
Table 7-2 Total volatile fatty acid (TVFA) concentration in reactors R1 to R6.	156
Table 7-3 Propionate-to-acetate (P:A) ratio in Pair 1, 2 and 3 reactors (day 1 – 85).....	158
Table 9-1 Physiochemical characteristics of the biomass feedstocks used for BMP tests....	192
Table 9-2 Physiochemical characteristics of the inoculum	192
Table 9-3 Summary of the results from experimental, Buswell equation and Gompertz models for the determination of the biochemical methane potential of selected biomass feedstocks	200

List of Figures

Figure 1-1 Map of Nigeria (EIA, 2016).....	2
Figure 2-1 Anaerobic degradation pathway. Adapted and modified from Bharathiraja <i>et al.</i> (2018).....	15
Figure 2-2 Cassava farm	18
Figure 2-3 Cassava production in Nigeria (a) Tuber (b) Peels and (c) edible starchy portion.	19
Figure 2-4 Rice farm in Nigeria.....	20
Figure 2-5 Napier grass (Elephant grass).....	21
Figure 2-6 Gamba grass	22
Figure 2-7 Guinea grass	24
Figure 2-8 Photo of Speargrass (<i>Imperata cylindrical</i>)	26
Figure 2-9 Relative growth rate curves of methanogens during AD at different temperatures (Lettinga <i>et al.</i> , 2001; Schön, 2010).....	33
Figure 2-10 The cellulose molecule showing the monomeric unit (Kumar <i>et al.</i> , 2009)	42
Figure 2-11 Effect of pretreatment on lignocellulosic biomass. Adapted from (Mosier <i>et al.</i> , 2005)	45
Figure 3-1 XRD analysis <i>showing</i> high peaks of potassium bicarbonate and potassium carbonate contents and other trace nutrients within the crystals from palm bunch ash-extract	54
Figure 3-2 XRD analysis showing high peaks of potassium bicarbonate and potassium carbonate contents and other trace nutrients within crystals from empty cocoa pod ash-extract	55
Figure 3-3 XRD analysis showing high peaks of potassium bicarbonate and potassium carbonate content and other trace nutrients within the crystals from plantain peels ash-extract	55
Figure 3-4 Batch Experimental Setup used for the determination of the BMP of substrates ..	64
Figure 3-5 Continuously stirred tank reactors (CSTR) setup with tubing connected to gas sampling bag, a variable speed overhead stirrer engine with stirring rod passing through Quickfit® flat head plates parallel center joint, a 10° side socket joint vacuum adapter, black	

insulating mat, k-type thermocouple inserted into the reactor using a red coloured rubber bung, and a control box fitted with Sestos temperature controllers.	69
Figure 4-1 Mean pH values inside the Pair 1, Pair 2 and Pair 3 reactors. Details of the feeding phase are presented in Figure 4-4.	79
Figure 4-2 Volatile solids (VS) reduction (%) in Pair 1, Pair 2 and Pair 3 reactors. Details of the feeding phases are presented in Figure 4-4.	81
Figure 4-3 Mean concentration of ammonium-N ($\text{NH}_4^+\text{-N}$) in Pair 1, Pair 2 and Pair 3 reactors over time	82
Figure 4-4 Mean concentration of total Kjeldahl-N (TKN) and organic nitrogen in Pair 1, Pair 2 and Pair 3 reactors over time	84
Figure 4-5 Comparison of mean COD_T variation in the Pair 1, Pair 2 and Pair 3 reactors from day 8 – 85	85
Figure 4-6 Volatile fatty acid concentrations in Pair 1, Pair 2 and Pair 3 reactors. Acetate (red), butyrate (black), formate (purple), isobutyrate (ash), isovalerate (yellow) and propionate (dark red), Refer to Table 4-1 for details of the organic loading rates and the corresponding days.	87
Figure 4-7 Mean concentration of alkalinity in the reactor: Pair 1 (black lines), Pair 2 (blue lines) and Pair 3 (red lines), and the mean total volatile fatty acid to total alkalinity (FOS: TAC) ratio over time	90
Figure 4-8 Stability check using propionate: acetate (P: A) ratios in the Pair 1, Pair 2 and Pair 3 reactors. Details of feeding regimes are presented in Table 4-1 and Figure 4-7.	91
Figure 4-9 Cumulative mean specific biogas production (SBP), cumulative mean volumetric biogas production (VBP) and mean methane contents (%) in biogas from the Pair 1, Pair 2 and Pair 3 reactors. The composition of the Pair 1, Pair 2 and Pair 3 reactors defined in Table 4-3. Point P and Q (day 93 – 103) represents a period of break in the feeding due to the failure of the AD reactors.	92
Figure 4-10 Cumulative mean specific methane production (cum SMP), specific methane production (SMP). Cum. means indicate the average of the cumulative volumes of methane produced in the Pair 1, Pair 2 and Pair 3 reactors. Other parameters are as defined in Figure 4-9.	93

Figure 4-11 Mean cumulative volumetric methane production (cum. Mean VMP) and mean specific methane production (Mean VMP) in the Pair 1, Pair 2 and Pair 3 reactors over HRT. Other parameters are as defined in Figure 4-9.....	97
Figure 4-12 Comparison of the mean specific methane production (SMP) of CSTR operating at different temperatures, before, during and after the AD process failure. Error bars represent +/- 2 standard error (SE) of the mean. Other parameters as defined in Figure 4-9.....	101
Figure 5-1 Mesophilic and thermophilic CSTRs showing overhead stirrers, a shaft with water-seal and gas-bags. Reactor vessels are obscured by gas bags. The working volume of each reactor was 1 L.....	108
Figure 5-2 Volatile solid reduction in the Pair 1 (Control), Pair 2 (supplemented), Pair 3 (Control), and Pair 4 (supplemented) CSTR over time. Table 5-3 contains more details on CSTR classification and supplementation	111
Figure 5-3 Mean pH in the Pair 1 (Control) unsupplemented and Pair 2 (supplemented) mesophilic, and Pair 3 (Control) unsupplemented and Pair 4 (supplemented) thermophilic CSTR over time. Supplementation involved the addition of ash-extract to CSTR.	112
Figure 5-4 Mean of Total Chemical Oxygen Demand (COD _T) and Ammonium-Nitrogen (NH ₄ -N) concentration inside the (Pair 1 (Control) unsupplemented and Pair 2 (supplemented) mesophilic and (Pair 3 (Control) unsupplemented and Pair 4 (supplemented) thermophilic CSTR over time. Values are the means from duplicate reactors within a pair.	114
Figure 5-5 Mean specific methane production from mesophilic Control 1, Pair 1(supplemented) and the thermophilic Control 2 and Pair 2 (supplemented) CSTR over time	117
Figure 6-1 Variation of pH in the Pair 1, Pair 2 and Pair 3 reactors under psychrophilic (27°C), mesophilic (37°C) and thermophilic (47°C) temperature conditions and organic loading rate over time. Values are the means from duplicate reactors within a reactor pair, green arrows indicate periods of supplementation with ash-extract (A - B), and no supplementation (O – A and B – C).....	125
Figure 6-2 Variations in the organic loading rate and the percentage destruction volatiles solids (VS) (%) in the Pair 1, Pair 2 and Pair 3 reactors from day 1 – 66. Values are the means from duplicate reactors within a pair, OLR is the organic loading rate as stated in Table 6-2.	127

Figure 6-3 Variation of mean total chemical oxygen demand(<i>CODT</i>), total Kjeldahl Nitrogen (TKN) and ammoniacal nitrogen ($\text{NH}_4^+\text{-N}$) in the Pair 1, Pair 2 and Pair 3 reactors with time. Values are the means from duplicate reactors within a pair (Table 6-2).....	129
Figure 6-4 Volatile fatty acids concentration in Pair 1 psychrophilic (27 °C), Pair 2 mesophilic (37 °C) and Pair 3 thermophilic (47 °C) CSTRs. Values are the means from duplicate reactors within a pair (Table 6-2).....	131
Figure 6-5 Inhibiting effects of acetic acid on propionate degradation rates $\text{mM} = \text{mmol. L}^{-1}$. Adapted from Felchner-Zwirello (2014).	132
Figure 6-6 Total VFA concentrations in the Pair 1, Pair 2 and Pair 3 AD reactors at the different temperature conditions. Values are the means values of the VFA from individual reactors within a pair. (Reactor temperatures as defined in Table 6-2).....	133
Figure 6-7 Mean specific methane production (SMP) and cumulative specific methane potential (SMP) for Pair 1, Pair 2 and Pair 3 reactors over time. Values are the means from duplicate reactors within a pair as defined in Table 6-2. The organic loading rate is presented in Figure 6-2.	135
Figure 6-8 Mean volumetric methane production (VMP) and cumulative volumetric methane production (VMP) for Pair 1, Pair 2 and Pair 3 reactors over time. Values are the means from duplicate reactors within a pair as referenced in Figure 6-4.....	136
Figure 6-9 Mean of specific methane production (SMP) and mean of volumetric methane production (VMP) for the Pair 1, Pair 2 and Pair 3 reactors from day 26 – 46 (2 nd HRT). Values are the means from duplicate reactors within a pair as defined in Table 6-2 and Figure 6-7.....	137
Figure 6-10 Mean of specific methane production (SMP) and mean of volumetric methane production (VMP) for the Pair 1, Pair 2 and Pair 3 reactors from day 47 – 66 (3 rd HRT). Values are the means from duplicate reactors within a pair as defined in Table 6-2.....	139
Figure 7-1 Mean volatile solids concentration, and mean volatile solids destruction (%), of Pair 1, Pair 2 and Pair 3 reactors over time. Dest. refers to the destruction of volatile solids	146
Figure 7-2 Mean concentration of ammoniacal nitrogen ($\text{NH}_4^+\text{-N}$), total Kjeldahl nitrogen (TKN) and total organic nitrogen (Organic-N) in the Pair 1, Pair 2 and Pair 3 reactors against time.	148

Figure 7-3 Free ammonia (NH ₃) in the Pair 1, Pair 2 and Pair 3 reactors with pH over time (See Equation 2-12)	149
Figure 7-4 Total chemical oxygen demand (COD _T) and pH in the Pair 1, Pair 2 and Pair 3 reactors over time.....	150
Figure 7-5 Concentration of volatile fatty acids (VFA) in the individual reactors in Pair 1 (R1 and R2), Pair 2 (R3 and R4) and Pair 3 (R5 and R6) reactors with time. The initial VFA or Pair 1 reactors was similar to Pair 2 & 3. Values in the graph represent mean values of the respective VFA from the CSTR.....	153
Figure 7-6 Total volatile fatty acid (TVFA), alkalinity and FOS:TAC ratio in the Pair 1, Pair 2 and Pair 3 AD reactors over time.....	160
Figure 7-7 Specific methane production from individual reactors in the Pair 1, Pair 2 and Pair 3 reactors over time. The arrow shows the point from which R4 suffered interruption due to temperature controller failure.....	162
Figure 7-8 Cumulative and specific methane production (SMP) from Pair 1, Pair 2 and Pair 3 reactors over time.....	163
Figure 9-1 Cumulative methane production of biomass feedstocks together with methane from blank, where A is the blank, B is Gamba grass, C is crystalline cellulose, D is Guinea grass, F is cassava waste, H is plantain peels and M is elephant grass.....	194
Figure 9-2 Daily methane production of the biomass feedstocks together with blank methane. Where A, B, C, D, F, H and M are as defined in the legend.....	194
Figure 9-3 Cumulative methane production of biomass feedstocks with EBP supplementation where A is blank (inoculum), G (mixture of perennial ryegrass, clover and timothy grass), I(mixture of Gamba and Guinea grass), J(mixture of rice straw and empty yam bean pod), K(mixture of rice straw and cassava waste), and L(mixture of rice straw and plantain peels).	196
Figure 9-4 Daily methane production from biomass feedstocks G, I, J, K and L as defined in the legends where A is the inoculum	197
Figure 9-5 Cumulative methane production of biomass feedstocks with inoculum A. E(rice straw + A), N (rice straw with 0.05 mL EPB ash-extract supplement + A), O(rice straw supplemented with 1.0 mL EPB ash-extract supplement + A), P(rice straw supplemented with	

2 mL EPB ash-extract + A), Q(rice straw supplemented with 0.05g EPB ash + A), T(rice straw + 0.15g EPB ash + A), and U(rice straw + 0.25g EPB ash + A). 198

Figure 9-6 Daily methane production from biomass feedstocks where A is the blank (inoculum). The names of the biomass feedstocks E, N, O, P, Q, T and U are as defined in the legends and in Figure 9-5. 198

List and definition of Abbreviations

AD	Anaerobic digestion
ADF	Acid detergent fibre
ADL	Acid detergent lignin
BMP	Biochemical methane potential
cBOD	Carbonaceous biochemical oxygen demand
CH ₄	Methane gas
CHP	Combined Heat and Power
C: N	Carbon-to-nitrogen ratio
COD	Chemical oxygen demand
COD _T	Total chemical oxygen demand
CSTR	Continuous stirred tank reactors
Cum	Cumulative volume (mL)
DP	Degree of polymerization
ECP	Empty cocoa pod
EPB	Empty palm fruit bunch
FOS	in German <i>Fluchtige Organische Säuren</i> (TVFA expressed in mg HAc.L ⁻¹)
FOS: TAC	Ratio of TVFA to total alkalinity (Ripley's ratio in English)
GC	Gas chromatography
HRT	Hydraulic retention time
IA	Intermediate alkalinity
NDF	Neutral detergent fibre

N mL	Millilitres in normal condition (gas volumes at 0 °C and an atmospheric pressure of 101.3 kPa)
OLR	Organic loading rate
PA	Partial alkalinity
P:A ratio	Propionate-to-acetate ratio
PP	Plantain peels
p-value	A statistical evidence to support a hypothesis
R1 – R6	CSTR from reactor 1 to reactor 6
R ²	Correlation coefficient
SBP	Specific biogas production (biogas yield) expressed in N mL Biogas.g ⁻¹ VS of substrate added
BPR	Biogas production rate (volume of biogas produced per volume of digester per day (m ³ . m ⁻³ . d ⁻¹).
SMP	Specific methane production expressed in N mL CH ₄ .gVS. added per day
TAC	in German <i>Totales Anorganisches</i> Carbonate (total alkalinity buffer expressed as mg. L ⁻¹ of CaCO ₃).
TKN	Total Kjeldahl nitrogen
TVFA	Total volatile fatty acid
TS	Total solid content
VFA	Volatile fatty acids
VMP	Volumetric biogas production expressed in N mL CH ₄ .L ⁻¹ reactor volume. d ⁻¹
VS	Volatile solids content (VS=TS + ash)

XRD

X-ray diffraction

Chapter 1 INTRODUCTION

1.1 The World energy consumption and the Nigerian experience

The primary energy consumption around the globe is mainly sourced from fossil fuels such as petroleum, natural gas and coal (Gupa, 2012; Jinsheng, 2009; Karimi, 2015; Meng, 2011; Said *et al.*, 2018; Wang *et al.*, 2018). Fossil fuels are known to be unsustainable due to their extremely low regeneration rates, that is, according to Energy-Insights (2011), it takes as much as 50 - 300 million years for crude oil to form compared to their daily usage. Towards the end of the year 2015, the known global fossil fuel reserves, namely crude oil, natural gas, and coal, were projected to last for just 51, 53 and 114 years respectively, based on the current rate of usage, and the reserve-production ratios (Chen, 2018; Wu, 2018). The implication is that is that, in around 60 years from now, there may be a global energy deficit. It is therefore imperative to investigate other potential energy resources that will be sustainable, renewable, affordable and environmentally friendly to replace fossil fuels, and to guarantee energy security. It is true that fossils are practically non-renewable and their combustion releases greenhouse gases (GHG) (Hamzehkolaei, 2018; Hatti-Kaul *et al.*, 2016; Rocco, 2018), however, many developed countries around the world, and some developing countries, can continue to use them as their source of constant energy supply for many decades.

The provision of a constant energy supply in most developing countries, especially in Nigeria, remains a challenging problem. Nigeria is the 7th most populated country in the world (Bureau, 2017), and is the largest oil producing country in Africa. The country has nearly a third of the continent's crude oil reserve (EIA, 2016), but ironically it suffers one of the worst energy crises in the world (Emodi, 2016). Nigeria (Figure 1-1) is geographically located in the tropical zone of West Africa between latitudes 4°N and 14°N and longitudes 2°2'E and 14°30'E and has a total area of 923 770 km² (FAO, 2013-2017).



Figure 1-1 Map of Nigeria (EIA, 2016)

Despite being an oil-dependent economy, Nigeria is mainly an agrarian country with a rich vegetation and abundant water resources that support good livestock production (FAO, 2013-2017). To date, only about 40% of Nigerians have access to electricity (Dahlquist, 2013; Eleri *et al.*, 2012), with up to 28 power cuts per day (Halff *et al.*, 2014), and this is made worse because about 92% of Nigerians live in poverty (Emodi, 2016). Most Nigerians depend on the use of private petrol or diesel-operated generators to provide electricity for their households and businesses, with the attendant risks of indoor emission of carbon monoxide and fire incidents. Sustainable energy supply is a major driver of technological, economical and industrial development around the world (Akuru *et al.*, 2017; Dahlquist, 2013; Gupta *et al.*, 2013; Jose, 2015; Wang *et al.*, 2018) and can bring significant benefits to Nigeria.

Therefore, for Nigeria to experience faster growth and development, there is an urgent need to exploit affordable and reliable sources of clean and renewable energy to build a sustainable energy supply which eventually will improve the economy, and the technological and social development of every sector of the economy.

1.2 Definition of biomass

The EU Directive 2003/30/EC defined biomass as the biodegradable fraction of products such as food wastes and agricultural residues (vegetable and animal substances), forestry, including degradable fractions of industrial and municipal wastes (EU-Commission, 2003; Nitsos *et al.*, 2013). Biomass stores solar energy within the organic matter through the process of photosynthesis (Abu-Dahrieh *et al.*, 2011; EIA, 2017; Emodi, 2016). Nigeria has abundant biomass reserves estimated to be equivalent to 88×10^2 MJ of energy, with shrubs and forage grasses alone producing about 200 million tons of dry biomass per year which is estimated to be equivalent to 2.28×10^6 MJ of energy (Emodi, 2016). Biofuels from lignocellulosic biomass such as forage grasses and shrubs are known as second generation biofuels. These biofuels are more sustainable than those from first generation biofuel (energy crops), which rely on the use of food-grade raw materials and consume valuable agricultural land reserves for their production (Nitsos *et al.*, 2013). Biomass could deliver energy in all forms – electricity, heat, liquid and gaseous transport fuels, and meet some of the present and future energy needs (Demirbas *et al.*, 2009) through processes such as combustion, gasification, pyrolysis and anaerobic digestion (Akuru *et al.*, 2017). In gasification, biomass is heated with a limited supply of oxygen to produce a synthesis gas which has usable energy content whereas pyrolysis yields a bio-oil when biomass is heated in the complete absence of oxygen. Anaerobic digestion (AD) produces methane-rich biogas when biomass is degraded by bacteria and archaea microbes also in the complete absence of oxygen (Akuru *et al.*, 2017). Biogas from the AD is a clean and economical renewable energy (Frigon & Guiot, 2010), and AD produces a nutrient-rich digestate which can be used as a soil amendment and fertilizer on agricultural land (Frigon & Guiot, 2010).

1.3 Energy demand and supply in Nigeria

Nigeria has the lowest net rates of electricity generation per capita in the world, and those that do have access face load shedding, blackouts, and reliance on private generators (EIA, 2016). At present, 72.9% of the electricity used in Nigeria comes from fossil fuels while 27.1% comes from hydropower (EIA, 2016; WorldBank, 2014). In 2005, it was reported that the estimated energy demand in Nigeria was 20,000 MW (Modi *et al.*, 2005), and now, the electricity capacity is about 6000 MW, while only about 4,000 MW is available to consumers (Akuru *et al.*, 2017; UNDP, 2015), a disparity which could worsen, considering the projected

electricity demand under economic growth scenarios of 7%, 10%, 11.5% and 13% between 2005 and 2030 (Monyei, 2017).

This energy deficit has led to about 70% of Nigerians not being connected to the national grid, and as a result, many people in rural communities rely heavily on the traditional use of burning biomass, wood fuel, candles, and kerosene, as their primary energy sources (UNDP, 2015), and only about 10% of the rural populace can access the available intermittent electricity supply (Akuru *et al.*, 2017). However, as of October 2018, the energy situation has worsened further, and this indicates the serious failure of fossil fuels and hydro resources to meet Nigeria's energy needs. Consequently, there is a real urgency to explore alternative renewable energy resources which might solve these seemingly intractable energy poverty problems.

1.4 Potential of agricultural wastes (biomass) as energy feedstocks

Most Nigerians, especially those dwelling in rural communities carry out subsistence farming which cumulatively produces millions of tons of biomass that is normally discarded as waste thereby polluting the environment. Nigeria's biomass energy resources have been estimated at 144 million ton. year⁻¹ (Janssen, 2012). Previous studies have reported that Nigeria's crop residues amount to about 83 million ton. year⁻¹, while animal waste accounts for 61 million ton. year⁻¹ of the total (Dahlquist, 2013). A number of researchers have also reported that Nigeria generates about 227,500 ton of fresh animal dung per day and about 20 kg of municipal solid waste per capita per year (Emodi, 2016; Okeh *et al.*, 2014). This figure suggests that animal manure alone could produce 6.8 million m³ of biogas assuming 1 kg of fresh animal manure typically produces 0.03 m³ of biogas (Emodi, 2016; Okeh *et al.*, 2014). Tranter *et al.* (2011) have stated the estimation of electricity generation from methane as follows:

- i Net calorific value of 1 m³ of methane = 35.85 MJ
- ii Electrical generation efficiency of combined heat and power unit = 35%
- iii 1 m³ of methane can generate 0.35 x 35.85 MJ = 12.5 MJ of electricity
- iv 1 MJ of electricity = 0.2778 kWh

If animal waste can generate about 60% methane, then as of 2015 animal manure alone could provide Nigerians with up to 6,800,000 (0.06) m³ x 12.5 MJ of electricity = 51,000,000 MJ,

or 14,167,800 kWh, or 14,168 MWh. This contrasts the current 6000 MWh which the country is struggling to generate from hydroelectricity, and therefore signifies that methane from animal manure alone could produce the energy needs of Nigeria.

The rich vegetation found across Nigeria consists of diverse types of unexploited plant biomass which potentially could be used as feedstock to produce biogas. Some of the most abundant biomass was selected for the current study includes: Cassava (*Manihot esculenta*) process wastes, Rice (*Oryza spp*) Straw, Napier Grass (*Pennisetum purpureum*), Gamba grass (*Andropogon gayanus*), Guinea grass (*Panicum maximum*), Speargrass (*Imperata cylindrica*) and Perennial Ryegrass (*Lolium perenne*). Other abundant types of biomass which have been processed into low-cost supplements and buffer materials to optimize AD processes include empty palm fruit bunch, empty cocoa pod, plantain peels, empty *Mucuna pruriens* pod and yam bean pod (*Sphenostylis stenocarpa*), traditionally known in Afikpo as ‘Azama’.

1.5 Status of AD technology in Nigeria

According to Dahlquist (2013), in 1982 the Federal Government of Nigeria, through the Energy Commission of Nigeria, established two Renewable Energy Centres in the country which were located at Sokoto and Nsukka. They also built a 20 m³ biogas plant at Mayflower Secondary School Ogun State which uses cow dung as feedstock, and another 10 m³ plant at NCERD Nsukka which was fed on cassava peel and poultry droppings. In addition, under the Africa 2000 low technology biogas systems project, the United Nations Development Programmes (UNDP) also introduced floating drum, balloon and tube anaerobic digesters in Yobe, Jigawa and Kano State, and another biogas plant in Kwachiri community in Kano State that utilizes cow dung to provide daily energy for a family of 40 people. Dahlquist (2013) also reported that more than 10 biogas plants of capacity 10 - 20 m³ which utilize cow dung, human excreta, piggery waste had been constructed by Sokoto Energy Research Centre (SERC) across Nigeria. However, despite several tertiary educational institutions carrying out biogas research in addition to the two biogas centers mentioned above, as of 2013 less than 20 pilot biogas projects had been built in Nigeria (Dahlquist, 2013).

However, the main biogas project in Nigeria, called the Cows-to-Kilowatts project, which started operation in May 2008, and is one of the largest biogas plants in Africa has the capacity to provide gas supply to 5400 homes at one quarter of the cost of liquefied natural gas (Brown & Stigge, 2017; Dahlquist, 2013). The design and construction of this biogas

plant were funded by the UNDP, and it was designed to produce 1500 m³.d⁻¹ of biogas containing 900 m³ methane.d⁻¹ for cooking, with an estimated useful life of 15 years, and expected to yield a return on investment within 2 years (Dahlquist, 2013).

In a contrasting report, Brown and Stigge (2017) stated that this AD plant, which was installed by the Nigerian branch of the Global Network for Environment and Economic Development, the University of Technology in Thonburi, Thailand, and UN Habitat's Sustainable project, actually had a reactor capacity of 3000 m³ and was designed to produce 1800 m³ methane. d⁻¹. According to the report, this AD plant was used to treat agro-industrial waste and produce 60 - 70% methane for cooking and gave a return on the investment of \$0.5 million after 3 years (Brown & Stigge, 2017). The plant also produced about 1500 L of phosphorus and nitrogen-rich digestate daily as an organic fertilizer, and this was sold to Oyo State Fertilizer Board for onward sales to urban and low-income farmers at about 5 percent of the cost of standard chemical fertilizer (Brown & Stigge, 2017; Dahlquist, 2013). In conclusion, biogas development is still in its infancy stage in Nigeria.

1.6 Challenges to bioenergy development in Nigeria

There are many challenges to bioenergy development in Nigeria. According to Akuru *et al.* (2017), one of the major setbacks is the lack of political willpower of the Nigerian government to put regulatory framework, standards, and incentives in place that would facilitate a shift from traditional biomass combustion to renewable energy sources. Another challenge is the lack of advanced technologies for supporting mid-size and large biogas plants, i.e. effective technology transfer (Brown & Stigge, 2017). Furthermore, the generation of bioenergy also requires experience, construction skills, operation and sludge handling skills. Cultural beliefs could also hamper the acceptance of using biogas from human or animal excrement for cooking or as fertilizer (Brown & Stigge, 2017).

Other important factors that hinder the proliferation of bioenergy technologies in Nigeria include the lack of credit facilities and high interest rates on bank loans, lack of information, overdependence on the government for energy, inadequate budgetary allocation on education and research, corruption among government officials, and ethnic and religious conflicts, especially the recently unchecked killings by the Fulani herdsmen across the country.

1.7 The potential use of biomass-derived supplement from ash for AD process optimization

Green plants absorb trace nutrients and other metals from soil solutions via their root hairs. These trace nutrients which are stored in plant tissues as aid to metabolism, can be extracted when the plant is incinerated to produce the inorganic remains – the ash. Ash is alkaline and contains essential trace elements which are beneficial to the anaerobic digestion process. These trace elements which can be extracted either via acid digestion, or by incinerating the biomass then dissolving the ash in water, followed by filtration and crystallization, can be used as a replacement for expensive trace elements as low-cost supplements that can optimize AD processes. There are several published articles on the importance of the addition of expensive commercially available trace nutrients and buffer agents as supplements that can boost or stabilize AD processes (Session 2.12). However, no previous work has been carried out to investigate the potential use of material derived from many locally abundant agricultural wastes as alternative and cheaper sources of these important AD supplements. Therefore, the current study is aimed at bridging this research gap and focusses on using these affordable low-cost ash-extracts to effectively improve AD processes, generate higher methane yields, and better conversion of the feedstock biomass. The ultimate goal of this research is to bring about an increase in the adoption of AD technologies in Nigeria as a means of solving the country's severe energy crises and help contribute towards poverty eradication.

1.8 Aim and objectives

1.8.1 Aim

To investigate the potential use of low-cost biomass residues (ash-extracts), as sources of trace elements and alkalinity for use as alternative pretreatment reagents for the optimization of AD processes utilizing selected lignocellulosic biomass feedstocks.

1.8.2 Objectives

1. To compare the effects feeding interval on the specific methane production (SMP) and volumetric methane production (VMP) of CSTR during the anaerobic digestion of grass silage.

2. To investigate psychrophilic anaerobic digestion of grass silage as a sustainable and affordable process in developing countries
3. To assess the effects of organic loading rate on the SMP from grass silage at psychrophilic, mesophilic and thermophilic temperatures.
4. To compare the recovery rates of psychrophilic, thermophilic and mesophilic CSTR after process failure following supplementation with biomass ash-extracts.
5. To determine the specific methane production (SMP) from a biomass feedstock consisting of seven types of grass silage and cassava processing waste under upper mesophilic (40 °C) and optimum thermophilic (55 °C) temperatures conditions both with and without EPB ash-extract supplementation.
6. To determine the effect of 10 °C degree differences in operating temperature of psychrophilic, mesophilic and thermophilic reactors on the specific methane production (SMP) and volumetric methane production (VMP) during the AD of a mixed lignocellulosic biomass feedstock.
7. To determine the effect of increasing the organic loading rate on the SMP, VMP and reactor stability of psychrophilic, mesophilic and thermophilic reactors during the AD of a mixed lignocellulosic biomass feedstock.
8. To investigate the effect of adding ash-extract supplements produced from empty palm fruit bunch (EPB) and empty plantain peels (EPP) on maintaining AD process stability and efficiency of reactors during the AD of a mixed lignocellulosic biomass feedstock.
9. To determine the effectiveness of empty palm fruit bunch (EPB) and empty cocoa pod (ECP) ash-extracts in providing alkalinity and buffering for the maintenance of pH within the optimum range for AD processes.
10. To determine whether EPB and ECP ash-extract supplements can maintain steady-state conditions in continuous AD reactors over extended operating periods.
11. To determine whether ash-extract supplements can restore the activity of AD reactors that are exhibiting a declining or failing performance.

1.9 Structure of the thesis

This thesis contains eight chapters, including the Introduction which has outlined the scope of energy problems in Nigeria, and the potential for solving these by adopting alternative and sustainable energy based on the AD.

Chapter Two is a Literature Review that details the application, advantages and disadvantages of anaerobic digestion, including optimization options, factors affecting AD process and choice of feedstock, determination of theoretical methane potentials of biomass. The chapter also looks at the importance of trace elements supplementation during AD processes and the cost implications which has made it unaffordable to low-income countries. It further explores the process of by which green plants freely absorb these trace nutrients from the soil water and the prospect of recovering the trace nutrients from plant biomass for use as low-cost supplements to enhance anaerobic digestion processes.

The third Chapter is concerned with the methodology. It contains details of the standard methods of analysis and other procedures adopted or modified from published literature. It presents information on the most abundant biomass feedstocks in Nigeria which can be harnessed to provide sustainable energy feedstocks. The chapter outlines the use of biomass ash-extracts as alternative supplements to expensive commercially available reagents for AD process optimization. The chapter also contains equations and some results from the physicochemical analysis/ characterization and results from compositional analysis of some of the biomass material used for this study, and the theoretical methane potentials of some biomass feedstocks derived from the Buswell equation.

Chapter Four presents the results and discussion from the continuously stirred tank reactors experiment which was performed to investigate the effect of feeding interval, operating temperature, organic loading rate and pH on the SMP and VMP of CSTR fed with a grass silage mixture of perennial ryegrass, clover and Timothy grass as feedstock.

Chapter Five contains the results and discussion from the second CSTR experiment which was carried out using various kinds of biomass ash-extracts in order to determine the effect of low-cost biomass extracts on the performance of thermophilic and mesophilic AD reactors during the co-digestion of tropical grass silage and cassava processing waste.

Chapter Six presents the results from the third CSTR experiment which was carried out to investigate the effect of 10 °C steps in operating temperature and increasing OLR on Specific Methane Production (SMP) during the AD of a mixed lignocellulosic feedstock.

Chapter 7 presents the results and discussion from CSTR experiments which focused on assessing biomass ash extracts as sources of buffer and trace nutrients supplements for

improved CH₄ production during the anaerobic co-digestion of cassava wastes and cattle slurry.

Finally, Chapter 8 draws upon the entire thesis and presents a summary and critique of the major findings from Chapters (3 – 7). It also includes the areas for further research identified during the study and some recommendations.

Chapter 2 Literature Review

2.1 Anaerobic Digestion – An Overview

Anaerobic digestion (AD) is a biochemical process which involves the decomposition of organic matter by a microbial consortium in the absence of oxygen to produce biogas – methane, carbon dioxide, partially degraded organic matter, known as digestate, new microbial biomass and inorganic matter (Ferreira *et al.*, 2013; Pellerá & Gidarakos, 2018; Teymoori Hamzehkolaei & Amjady, 2018). Strict anaerobic archaea methanogens, which belong to the taxon Euryarchaeotic, and which are also prokaryotic microorganisms, produce methane which is the most important product of anaerobic digestion, as an end-product of their metabolism (Hackstein & van Alen, 2010). The degradation of biomass during the AD process is mostly carried out by obligate anaerobes which can only live and multiply in the absence of oxygen (Bajpai, 2017), which is why anaerobic digestion process must be carried out in closed reactor vessels in order to achieve efficient degradation of the biomass. The AD process can be applied to the digestion of agricultural residues, wastewater, and other biological wastes as an effective method for waste treatment, and for production of renewable energy – produced biogas can be used to generate electricity through internal combustion engines, steam turbine generators, or via combined heat and power (CHP) (EIA, 2017; Love & Bryant, 2017; Oreopoulou & Russ, 2006; Radu *et al.*, 2014; Teymoori Hamzehkolaei & Amjady, 2018; Wheatley *et al.*, 1997).

Being one of the longest established biofuel technologies, anaerobic digestion was used in sewage works in the Exeter (UK) and Boston (USA) in the late Victoria times to produce methane used for street lighting. Methane gas produced via AD was also used in Leprosy hospital in India in the 19th century to provide light for the hospital (Love & Bryant, 2017). According to Gerardi (2003), the first anaerobic digesters used to degrade domestic sewage sludge were built over 100 years ago at Vesoul in eastern France. Presently, the AD process is frequently used to digest municipal sewage sludge and food processing wastes at large scale (Gerardi, 2003). However, small AD reactors have also been designed using brick, concrete and polyethylene, and are common in China (8 million) and India (4.5 million), and are expanding rapidly into central and South America, as well as other developing countries, as affordable sources of energy and agricultural fertilizer (Brown & Stigge, 2017).

2.2 Advantages of Anaerobic digestion of biomass

Anaerobic digestion reduces waste loads, and hence reduces the land requirement for waste disposal, and the cost of construction and operation of landfills (Chen *et al.*, 2008; de Souza, 2013; Karthikeyan *et al.*, 2016). It improves the dewatering of sludge which results in cheaper sludge handling and disposal costs (De Mes *et al.*, 2003; Meyer & Powers, 2011; Pullen, 2015; Wheatley *et al.*, 1997).

According to the UN, livestock is responsible for 18% of global greenhouse gas emission (Siegel & Nelder, 2008). This GHG emission as methane, which comes from undigested manures such as livestock and poultry wastes, can be mitigated using AD reactors, where the gas could be recovered for energy purposes or flared (Acton, 2012; Hohenstein, 2011; Karimi, 2015; Korres, 2013; Net, 2010). Thus, AD processes effectively and efficiently reduce CO₂ and methane emissions which significantly reduces GHG emission into the atmosphere (de Souza, 2013; Meyer & Powers, 2011; Tranter *et al.*, 2011).

Anaerobic digestion produces clean fuels from renewable feedstocks (Chen *et al.*, 2008; Dahlquist, 2013; De Mes *et al.*, 2003; Love & Bryant, 2017; Wheatley *et al.*, 1997), which potentially reduces over-dependence on fossil fuels (Oreopoulou & Russ, 2006). The biogas from AD process can be purified further to make it acceptable for use as a transport fuel or for electricity generation via CHP systems (de Souza, 2013; Karthikeyan *et al.*, 2016; Management Association, 2017; Pullen, 2015; Teymoori Hamzehkolaei & Amjady, 2018). Previous studies have also reported that AD effectively reduces 80 - 90% of the odour (H₂S, NH₃, etc.) (De Mes *et al.*, 2003; Klemes *et al.*, 2008; Meyer & Powers, 2011).

The AD process also converts up to 70% of the nitrogen compounds in the waste to ammonia and retains P and K which together are essential components of fertilizers (Klemes *et al.*, 2008). Therefore, digestate can be added to soil to serve as an excellent fertilizer to improve crop yields (Brown & Stigge, 2017; Tranter *et al.*, 2011; Wheatley *et al.*, 1997). This is possible because sludge from the AD is stable, rich in nutrients and biologically active, enabling them to stimulate microbial activities in the soil and save farmers the high cost of buying mineral fertilizers. The AD process effectively inhibits the growth of pathogenic bacteria, protozoa, and viruses due to the challenging biological conditions inside the reactor provided by organic acids, high temperature, exposure time and lack of oxygen (Klemes *et al.*, 2008; Love & Bryant, 2017; Meyer & Powers, 2011). Thus, when recycling of effluent is

incorporated, the AD can help in the control of microbial pollution in the environment by preventing the release of the process microbes into the environment.

The digestate and biosolids produced during anaerobic digestion can also serve as additives to cement (Pullen, 2015). Thus, the adoption of AD process for energy recovery and for production of nutrient-rich digestates for use as organic fertilizer, can help developing countries to grow rapidly in terms of human capacity, agriculture and infrastructure.

2.2.1 Disadvantages of anaerobic digestion

According to Riffat (2012), optimal operation of the AD process normally requires a relatively high temperature (35 °C), long start-up time to build sufficient biomass due to the slow growth rate of methane-forming bacteria; and may also require the addition of chemicals to maintain the required levels of alkalinity and nutrients in the reactor. There is also strict regulation of grid gas quality which requires that the biogas has to be refined from 50 – 70 % methane, 20 – 25 % CO₂ to over 97 % methane and that it should be free from oxygen, hydrogen, nitrogen, other trace gases and odor (Pullen, 2015). Sometimes, the digestion process can be upset by the presence of toxic substances, generate odours due to the formation of fatty acids. Wheatley *et al.* (1997) also highlighted high capital costs, long retention time, long start-up periods, and the cost of heating as some of the disadvantages of AD treatment. Among the factors mentioned, the high cost of chemicals and cost of heating the AD plants are the key hindrances to the development of AD technology in many developing countries, especially in poor countries with low temperatures.

2.3 The AD process degradation pathway

Anaerobic degradation is a highly complex and dynamic process that combines microbiological, biochemical and physicochemical processes (Angelidaki *et al.*, 2009). It is a multi-stage biochemical process that involves several reactions and different groups of microorganisms – bacteria and archaea and follows a complex metabolic pathway in transforming complex organic matter into biogas (Ferreira, 2013). According to Yang *et al.* (2011), degradation of lignocellulosic biomass is naturally carried out by glycosyl hydrolase (glycosidase) enzymes that are produced by different microbes in specific microbial communities. These AD process microbes and methane-forming archaea break down organic matter via a sequential degradation pathway (Figure 2-1) which is divided into four stages,

namely: disintegration and hydrolysis, acidogenesis (fermentation), acetogenesis and methanogenesis.

2.3.1 Disintegration and hydrolysis

This is usually the rate-limiting step during anaerobic digestion processes because it governs the growth of microbial biomass conversion, the removal of solids and uptake of liquid substrates from the waste environment, hence it determines the rate of other the organic decomposition steps (Miller & Clesceri, 2002). Many microorganisms produce extracellular enzymes mainly hydrolases, e.g. lipases, cellulases, and proteases, which carry out the degradation of complex molecules such as lipids, carbohydrates, and proteins into smaller sub-units that can be assimilated by the microbial cells (Ferreira, 2013). Simple soluble molecules produced from the feedstock biomass can penetrate the cell membranes of the fermentative bacteria where they are metabolized, converted into simpler compounds, and excreted in the form of volatile fatty acids, alcohols, lactic acid, carbon dioxide, hydrogen, ammonia, hydrogen, sulfide, and produce new bacterial cells (Schön, 2010). The hydrolysis rate during anaerobic digestion process depends on: temperature of the anaerobic digester, particle size and shape of the feedstock biomass, pH of the reactor medium, residence time of the feedstock in the reactor, composition of the feedstock (lignin, carbohydrate, protein and fat contents), concentration of NH_4^+ -N, and concentration of hydrolysis intermediate products such as VFAs (Lenihan *et al.*, 2010; Von Sperling & de Lemos Chernicharo, 2005). The most important hydrolytic bacteria are *Bacteroides*, *Bifidobacteria*, and *Clostridium* (Gerardi, 2006). The hydrolysis rate of a single substrate such as lignocellulose can be represented by (Equation 2-1 and Equation 2-2), which incorporates the mass concentrations of the substrates (Miller & Clesceri, 2002)

$$S = S_0 \exp(-k_h X t) \quad \text{Equation 2-1}$$

$$\frac{dS}{dt} = (-k_h) S_0 \exp(-k_h X_h t_{total}) \quad \text{Equation 2-2}$$

where S is the available organic material, or dry weight of volatile organic matter, organic carbon or soluble COD concentration of the material (S_i), X is the mass of organisms over the

period, t and $-Kh$ represents the anaerobic rate of hydrolysis (expressed as day^{-1}). For a soluble organic substrate.

2.3.2 Acidogenesis (fermentation)

During the fermentation process, diverse groups of fermentative or acid-forming bacteria transport the soluble products from the disintegration and hydrolysis step inside their cells and convert these products to organic acids such as formate, acetate, lactate, propionate, and butyrate (Gerardi, 2006; Von Sperling & de Lemos Chernicharo, 2005). Other products formed at this step include: ethanol, pyruvates, ammonia, hydrogen sulfide, hydrogen, and carbon dioxide which are simple substrates for use by methane-forming bacteria (Ferreira, 2013).

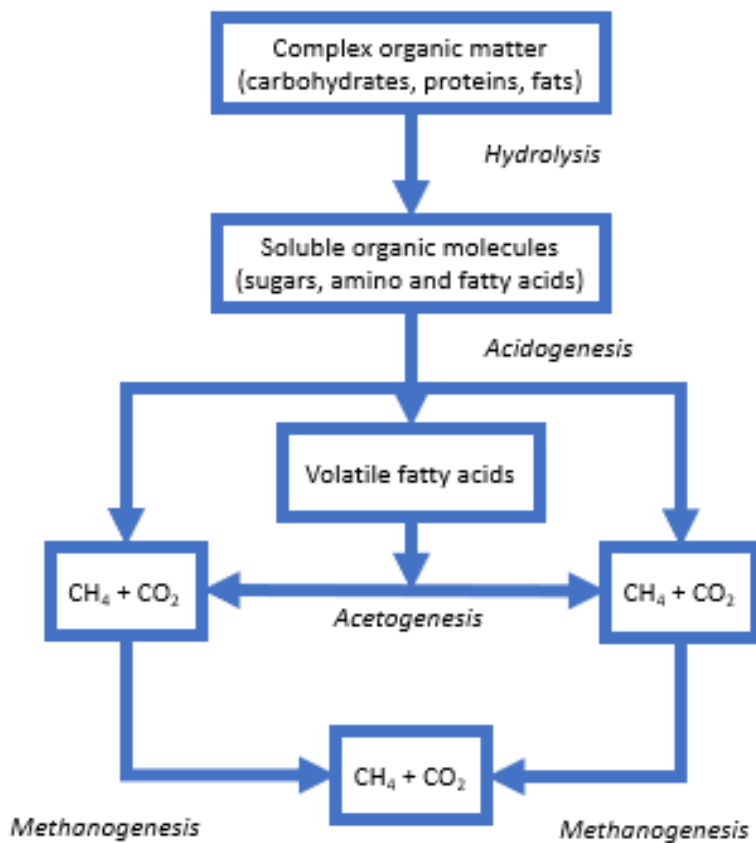


Figure 2-1 Anaerobic degradation pathway. Adapted and modified from Bharathiraja *et al.* (2018)

2.3.3 Acetogenesis

In this stage, obligate hydrogen-producing acetogenic bacteria oxidize propionate and higher VFAs to acetate, hydrogen and carbon dioxide, which are substrates used directly by methane-producing archaea (Schön, 2010; Von Sperling & de Lemos Chernicharo, 2005).

The process is favored by low hydrogen concentrations, thus a syntrophic relationship exists between the hydrogen consumers (hydrogenotrophic methanogens) and the acetogens in order to regulate the hydrogen and propionate concentration and control the entire digestion process (Ferreira, 2013). When these processes are not balanced, this usually leads to a drop in pH due to the presence of H⁺ from the accumulation of VFA in the aqueous solution. However, normally the hydrogenotrophic methanogens, which include the genera *Methanobacterium*, *Methanospirillum* and *Methanobrevibacter* use the hydrogen and CO₂ to produce methane, keeping hydrogen concentrations low (de Lemos Chernicharo, 2007; Gerardi, 2006; Korres, 2013). Low concentration of hydrogen (5 – 50 ppm) has been reported to favour the formation of acetic acid (Singh *et al.*, 2015). However, excess hydrogen concentration decreases acetic acid concentration and increases the formation of organic acids such as propionic and butyric acids which are toxic to the methanogens (Singh *et al.*, 2015; Von Sperling & de Lemos Chernicharo, 2005). The acetoclastic methanogens can only directly utilize acetate from the acidogenic phase to produce methane. It has also been reported that about 50% of soluble COD is converted into propionic and butyric acids which the acetogens further break down into acetic acid and hydrogen (Von Sperling & de Lemos Chernicharo, 2005).

2.3.4 Methanogenesis

At this final stage of the anaerobic digestion process, the methanogenic archaea, mainly acetoclastic methanogens and the hydrogenotrophic methanogens convert the products from acetogenesis in the forms of acetic acid, hydrogen, CO₂, formic acid, methanol, methylamines and CO into biogas (Von Sperling & de Lemos Chernicharo, 2005). These methane-forming bacteria (methanogens) produce methane by using the acetate and/or CO₂ and hydrogen (Klemes *et al.*, 2008; Von Sperling & de Lemos Chernicharo, 2005). *Methanosaeta* is a filamentous acetoclastic methanogen and dominates when there is a low concentration of VFA and ammonia in a reactor whereas *Methanosarcina* is a hydrogenotrophic methanogen and dominates in the presence of high VFA and high ammonia concentrations (Ferreira, 2013). According to Khanal (2011a), *Methanosarcina* accounts for the stability of the AD process, and its dominance is maintained during short SRT or high acetate concentration.

2.4 Potential biomass for biomethane production

Biodegradable organic matter can be used as feedstock for bioenergy production. Examples of common biodegradable biomass feedstocks include: food processing wastes (potatoes, fruits,

restaurant wastes, etc.); municipal solid wastes (biodegradable components), lignocellulose (straw e.g. rice, wheat, corn straw, etc. and grass silage); cellulose (paper, cardboard, cellulose powder); animal waste (poultry, cow, pig dung) and sludge (sewage). In Europe, especially Germany and Austria, many farmers use grass silage as an anaerobic digestion feedstock to produce biogas (Nizami & Murphy, 2010). However, this section provides details of some of the potential biomass feedstocks from Nigeria that have been used in the current study, as listed in Section 1.4.

2.4.1 Perennial Ryegrass (*Lolium perenne*)

Perennial ryegrass (*Lolium perenne* L.) is a grass from the family Poaceae, native to Europe, temperate Asia, and northern Africa but now widely cultivated and naturalized around the world (Bassam, 2010; Casler & Duncan, 2003), but most extensively used for forage in Europe and United States (Casler & Duncan, 2003). Its leaves are dark green with smooth and glossy lower surface (Bassam, 2010). It is propagated using seed and is of great importance in being utilized as animal feed (Bassam, 2010). It can grow between 10 to 90 cm high with erect or prostrate stems with 2-4 smooth nodes and mid-green leaves (Casler & Duncan, 2003). The leaves and stems of the grass are generally more digestible than other grass species (Boller *et al.*, 2010). The grass is also used on winter-games parks, pitches, roadsides, heavy-duty lawns, landscaping areas, tennis courts, cricket fields, golf tees and fairways (Casler & Duncan, 2003). It has a high content of water-soluble and non-structural carbohydrate (Korres, 2013; Yamada & Spangenberg, 2010), and lower concentrations of crude fibre (Korres, 2013; Lichtfouse, 2011). In addition to its use for forage and feed purposes, perennial ryegrass is now considered as a candidate biomass for conversion into biofuels for energy production in the form of heat and electricity (Bassam, 2010). This is because the grass contains up to 40% soluble sugar which can be fermented easily to biofuel such as ethanol, while the remaining cellulose can either be ensiled for animal feed or further broken down with enzymes to produce more biogas (Bassam, 2010; Lichtfouse, 2011). Therefore, perennial ryegrass is one of the potential AD feedstocks which could be used to reduce the energy crisis in Nigeria.

2.4.2 Cassava (*Manihot esculenta Crantz*) process wastes

Cassava is a dicotyledonous plant belonging to the plant family called *Euphorbiaceae* which originated and was domesticated in South America in about 4000 - 2000 BC and is now a major staple food crop in different parts of the world (Bassam, 2010). It is a vital energy crop

with high energy potential; and is one of the richest fermentable substances for biofuel production, structurally comprising three tissues namely: peel (10 – 20 %), cork layer (0.5 – 2.0 %) and an edible portion (80 – 90 %) (Bassam, 2013). Cassava (Figure 2-2) is a major agricultural crop produced by almost every rural household in Nigeria, because of ease of cultivation, high calorie content and ease of converting it to different forms of food products such as garri, Abacha, starch, tapioca, flour, fufu, chips, alcohols, crackers, bread, pasta, etc (Cushion *et al.*, 2009).



Figure 2-2 Cassava farm

Cassava is grown in over 90 countries around the world (Muchie & Baskaran, 2012). However, Nigeria is the largest producer of cassava globally (Cushion *et al.*, 2009; Ghosh, 2017; Muchie & Baskaran, 2012; Mussagy *et al.*, 2009).

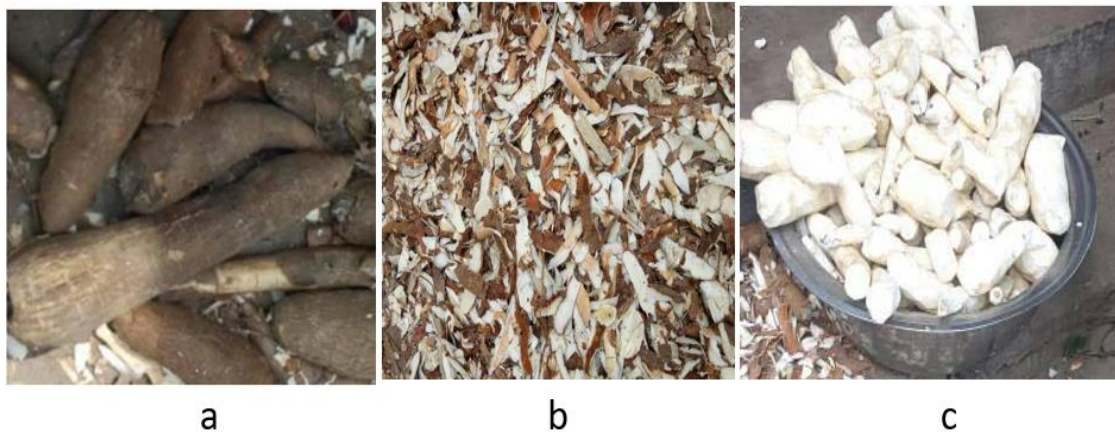


Figure 2-3 Cassava production in Nigeria (a) Tuber (b) Peels and (c) edible starchy portion.

The crop is tolerant to drought, can grow well on marginal lands and matures within eight months, though its harvest can be delayed for two years or beyond, a characteristic that makes it ideal for use as insurance against food shortage (Cushion *et al.*, 2009). Cassava contains different concentrations of toxic hydrogen cyanide (HCN) depending on the variety (Hahn *et al.*, 1992). However, HCN is often reduced significantly during cassava processing which generates enormous amounts of waste which are left to decompose, dried and burnt, or discarded into nearby streams, polluting the environment. However, since the dry root of cassava contains about 80% fermentable starch (Bassam, 2013), the processing waste, especially the peels and starch-rich water from the milling process, could be converted to biogas via anaerobic digestion. This would not only add value to the residue but would go a long way in providing farmers with sufficient energy for processing cassava into other refined products instead of relying on the traditional burning of wood as is currently practiced.

2.4.3 Rice Straw (*Oryza spp*)

Rice (*Oryza sativa* or *Oryza glaberrima*) is a cereal food crop which belongs to the grass family Poaceae which are native to tropical and subtropical southern Asia and southeastern Africa (Gnanamanickam, 2009). It is recognized as one of the most important crops in the world that provides the main source of energy for more than half of the world population (Gnanamanickam, 2009). Rice production accounts for 30% of the total global cereal production and by the year 2025, an estimation of 4.6 billion people will depend on rice for their daily nourishment (Gnanamanickam, 2009). Globally, Asia ranks the highest in rice production with an output of 667.6 million tons, America (37.2 million tons), Africa (20.9 million tons), Europe (3.9 million tons) and Oceania (1.7 million tons). In technical terms,

this amount of rice straw could potentially produce 205 billion liters of bioethanol per year, which is the largest potential amount possible from a single biomass feedstock (Demirbas *et al.*, 2011).



Figure 2-4 Rice farm in Nigeria

Nigeria is the largest producer of rice in West Africa with an average production of 3.2 million tons of paddy rice a year amounting to about 2 million tons per year (Janssen, 2012). Over 70% of the states in Nigeria grow rice as a major cereal crop which usually produces a huge amount of post-harvest wastes which are often burnt in open fires in the rice fields as part of the land preparation for the next planting season. Harvesting and processing of rice for food generate two major wastes – rice straw which is the leafy portion with the stem which is often left behind in heaps in the farm for open burning or to degrade over time while the husk refers to the waste generated from the rice milling processes. Among different agricultural wastes, rice straw is one of the most abundant renewable lignocellulosic biomass resources in the world and it is typically composed of cellulose (32 – 47 %), hemicellulose (19 – 27 %), and lignin (5 – 24 %) (Wang *et al.*, 2015). Research has shown that a harvest of 1 kg of the rice grain is accompanied by the generation of approximately 1 - 1.5 kg of rice straw (Kaur & Phutela, 2016). However, instead of burning, rice straw could serve as a renewable raw material for biogas production via anaerobic digestion, and potentially this biogas could

substitute fossil fuels for the provision of both electricity, heat and other economic benefits for the people.

2.4.4 Napier Grass (*Pennisetum purpureum* Schum)

Napier grass, also commonly known as elephant grass (*Pennisetum purpureum*), is one of the major fast-growing green herbaceous perennial grasses that cover many tropical savannah grasslands in Nigeria. The grass belongs to the Poaceae family and is native to tropical Africa (Zhang & Dincer, 2016). It grows well on marginal lands and is often used for cattle feed and cultivated as forage. Napier grass can grow up to 4 m in height and has more productivity than switchgrass, *Miscanthus*, or food crops (Jansen, 2012). It is one of the highest yielding tropical grasses and a very versatile species that can be grown under a wide range of conditions (dry or wet) and production systems, and could serve as a substrate for biogas production, substituting fossil fuels (Zhang & Dincer, 2016).



Figure 2-5 Napier grass (Elephant grass)

Napier grass can grow 3 meters high every 45 days, which implies that it can be harvested 6 times a year with a yield of about 40 tonnes per ha giving an annual production of 240 tonnes per hectare per year (Jansen, 2012). Napier grass has a deep root system that is fairly drought resistant. Its tender and young leaves are good animal feed. Being an aggressive invasive

plant, local farmers spend a lot of money in cutting or weeding the grass using crude implements. This is often necessary to prevent it from outcompeting and suppressing other crops in cultivated farms. However, instead of burning which leads to environmental pollution, Napier grass is rich in cellulosic fiber is an excellent and cheap AD feedstock for producing biogas that would help to solve Nigeria's enormous energy crises.

2.4.5 Gamba grass (*Andropogon gayanus*)

Gamba grass, *Andropogon gayanus* is a gigantic African grass (Russell-Smith *et al.*, 2009; Wormworth & Sekercioglu, 2011). It has been introduced into different parts of the world, including Australia, Brazil, etc., as improved pasture species for cows (Russell-Smith *et al.*, 2009; Weber, 2017), and farmers prefer the grass because it produces bigger leaves than many native kinds of grass (Freeman *et al.*, 2011). The grass can grow up to 4 m high and has a standing biomass up to about 17 ton. ha⁻¹ (Cochrane, 2010), which can reach up to 30 ton. ha⁻¹ (Russell-Smith *et al.*, 2009). Gamba grass is an aggressive colonist of native savannah and results in fire cycle with intense fire which reduces canopy in the ecosystem (Russell-Smith *et al.*, 2009). Due to high fuel load, gamba grass has been reported to have the potential to produce fires up to seven times more likely than native grasses (Moran, 2005; Stow *et al.*, 2014).



Figure 2-6 Gamba grass

Some researchers have also reported that the intensity of fire from burning Gamba grass is at least eight times that of native grasses during early dry seasons (Cochrane, 2010; Wormworth

& Sekercioglu, 2011) because the grass accumulates more biomass than native grasses (Weber, 2017). This burning increases the release of stored carbon from trees which catch fire unintentionally from the burning grass, and that adversely affects the ecosystem and constitutes a threat to the country's biodiversity because the fire from the grass destroys tree canopies which also increases GHG emission (Wormworth & Sekercioglu, 2011). In Nigeria, Gamba grass chokes up other grasses to remain the only dominant species in many grasslands and often initiates seasonal fire cycles which decrease tree canopy cover making the soil vulnerable to erosion. In addition to hand-pulling, weeding and application of herbicides, Gamba grass can be controlled by grazing (Cochrane, 2010). However, only an insignificant amount of this vast biomass is grazed, which often leaves a large mass of unutilized Gamba grass to initiate intense fire outbreaks annually. Thus, harvesting Gamba grass regularly, and using it as feedstock for the AD to produce methane could effectively help to control the spread of the grass, as well as reduce the environmental concerns associated with the grass in the environment.

2.4.6 Guinea grass (*Panicum maximum*)

Guinea grass (*Panicum maximum*) is a perennial tropical grass that mainly grows as a weed in cultivated fields, pastures and roadside all year round (Veziroğlu et al., 1987), and is the most well-known of all tropical grasses (Warren, 1924). The grass is native to Africa, has long narrow leaves, and produces a seed head that resembles rice, and can grow up to 1 – 1.5 m tall (Boonman, 2013; Charrier, 2001; Service, 2010). The grass was spread from Africa to different continents, especially during the era of the slave trade, where it was used to make bedding and packaging materials for assisted migrants (Boonman, 2013), and now, it has spread to nearly all tropical countries as high-protein fodder for livestock (Service, 2010). Guinea grass is capable of colonizing cultivated land on the coast, and elsewhere where it grows as a secondary grass (Boonman, 2013). The grass grows very well in well-drained soils, and sunny areas, but can also tolerate a wide range of environmental conditions (Service, 2010). According to Moran (2005), there is a renewed interest in Guinea grass (*Panicum maximum*) as an alternative pasture crop.



Figure 2-7 Guinea grass

The grass is adapted to both the tropics and subtropics and is even tolerant to shading, and hence has a role in agroforestry plantation and can yield biomass which is equivalent to Napier grass under certain conditions. This grass can be harvested every 4 weeks (Moran, 2005) i.e. 10 to 12 times per year. Its maximum dry matter production is about 30 tons. hectare⁻¹.year⁻¹ generating a plentiful supply for intensive livestock farms (Charrier, 2001).

However, this grass also spreads aggressively and can build very high fuel loads which can increase fire risk. It develops a broad fire-adapted underground rhizome that enables it to survive fire better than many other native kinds of grass, and normally sprouts new growth after the fire, thus increasing its dominance on the land after fire incidence. It is resistant to drought and a large amount of biomass it produces hot fires that destroy the native vegetation (Service, 2010). It has a sixty-day regrowth cycle during hotter months and a ninety-day period during the cooler months (Bergin, 2004). In Nigeria, Guinea grass is only used in pastures for livestock, while significant unutilized biomass from the grass which is often left to spoil, burnt or abandoned to trigger annual intense bushfire could be utilized as a dependable biomass feedstock resource to produce biogas.

2.4.7 Speargrass (*Imperata cylindrica*)

Speargrass (*Imperata cylindrica*), is an aggressive invasive rhizomatous perennial weed (Brink, 2012; Labrada *et al.*, 1994; Singh, 2014). It belongs to the plant family Poaceae, and its widely distributed throughout the tropics and subtropical regions of Africa, India, etc (Brink, 2012). The grass has been identified as one of the major invasive perennial weeds posing problems in crop production in Nigeria (Chikoye *et al.*, 2005), and is recognized as one of the 10 worst weeds in the world (Brink, 2012). It can grow on all continents, except Antarctica (Labrada *et al.*, 1994). The stem of Speargrass can be solitary or tufted with flat, rolled or stiffly erect leaf blades, and is classified as an invasive weed in different parts of the world including the United States (Xu & Zhou, 2017). Speargrass is suitable for mulching, erosion control, slope stabilization (Brink, 2012), papermaking, animal feeds and traditional medicine (Labrada *et al.*, 1994). Speargrass is propagated sexually by seeds and vegetatively by underground roots, which enables it to be drought-resistant (Brink, 2012; Chikoye *et al.*, 2005; Labrada *et al.*, 1994; Xu & Zhou, 2017). The grass produces cylindrical panicles which are copiously hairy (Xu & Zhou, 2017). It has a needle-like sprouts that can pierce farmers feet, eyes, palms, etc during weeding (Chikoye *et al.*, 2005), and has rhizomes that are extremely competitive, highly resistant to heat and breakage, and can penetrate the soil up to 1.2 m deep and invade the roots of other plants causing them to rot or to die (Brink, 2012). It outcompetes other plant species for resources, gaining an advantage over indigenous plants (Xu & Zhou, 2017). The grass mostly grows near rivers and seashore sands, disturbed grassy places and cultivated lands (Xu & Zhou, 2017). Its dry matter yield is about 2 - 12 tons. ha⁻¹ per year⁻¹ although 11 tons. ha⁻¹ of leaves and 7 tons. ha⁻¹ of rhizomes has also been recorded in Indonesia (Brink, 2012).

Speargrass also causes mouth and tongue injuries to animals that graze on it, and generally reduces the market value of crops especially tubers which it causes to rot (Chikoye *et al.*, 2005). In Nigeria, many farmers have abandoned their farmlands due to Speargrass invasion because of the high amount of effort, time and money required to control its spread. It is easily spread when there is stress such as burning, cutting or drought (Labrada *et al.*, 1994) and competes with crops for space, fertilizer, nutrients, and water, and harbors pests and insects (Chikoye *et al.*, 2005; Labrada *et al.*, 1994). It also initiates intense frequent bushfire in farms, and fallow lands and the seedlings establish very well after every bushfire (Labrada *et al.*, 1994). Speargrass can only produce viable seeds after cross-pollination.



Figure 2-8 Photo of Speargrass (*Imperata cylindrical*)

Speargrass can tolerate temperatures as low as -15°C when dormant and can withstand waterlogging (Brink, 2012). In Nigeria, Speargrass is mostly controlled by hand pulling, hoeing or burning which are often ineffective. Some researchers have reported that the use of herbicides such as Glyphosate and intercropping it with *Mucuna* is a more effective control of the grass (Chikoye *et al.*, 2005). Although Speargrass is a low-quality forage, research has shown that at a very young growth stage it may have digestibility up to 70 %, which reduces to below 40 % after 150 days (Brink, 2012). Thus, the grass could be more effectively controlled by harvesting it young and using it as a substrate for biogas production to solve the energy poverty problems in Nigeria.

2.5 Factors that determine the biogas potential of feedstocks

The chemical composition of feedstocks affects their digestion efficiency during anaerobic digestion (Karthikeyan *et al.*, 2016). Other factors that affect the biogas potential of any given biomass feedstock include: the feedstock material itself, the dry matter content, the actual energy content of the feedstock, retention times of the feedstock in the digester, the purity of

the feedstock, the type of AD plant and its operational conditions (De Mes *et al.*, 2003; Pullen, 2015).

AD feedstocks which are rich in lipids and proteins produce higher volumes and percentages of methane gas because they contain organic matter which is easily biodegradable (Table 2-1), unlike lignocellulose which has a high content of lignin which is recalcitrant to decomposition especially when digested as mono-substrate.

Table 2-1 Theoretical Biogas potentials of pure samples from selected substrate components

Substrate	Composition	Biogas yield (L/g VS)	CH ₄ L/g VS (STP)	CO ₂ (% by volume)
Carbohydrates	(C ₆ H ₁₀ O ₅) _n	0.790	0.415	50
Lipids	C ₅₇ H ₁₀₄ O ₆	0.125	1.014	32
Proteins	C ₅ H ₇ NO ₂	0.700	0.496	29
Acetate	C ₂ H ₄ O ₂	-	0.373	-

Source: (Angelidaki & Sanders, 2004; Oreopoulou & Russ, 2006)

Feedstock that has high content carbon sources and nutrients, especially C, N, and P can achieve efficient biodegradation during anaerobic digestion. The ratios of carbon to nitrogen and nitrogen to phosphorus are the most important parameters for predicting the success of the degradation process. Typical values of these recommended ratios are: C:N = 10:1 to 30:1, N:P = 5.1 to 7.1 and overall COD: N:P = 420:7:1 to 1500:7:1 (Schön, 2010).

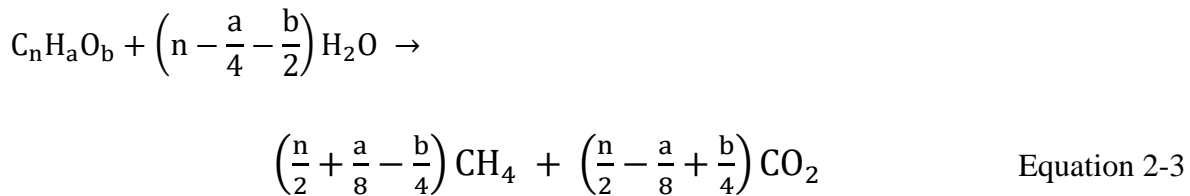
2.6 Biomethane potential of feedstocks

The energy value, in terms of methane content, of any given biomass feedstock, can be estimated theoretically by using an empirical formula, or data obtained from the compositional analysis. However, in the laboratory, the biochemical methane potential (BMP) test can be used to determine the actual methane production under various operational conditions.

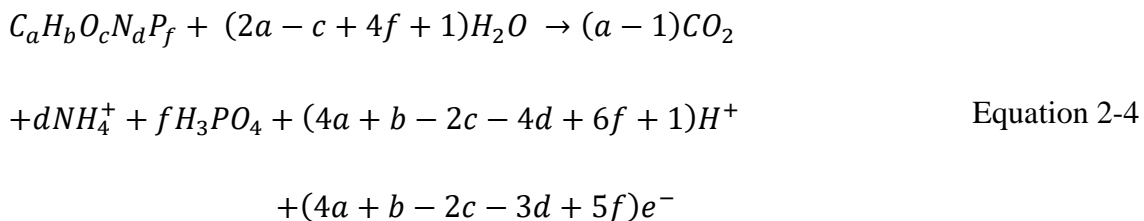
2.6.1 Determination of the theoretical energy value of biomass feedstocks

A feedstock has a maximum amount of methane it can produce based on its carbon content, and this can be quantified by putting the chemical composition of the wastes into the Buswell and Mueller equation (Equation 2-3). The volume of empirical methane production estimated theoretically cannot be achieved in practice because microorganisms use a portion of the carbon and energy gained from the catabolic destruction of the feedstocks for the growth and maintenance of their biomass (anabolic processes), while some portion of the biomass feedstock is not biodegradable (Angelidaki & Sanders, 2004; de Lemos Chernicharo, 2007; Mohee & Mudhoo, 2012; Wellinger, 2013). This could also be due to inhibition from other components in the feedstock and from inadequate time for hydrolysis.

The energy potential can be estimated using the stoichiometric oxidation relationship of the chemical composition of the biomass feedstock identified by Buswell and Mueller (1952).



where $C_nH_aO_b$ represents the empirical composition of the feedstock, where the values of the number of atoms a, b and c are determined by elemental analysis. Similarly, the standard wastewater analysis parameter can be used to determine gas yields. Typically, for every 1 g of COD destroyed in AD operating at 35 °C, 395 mL of CH_4 gas is produced. According to Frigon and Guiot (2010), some other important nutrient parameters in AD reactors such as volatile solids (VS), chemical oxygen demand, total organic carbon (TOC), total organic nitrogen (TON), and total phosphorus, can be theoretically determined using a more robust empirical formula given in Equation 2-4.



where

$$\begin{aligned} \text{VS (g)} &= 12a + b + 16c + 14d + 32f \\ \text{COD (g)} &= 32a + 8b - 16c - 24d + 40f \\ \text{Total Organic carbon (g)} &= 12a \\ \text{Total Organic Nitrogen (g)} &= 14d \\ \text{Total Phosphorus (g)} &= 32f \end{aligned}$$

The theoretical methane potential (TMP) of a substrate $C_nH_aO_bN_cS_d$ from compositional analysis expressed as $\text{m}^3 \text{CH}_4 \cdot \text{kg}^{-1}$ substrate converted at STP can also be simply calculated using Equation 2-5 and Equation 2-6 from Frigon and Guiot (2010) and Angelidaki and Sanders (2004), respectively:

$$TMP = \frac{22.4 \left(\frac{n}{2} + \frac{a}{8} - \frac{b}{4} - \frac{3c}{8} - \frac{d}{4} \right)}{12n + a + 16b + 14c + 16d} \text{ (L CH}_4 \cdot \text{g}^{-1} \text{VS added)} \quad \text{Equation 2-5}$$

or represented as in Equation 2-6

$$TMP = \frac{22.4 \left(\frac{n}{2} + \frac{a}{8} - \frac{b}{4} \right)}{32 \left(n + \frac{n}{4} - \frac{b}{2} \right)} \text{ (L CH}_4 \cdot \text{g}^{-1} \text{VS added)} \quad \text{Equation 2-6}$$

when only the composition of carbon, nitrogen, and oxygen are known, where 22.4 is the molar volume of an ideal gas ($\text{L STP} \cdot \text{mol}^{-1}$). Due to non-degradable components of biomass, in practice, the actual methane yield from anaerobic digestion plants does not often exceed 60% of the TMP value (Frigon & Guiot, 2010). The use of TMP to estimate BMP is simple. However, the TMP value of methane obtained is always higher than the actual methane yield from BMP experiments as it does not consider factors such as inhibition, hydrolysis time, biodegradability and proportion of the carbon in the feedstock used for new biomass synthesis (Mohee & Mudhoo, 2012).

The nutritional composition and fatty acids content of a given biomass feedstock can also be used to estimate the theoretical methane potential of biomass as shown in Equation 2-7.

$$\begin{aligned}
&TMP, \beta_{oTheo} (L CH_4 g VS^{-1}) \\
&= 0.415(carbohydrates) + 0.496(proteins) \\
&+ 1.014(lipids) + 0.373(acetate) + 0.530(propionate)
\end{aligned}
\tag{Equation 2-7}$$

where the carbohydrates, proteins, lipids, acetate, and propionate are expressed as the % of the volatile solids (VS) and the methane potential expressed at STP (Zamorano, 2008).

2.6.2 Biochemical Methane Potential (BMP) Assay

The biochemical methane potential (BMP) assay established by McCarty (1964) and his research group is a simple and inexpensive laboratory procedure used to estimate the anaerobic digestibility of a biomass feedstock and its toxicity under anaerobic conditions (Owen *et al.*, 1979; Riffat, 2012; Rouches *et al.*, 2017). The results from the test show the ultimate methane (or biogas) produced from a given weight of biomass feedstock (Angelidaki *et al.*, 2009; Mohee & Mudhoo, 2012), which serves as a key parameter for the design and operation of full-scale anaerobic digestion plants (Abu-Dahrieh *et al.*, 2011). The maximum specific methane yield obtained from anaerobic digestion of the substrate feedstock is expressed as $m^3 CH_4.kg^{-1}VS$ added. The value of the observed methane yield from the BMP test divided by the theoretical methane yield (TMY), is the biodegradable fraction of the substrate (Dahlquist, 2013). A comprehensive method for carrying out BMP assay has been reported in the German Standard Procedure for Fermentation of organic materials (VDI. 4630, 2006).

2.7 Process parameters that affect the performance of anaerobic digestion

The performance of the AD process is influenced by several factors inside the reactor, especially temperature, pH value, alkalinity, anaerobic conditions, characteristics of waste, nutrients supply (e.g. micro and trace elements), organic and hydraulic loading rate, volatile fatty acid concentration, mixing, presence of inhibitors and toxic substances in the reactor (Schön, 2010; Van Haandel, 2007).

2.7.1 Temperature

Temperature has been reported to be the most important factor that controls the rate of anaerobic digestion and biogas production process (Klemes *et al.*, 2008). Temperature is a

critical factor that determines the performance of the AD because it primarily controls the rate of the biochemical processes, especially the hydrolysis phase, which has been reported by many studies to be the rate-limiting phase (Bajpai, 2017; Ferreira *et al.*, 2013; Khanal, 2011c; Nayono, 2010; Van Haandel, 2007). A fall in temperature could lead to decrease in microbial activity and biogas production, whereas an increase in temperature could increase microbial activity but could also lead to the death of some bacteria (Klemes *et al.*, 2008). Potentially, for every 10 - degree rise in temperature, the rate of reaction can double (Bajpai, 2017), however, this is subject to the limitations above.

Several studies have shown that AD processes can be operated with three broad temperature ranges based on the three anaerobic bacterial thermal groups, namely: cryophiles (psychrophiles), mesophiles, and thermophiles (Cheng, 2009; Klemes *et al.*, 2008; Riffat, 2012; Schön, 2010), as presented in Table 2-2.

Table 2-2 Classification of anaerobic digesters by temperature

Anaerobic process	Operating temperature (°C)	Optimum Temperature (°C)	Operating HRT (Days)	Microbial growth and digestion rates	Tolerance to Toxicity
Cryophilic	10 - 25	> 20	> 50	Low	High
Mesophilic	30 - 40	35	25 - 30	Medium	Medium
Thermophilic	50 - 60	55	10 - 15	High	Low

Anaerobic digesters operated under cryophilic (psychrophilic) temperatures are characterized by low degradation rates and low methane productivity. They are normally run at longer solid retention times (SRT) and low organic loading rates (Schön, 2010). A study by Chen *et al.* (2016) on the AD of tomato plant waste conducted at cryophilic room temperatures (20 - 25 °C) and a mesophilic temperature (37 ± 1 °C) in a batch test, showed that the digesters achieved higher performance under mesophilic temperatures.

Another study carried out by Da Ros *et al.* (2017) on the anaerobic co-digestion of winery wastewater sludge and wine lees in pilot plants operated at mesophilic and thermophilic conditions, showed that the digestion process was stable for a long period at a mesophilic

temperature (37 °C) with an average biogas production of $0.386 \text{ m}^3 \cdot \text{kg}^{-1} \text{COD}_{\text{fed}}$ compared to the thermophilic reactor which failed after one HRT (23 days) due to VFA accumulation.

Thermophilic anaerobic digesters can tolerate higher loading rates, smaller reactor size due to shorter retention time, have higher methane productivity due to faster growth of microbes, and higher pathogen inactivation (Schön, 2010). A study by Streitwieser (2017) also revealed that the activation energy and degradation rate of thermophilic AD processes are higher than the mesophilic regimes. However, another study by Capson-Tojo *et al.* (2017) on the AD of microalgae under mesophilic (35°C) and thermophilic (55°C) temperatures in batch and continuous reactors, also showed that although thermophilic reactors had higher hydrolysis rates in terms of soluble COD production, these did not improve the methane productivity compared to the mesophilic reactors.

The main disadvantages of thermophilic AD reactors are the decreased process stability that arises from the higher growth rate of microbes at the shorter SRT, and this can lead to incomplete digestion, which eventually increases the washout of microorganisms from the reactors (Schön, 2010). Although Da Ros *et al.* (2017) were able to overcome the instability challenges of running thermophilic reactors and improved the process by the addition of trace elements (iron, cobalt, and nickel) as supplements, they reported that the produced sludge from the process (digestate) had poor dewatering properties.

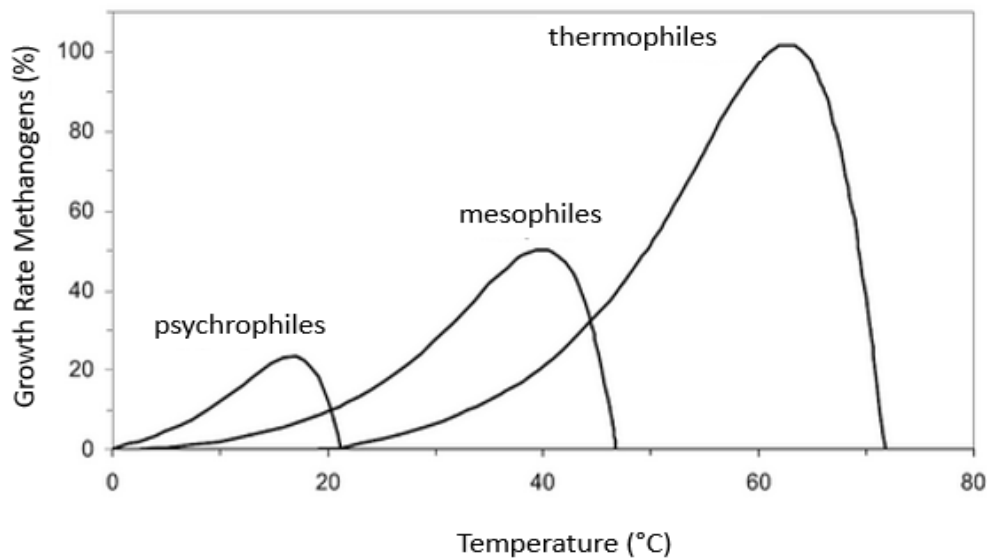


Figure 2-9 Relative growth rate curves of methanogens during AD at different temperatures (Lettinga *et al.*, 2001; Schön, 2010)

Within each temperature range, the growth rates of bacteria increase exponentially with temperature according to the Arrhenius equation until the optimum temperature is reached beyond which, the growth rate begins to decline exponentially as the temperature reduces the bacterial metabolism by denaturing macromolecules such as enzymes (Schön, 2010).

Bacterial growth (Figure 2-9) is not limited to these classes of temperature, as some bacteria can survive over a wide range of temperatures, including temperatures as low as 0°C (Riffat, 2012).

2.7.2 pH

The pH of a solution, which is defined as the negative logarithm of the hydrogen ion concentration (H^+) (Equation 2-8), is an important factor that determines the optimal growth and maximum enzymatic activity of different microbial groups, as well as the equilibrium conditions of the AD system during the degradation process (Schön, 2010). Thus, maintaining a suitable pH during AD operation is an important factor for controlling the performance of the digestion process because a slight change in pH adversely affects the different stages of AD process to different degrees (Bajpai, 2017; Khanal, 2011c), and may signify the start of VFA accumulation (Boe *et al.*, 2010).

$$pH = -\log[H^+] = \log \left[\frac{1}{[H^+]} \right] \quad \text{Equation 2-8}$$

Lue-Hing (1998) reported that a pH value between 6.6 and 7.4, when the carbon dioxide content of the biogas varied from 30 to 40%, indicates that the bicarbonate alkalinity (which is approximately equal to total alkalinity) in the reactor ranges between 1000 and 5000 mg.L⁻¹ as CaCO₃. According to Klemes *et al.* (2008), methanogens will begin to die at a pH below 6.5 due to acidification, and this will lead to the reduction or inhibition of biogas production. Therefore, it is preferable to maintain the pH inside the digester at a near neutral value of 7 in order to ensure stable operation (Van Haandel, 2012, 2007).

2.7.3 Alkalinity

Alkalinity value defines the buffering capacity, or the ability of the reactor contents to resist changes in pH (Federation, 2007; Von Sperling & de Lemos Chernicharo, 2005). Buffering capacity refers to the capacity of the digester medium to neutralize the acids produced during the degradation process in order to reduce pH change (Ferreira *et al.*, 2013). During the AD process, CO₂ which is one of the products forms bicarbonate which provides a buffering system within the reactor, and that helps to maintain the required pH (Van Haandel, 2012, 2007).

According to Schön (2010), a reduction in pH could be due to acid contained in the substrates, the formation of VFA (e.g. acetic acid) during the digestion process, or when the CO₂ produced during the fermentation and methanogenesis stages is solubilized in water to form carbonic acid (Equation 2-9):



The high partial pressure of H₂ can also inhibit propionic acid-degrading bacteria causing the accumulation of high concentrations of volatile fatty acids (VFA), such as butyric and propionic acids (Khanal, 2011c), and this causes a reduction in pH. This condition requires that adequate amounts of alkalinity are present to buffer the reaction process in order to resist the drop in pH (Schön, 2010) since low pH reduces the activity of the methanogens (Khanal, 2011c). Research has shown that bicarbonate alkalinity >1000 mg.L⁻¹ as CaCO₃ is required in order to maintain pH in the digester above 6.8, and consequently, the alkalinity in large scale the AD plants is maintained between 1000 - 5000 mg.L⁻¹ as CaCO₃ (Federation, 2007; Khanal, 2011c). However, to maintain more stable operation, a pH range of 7.0 – 7.2, alkalinity 4000 – 5000 mg.L⁻¹ CaCO₃, is recommended (Andreoli, 2007). Some examples of

chemicals which are commonly used to maintain bicarbonate alkalinity in anaerobic digesters are presented in Table 2-3.

Table 2-3 Alkalinity equivalent weight ratios (Federation, 2007)

Chemical name	Formula	Ratio
Anhydrous ammonia	NH ₃	0.32
Aqua ammonia	NH ₄ OH	0.70
Anhydrous soda ash	Na ₂ CO ₃	1.06
Caustic soda	NaOH	0.80
Hydrated lime	Ca(OH) ₂	0.74

It has been reported that instead of using alkali to increase the buffering capacity of the AD process, liquid digestate could be used to save cost (Oreopoulou & Russ, 2006). Research has also shown that addition of the right amount of sodium bicarbonate is often preferred due to its high solubility, long-lasting effect, low toxicity, and the fact that it can significantly consume gas-phase CO₂ and improve the pH when added directly (Li, 2016). A detailed procedure for determining the right amount of reagent to add to an AD in order to provide the required alkalinity has been published (Federation, 2007). However, the use of commercial high purity chemicals to control pH in AD reactors is expensive and may not be affordable to people from low-income countries, and therefore the use of very cheap locally available alkaline-rich waste materials such as biomass ash and its extracts might be a better alternative.

2.7.4 Effect of mixing on the AD process

The good operational conditions in high-rate AD reactors that provide an optimum environment for microorganisms can be achieved through adequate mixing, together with heating, uniform feeding rates and correct thickening of the feed sludge (Federation, 2007; Schön, 2010). The benefits of effective digester mixing are:

- It enhances in a uniform distribution of incoming substrate throughout the digester
- It improves the contact of the substrate with the microorganism
- Mixing provides uniform heating for all the reactor contents

- It reduces the formation of scum layers and accumulation of settled sludge at the bottom of the reactor
- It increases the dilution of inhibitors- including toxic substances, unfavorable pH, and balances the temperature of the feedstock
- It enhances the phase separation of the biogas from the digester liquid.

2.7.5 Solid residence time (SRT)

This refers to the period that solids are retained in the digesters and is determined by the characteristics of the substrate, as easily degradable substrates require short SRT, while substrates which are hard to degrade (lignocellulose) are digested with long SRT (VDI. 4630, 2006). It controls the type of microorganisms that can grow in the reactor and the biogas yield (Korres, 2013; Schön, 2010; Singh *et al.*, 2015). Short retention time can increase gas production rates but gives poor gas yields in terms of the VS converted, while long retention time essentially leads to increase in the specific gas yield but decreases in the volumetric gas production rate which is expressed as $\text{m}^3 \text{CH}_4 \cdot \text{m}^{-3} \cdot \text{d}^{-1}$ (Cheng, 2009; Schön, 2010).

2.7.6 Organic loading rate

This refers to the amount of substrate (volatile solids, kg or kgCOD) or other measure of organic matter introduced into the digester per reactor volume (m^3) in a day (d). It is an important parameter used in the determination of the size and operation of AD digesters during the design process. It is calculated as shown in Equation 2-10.

$$\text{OLR} = \frac{Q \cdot C}{V} = \frac{C}{\text{HRT}} \quad \text{Equation 2-10}$$

where OLR is the organic loading rate ($\text{kgVS} \cdot \text{m}^{-3} \cdot \text{d}^{-1}$ or $\text{kgCOD} \cdot \text{m}^{-3} \cdot \text{d}^{-1}$), Q the influent flow rate ($\text{m}^3 \cdot \text{d}^{-1}$), C the concentration of volatile solids in the substrate ($\text{kgVS} \cdot \text{m}^{-3}$) and V the reactor volume (m^3) (Nayono, 2010; Schön, 2010). For a CSTR with no recirculation, the SRT is equal to the HRT, whereas SRT is higher than HRT in reactors that incorporate solids recycle (de Lemos Chernicharo, 2007; Korres, 2013; Schön, 2010). As shown in Equation 2-10, OLR is inversely proportional to HRT which signifies its dependence on retention time, in addition to the process temperature. This indicates that an increase in OLR at lower temperatures would require longer retention time.

2.7.7 Redox Potential or Oxidation-Reduction Potential (ORP)

The activity of microbes inside AD reactors is influenced by the redox potential (Table 2-4) in of system. The ORP measured in millivolts (mV) can be defined as the tendency of chemical species such as molecules and radicals in the AD to gain electrons and then undergo reduction (Rosato, 2017). Values of ORP between 0 and – 2000 mV indicate anaerobic process (Rosato, 2017), and according to Khanal (2011c), maintaining ORP value around -200 to -350 mV in the AD at pH 7.0 provides a competitive advantage to the growth of obligate anaerobes within the reactor mixture.

Table 2-4 Oxidation-Reduction Potential (ORP) and bacterial activity in AD reactors

ORP (mV)	Bacteria Activity
+300	O ₂ is available and used to degrade BOD
+100 to -100	NO ₃ ⁻ available and used to degrade cBOD: denitrification occurring
< -100	SO ₄ ²⁻ available and used to degrade cBOD: sulfate reduction and acid production occurring
< -200	Anaerobic fermentation and acid production occurring
<-300	Methane and H ₂ S production occurring

Adapted from (Gerardi, 2006)

During AD processes, the production of CO₂ is due to oxidation process of organic carbon while the formation of methane is a reduction process of the organic carbon (Rosato, 2017). An increase in the oxidation-reduction potential above -300 mV due to the presence of sulfate and nitrate in the digester, inhibits the activity of the methane-forming bacteria, and methane production, but does not inhibit the activity of acidogenic bacteria (Gerardi, 2006). Therefore, such conditions may lead to instability.

2.7.8 Toxicity and inhibition

Methanogens are very sensitive to the presence of toxic materials in the AD feedstock or reactor. Some of these toxic materials, for instance, weak acids and bases produced during the digestion process become toxic and dissociated due to pH (Van Haandel, 2012, 2007). Toxicity exerts adverse irreversible effects on the microbial metabolism during the AD process. Inhibition, on its own, is reversible and precedes toxicity. Inhibition takes place

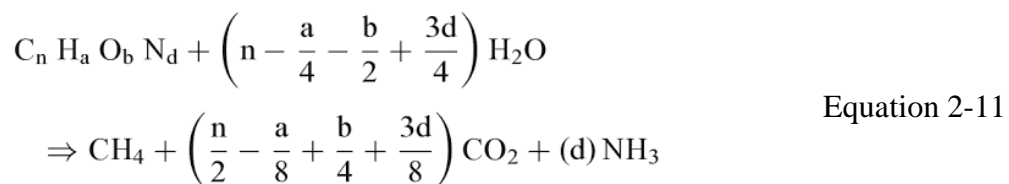
when there is a small increase in the concentration of a compound leading to reversible impairment of the biological process, either by affecting microbial cell structures or the enzymes that carry out metabolism during anaerobic digestion process (Gerardi, 2006; Holland, 2013; Korres, 2013; Schön, 2010; Stronach *et al.*, 2012). Inhibitors are chemical substances such as ammonia, sulfide, metals and some organic compounds which negatively affect or retard microbial growth in the AD, leading to decrease or a complete cessation of methane production (Chen *et al.*, 2008; Cheng, 2009; Wang *et al.*, 2010).

2.7.8.1 Oxygen inhibition

Traces of oxygen in AD inhibit the methane-forming archaea which are strict anaerobes (Schön, 2010; Van Haandel, 2012, 2007; Wang *et al.*, 2010), and these die in the presence of free molecular oxygen (Gerardi, 2003). Free molecular oxygen does not actually kill obligate anaerobes such as the methanogens, but they are killed by highly toxic superoxide (O_2^-) and hydrogen peroxide (H_2O_2) which are formed when free oxygen enters the bacterial cell (Gerardi, 2006).

2.7.8.2 Ammonia inhibition

Ammonium is produced when protein is degraded, and the quantity produced in the AD digester is a function of the total nitrogen in the substrate and the rate of protein degradation (Poltronieri, 2016; Van Haandel, 2012, 2007). The quantity of ammonia contained in a substrate can be estimated by stoichiometry using the Buswell equation as shown (Equation 2-11) as follows:



where $C_n H_a O_b N_d$ represents the chemical formula of the biodegradable organic material undergoing complete anaerobic degradation process. H_2O , CH_4 , CO_2 and NH_3 are expressed in litres(L), mL.gVS.d⁻¹, mg.L⁻¹, respectively.

The main forms of inorganic nitrogen in the anaerobic digester are the ammonium ion (NH_4^+) and free ammonia (NH_3) (Chen *et al.*, 2008), and together these constitute the total ammoniacal nitrogen (TAN). When the ammonium concentration is too low it will cause

nitrogen shortage in the reactor which will limit the growth of the bacteria leading to poor or suboptimal process performance (Poltronieri, 2016). Conversely, when the ammonium concentration is excessive (Table 2-5), it can often lead to reactor failure due to ammonia inhibition (Poltronieri, 2016). This inhibition is due to the diffusion of free ammonia into the cell membrane and causes proton imbalance and/or potassium deficiency inside the cell of methanogenic archaea (Chen *et al.*, 2008; Gübitz *et al.*, 2015). The level of ammonia inhibition in AD depends on the organic composition of the feedstock, inoculum and the pH and temperature inside the digester (Chen *et al.*, 2008). pH affects the equilibrium ratio of free ammonia to ammonium ion in the anaerobic digester. The ranges of ammonia concentrations and their effects are presented in Table 2-5.

Table 2-5 Effect of ammonia nitrogen on anaerobic digestion at neutral pH

Ammonia concentration (as N, mg/L)	Effect
50 – 200	Beneficial
200 – 1000	No adverse effect
1500 – 3000	Inhibitory at pH 7.4 to 7.6
Over 3000	Toxic at pH > 7.6

Source: (Von Sperling & de Lemos Chernicharo, 2005)

Therefore, it is the free unionized (non-dissociated) form of ammonia (FAN), which is very toxic to methanogens, especially at concentrations higher than 3000 mg. L⁻¹ where it is toxic at all pH values. If the value of TAN is known, FAN can be estimated using Equation 2-12 (Shi *et al.*, 2017):

$$C_{FAN} = \frac{C_{TAN}}{1 + \frac{10^{-pH}}{K_a}} \quad \text{Equation 2-12}$$

where, C_{FAN} and C_{TAN} are the concentration of free ammonia and the total ammonia nitrogen, respectively, K_a = 1.097 x 10⁻⁹ at 35 °C is the ammonia dissociation constant.

2.7.9 Volatile fatty acids

Volatile fatty acids (VFA) are intermediate products formed during the anaerobic degradation process. VFA can exert toxicity if the rate of their production exceeds the rate of consumption

in a reactor, thereby disrupting the equilibrium of the process due to the formation of high concentrations of unionised acids which can diffuse through the cell membrane of bacteria (Gerardi, 2006; Schön, 2010; Van Haandel, 2012, 2007). High concentrations of unionized volatile acids like acetate, butyrate, and propionate reduce the alkalinity which results in a fall in the reactor pH. Propionate has been reported to be the most inhibitory VFA to the AD process, particularly when present at a concentration $> 5 \text{ mg.L}^{-1}$ (Gerardi, 2003; Oreopoulou & Russ, 2006).

2.7.10 Aromatic, phenolic and chlorinated hydrocarbons

These hydrocarbons are toxic to methanogens, especially chloroform (CHCl_3), when present at a concentration above 1 mg.L^{-1} (Gerardi, 2006; Wang *et al.*, 2010). Aldehydes, especially formaldehyde (HCHO), are very toxic to methanogens when present at concentrations above 100 mg.L^{-1} . Some aromatic compounds such as toluene, phenols, benzene also inhibit methanogenic activities during AD (Gerardi, 2006; Wang *et al.*, 2010). The presence of industrial wastes containing chlorinated organics and biocides can also result in immediate toxic effects when added into the reactor. Such materials are naturally toxic, and exert irreversible toxic effects on the metabolic process, unlike ordinary inhibitory substances (Van Haandel, 2012, 2007). Similarly, tannins which are phenolic compounds contained in apples, beans, cereals, bananas, and coffee are potentially toxic to methanogens and are believed to inhibit specific enzyme sites in the microbes (Gerardi, 2006).

2.7.11 Sulfate and sulfide inhibition

Sulfur is an essential nutrient for most microorganisms and is a vital component of the cells of the methanogenic archaea. A concentration in the range $1 - 25 \text{ mg.L}^{-1}$ supports the growth of methanogens (Chen *et al.*, 2008; Gerardi, 2003). According to Gerardi (2006), 1.5 g of sulfate is reduced to hydrogen sulfide when SRB degrade 1 g of COD. Sulfate does not actually inhibit methanogens but SRB such as *Desulfuromonas*, *Desulfovibrio*, and *Desulfomonas* outcompetes methanogens for substrates. Also, the reduction of sulfate by SRB produces hydrogen sulfide (H_2S) and sulfide ions (HS^- , S^{2-}) which strongly inhibit the AD process, particularly at concentrations above $150 - 200 \text{ mg.L}^{-1}$ (Gerardi, 2003; Schön, 2010; Wang *et al.*, 2010). Sulfide inhibition is also pH dependent because only the unionized H_2S can easily diffuse through the cell membrane and cause toxicity (Gerardi, 2006; Schön, 2010). Therefore, pH values below pH 7 will increase the toxic hydrogen sulfide concentration and reduce the free sulfide ion concentration (Gerardi, 2003; McCartney, 1991).

In general, sulfide can be tolerated by methanogens when its concentration is below 50 – 100 mg.L⁻¹ (Van Haandel, 2012, 2007). The toxicity caused by sulfide can be reduced by adequate pH control, adding ferrous salts which will form insoluble iron sulfide (Haghighi Mood *et al.*, 2013). Recycling the digested sludge to enhance the growth of sulfide-tolerant bacteria, and dilution of the feed and scrubbing of the biogas to strip the H₂S gas and reduce aqueous concentrations (Van Haandel, 2012, 2007; Wang *et al.*, 2010).

2.7.12 Metal inhibition

Metals such as sodium (Na), potassium (K), calcium (Ca), magnesium (Mg) and other trace metals, are important to methane-producing microorganisms when available at the correct concentrations in the AD reactor (Chen *et al.*, 2008; Gerardi, 2006; Khanal, 2011b; Nayono, 2010; Schön, 2010). Salts from minerals or organic matter contain cations such as Na, K, Mg and Ca; transition metals with beneficial effects in low concentration such as Fe, Cu, Zn, Ni, Co, Mn, Cr (see Section 3.2.1, Table 3-3 and Table 3-4), and other heavy metals which are not important to the AD process such as Cd, Pb, Al and Hg, are also found frequently in digesters (Chen *et al.*, 2008; Gerardi, 2006; Schön, 2010; Van Haandel, 2012, 2007).

According to Lue-Hing (1998), Cu, Zn, and Ni are toxic to methane-producing archaea at low concentrations, but most of the transition metals such as Fe and Al are insoluble near the neutral pH and therefore are not toxic. However, research has shown that the toxicity of heavy metals can be neutralized when they react with sulfide inside the reactors to precipitate the insoluble metal sulfide of their toxic metals (Bajpai, 2017; Gerardi, 2003; Hatti-Kaul *et al.*, 2016; Khanal, 2011a; Van Haandel, 2012, 2007).

2.8 Lignocellulosic biomass as AD substrate

Lignocellulosic substrates are mainly composed of plant or crop residues and are the most abundant biomass resources on earth (Gupta & Tuohy, 2013). Lignocellulose is contained within the non-edible part of plants (Tong *et al.*, 2013), and it is made up of three biological polymers namely: cellulose, hemicellulose, and lignin (Dahlquist, 2013; Harmsen *et al.*, 2010; Nitsos *et al.*, 2013). The relative composition of these polymers in woody biomass are: cellulose (40 - 50%), hemicellulose (20 - 30%); lignin (20 - 35%); and other extractable (0 - 10%) (Barnett & Jeronimidis, 2009). The cellulose and hemicellulose components are simple polymers of sugars and therefore are readily used as a source of fermentable sugar by anaerobic microorganisms (Gupta & Tuohy, 2013).

2.8.1 Cellulose

The cellulose $(C_6H_{10}O_5)_n$ is the major structural constituent of plant cell walls that provides structural support to the plant, and the most abundant renewable organic resource on earth (Chen *et al.*, 2016). It is a highly insoluble crystalline carbohydrate polymer that is not digestible by humans (Agbor *et al.*, 2011; Harmsen *et al.*, 2010). Cellulose comprises of a chain of cellobiose made up of pure dehydrated repeating units of D-glucose units joined by β -1, 4-glycoside linkages (Agbor *et al.*, 2011; Chen *et al.*, 2016; de Souza, 2013). A single molecule of cellulose contains about 10,000 molecules of glucose units (O'Rear, 2012). Although cellulose (Figure 2-10) is an unbranched polymer which is not soluble in water, it can be hydrolyzed during anaerobic digestion to produce D-cellobiose (β -1, 4-bond) which can be completely hydrolyzed to release D-glucose (Agbor *et al.*, 2011; Dahlquist, 2013).

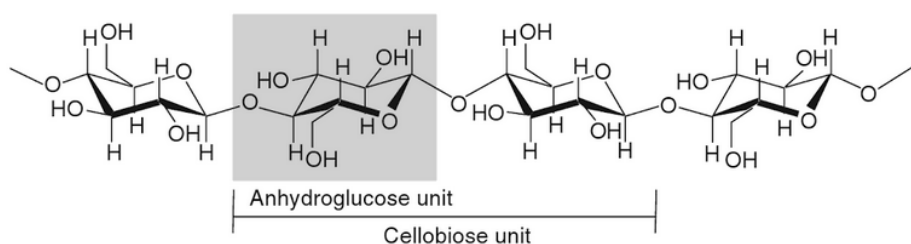


Figure 2-10 The cellulose molecule showing the monomeric unit (Kumar *et al.*, 2009)

Cellulose supramolecular structure consists of chains (20-300) of highly ordered (crystalline) and densely packed parallel fibrous-like rod structures called microfibrils which bundle together to form the cellulose fibers (Agbor *et al.*, 2011; Yang *et al.*, 2011). The structural anchor and strength of the cellulose structure are provided by the intramolecular and intermolecular H-bonds and van der Waals' forces (Barnett & Jeronimidis, 2009). Cellulose is soluble in aqueous sodium hydroxide solution at different concentrations (7 – 10 % NaOH) below room temperature, especially from -10 to 4 °C (Qi, 2016). The high solubility of cellulose in pure commercial grade NaOH solution indicates that it might also be deconstructed and solubilized by using NaOH-rich ash extracts from burned natural biomass at different concentrations and temperatures, and potentially increase its enzymatic conversion to biogas via anaerobic digestion.

2.8.2 Hemicellulose

Hemicellulose is a complex carbohydrate with a lower molecular weight than cellulose and provides support for the cell wall in the plant (Dahlquist, 2013; Hendriks & Zeeman, 2009).

It consists of 20 – 50 % of lignocellulose biomass and it is the second most abundant polymer in the biomass (Agbor *et al.*, 2011). Hemicellulose is made up of subunits of five-carbon (xylose and arabinose) and six-carbon (glucose, mannose, and galactose) sugars, and their respective sugar acids, which have a random amorphous structure with low mechanical strength. It can be represented by the formula $(C_5H_8O_4)_n$ where n is the degree of polymerization (DP), which represents the number of monomeric units in the hemicellulose macromolecule, and which usually occur in the range of 100 - 200° (Basu, 2013; Wang, 2014). It is structurally connected to the cellulose by hydrogen bonds and van der Waals forces (O'Rear, 2012), and can dissolve in dilute weak acids (Basu, 2013). The most abundant component of hemicellulose is xylan which is majorly found in agricultural plants such as grasses and straw and is reported to be partially degradable under mesophilic conditions (Dahlquist, 2013).

In softwood, the hemicellulose is present mainly as glucomannan (Agbor *et al.*, 2011), and is branched with short lateral chains which are hydrolyzable (Barnett & Jeronimidis, 2009). This implies that hemicellulose could also be easily deconstructed using highly alkaline biomass-derived ash extracts and locally available alkaline materials from Nigerian crop wastes to make biogas production process cheap, affordable and efficient.

2.8.3 Lignin

Lignin has an amorphous polyphenolic and hydrophobic structure of three-dimension phenylpropane (C₉ units); and is contained within the cell wall of vascular plant cell walls, and also possess strong resistance to oxidation and biodegradation (Agbor *et al.*, 2011; Dahlquist, 2013; de Souza, 2013; Harmsen *et al.*, 2010; Kumar *et al.*, 2009). Its resistance to biodegradation constitutes the most significant factor limiting biodegradability of lignocellulosic biomass during anaerobic digestion (Rouches *et al.*, 2017). This recalcitrant lignin tightly connects the hemicellulose and the cellulose, thereby making it difficult for hydrolytic enzymes to access the cellulose (Dahlquist, 2013).

The lignin molecules in the grass are the same as those in the wood and contain mostly aromatic glycerol-β-aryl-ether bonds like softwood (Basu, 2013; Dahlquist, 2013). The number of carbon-carbon bonds (β-5 and β-β) in structural units is higher than in hardwood. When lignin is subjected to the mechanical action, enzymes or chemical reagents, its 3-D structure is degraded into smaller fragments (Basu, 2013; Cheng *et al.*, 2016). The presence of hydroxyls and many polar groups in the lignin structure, form strong intra and intermolecular

hydrogen bonds (Basu, 2013; Brodeur *et al.*, 2011). Lignin is mostly insoluble in solvents but can be separated into soluble and insoluble lignin via degradation or condensation processes (Cheng *et al.*, 2016). The best solvent for separating lignin is acetyl bromide and hexafluoroisopropanol (HFIP) in acetic acid (Cheng *et al.*, 2016). When softened, lignin becomes sticky and has adhesive properties (Cheng *et al.*, 2016), which makes it act as a binder between macromolecules within cells, making them remarkably resistant to impact, compression and bending (Harmsen *et al.*, 2010; Yang *et al.*, 2011). In the current study, it is likely that the natural alkaline extracts from plant biomass, may have some intrinsic properties that could enhance the deconstruction of the lignin walls during pretreatment because they have high contents of alkaline metals and several trace nutrients (Table 3-2) which could potentially enhance the softening of hard tissues in plants.

2.9 Pretreatment of lignocellulosic biomass

According to de Souza (2013), microorganisms can naturally produce and secrete carbohydrate-active enzymes, that work synergistically to degrade the plant cell walls to release sugars monomers such as glucose, which can be used as a substrate for the metabolism microorganisms that produce biogas. However, the release of glucose is often resisted by the architecture of the plant's cell walls, which reduces the ability of the microorganisms to adjust their metabolism and subsequently degrade it (de Souza, 2013). This problem can be overcome by subjecting the biomass to appropriate pretreatment steps. Pretreatment of lignocellulosic biomass (Figure 2-11), increases the surface area and porosity, disrupts or removes the lignin, breaks down the hemicellulose polymers and de-crystalize the cellulose, to make the cellulose or hemicellulose more accessible to the hydrolytic enzymes that convert the carbohydrate polymers into fermentable sugars (Ayoub & Lucia, 2017; Hakeem *et al.*, 2014; Kumar *et al.*, 2009; Mosier *et al.*, 2005).

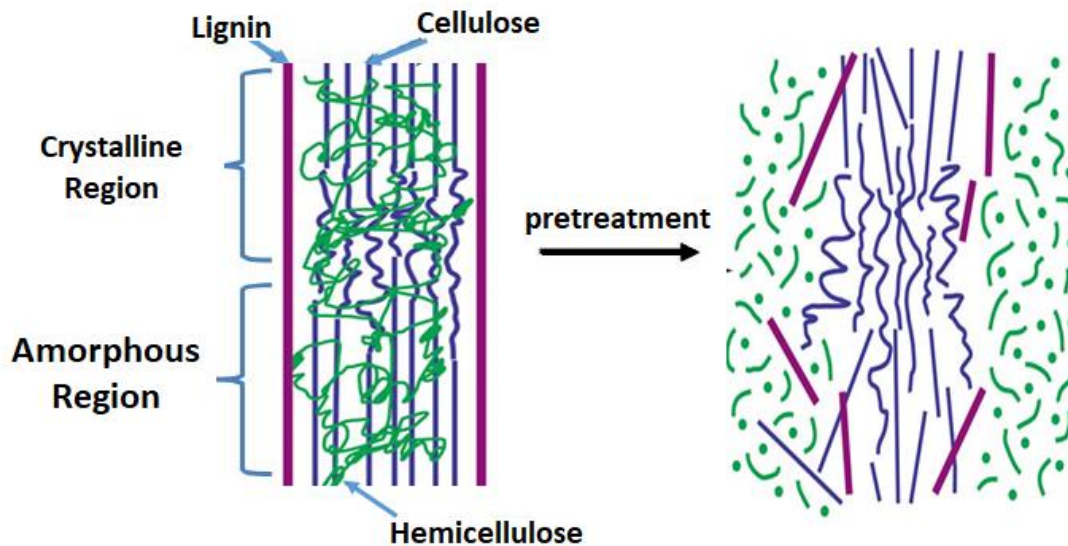


Figure 2-11 Effect of pretreatment on lignocellulosic biomass. Adapted from (Mosier *et al.*, 2005)

Pretreatment should essentially improve the release of sugars, avoid the formation of degradation by-products that would inhibit the downstream processes, and must be cost-effective (Ayoub & Lucia, 2017; Brodeur *et al.*, 2011; Kumar *et al.*, 2009; Sun & Cheng, 2002). The choice of suitable pretreatment depends on the structure of the biomass, energy potential of the biomass, end-user disposal practices and other technical, economic and environmental considerations (Gupta & Tuohy, 2013; Wong *et al.*, 2016). Thus, there is no preferred pretreatment method that is universally applicable to all kinds of biomass. There are several literature reviews on pretreatment methods for lignocellulosic materials (Brodeur *et al.*, 2011; Harmsen *et al.*, 2010; Sun & Cheng, 2002). These state that pretreatment can be physical, physicochemical, mechanical, thermal, biological, or a combination of these processes, depending on the need to improve the degradation of the biomass (Agbor *et al.*, 2011; Wong *et al.*, 2016; Yang *et al.*, 2011). A good comparison of the different type of pretreatment methods currently used for lignocellulosic biomass has been published by (Mondal & Dalai, 2017).

Physical pretreatment, especially air-drying will likely be the simplest, most affordable and most practicable kind of pretreatment of biomass that could be used by people living in tropical and developing countries because of the abundant sunlight. The use of sunlight to pretreat lignocellulose biomass can be achieved by subjecting the biomass to a UV-induced degradation (Luque & Balu, 2013), during which the lignin strongly absorbs UV energy to its double bond, and undergo surface degradation (Jawaid *et al.*, 2017). Chemical pretreatment which is often done using acids and alkali reagents is not only expensive but requires

recovering of the pretreated biomass by neutralization and filtration before further processing (Clark & Deswarte, 2014). Similarly, cost of enzymatic pretreatment accounts for about 25% biogas total processing expenses (Lupoi *et al.*, 2016). However, in many developing countries of the world, including Nigeria, there are many bio-resources that are acidic and alkaline in nature, which have not been investigated as possible low-cost substitutes for the pretreatment of biomass, and these resources when exploited, may improve the solubilization of biomass to a degree that is comparable to chemical pretreatment processes.

2.10 Mono-digestion and co-digestion of lignocellulosic biomass

Research has shown that grass is an excellent energy crop, and that depending on its biogas potential, it could be classified as either as a high yielding, or a low energy input perennial crop (Nizami & Murphy, 2010). Despite a large amount of research on the AD, investigations on the mono-fermentation of grass silage are uncommon (Koch *et al.*, 2010). However, a recent study by Zealand *et al.* (2017) has shown that it was feasible to mono-digest rice straw in an AD digester to produce biogas, which could be used by CHP technology to provide renewable energy. According to Beline *et al.* (2017), livestock manures can as well be used as AD feedstock because they are rich in nitrogen which could provide a buffer to manage the digestion process and important trace nutrients, that can enhance the biological process. Animal manure often contains lignocellulosic components, however, using livestock manure as mono-substrates in the AD is difficult because of their low energy yield compared to their volumes (Beline *et al.*, 2017). Thus, combining waste materials, especially food processing wastes, wastes from slaughterhouses, etc., with other substrates, especially agro-industrial wastes, can improve biogas production without major cost implications (Beline *et al.*, 2017). Co-digestion essentially improves the nutrient balance of the feedstock and the C:N ratio which is necessary to make the digestion process more stable. According to several studies, balanced C:N ratio required to improve the stability and efficiency of an AD process ranges between 20 – 30: 1 (Demirbas, 2008; Korres, 2013; Lee *et al.*, 2016; Soni, 2007). A balanced C:N ratio shows that the nitrogen in the feedstock will be sufficient for the degradation of carbon and such would enhance the rate of biogas produced (Demirbas, 2008; Lee *et al.*, 2016). Therefore, it can be concluded that co-digestion of wastes improves the efficiency of the AD reactor and economic feasibility of the biogas production process.

2.11 Optimisation of the AD process using conventional supplements

Some of the inorganic and organic additives commonly used as supplements to improve AD performance include: (i) micro or trace nutrients (Ni, Mo, Co, Se, Fe and W), (ii) macronutrients (P, N and S), and (iii) ashes from incinerators (Romero-Güiza *et al.*, 2017). Choong *et al.* (2016) also stated that trace elements such as iron (Fe), nickel (Ni) and cobalt (Co) are the most studied and desirable, and their correct combination as supplements, especially for the mono-digestion of micronutrient-deficient substrates, can have positive impacts. These impacts include improved digester stability with greater organic matter degradation, low VFA concentrations, and higher biogas production.

Research has also identified that when enzymes are dosed directly into AD reactors, they degrade the substrate faster than microbes because of their high solubility and mobility (Romero-Güiza *et al.*, 2016). A recent study by Romero-Güiza *et al.* (2017) also showed that biological additives such as microbial inocula, which was rich in hydrolytic or methanogenic microorganisms (bioaugmentation), and enzymes, increased the efficiency of the AD process. Direct addition of enzymes and microorganisms such as *Clostridium cellulolyticum* has also been reported to improve the hydrolytic stage of the AD by increasing the degradation of lignocellulose (Hatti-Kaul *et al.*, 2016).

Although the addition of chemical and biological materials into AD reactors can enhance the process stability and biogas yield, due to improved microbial growth, a recent study has shown that N and P additions did not enhance specific CH₄ yields from rice straw (Zealand *et al.*, 2017). In some research, biochar, magnetite, granulated activated carbon, graphite, and carbon cloth have been added to methanogenic AD reactors to improve the degradation of organic acids, leading to an increase in methane production (Hatti-Kaul *et al.*, 2016).

2.12 Optimisation of the AD process using biomass-derived low-cost supplements

The importance of trace nutrients supplementation during the operation of AD reactors, and the limitations to its use in low-income countries have been discussed in Section 1.7. However, these essential AD supplements which are commercially available but expensive, are naturally and freely absorbed by green plants from a pool of ions in the soil through their roots by diffusion, mass flow or root interception (Kabata-Pendias & Mukherjee, 2007; Saha *et al.*, 2017). Plants absorb trace nutrients at varying concentrations depending on the nutrient supply rate from the soil, the length of the plant's root and the root activity (Zhang, 2017).

These trace nutrients enhance the plant's growth, productivity and the quality of fruits it produces (Chojnacka & Saeid, 2018; Naeem *et al.*, 2017; Srivastava, 2012). In plants, these absorbed trace elements such as Cu, Fe, Mn and Zn help to activate enzymes or can be incorporated into the metalloenzymes of electron transfer systems; while Al, Cu, Co, Mo, Mn, and Zn are believed to be responsible for the protection of drought-resistant varieties of plants (Kabata-Pendias, 2000). The concentration of trace nutrients absorbed by plants varies with different species (Sharma, 2018); and plants that can accumulate over 0.1% of Pb, Co, Cr, Cr and more than 1% of Mn, Ni, and Zn in their shoots are referred to as hyperaccumulators (Han, 2007). Once absorbed, Mn, Zn, B, Mo, Se, and Cd are readily translocated to the plant tops, while heavy metals are mostly stored in the root regions (Alloway, 1995). Through the incineration of woody plant, woody biomass ash is produced. Wood-ash produced thermally from chemically untreated woody biomass such as straw, cereals, hay, woodchips, bark, sawdust and other agricultural residues is non-hazardous (Röser *et al.*, 2008; Van Loo & Koppejan, 2012). According to Abdel-Jawad (2001), ash from the combustion of biomass contains much of the inorganic minerals contained in the original biomass. Thus, ash from agricultural residues contains minerals including trace elements which can be extracted to potentially serve as a supplement for the optimization of the AD process, especially in developing countries around the world. This concept will be presented in further details in this thesis to contribute to the growing research on AD process, as the current study will offer some important insights into low-cost AD process optimization for sustainable bioenergy production especially in low-income and developing countries.

Chapter 3 Materials and Methods

3.1 Biomass Feedstocks

The grass silages (gamba grass, guinea grass, elephant grass, spear grass), agricultural wastes (rice straw, cassava process wastes, empty palm bunch, empty cocoa pod) and local potash, were field collected in Nigeria during the dry season. These biomass feedstocks were air-dried locally for 14 days by spreading them on clean concrete pavements where they dried under direct sunlight to a moisture content below 10%, as specified in the US National Renewable Energy Laboratory Analytical Procedure (LAP) (Sluiter *et al.*, 2008). After drying the biomass feedstocks, each species was cut into smaller pieces (about 2 cm) using scissors, and then packed in air-tight polythene bags in which they were transported to Newcastle University for this study. Some of the physiochemical characteristics of the biomass feedstocks are presented in Table 3-1.

Table 3-1 Main characteristics of the biomass feedstocks

Parameters	Rice	Elephant	Gamba	Guinea	R. T.C	Speargrass	Cassava	Cassava
	straw	grass	grass	grass	grass		starch	peels
	Values							
MC (%)	7%	9%	9%	6%	7%	7%	12%	6%
VS (%)	82%	87%	81%	89%	79%	94%	90%	84%
TS (%)	93%	91%	91%	94%	93%	93%	88%	94%
C/N ratio	48:1	24.2:1	36:1	36.4:1	25:1	63.9:1	223:1	65:1
Lipids	1.9%	0.6%	0.5%	1.3%	2.4%	0.9%	ND	ND

R. T. C – A mixture comprising of perennial ryegrass, Timothy and clover grasses

ND - Not determined,

MC – Moisture content (%)

TS- Total solids (expressed as % dry mass)

VS – Volatile solids (expressed as %TS)







Similarly, a mixture of co-cropped grasses consisting of perennial ryegrass, clover and timothy grass was collected from a grass silage storage depot at Cockle park farm located in

Newcastle upon Tyne, where it is harvested, ensiled and used as a co-digestion feedstock for the commercial AD plant situated on the farm. Every biomass feedstock used for the current study was ground to a powder using a food blender and then sieved to pass a 1 mm sieve. Representative samples were taken and characterized for total solids (TS), volatile solids (VS), chemical oxygen demand, and then carbon, nitrogen, hydrogen, phosphorus and oxygen contents according to standard analytical procedures as listed in Table 3-8.

3.2 Preparation of low-cost AD supplements

The low-cost supplements which were used as alternative sources of trace nutrients and reactor buffering reagents were all prepared using the selected agricultural wastes presented in Table 3-2.

Table 3-2 Selected agricultural wastes used to produce low-cost AD supplements

S/N	Name of biomass (waste)	Photo	Crystals from biomass
1	Empty palm fruits bunch EPB		
2.	Empty cocoa pod (ECP)		
3	Plantain peels (PP)		

Procedure:

Ash from empty palm fruit bunches (EPB) was collected from a heap of burnt empty palm bunches in a commercial palm plantation located in Umuahia Nigeria. The empty cocoa pod (ECP) and plantain peels (PP) in Table 3-2 were also collected from individual cash crop plantations located in Afikpo-North, Nigeria. Some quantities of dried empty palm fruit bunch, dried cocoa pod and plantain peels shown in Table 3-2, were also collected and brought to Newcastle University for ashing, extraction and characterization. Each type of ash-extract was prepared by dissolving 500 g of the ash in 1 L of distilled water. The mixture produced was filtered using a vacuum filtration apparatus fitted with Whatman™ Grade 1 Qualitative Filter Circles of 90mm diameter. Soluble extracts (filtrate) from each of the biomass was then dried at 105 °C for a period of 3 - 5 days to produce alkaline salts (crystals). The salt produced by the biomass feedstocks are presented in Table 3-2. From each of these dried extracts (crystals), 1 g of each salt was weighed and re-dissolved in 1 L of distilled water, and from this solution, a sample of each salt solution was taken for analysis to determine its elemental composition as described in Section 3.2.1. Some of the crystals were sent to the XRD laboratory in the chemistry department at Newcastle University where they were analyzed to determine the abundance of each type of chemical compounds present in the biomass-derived salts using X-ray diffraction (XRD) (

Figure 3-1 - Figure 3-3).

3.2.1 Elemental composition of selected biomass feedstocks

This was carried out by the wet ash procedure described by Nielsen (2017), which involved the digestion of the 1 g dried and powdered sample of the biomass in a 100 mL conical flask which was placed in a fume cupboard. About 10 mL of concentrated H₂SO₄ and 10 mL of concentrated HNO₃ acids (from Sigma-Aldrich, UK) were added to the biomass. This mixture of acids and biomass was placed on a hot plate and heated at 120 °C for about 15 minutes, during which effervescence occurred accompanied by the release of reddish-brown coloured nitrogen (IV) oxide (NO₂) gas. The addition of the acids continued as the digestion progressed, until all the biomass was completely digested, which was evidenced by the formation of a light yellowish solution and then no further release of NO₂ gas. The digestate was then transferred to a 100 mL standard volumetric flask and was made up to 100 mL using distilled water. A sample from this solution was then sent to an analytical laboratory located in the Devonshire building in Newcastle University for the determination of its elemental

composition using a Varian Vista MPX axial ICP-OES with CCD detector in accordance with the analytical procedure described in the Standard Methods for the Examination of Water and Waste Water 20th Edition (APHA 3120 C). The elemental analysis of each sample of the biomass feedstocks and supplements was carried out in triplicates. The mean composition of the metals from each sample are presented in Table 3-3 and Table 3-4.

Table 3-3 Elemental analysis of some selected biomass feedstocks for their metal composition

Metals (mg/g)	Concentration (mg.g ⁻¹)				
	Elephant	Gamba	Rice Straw	Speargrass	Guinea
Al	21.6	3.83	1.21	4.58	2.65
Ca	66.3	42.5	43.5	41.1	59.2
Co	0.37	<0.01	0.11	0.07	0.03
Cu	0.91	0.24	0.24	0.26	0.19
Fe	237	4.37	51.9	35.2	21.1
K	193	83.1	112	98.4	129
Mg	31.6	26.7	4.40	8.50	23.8
Mn	5.20	3.88	4.18	1.12	2.08
Na	4.2	6.4	2.4	2.4	4.3
Ni	35.1	0.08	8.29	5.12	2.69
P	39.4	26.0	13.8	8.3	12.8
Pb	<0.05	<0.05	<0.05	<0.05	<0.05
S	14.2	24.8	7.2	12.6	16.9
Se	<0.1	<0.1	<0.1	<0.1	<0.1
Zn	0.54	0.49	0.35	0.22	0.69

Note: Each test on the biomass was carried out in triplicate

Table 3-4 Elemental analysis of biomass ash-extracts used as supplements for the AD process optimization

Sample	Concentration (mg. g ⁻¹)													
	Al	Ca	Co	Cu	Fe	K	Mg	Mn	Na	Ni	P	S	Se	Zn
EPB	0.4	0.5	<0.01	0.02	0.06	3746	1.2	0.03	22	0.07	187	107	<0.1	0.04
PP	0.1	0.5	<0.01	<0.01	<0.01	4302	0.2	<0.01	17.5	0.03	109	50.4	<0.1	<0.01
ECP	0.2	2.7	<0.01	<0.01	<0.01	4059	1.3	<0.01	12.8	0.02	6.1	124	<0.1	<0.01

EPB – Empty palm bunch ash extract;
 PP – Plantain peels ash extracts and
 ECP – Empty cocoa pods ash extracts

3.2.2 Determination of the abundance of the major chemical compounds in some selected crystals from biomass ash-extract

The salts samples produced from the biomass ash described in Section 3.2, were sent to the XRD laboratory located at the Chemistry department in Newcastle University. The results obtained from the analysis are as shown in

Figure 3-1 – Figure 3-3.

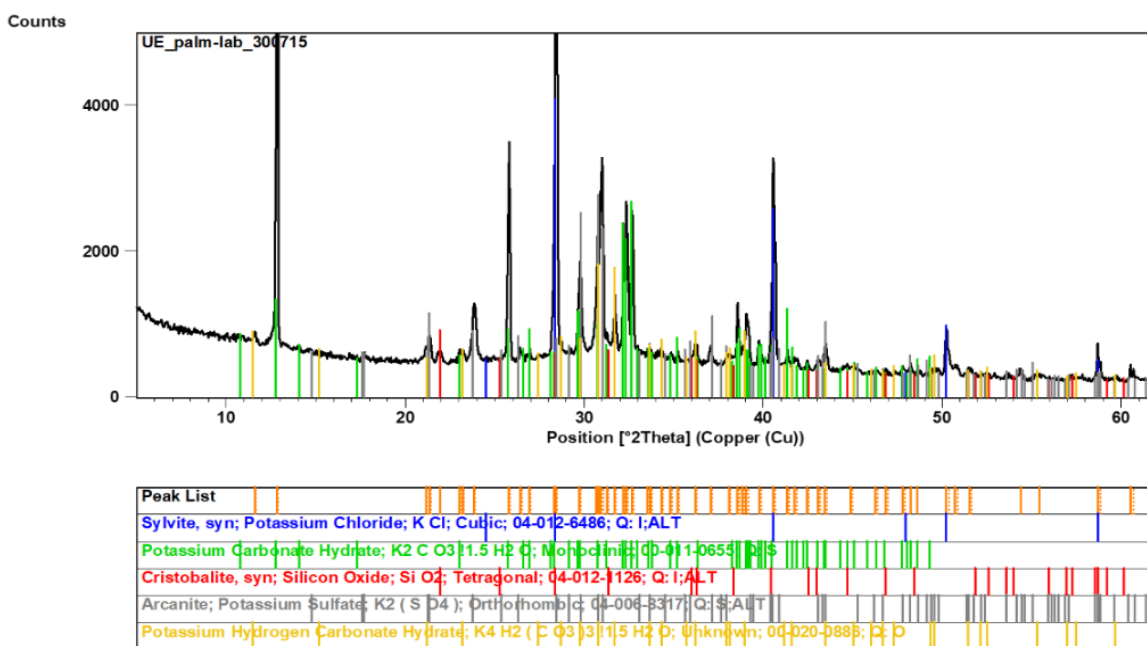


Figure 3-1 XRD analysis showing high peaks of potassium bicarbonate and potassium carbonate contents and other trace nutrients within the crystals from palm bunch ash-extract

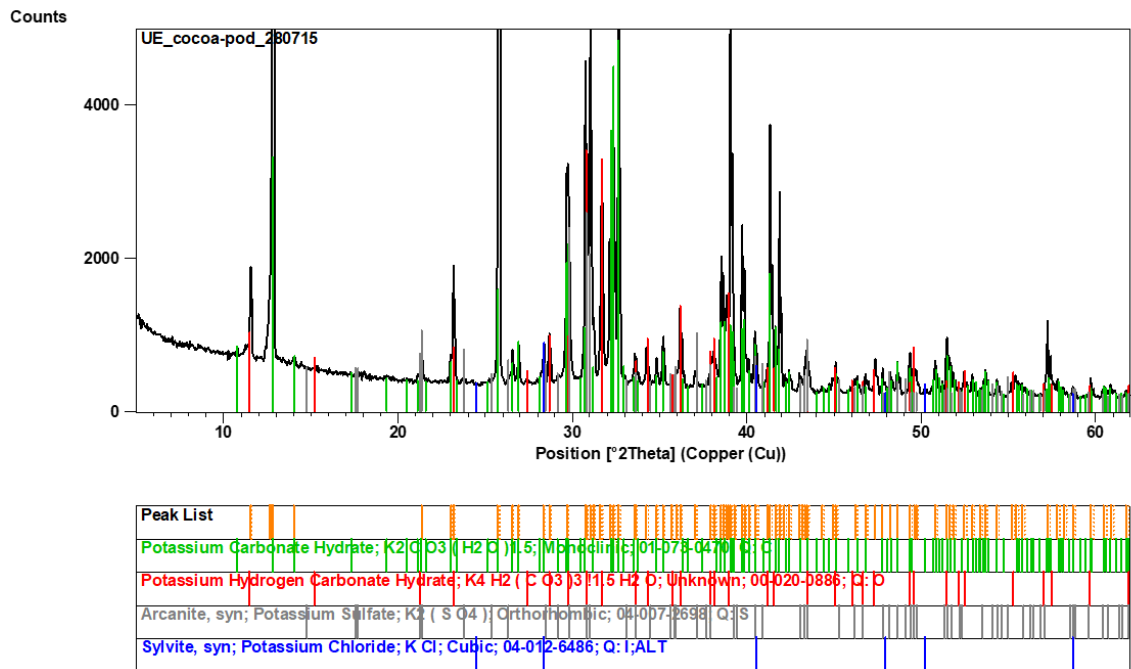


Figure 3-2 XRD analysis showing high peaks of potassium bicarbonate and potassium carbonate contents and other trace nutrients within crystals from empty cocoa pod ash-extract

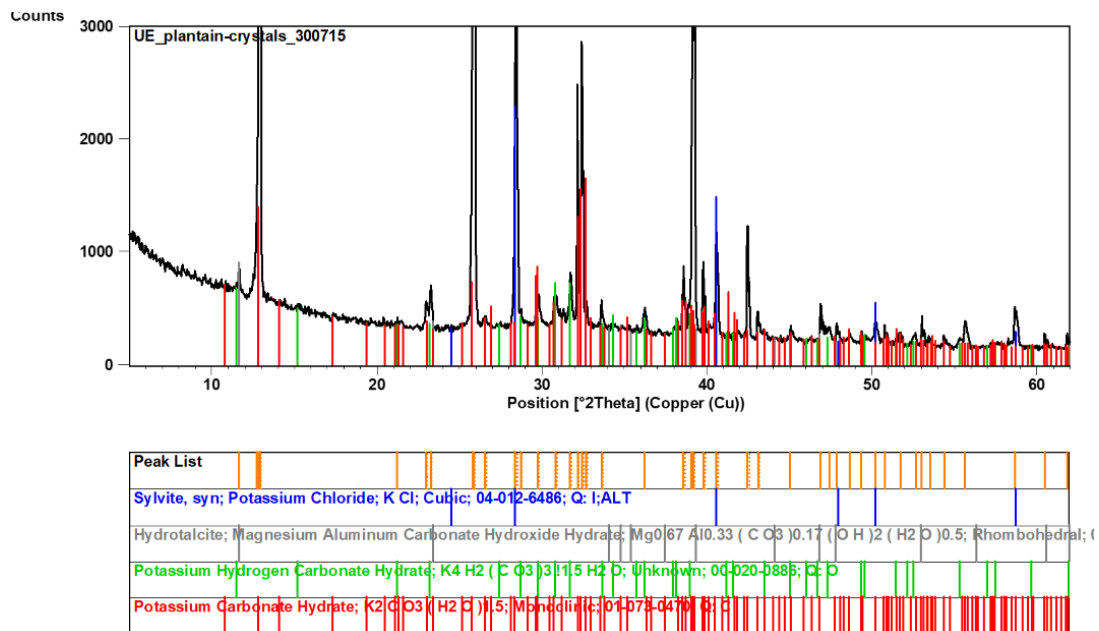
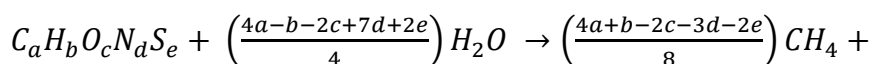


Figure 3-3 XRD analysis showing high peaks of potassium bicarbonate and potassium carbonate content and other trace nutrients within the crystals from plantain peels ash-extract

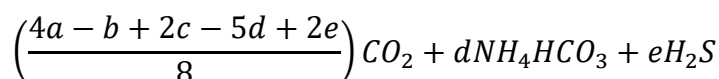
3.2.3 Analysis of carbon, nitrogen, oxygen, nitrogen and sulfur contents of selected biomass feedstocks

The carbon, nitrogen, and sulfur contents from 1 gram of the powdered biomass from each biomass feedstock was measured to an accuracy of $\pm 1\%$ using an Elementar VarioMAX CNS analyzer at the Drummond building GC/MS laboratory in Newcastle University. The analysis involved combustion of the biomass feedstock at 1145°C in an oxygen atmosphere. However, the oxygen contents of each biomass were measured by the Elemental Microanalysis Laboratory, UK using Thermo elemental analyzer model NA2000, configured for oxygen analysis. The hydrogen content was determined using Carlo Erba EA1108 Elemental Analyser using the dynamic flash combustion gas chromatography technique (Pella & Colombo, 1973). The data obtained from the above analysis were then used to generate the stoichiometric formula of each biomass and the theoretical biochemical methane potentials (TMP) presented in

Table 3-5 by using the Buswell Equation 3-1.



Equation 3-1



where the $TMP = \left(\frac{4a+b-2c-3d-2e}{8}\right)CH_4$ is expressed in $\text{mL CH}_4\cdot\text{g}^{-1}\text{VS}$ added

Table 3-5 Stoichiometric formula and TMP of various biomass feedstocks used for this study

S/N	Biomass	Stoichiometric formula	TMP, L CH ₄ .Kg ⁻¹ . VS
1	Perennial Ryegrass. Clover and Timothy grass	$C_{396}H_{666}O_{237}N_{24}S + 154H_2O$ $\rightarrow 213CH_4 + 159CO_2 + 24NH_4HCO_3 + H_2S$	498
2	Gamba grass	$C_{619}H_{1135}O_{396}N_{29}S + 188H_2O$ $\rightarrow 341CH_4 + 249CO_2 + 29NH_4HCO_3 + H_2S$	500
3	Elephant grass	$C_{659}H_{1299}O_{439}N_{38}S + 181H_2O$ $\rightarrow 368CH_4 + 253CO_2 + 38NH_4HCO_3 + H_2S$	491
4	Rice straw	$C_{813}H_{1504}O_{560}N_{48}S + 242H_2O$ $\rightarrow 436CH_4 + 329CO_2 + 48NH_4HCO_3 + H_2S$	467
5	Guinea grass	$C_{570}H_{1143}O_{376}N_{21}S + 134H_2O$ $\rightarrow 326CH_4 + 223CO_2 + 21NH_4HCO_3 + H_2S$	510
6	Cassava waste	$C_{1578.8}H_{2967.1}O_{1403.7}N + 135.2H_2O$ $\rightarrow 809.4 CH_4 + 769.4.4CO_2 + NH_4HCO_3$	409

The results were validated using the online biogas app (OBA) available online at: <https://biotransformers.shinyapps.io/oba1/> (Accessed 16/09/2018)

3.2.4 Estimation of cellulose, hemicellulose and lignin contents in biomass feedstocks

Several lignocellulosic biomass feedstocks were used in the current study. However, the determination of their lignocellulosic composition, such as their cellulose, hemicellulose and lignin contents were only carried out using the Elephant grass, Gamba grass and Guinea grass. The experiment was performed in accordance with the protocol developed by Van Soest (1963), and following the analytical procedures described by Goel (2007) & Sharma (2008).

All the reagents used for this analysis were of analytical grade and were purchased from Sigma/Aldrich, UK

3.2.4.1 Estimation of cellulose

The cellulose contents of the biomass feedstocks were determined using the following reagents:

1. Acetic nitric reagent (150 ml of 80% acetic acid + 15 ml of concentrated HNO₃)
2. Anthrone reagent (0.2% anthrone in concentrated 67% H₂SO₄ which was prepared fresh before use)

Procedure:

About 1 g of powdered biomass from the air-dried sample (< 1mm) was added to a boiling tube, followed by 3 ml of acetic nitric reagent, and then mixed using vortex mixer. The mixture formed was boiled in a water bath for 10 minutes, then cooled and centrifuged for 20 minutes to extract the supernatant which was then discarded. The residue left was then washed with D.I water, centrifuged, and the supernatant discarded. Furthermore, 10 ml of 67% H₂SO₄ was added to the residue and this produced a mixture which was left to stand for 1 hour to form a solution. From this solution, 1 ml volume was taken using a pipette into a 100 mL volumetric flask and was diluted to 100 mL using D.I water. From this dilute solution, 1 ml was pipetted into a test tube, followed by the addition of 10 ml of anthrone reagent in order to determine the cellulose content (x) in the biomass. In order to accurately estimate this cellulose content, a cellulose standard containing 100 mg of crystalline cellulose was also measured and prepared the same way as described for the sample, and then dilute to the concentrations shown in Table 3-6. The contents of the test tubes were subsequently boiled in water bath for 10 minutes and cooled. The absorbance of each tube was measured at 630 nm wavelength.

Table 3-6 Procedure for the determination of the cellulose contents in biomass feedstock

Reagents (ml)	Blank	1	2	3	4	5	6	7	8	9	10	x
Standard cellulose	-	0.1	0.2	0.3	0.4	0.5	0.6	0.7	0.8	0.9	1.0	1.0
Distilled water	1.0	0.9	0.8	0.7	0.6	0.5	0.4	0.3	0.2	0.1	-	-
Anthrone reagent	10.0	10.0	10.0	10.0	10.0	10.0	10.0	10.0	10.0	10.0	10.0	10.0

A standard curve was then prepared and was used to calculate the amount of cellulose present in the sample by using the equation of the line of best fit (Equation 3-2)

$$y = mx + c. \quad \text{Equation 3-2}$$

where x is the cellulose content (%), c is a constant, and y is the absorbance measured by the spectrophotometer for each sample dilution.

3.2.4.2 Estimation of neutral detergent fibre (NDF) or plant cell-wall contents

The NDF contents of the biomass feedstock were determined the modified Van Soest and Wine (1967) procedure as contained in Faithfull (2002). The chemical reagents used include:

1. Neutral detergent solution: Prepared by dissolving 30 g of sodium dodecyl sulfate, 18.61 g of sodium borate decahydrate, 6.81 g of sodium borate decahydrate, and 4.56 g of anhydrous disodium hydrogen phosphate in 1 litre of distilled water and stirred to dissolve the mixture. Weighing was carried out with an extraction fan on, and while wearing dust masks because sodium dodecyl sulfate dust irritates the lungs. The pH of the mixture was adjusted to 6.9 – 7.1 using 1 N NaOH solution. About 10 mL of triethylene glycol was then added to the solution to prevent foaming.
2. Acetone

Procedure.

About 0.5 g of powdered biomass from the air-dried sample (< 1 mm) was weighed and transferred to a 500-ml round-bottom flask (socket size 34/35). After that, 100 mL of neutral

detergent solution was measured and added to the biomass in the flask at room temperature. This mixture, containing the biomass and the neutral detergent solution was then transferred to the Kjeldahl heating unit. On the Kjeldahl heating unit, a coil condenser ground glass cone with size 34/35 was connected to the round-bottomed flask. Subsequently, a steady supply of water was turned on while the mixture was heated to boil. At boiling point, the heating regulator was turned down and the heated mixture was allowed to simmer for 60 minutes. This period, the flask was occasionally swirled and squirted with a little amount of D.I water to wash back samples from the flask walls and condenser respectively, into the detergent. The mixture in the flask was then transferred to No. 1 sintered glass crucible (previously dried at 500 °C for 30 minutes and cooled in a desiccator). After cooling, the mixture in the flask was filtered by applying gentle suction using a vacuum pump. After the first suction, the mat of sample fibre in the crucible was then broken into small pieces using a glass rod, and then washed twice, by filling the crucible with very hot water (80 – 90 °C) and repeating the filtration step. The washing and drying were also repeated twice using acetone, and then allowed to dry in a fume cupboard to remove the acetone. The acetone-free solid obtained was dried overnight at 100 °C oven, then cooled in a desiccator and weighed. The crucible with its NDF content was afterward placed in a cool muffle furnace, and its temperature increased to 500 °C for 3 hours to ash the sample. This ashed sample was finally removed from the furnace, cooled in a desiccator and weighed to determine the % of NDF in the sample, and the % of ash in the NDF as follows:

$$\begin{aligned} \text{Neutral detergent fibre (\%)} & \qquad \qquad \qquad \text{Equation 3.1} \\ &= \frac{\text{Weight of fibre}}{\text{Weight of original sample}} \times 100 \end{aligned}$$

$$\begin{aligned} \text{Neutral detergent fibre (\%)} & \qquad \qquad \qquad \text{Equation 3.2} \\ &= \frac{\text{Weight of fibre}}{\text{Weight of original sample}} \times 100 \end{aligned}$$

3.2.4.3 Estimation of hemicellulose using the Neutral Detergent Fibre Method (NDF)

The total hemicellulose contents of the biomass feedstocks were determined using the following reagents:

1. Neutral detergent solution: Prepared by dissolving 18.61 g disodium ethylenediaminetetraacetate, and 6.81 g of sodium borate decahydrate, in 200 ml of distilled water. The mixture formed was then heated and stirred to dissolve all the solids. About 200 ml of distilled water was added to 4.36 g of anhydrous disodium hydrogen phosphate which was placed in a separate beaker, and then heated to dissolve the salt. Both solutions were then mixed thoroughly, and the pH adjusted to range between 6.9 and 7.1. The volume of the mixture was then raised to one litre using distilled water.
2. Acetone
3. Anhydrous sodium sulfite
4. Decahydronaphthalene (reagent grade)

Procedure:

About 1 g of powdered biomass from the air-dried sample (< 1 mm) was weighed into a beaker of a refluxing apparatus. This was followed by the addition of 10 mL of cold neutral detergent solution, 2 mL of decahydronaphthalene, and 0.5 g sodium sulfite solution. The mixture produced was then heated for 5 – 10 minutes. Heating was reduced when the mixture started to boil, and that was done in order to avoid foaming. The contents in the beaker were refluxed for 60 minutes at boiling temperature, and then filtered through sintered glass (G-2), followed by washing with hot water. The residues in the sintered glass were further washed twice with acetone before being transferred to a weighed crucible and dried at 100 °C for 12 hours. The crucible, together with its contents was then cooled in a desiccator and weighed to estimate the weight of its content.

Hemicellulose = Neutral detergent fibre (NDF) – Acid detergent fibre (ADF)

3.2.4.4 Estimation of Acid Detergent Fibre (ADF)

The acid detergent fibre (ADF) contents of the biomass feedstocks, were determined using the following reagents:

1. Acid detergent solution: Prepared by dissolving 20 g of Cetyl trimethyl ammonium bromide (CTAB) in 1 litre of 1N sulphuric acid.
2. H₂SO₄ (72% w/v)

3. Acetone
4. Sintered funnel (G-2)
5. Round bottomed flask with refluxing apparatus
6. Muffle furnace

Procedure:

About 1 g of powdered biomass from the air-dried sample (< 1 mm) was weighed into the beaker of the refluxing apparatus, followed by the addition of 100 mL of acid detergent solution. The mixture was heated for 10 minutes, and then the heating was reduced as the mixture started to boil in order to prevent foaming. Subsequently, the beaker was removed from the heater, cooled, and then its contents were filtered through a sintered funnel (G-2) on a filter manifold by suction. The contents were again rinsed twice into the crucible with hot water, and then filtered. Furthermore, the washing of the contents of the crucible was carried out two more times with acetone, using the same procedure, until the filtrate became colourless. The crucible and its contents were then dried in a hot air oven at 100 °C (overnight). After the drying, it was cooled in a desiccator and weighed. The percentage (%) acid detergent fibre was then calculated as shown in Equation 3-3.

$$\text{Acid detergent fibre (\%)} = \frac{\text{Weight of the fibre}}{\text{Weight of the sample}} \times 100 \quad \text{Equation 3-3}$$

3.2.4.5 Estimation of Acid Detergent Lignin (ADL)

The acid detergent lignin (ADL) contents of the biomass feedstocks, were determined using the following reagents:

1. 72% (w/v) H₂SO₄: Prepared by dissolving 583 mL of pure concentrated sulphuric acid in 417 mL of distilled water in a volumetric flask, with occasional stirring. The process was very hot and was cooled in a water bath.

Procedure:

The acid detergent lignin was determined by transferring the ADF to the sintered crucible, followed by addition of 50 ml of 72% H₂SO₄ (15 °C) and stirring the mixture with a stirring rod to smooth the paste and break the lumps. With the glass rod still left inside the volumetric flask to break the lumps, the flask was refilled with sulphuric acid and stirred

hourly as the acid drained away. The addition of acid was repeated twice, with the crucible temperature kept at 20 – 23 °C for 3 h, and then the mixture was filtered to remove the acid. This was followed by washing the content with hot water until all the acids were washed out. The crucible was then dried in a hot air oven at 100 °C overnight and weighed. Afterward, the residue was placed in a muffle furnace at 550 °C for 3 h, cooled and weighed to estimate the ADL as shown in Equation 3-4.

Acid detergent lignin (ADL) %

$$= \frac{\text{Weight of crucible + lignin} - (\text{Weight of crucible})}{\text{Weight of sample}} \times 100 \quad \text{Equation 3-4}$$

The results obtained from the experiment described in Section 3.2.4.1, 3.2.4.2, 3.2.4.4, and 3.2.4.5 are presented in Table 3-7.

Table 3-7 Results from the determination of cellulose, hemicellulose and lignin contents in Elephant grass, Guinea grass and Gamba grass

Lignocellulosic Biomass	DM (g)	MC (%)	ODM (%)	Ash (%)	NDF (%)	ADF (%)	ADL (%)	Hemi-cellulose (%)	Cellulose (%)
Elephant grass	0.95	5%	86%	19%	67%	46%	7%	21%	40%
Guinea grass	0.96	4%	93%	10%	73%	54%	10%	19%	44%
Gamba grass	0.95	5%	96%	9%	70%	53%	10%	17%	43%
NDF	= Hemicellulose + Cellulose + Lignin + Minerals								
ADF	= Cellulose + Lignin + Minerals								
Cellulose	= ADF – Residue after extraction with 72% H ₂ SO ₄								
Lignin	= Residue after extraction with 72% H ₂ SO ₄ – Ash								

3.3 Seed sludge (reactor Inoculum)

The fresh inoculum for AD reactors was collected from an active mesophilic anaerobic digestion plant used to co-digest cattle slurry and ryegrass at Cockle park farm in Newcastle upon Tyne. It was sieved using a 5 mm sieve to remove solid particles to make it homogeneous. Degassing was carried out by incubating the inoculum at 37 °C, which was the operational temperature of the AD plant from which it was collected. The degassing

process was protracted for about 10 – 14 days until daily methane production was less than 1% of the cumulative methane production was observed). After the degassing, the inoculum was mixed with the substrates at various ratios and the biomethane production was determined in accordance with the procedure published in (VDI. 4630, 2006).

3.4 Experimental Procedures

3.4.1 Batch Reactors – Biomethane Potential (BMP) Assay

All the BMP assays were performed in 500 ml reactor vessels and were carried out in triplicates for each condition tested, including blanks and controls. After filling the reactors, they were flushed with N₂/CO₂ (80/20% as volume) for about 10 seconds to drive off ammonia and oxygen, and that kept the pH at neutrality and maintained anaerobic conditions inside the reactor vessels. Every flushed reactor vessel was immediately closed with a rubber stopper (Figure 3-4). Different masses of biomass feedstocks were used in the BMP tests to ensure that the BMP was not underestimated due to potential inhibition from substrate overloading, with inoculum to feedstock ratios ranging from 6:1 – 2:1.



Figure 3-4 Batch Experimental Setup used for the determination of the BMP of substrates

A blank assay containing only inoculum and water was used to determine the background methane production from the inoculum, which was subtracted from the methane production obtained in the sample assays. Control assays using cellulose and acetate as substrates were also set up to confirm the viability of the inoculum. Mixing was carried out at least once a day

by swirling the reactor bottles for about 15 seconds. This helped to facilitate the contact between the bacteria and substrate, to prevent accumulation of substrates and intermediate products in the medium by providing homogenous conditions inside the reactors. The daily volumes of biogas produced were collected using the 1-litre Supel™-Inert Multi-Layer Foil Gas Sampling Bag with Thermogreen® LB-2 Septa equipped with Screw Cap Valve (SCV) purchased from Sigma-Aldrich UK. Each reactor was connected to its own gas sampling bags via a 6 mm PVC tube fitted with a clip and attached to a metal tube passing through the rubber bung that was used to as stopper for each reactor bottle.

The biogas volumes produced by each reactor bottle were measured daily for periods ranging from 28 to 40 days, and their methane content determined using a Carlo Erba HRGC 5160 gas chromatograph equipped a flame ionization detector, an electron capture (ECD) detector, and an on-column MFC injector with a split/splitless controller. The GC was operated at oven temperature set at 150 °C and utilized helium gas as the carrier gas. The injection of the biogas from the reactors into the GC was carried out following the procedure described in Section 3.4.2.

3.4.2 GC method for Methane Analysis

Methane analysis was conducted by injecting about 50µL, 40µ, 30µ, 20µ, and 10µ L volumes of a known standard calibration CH₄ gas into the GC using a 100 µL SGE Gas Tight Syringe with Luer Lock which was purchased from Sigma-Aldrich, UK. The methane peaks were captured by an Atlas software (Fisher Scientific), and these were then plotted against the % CH₄ content in each µL of standard injected in Microsoft Excel. The straight-line graph from this plot produced the equation of a straight line: $A = mx + c$; where A represents the areas occupied the standard gas, while m and c are constants. This equation was then used to determine the concentration of methane in the biogas by substituting the area (A) in the equation with the area of the peak produced in the GC by the biogas from the reactors. The percentage of methane was then established by finding the values of x from the equation above. This percentage of methane was then multiplied by the total volume of biogas to determine the actual volume of methane gas produced. In order to achieve this, the normal volume of the gas was calculated using Equation 3-5 which included headspace correction and water vapour content to obtain the volume of CH₄ in the dry state at STP as described in VDI. 4630 (2006).

$$V_0^{tr} = V \cdot \frac{(p - p_w) \cdot T_0}{P_o \cdot T} \quad \text{Equation 3-5}$$

where

V_0^{tr} volume of the dry gas in the normal state in Nm

V volume of the gas in the gas bag in mL

p pressure of the gas phase at the time of reading in hPa

p_w Vapour pressure of the water corresponding to the ambient (room) temperature, in hPa

T_0 Normal temperature, $T_0 = 273$ K

P_o Normal pressure, $P_o = 1013$ hPa

T Temperature of the biogas gas which is equivalent to the ambient room temperature in K at time of measurement.

The methane content of the dry biogas volume obtained with Equation 3-5 was estimated using Equation 3-6 (VDI. 4630, 2006).

$$C_{CH_4}^{dry} = C_{CH_4}^{moist} \frac{p}{p - p_w} \quad \text{Equation 3-6}$$

where

$C_{CH_4}^{dry}$ is the methane content (%) in the dry biogas

$C_{CH_4}^{moist}$ is the methane content (%) in the moist or raw biogas produced

p is the pressure of the gas phase at the time of reading expressed in hPa

p_w is the vapour pressure of water at ambient (room) temperature, see Annex A for the vapour pressure table

The biogas contents were also subjected to headspace correction using Equation 3-7 to account for the biogas contained at the headspace of the fermentation apparatus (VDI. 4630, 2006).

$$C_{korrr}^{tr} = C_{t2}^{tr} + (C_{t2}^{tr} - C_{t1}^{tr}) \frac{V_K}{V_B} \quad \text{Equation 3-7}$$

where

C_{korrr}^{tr} is the correct concentration of the biogas in the dry gas in % by volume

C^{tr} is the measured concentration of biogas component in the dry gas in % by volume

V_K is the headspace volume, in mL

V_B is the volume of biogas produced, in mL

t time of measurement ($t_2 > t_1$)

The volumes of methane measured in the first 7 days were used to plot the experimental curve which was then used to define the hydrolysis constant for the first order hydrolysis model:

$$\frac{ds}{dt} = -k_h S \quad \text{Equation 3-8}$$

where S is the biodegradable substrate, t the time and k_h the first order hydrolysis constant.

From the experimental data, the value of the ultimate methane production and the methane produced time, t are related as shown in Equation 3-9:

$$\ln \frac{B_\infty - B}{B_\infty} = -k_h t \quad \text{Equation 3-9}$$

where: B_∞ is the cumulative CH_4 (ultimate) production at 7th day, B is the daily methane production within the reference time during which the hydrolytic constant was determined.

See Annex A for a summary of the results from the BMP tests.

3.4.3 Kinetic analysis of BMP data

This was carried out by modeling the cumulative methane volume produced using Gompertz Equation 3-12, to establish the relative biodegradability and the methane yield of each substrate and to see the difference in trends between the experimental data (Equation 3-10), and the values from a model equation using first order kinetics. The biodegradability constants, K was determined using Equation 3-11 while the Gompertz Equation 3-12 was used to determine other parameters.

$$BMP = \frac{\text{Sample } CH_4 - \text{Control } CH_4}{\text{mass of biomass feedstock (VS)}} = LCH_4 \cdot kg^{-1}VS \quad \text{Equation 3-10}$$

$$Y(t) = Y_m \cdot (1 - \exp^{-kt}) \quad \text{Equation 3-11}$$

$$M(t) = P \cdot \exp \left\{ -\exp \left[\frac{R_{max} \cdot e}{P} (\Delta - t) \right] + 1 \right\} \quad \text{Equation 3-12}$$

where Y (t) is the cumulative biomethane yield (L CH₄) at a digestion time t (days), Y_m is the maximum biomethane potential (L CH₄ · kg⁻¹ VS added · d⁻¹) of substrate added, k is the decay constant (days⁻¹) and it measures the rate of degradation. M (t) is the cumulative biomethane yield (L CH₄ · kg⁻¹ VS) at a given time t (days). P is the maximum biomethane potential (L CH₄ · kg⁻¹ VS) of the substrate from the BMP test. R_{max} is the maximum biomethane production rate (L CH₄ · kg⁻¹ VS added · d⁻¹). Δ the lag phase measure how long it takes (days) before the methane production starts to occur while R² is a measure of the fitness of the biomethane curve on the kinetic model.

3.5 Continuous stirred-tank reactors (CSTR)

The CSTR consisted of six Quickfit[®] borosilicate culture vessels each of 5 litres capacity purchased from Sigma-Aldrich, United Kingdom. These vessels were covered with Quickfit[®] flat headplate which had parallel center joints, ST/NS: 19/26, and a 10° side socket joint vacuum adapter with screw-thread (ST) connector for flexible tubing. The headplate seal was made air-tight using a white silicone sealant and a high vacuum grease purchased from VWR UK. Each reactor was also fitted with a 60 cm stainless steel stirring rod with 20 cm stirring bar passing through the center joint of the head plate with a water seal and clamped to a variable speed overhead stirrer engine, and each of the reactors was fully mixed by setting its

own overhead stirrer at the speed of 120 rpm. In the current study, different experiments were carried out with reactors working volumes ranging from 4 – 5 litres, feeding were also carried out at an OLR ranging from 1.0 to 2.0 kgVS.m⁻³.d⁻¹), and a hydraulic retention time (HRT) ranging from 20 - 25 days. Except for the experiment with perennial ryegrass where the effect of discontinuous feeding and continuous daily feeding regimes was investigated, feeding of all the reactors was done once a day at approximately 24 h intervals throughout the study. The complete setup for the continuously stirred tank reactors (CSTR) is as shown in Figure 3-5.



Figure 3-5 Continuously stirred tank reactors (CSTR) setup with tubing connected to gas sampling bag, a variable speed overhead stirrer engine with stirring rod passing through Quickfit[®] flat head plates parallel center joint, a 10° side socket joint vacuum adapter, black insulating mat, k-type thermocouple inserted into the reactor using a red coloured rubber bung, and a control box fitted with Sestos temperature controllers.

Non-adhesive wire wound Silicon heating pads (190 x 415 mm, 230V), with 1M lead purchased from Holroyd Components Ltd United Kingdom, were used to provide heating for all the reactors. These heating pads were wrapped around the reactors by means of hooks and springs attached to them. A black insulating mat was also used to cover the heating pad in each of the reactors to minimize heat loss. The temperature inside each reactor vessel was monitored using a K-thermocouple probe on a Sestos temperature controller inserted into the reactor mixture, which controlled output to the heater pads. The pH inside the reactors was

also measured daily using a Thermo Scientific™ Orion Star™ A326 pH/Dissolved Oxygen Portable Multiparameter Meter. Physico-chemical parameters, such as: total solids (TS), volatile solids (VS), chemical oxygen demand, ammonium nitrogen ($\text{NH}_4^+\text{-N}$), total Kjeldahl nitrogen (TKN), alkalinity and volatile acid concentrations were measured weekly according to standard methods (APHA., 2005). Stability of the process in terms of total volatile fatty acid (TVFA) to alkalinity (FOS: TAC) ratio was also determined as earlier described in Section 3.6.

Daily biogas production from each reactor was collected using a 10 L Supel™-Inert Multi-Layer Foil Gas Sampling Bag fitted with a Thermogreen® LB-2 Septa and a Push/Pull Lock Valve (PLV), which was connected to one of the outlets on the Quickfit® reactor's head plate. The methane content (%) in the biogas was measured as described in Section 3.4.2.

Monitoring and Analysis. A summary of all the operational parameters which were monitored, and the analytical procedures used are shown in Table 3-8.

Table 3-8 Important parameters monitored during the anaerobic digestion processes in continuous reactors

Parameter	Units	Test method	Target	Frequency
Temperature	°C	Meter	36 - 38 °C	Daily
pH	pH units	4500-H ⁺ B, pH Meter	6.8 – 7.2	Daily
Gas production	Litres	Gas Bags	Variable	Daily
Gas composition	%	Gas chromatograph	50 – 65% CH ₄	Daily
Sample volume	mL	VDI 4630	200 – 250 mL	Weekly
Total solids	%	APHA 2540 B	-	Weekly
Volatile solids	%	APHA 2540 B	-	Weekly
Alkalinity	mg. L ⁻¹	APHA 2320 ⁴	1500 – 5000	Weekly
Volatile acids	mg. L ⁻¹	APHA 5560 C	50 – 330	Weekly
FOS:TAC ratio	Nil	Calculated	0.1 - 0.2	Weekly
Organic loading rate	g.L ⁻¹ . d ⁻¹	Measuring cylinder	1 – 2g VS. L ⁻¹ . d ⁻¹	Daily
COD	mg. L ⁻¹	APHA 5220B open reflux	Variable	Weekly
NH ₄ -N	mg. L ⁻¹	APHA 4500-NH ₄ -N B&C	50-1500	Weekly
TKN-N	mg. L ⁻¹	APHA 4500-N _{org} B	100-1600	Weekly

VDI = in Germany *Verein Deutscher Ingenieure* (VDI. 4630, 2006)

FOS	=	in German <i>Fluchtige Organische Säuren</i> (TVFA expressed in mg HAc.L ⁻¹)
TVFA	=	Total volatile fatty acid concentration
HAc	=	Acetic acid equivalent,
TAC	=	in German <i>Totales Anorganisches Carbonate</i> (total alkalinity buffer expressed as mg.L ⁻¹ of CaCO ₃).
APHA	=	American Public Health Association, USA (APHA, 2005 #2467).

The destruction/reduction of volatile solids in the reactors was estimated using Equation 3-13.

$$\text{Volatile solids reduction (\%)} = \frac{(VS_{in} - VS_{out}) \times 100}{[VS_{in}]} \quad \text{Equation 3-13}$$

where VS_{in} represents the percentage of VS in the feed going into the reactor and VS_{out} represents the percentage of volatile solids in samples taken from the AD reactor. VS measurement was carried out following the standard method mentioned in Table 3-8.

3.6 Stability of the AD process

3.6.1 Determination of Total volatile acid (FOS) and Total Alkalinity (TAC) ratio

The stability of anaerobic digestion process was determined by the ratio of the volatile fatty acids (VFA) to the alkalinity otherwise known as Ripley ratio, IA/PA ratio, VFA/bicarbonate ratio or FOS:TAC ratio (Lossie & Pütz, 2008; Shetty *et al.*, 2017). This was measured by titration as described by Lossie and Pütz (2008) and Federation (2007), which involved a two-stage titration during which the values of the bicarbonate alkalinity and the alkalinity due to volatile acids were estimated as follows:

- titration up to pH 5.75: the first stage of titration provides the partial alkalinity (PA), practically equivalent to the bicarbonate alkalinity
- titration up to pH 4.3: the second stage of titration provides the intermediate alkalinity (IA), practically equivalent to the alkalinity of the volatile acids.

$$\begin{aligned} \text{BA} &= [\text{TA} - (0.85 \times 0.83 \times \text{TVA})] && \text{Equation 3-14} \\ &= \text{TA} - 0.71 \times \text{TVA} \end{aligned}$$

where:

BA = bicarbonate alkalinity (as mgCaCO₃.L⁻¹), TA = total alkalinity (as mgCaCO₃.L⁻¹), VFA = concentration of volatile fatty acids (as mg acetic acid.L⁻¹), 0.85= correction factor that considers 85% of ionization of the acids to the titration endpoint, and 0.83 = correction factor from acetic acid into alkalinity. The results from the estimation of FOS:TAC ratio (Table 3-9) were then used to determine the correct amount of buffering agent (bicarbonate) to dose into the reactor to maintain optimum buffering capacity within the digester.

Table 3-9 Ripley ratio, FOS:TAC ratio, intermediate alkalinity (IA) : partial alkalinity (PA) ratio or Volatile acids and alkalinity ratio (Andreoli *et al.*, 2007)

FOS: TAC	Indication	Action to be taken
> 0.6	Excessive organic load	Stop feeding the reactors
0.5 – 0.6	High organic load	Reduce feedstock input
0.4 – 0.5	The AD reactor is at the limit	Monitor the reactors carefully
0.3 – 0.4	Ideal condition for biogas production	Keep feedstock input constant
0.2 – 0.3	Insufficient organic load (under-fed reactors)	Increase the feedstock input gradually
<0.2	Extremely low organic load	Increase feedstock input quickly

3.7 Data analysis

The data obtained from the current study were analyzed using the statistical packages SPSS version 17.0, Microsoft Excel 2016 (Microsoft Corporation, USA). Kinetic models which were used to predict the expected results, degradation constants and hydrolysis rates were carried out by fitting the experimental data on the Gompertz equation using the curve fitting tools in MATLAB R2016a. All analyses were based on a 5% statistical significance level for all parameters tested, and results are presented within ± 2 S.D. Correlation and regression analysis, analysis of variance paired samples T-tests (2- tailed), etc. were also used to determine the statistical significance of the differences between the mean values of the results obtained from different experiments carried out in the current study.

Chapter 4 Effect of feeding interval, operating temperature, organic loading rate and pH on the SMP and VMP of CSTR fed with a grass silage mixture of perennial ryegrass, clover and Timothy grass as feedstock

ABSTRACT

A mixture of grasses consisting of perennial ryegrass, clover and timothy grass which were co-cultivated was used for the current study. The experimental set up consisted of six anaerobic continuously stirred tank reactors (CSTR) assembled in three pairs as follows: psychrophilic (Pair 1), mesophilic (Pair 2), and thermophilic (Pair 3). A near-neutral pH 6.8 – 7.2 was maintained in all the reactors using a 1N ammonium bicarbonate solution. All the CSTR were acclimatized for 7 days (day 1 – 7). The period of irregular daily feeding intervals lasted from day 8 – 93, whereas regular daily feeding lasted from day 104 – 140. The organic loading rates (OLR) used from day 1 – 7, 8 – 56, 57 – 93 and 109 – 120 were 1.48, 1.0, 1.5 and 1.5 gVS.L⁻¹.d⁻¹, respectively. All the CSTR were operated at a hydraulic residence time, HRT of 20 days. During the period of regular daily feeding intervals (day 104 – 140), the pH of all the CSTR was maintained at the near-neutral range with biomass ash-extracts supplement. The results obtained showed that the mean SMP from the Pair 1, Pair 2 and Pair 3 reactor measured at 33-day intervals, calculated from day 25 -58 (irregular feeding intervals) were 294.5, 433.5 and 370.2, N mL CH₄.g⁻¹VS added.d⁻¹, respectively. Similarly, the SMP of all the paired reactors from day 60 – 93 (failing state) were 140, 273.8 and 231.1 N mL CH₄.g⁻¹VS added.d⁻¹ respectively; while from 109 – 120 (regular feeding intervals/recovery), the SMP from the Pair 1, Pair 2 and Pair 3 reactors were also 185.1, 160.8 and 318.2, N mL CH₄.g⁻¹VS added.d⁻¹ respectively. None achieved steady-state conditions which suggest that the application of irregular daily feeding intervals in feeding AD reactors is not likely an effective practice for achieving sustainable biogas production in a long run. The addition of NH₄HCO₃ as supplement provided a good buffering condition in the digestion process, but later it led to a souring problem, probably due to the accumulation of excess ammonia, ammonia inhibition, and then a subsequent decrease in pH and gas production, and acidification. However, the addition of ash-extracts prepared from agricultural biomass waste was shown to enhance the recovery of the failed AD reactors due to its richness in essential trace element and high alkalinity content, both of which are necessary for optimal bacterial growth.

Keywords— *Anaerobic digestion, discontinuous feeding, Perennial ryegrass, Specific Methane Production, supplements, temperature*

Objectives

The objectives of the current study were:

1. To compare the effects feeding interval on the specific methane production (SMP) and volumetric methane production (VMP) of CSTR during the anaerobic digestion of grass silage.
2. To investigate psychrophilic anaerobic digestion of grass silage as a sustainable and affordable process in developing countries
3. To assess the effects of organic loading rate on the SMP from grass silage at psychrophilic, mesophilic and thermophilic temperatures.
4. To compare the recovery rates of psychrophilic, thermophilic and mesophilic CSTR after process failure following supplementation with biomass ash-extracts.

4.1 Materials and methods

The materials and methods used in this study are summarized in Table 4-1 while the characteristics of the biomass feedstock and inoculum are presented in Table 4-2. The reagents added to all the reactors as supplements during the irregular daily feeding intervals and regular daily feeding intervals were ammonium bicarbonate (NH_4HCO_3) (BioUltra grade, Sigma-Aldrich, UK), and empty palm bunch ash-extract (Table 3-2).

Table 4-1 Summary of the materials and methods

Material	Source/Description
Inoculum	Cockle Park farm, Morpeth, UK
Mixture of perennial Ryegrass, White Clover & Timothy	Preparation: Spread and dried at room temperature for 4 weeks, ground and sieved to < 1mm and stored in an air-tight container at 4 °C prior to use. See Chapter 3, Table 3-1 for results obtained from the physicochemical analysis of the grass silages.
CSTR	Setup: See the procedure described in Section 3.5
Feeding plan	Once daily at irregular (discontinuous) feeding intervals.
Organic loading rate (OLR)	1.48 gVS.L ⁻¹ . d ⁻¹ (day 1 - 7) acclimatization 1.00 gVS.L ⁻¹ . d ⁻¹ (day 8 – 56) irregular feeding interval 1.50 gVS.L ⁻¹ . d ⁻¹ (day 57 – 93) irregular feeding interval 1.50 gVS.L ⁻¹ . d ⁻¹ (104 – 109) regular feeding without supplementation 1.50 gVS.L ⁻¹ . d ⁻¹ (110 – 125) regular feeding with supplementation 1.50 gVS.L ⁻¹ . d ⁻¹ (126 – 140) regular feeding without supplementation

Table 4-2 Characteristics of the biomass feedstock and inoculum

Analysis	Abbreviation	Inoculum	Feedstock
Moisture content (%)	MC	87%	7
Total solids (%)	TS	1%	93
Volatile solids (% in TS)	VS	61%	79
pH value	pH	7.8	x
Chemical oxygen demand (mg L ⁻¹)	COD	14,333.3	x
Total Kjeldahl Nitrogen (mg L ⁻¹)	TKN	2,415	x
Ammonium nitrogen (mg L ⁻¹)	NH ₄ ⁺ - N	2,016	0.84
Alkalinity (mg CaCO ₃ L ⁻¹)	TAC	19,550	x
Carbon (%)	C	x	43.6
Hydrogen (%)	H	x	6.1
Nitrogen (%)	N	x	3.09
Oxygen (%)	O	x	34.8
Sulphur (%)	S	x	0.29
Carbon to nitrogen ratio	C: N	X	25:1
Lipids (%)		x	2.4

The physicochemical parameters monitored and analyzed, as well as their test procedures and sampling frequencies are presented in Table 3-8. Similarly, the CSTR used for the current study were grouped in pairs as shown in Table 4-3.

Table 4-3 Summary of CSTR operating conditions

Reactors name	Composition	Temperature
Pair 1	R1 and R2	Psychrophilic (25 ± 2 °C),
Pair 2	R3 and R4	Mesophilic (40 ± 3 °C)
Pair 3	R5 and R6	Thermophilic (60 ± 2.5 °C)

All the reactors were fed once per day throughout the experiment. During the periods of irregular daily feeding intervals, the time difference between each feed were less than 11 hours, whereas as other times, the time difference were over 30 hours. However, during the

period of regular daily feeding, the reactors were also fed once per day, but at 24 ± 1 hourly intervals.

4.2 Results and discussion

4.2.1 Operational parameters

4.2.1.1 Effects of temperature and pH

The mean temperatures of Pair 1, Pair 2 and Pair 3 reactors were 25 ± 2 °C, 40 ± 3 °C, and 60 ± 2.5 °C, respectively. This implies that temperature variations recorded in all the reactors deviated from mean values approximately by ± 3 °C/day, which is higher than the maximum temperature variation of ± 1 °C/day recommended for anaerobic digestion plants in order to maintain stability (Grady Jr, 2011). However, these variations in temperature did not result to any noticeable negative effect on the performances of the reactors, especially the Pair 2 (mesophilic) CSTR. That is, despite temperature variations, overall, the Pair 2 reactors performed better than the Pair 1 and Pair 3 CSTR both in terms of stability and methane production. This better performance achieved by Pair 2 reactors agrees with Shah (2014) and Harzevili and Hiligsmann (2017), who reported that mesophilic bacteria can tolerate temperature fluctuations within ± 3 °C without significant variation in methane production.

The pH inside the AD reactors is another important parameter that was monitored in the current study because previous studies have shown that any deviation from optimum mean pH 6.8 – 7.4 can substantially affect AD digesters performance by decreasing the bacterial growth and the activity of the anaerobic microbes, which can lead to a considerable reduction in daily biogas production and digester failure (Andreoli, 2007; Grady Jr, 2011). The decision to maintain pH of the CSTR within the optimum range was necessary because studies have also shown that operating AD reactors around pH 7.0 – 7.2 enhances the activities of the methanogenic bacteria (Andreoli, 2007; Hobson *et al.*, 1981). The summary of the statistical comparison of the mean values of the pH in each pair of CSTR condition from day 1 – 140 are presented in Table 4-4.

Table 4-4 Comparison of the pH in the Pair 1, Pair 2 and Pair 3 reactors

	Pair 1	Pair 2	Pair 3
Descriptive	Psychrophilic	Mesophilic	Thermophilic
Statistics	(25 ± 1 °C)	(40 ± 1 °C)	(60 ± 1 °C)
Mean	7.01	7.11	7.22
Mode	7.05	7.160 ^a	7.18
Std. Deviation	0.74	0.76	0.78
Maximum	7.58	7.71	7.84

Table 4-4 suggests that the mean pH of all the CSTR was within the desired optimum range, remaining near neutral possibly due to daily supplementation of all the reactors with the ammonium bicarbonate solution. However, this was not true during the AD process failure, phase B (Figure 4-10 and Figure 4-12) during which even the addition of NH_4CO_3 could not prevent the reactors from failing due to rapid consumption of alkalinity by high concentration of VFA (Figure 4-6) which caused the pH to fall below pH 6 (Figure 4-1). The changes in the pH of the reactors due to the addition of the bicarbonate supplement is as shown in Figure 4-1.

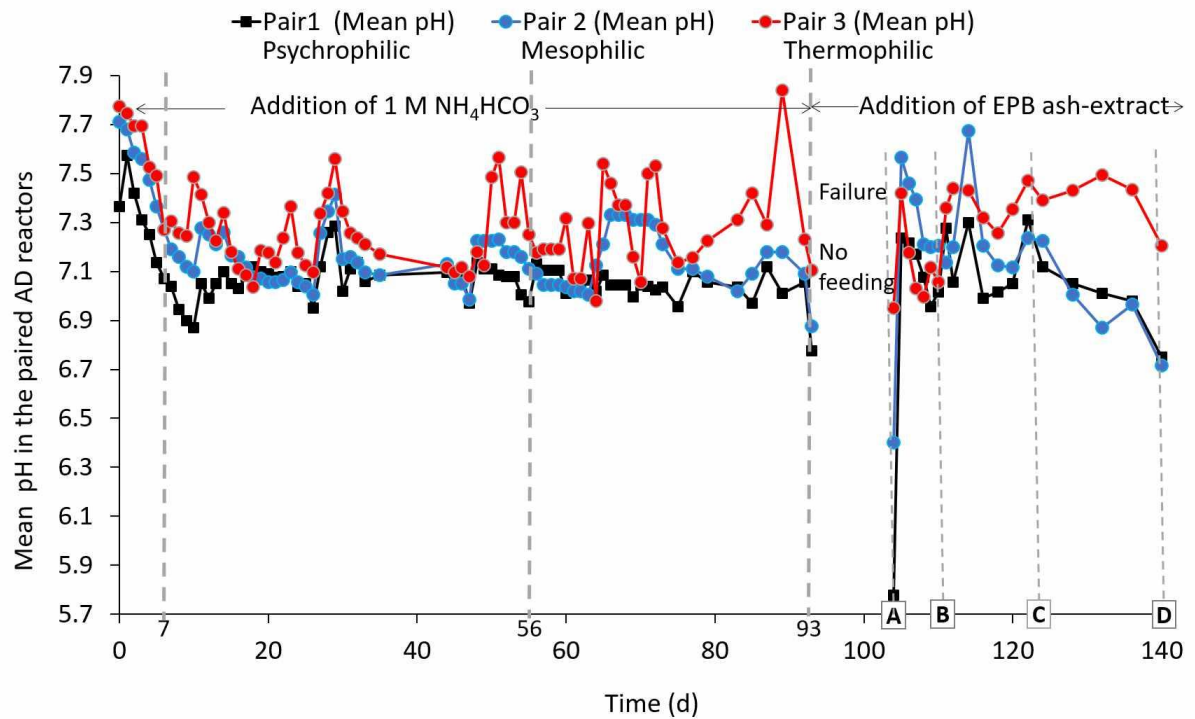


Figure 4-1 Mean pH values inside the Pair 1, Pair 2 and Pair 3 reactors. Details of the feeding phase are presented in Figure 4-4.

However, with the addition of NH_4HCO_3 supplements to all the CSTR (Figure 4-1), it was found that the stability of the pH values, or the ability of the CSTR to retain pH after supplementation, increased with temperature. Since research has shown that pH shows the alkalinity situation in the AD reactors de Lemos Chernicharo (2007), then it is possible that these behaviours of pH in Pair 1, Pair 2 and Pair 3 reactors during their supplementation with equal amount of NH_4HCO_3 indicate that the ability of the CSTR to retain alkalinity is directly proportional to operating temperature, which could be mathematically expressed as shown in Equation 4-1.

$$\text{Alkalinity (Alk)} = k T (^{\circ}\text{C}) \quad \text{Equation 4-1}$$

where k is a constant of proportionality which may be influenced by the concentration of volatile solids and concentration of supplements added to the CSTR.

Thus, operating AD reactors at low temperatures as in the case of Pair 1 reactors would necessitate more expenditure on supplementation to minimize the accumulation of VFA which acidifies the CSTR causing it to fail. This explains why an extra volume of the ammonium bicarbonate supplement was required to maintain adequate pH in the Pair 1 reactors, compared to Pair 2 and Pair 3 reactors. Although ammonium bicarbonate was used

as a supplement in the current study, however, de Lemos Chernicharo (2007) noted that the high cost of the reagent is a major impediment to its use as AD process supplements. Contrary to expectations, souring still occurs in all the reactors from day 70 despite supplementation of ammonium bicarbonate. This instability problem in all the CSTR was likely not only due to discontinuous/irregular feeding, but also due to an increase in the OLR from 1.0 to 1.5 gVS.L⁻¹.d⁻¹ on day 57, which increased instability and souring in the reactor due to overloading (Figure 4-10). This was followed by rapid acidification in all the reactors due to increases in VFA concentrations (Table 4-6), emission of pungent odour from both the reactors and the biogas, and daily decrease in volumetric biogas production and methane contents, which are all signs of overloading (Figure 4-10). These results also agree with that of Kim *et al.* (2002) who during a study comparing the performances and stability of mesophilic and thermophilic AD reactors found that increasing OLR stimulated acidogenesis in the reactors leading to the production of more VFA and H⁺ which cause the AD reactors to fail due to pH<5.

4.2.2 OLR and VS destruction

During the period of acclimatization (day 1 – 7), there was a substantial drop in pH of the reactors from 7.84 to 6.8, probably due to the rapid consumption of alkalinity by the slightly acidic biomass feedstock that was fed to the reactors. This situation was controlled by dosing ammonium bicarbonate solution to restore the pH to the range of 6.8 – 7.2, and then reducing the daily feeding as described in section 4.1. The volatile solids destruction of the reactors varied from 27% to 82.52% across the reactors, with a mean of 61.9, 68.5 and 63.5% for Pair 1, Pair 2 and Pair 3 reactors, respectively (Figure 4-2). The percentage destruction of volatile solids (VS) was directly proportional to the amount of biogas produced (Figure 4-9), but inversely proportional to the OLR. The extent of destruction of VS in the digesters also varied with the time of feeding and sampling of the reactors. Thus, due to the irregular daily feeding pattern adopted for the study, higher VS destruction was recorded at longer feeding intervals, that is when feeding times was over a 24 h interval, while lower destruction was recorded at lower feeding intervals, that is when the feeding interval was less than 24 h.

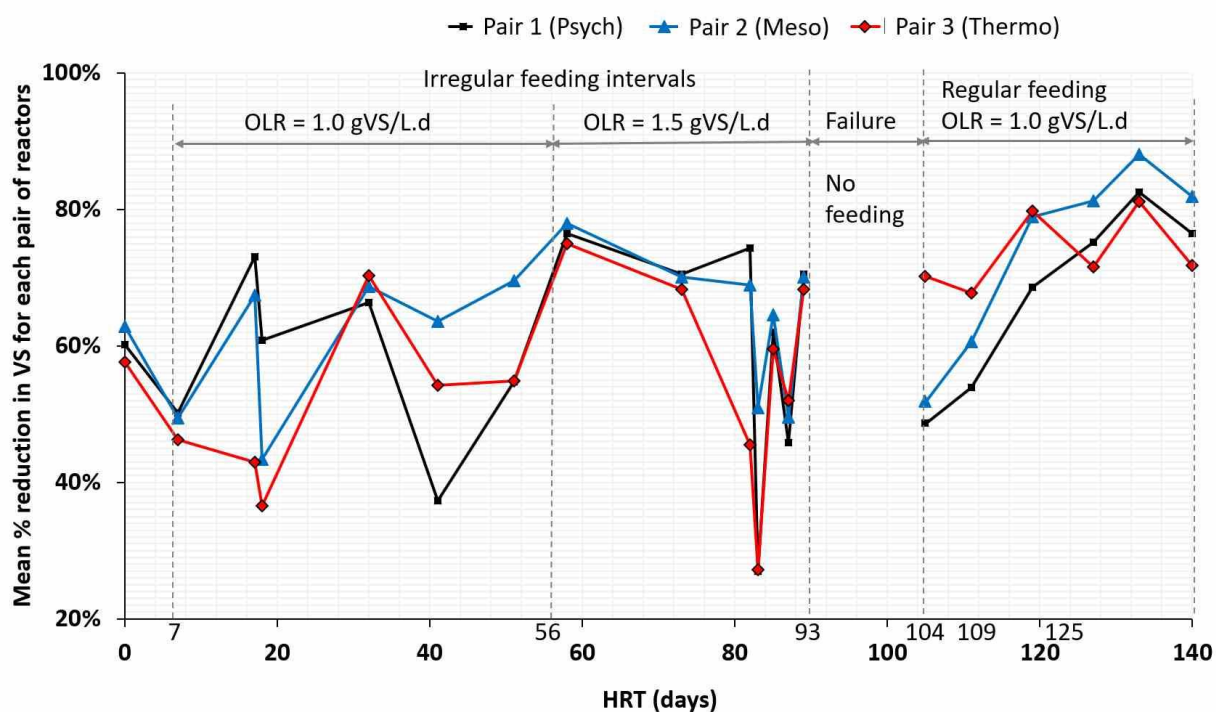


Figure 4-2 Volatile solids (VS) reduction (%) in Pair 1, Pair 2 and Pair 3 reactors. Details of the feeding phases are presented in Figure 4-4.

Lower intervals between feeding times resulted in the accumulation of VS inside the reactors which led to the problem of overload at different times, especially from day 57 when OLR was increased (Table 4-1), frequent pH drops (Figure 4-1), and instability during the study. This result agrees with Holland (2013), who reported that overloading an AD digester with excessive feed leads to the faster production of VFA at a rate which exceeds that which the methanogens can convert to methane gas. Such situation can lead to the accumulation of unconverted VFAs leading to the acidification of the digesters, a fall in pH to a value < 6, and can result in the death of methanogenic archaea and total process failure. The thermophilic anaerobic digesters, Pair 3 showed good volatile solids destruction rates, which were higher than that of the Pair 1 (psychrophilic) reactors, but comparable to that of the Pair 2 (mesophilic) reactors.

4.2.3 Variation of ammonium nitrogen, TKN nitrogen, and COD

Ammonium ion (NH_4^+) is an essential source of nitrogen nutrient needed by bacteria for their metabolism. However, at high pH, most of the NH_4^+ converts to free ammonia which is toxic to methane-forming bacteria (de Lemos Chernicharo, 2007; Gerardi, 2003; Jha & Schmidt, 2017). In the current study, the mean concentration of ammoniacal nitrogen/ammonia during start-up was $2,618 \text{ mg.L}^{-1}$ due to the high ammonia content of the cattle slurry component of

the inoculum used. However, this concentration decreased continuously over time in all reactors as shown in Figure 4-3 until over 80% of the original concentration had been washed out. According to Gerardi (2003), ammoniacal-nitrogen (NH_4^+) in an AD digester in the range of 50-200 mg.L^{-1} has a beneficial effect, when present at the range of 200 - 1000 mg.L^{-1} , ammonia-N has no adverse effect on the AD process. However, it was reported that ammonia-N concentration ranging from 1500 – 3000 mg.L^{-1} has inhibitory effect at pH level over 7.4, and at such toxic concentration, biogas production is reduced (Wellinger, 2013).

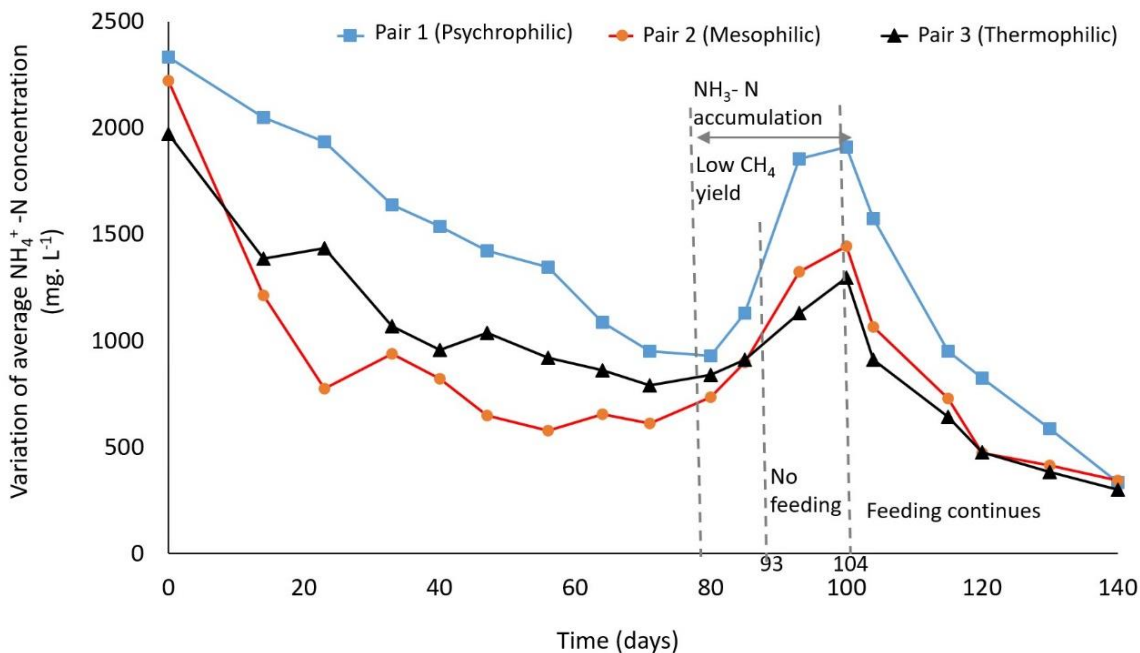


Figure 4-3 Mean concentration of ammonium-N (NH_4^+ -N) in Pair 1, Pair 2 and Pair 3 reactors over time

One major issue with the Pair 1 reactors was that being low-temperature reactors, they had high ammonia-N concentration which is a problem due to potential inhibitory characteristics of ammonia when present at high concentrations. The mesophilic reactors (Pair 2) which had the lowest ammonia-N concentration, performed better than both Pair 1 and Pair 3 reactors. The concentration of ammonia-N in the thermophilic reactors (Pair 3), was just slightly higher than that of the mesophilic reactors. The higher concentration in the thermophilic reactors was expected because Engineers (2008) had earlier stated that among the different types of ammonia compounds present, that ammonium bicarbonate is the most sparingly soluble in water, and that its solubility increases with temperature as shown in Table 4-5.

Table 4-5 Solubility of ammonium bicarbonate at different temperatures (Engineers, 2008)

Temperature (C)	0	10	20	30	40	50	60
Solubility (%)	10.6	13.9	17.8	22.1	26.8	31.6	37.2

In agreement with Engineers (2008), Shah (2014) also stated that ammonia toxicity increases with temperature and that thermophilic processes are more susceptible to ammonia inhibition at ammonia concentration > 80 mg/L.

A previous study by Jha and Schmidt (2017), also found that lower inhibitory effect of ammonia occurred at mesophilic compared to the thermophilic temperatures. In another study, Paul and Dutta (2018) showed that AD plant operated at thermophilic temperatures are more prone to failure especially at pH >7.4 due to free ammonia inhibition because the release of free ammonia increases with the temperature of the anaerobic digestion process. This release of ammonia at a higher temperature may be due to volatilization or stripping of the ammonia molecules.

Furthermore, the results from the analysis of the total Kjeldahl nitrogen (TKN) and organic nitrogen concentrations in the reactors presented in Figure 4-4, shows that the TKN in the Pair 1, 2 and 3 reactors decreased from 2,588 – 1,218 mg.L⁻¹; 2,501 – 696.5 mg.L⁻¹ and 2,257.1 – 735 mg.L⁻¹ respectively. The organic-N contents in the three Pairs of reactors also decreased from 903.6 – 105 mg.L⁻¹; 770 – 178.5 mg.L⁻¹ and 567 – 144.7 mg.L⁻¹ for the Pair1, 2 and 3 reactors respectively. From the data, it is apparent that the concentration of both the TKN and organic-N recorded in all the reactors were far lower compared to the results obtained from other experiments carried out in the current study using different grass silages (Section 6.2.2) and Figure 6-3).

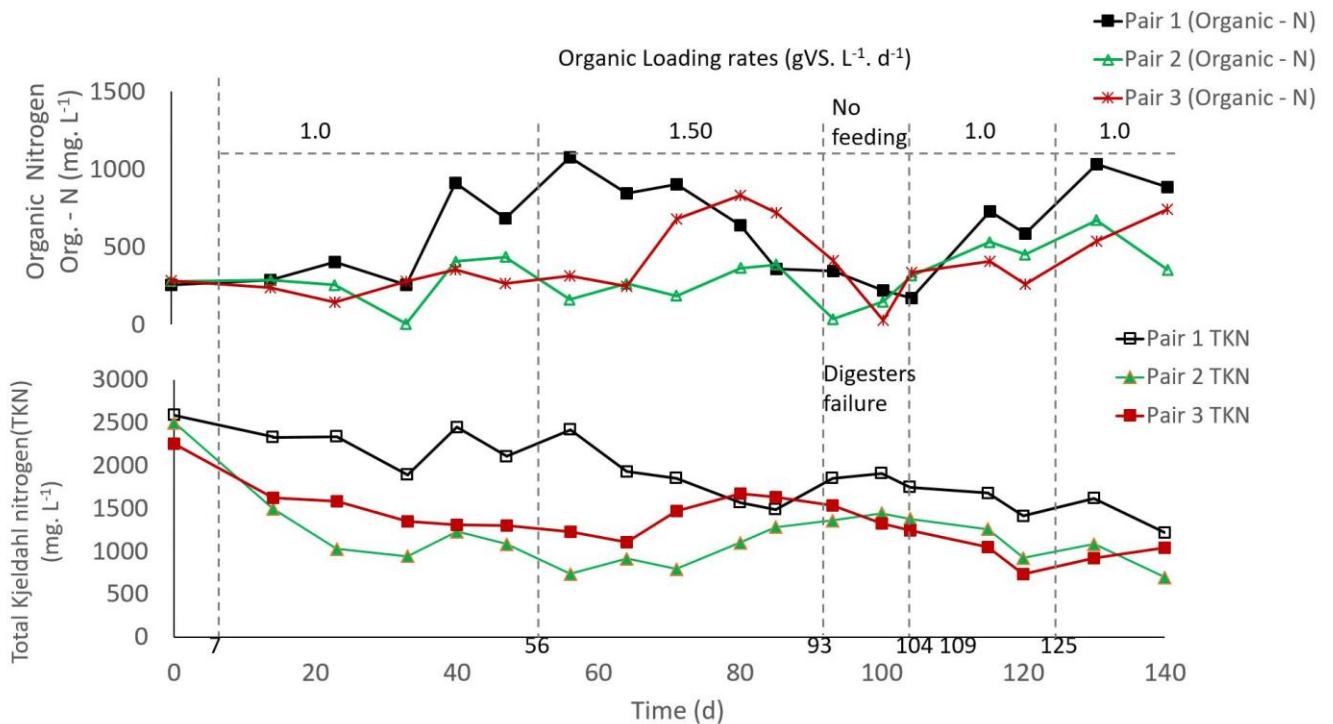


Figure 4-4 Mean concentration of total Kjeldahl-N (TKN) and organic nitrogen in Pair 1, Pair 2 and Pair 3 reactors over time

The higher concentration of the organic nitrogen in Pair 1 reactors led to suboptimal biogas production (Figure 4-9, Figure 4-11 and Figure 4-12), and this could be because the daily addition of ammonia bicarbonate introduced a high organic nitrogen contents in the reactors which led to the release of free ammonia at inhibitory concentrations. The presence of high concentration of free ammonia in AD reactors inhibits the methanogenic activities by increasing the energy required for their maintenance, alters their intracellular pH, decreases in their intracellular potassium contents and inhibits the specific enzymatic reactions of the archaea methanogens (Zhu, 2017).

The boxplot (Figure 4-5) represents the variability in the total chemical oxygen demand in all the AD reactors. The total concentration of the chemical oxygen demand (COD_T) in the reactors showed an increasing pattern from day 1 – 7 because of the daily loading of the reactors with biomass feedstocks without any removal (Figure 4-4). This corresponds to the period of initial VFA accumulation during the acclimatization period. However, from day 8 onwards, a higher COD_T reduction occurred when feeding was delayed beyond 24 h, and that statistically correlated with the methane production ($R^2 = 0.79$) (Figure 4-11). Thus, reduction in COD_T removal (Figure 4-5) corresponded with a reduction in VS removal (Figure 4-2), from the digesters, and that was predominant in the Pair 1 reactors (psychrophilic), and

especially during very close feeding intervals during the irregular daily feeding process. From Figure 4-5, it is clear that the mean concentration of COD_T in all the reactors was increased from the 1st quartile (25% percentile) to the 3rd quartile (75% percentile) with their medians all within the 1st quartile. The outliers represent values of CODs high than expected in the reactors correspond to the periods of high operational instability due to increasing concentrations of VS and high COD_T in the Pair 1 (psychrophilic) and Pair 3 (thermophilic reactors).

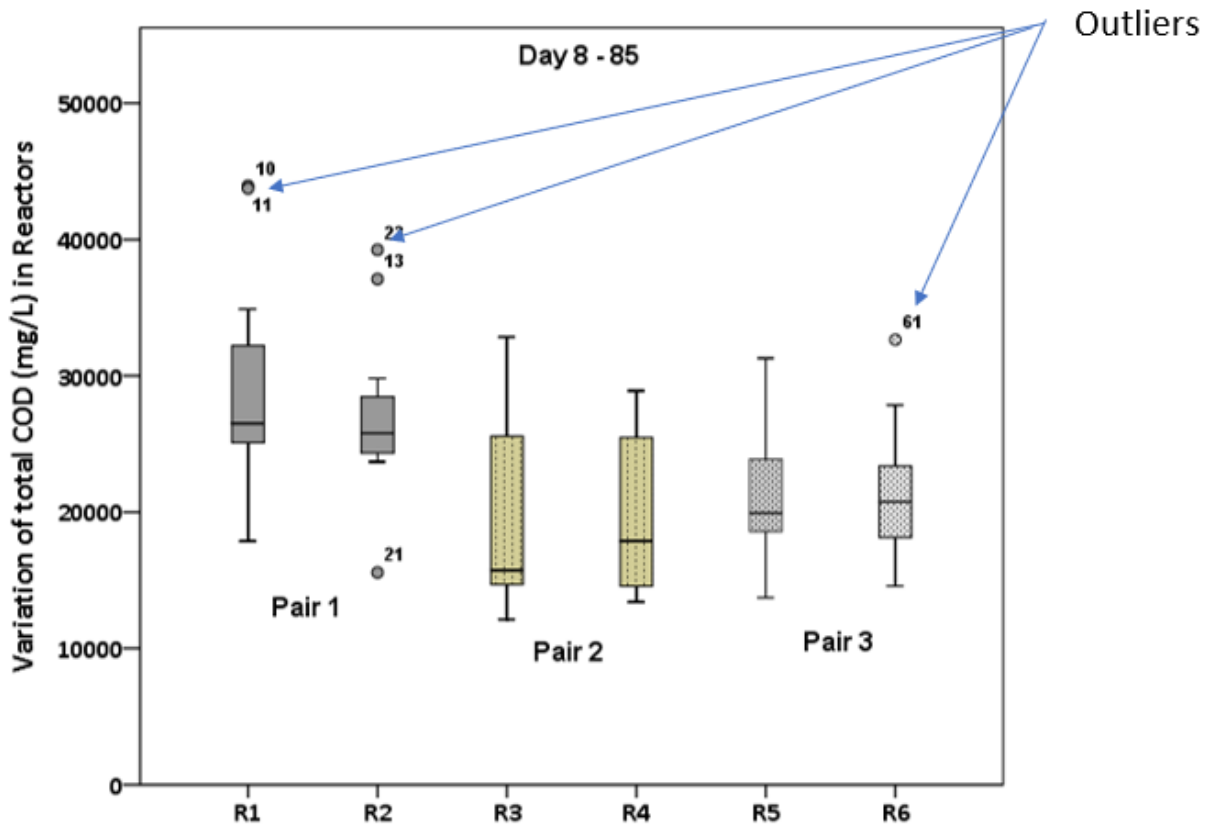
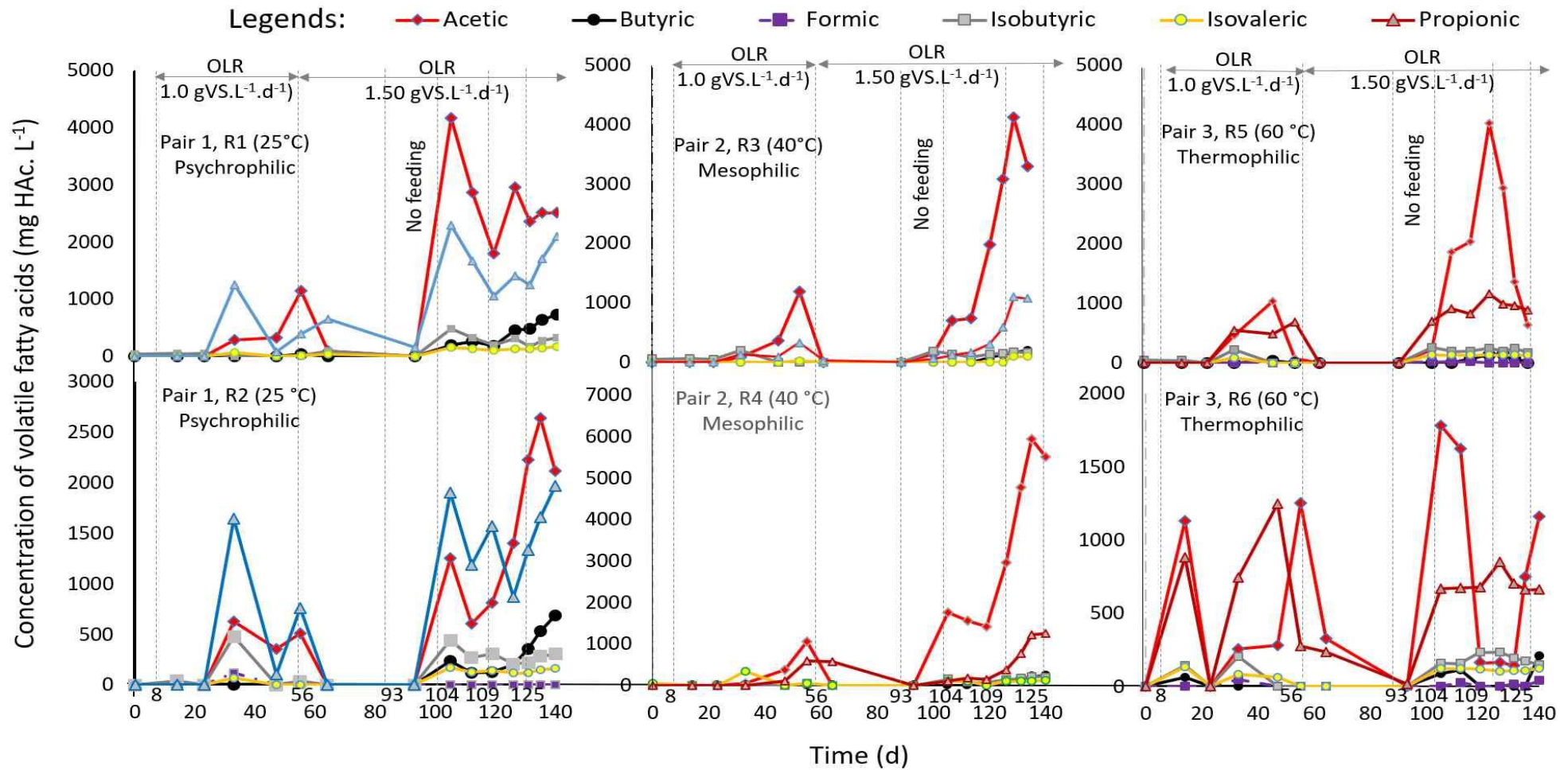


Figure 4-5 Comparison of mean COD_T variation in the Pair 1, Pair 2 and Pair 3 reactors from day 8 – 85

One other major observation from these reactors was that their COD_T removal was directly proportional to the operating temperatures, which was why more COD_T removal was recorded in the thermophilic (Pair 3) reactors (Figure 4-5). Statistically, the Tukey's one-way Post Hoc Multiple Comparisons ANOVA which was used to compare the COD_T data from the psychrophilic, mesophilic and thermophilic reactors, with an assumption of equal variances, equally showed that the mean difference in the value of the COD_T between each pair of reactor conditions was significant at 0.05 level. This further validates the earlier observation that the degree COD_T removal was related directly with the operating temperature.

4.2.4 Volatile fatty acid inhibition and alkalinity

The formation of VFA in the AD is regarded as one of the most important parameters for monitoring the performance of the digestion process due to their inhibitory effects when present in undissociated states or at high concentrations (Harzevili & Hiligsmann, 2017; Stronach *et al.*, 2012), and Sawyer et al, (2003) as quoted in (Khanal, 2011a) reported that the value VFA often ranges between 50 – 250 mg HAc.L⁻¹ in a healthy anaerobic system. In the current study, the concentration of VFAs observed in the reactors increased in the order: acetate>propionate> butyrate> isobutyrate> isovalerate> formate, from day 1 – 140. This shows that acetate had the highest concentration while the formate had the lowest concentration among the VFA produced in all the reactors during this study. However, the concentration of formate was so low and was only detected in the thermophilic reactors (Pair 3), just after failure (Table 4-6). The VFA profiles for Pair 1, Pair 2 and Pair 3 reactors are shown in Figure 4-6.



1

2 Figure 4-6 Volatile fatty acid concentrations in Pair 1, Pair 2 and Pair 3 reactors. Acetate (red), butyrate (black), formate (purple), isobutyrate (ash),
 3 isovalerate (yellow) and propionate (dark red), Refer to Table 4-1 for details of the organic loading rates and the corresponding days.

From the graphs in Figure 4-6, the irregular daily feeding contributed to instability during the AD process which is evident from the intermittent accumulation of VFA from the startup, especially in the psychrophilic reactors (Pair 1) and reactor R6 (Pair 3). The results also show that increasing the organic loading rate from 1.0 to 1.5 g VS.L⁻¹.d⁻¹ brought about a rapid increase in VFA accumulation on day 56. However, with the regular use of ammonium bicarbonate to buffer the reactors, no detrimental effect was observed on the methane production at this point. However, on day 56, the Pair 2 (mesophilic reactors) had accumulated high concentrations of VFA > 1,500 mg HAc.L⁻¹ despite the addition of the bicarbonate alkalinity. The other two pairs of reactors started producing biogas with a pungent odour, due to the accumulation of very high concentrations of VFA. The highest concentrations of VFA recorded in the reactors are shown in Table 4-6.

Table 4-6 Maximum concentrations of VFAs detected in the Pair 1, Pair 2 and Pair 3 reactors during the period of instability in the AD reactors (day 55 – 140)

Anaerobic CSTR		Concentration (mg. L ⁻¹)					
		Acetate	Butyrate	Formate	Isobutyrate	Isovalerate	Propionate
Pair 1	R1	4170.1	727.7	0	473.0	162.7	2288.5
	R2	2636.2	685.3	117.8	476.3	171.2	1971.4
Pair 2	R3	4121.9	201.0	0	192.6	102.2	1098.6
	R4	5944.3	230.6	0	218.2	338.8	1256.4
Pair 3	R5	4016.5	147.2	22.8	254.8	138.1	1151.5
	R6	1782.5	210.1	45.1	237.2	134.8	1249.1

Figure 4-5 and Table 4-6 show that the peak concentrations of acetate were highest followed by propionate and then butyrate. However, research has shown that acetate is the least toxic VFA produced during the AD process, and that propionate at a concentration > 3000 mg.L⁻¹, can inhibit AD processes adversely, and could lead to the process failure, unless an inoculum was previously acclimatized to these high concentrations (Stronach *et al.*, 2012). Khanal (2011a) also reported that VFA concentrations above 2,000 mg HAc.L⁻¹ inhibit the

methanogens. Propionate inhibition occurring in AD reactors when detected at a concentration ranging between 1000 – 5000 mg.L⁻¹ has also been recorded (Stronach *et al.*, 2012), according to (Vertes *et al.*, 2011), propionate can inhibit archaea methanogens even at neutral pH.

Although acetate is presumed to be the least toxic VFA to AD processes, high concentrations of acetate reduce the buffering capacity of the digesting sludge which causes the pH to drop (souring) (Holland, 2013), and indicates the failure of acetoclastic methanogenesis (Grady Jr, 2011; Stronach *et al.*, 2012). Propionate, iso-butyrate, and valerate have also been reported to be the most significant volatile fatty acids that are affected by ammonia inhibition (Shi *et al.*, 2017). According to Wheatley *et al.* (1997), when there is shock load during the operation of AD reactors, there is high potential for disruption to occur because the growth rate of the acid-forming bacteria is more rapid than that of the methanogenic archaea, and that can result in an increase in acid concentration, reduction in alkalinity and changes in biogas composition. To prevent process upset occurring during AD operation, Wheatley *et al.* (1997) also stated that it is better to separate the acidogenic and the methanogenic stages of the process in two different reactors (2-stage system) to enable the acidogenic reactor to act as the buffering tank which helps prevent possible shock in the methanogenic reactor. Process upset, or shock can also be prevented from occurring during AD process by ensuring that adequate amount of alkalinity is present in the reactors.

The recommended range of alkalinity in the AD is 4000 - 5000 mg.L⁻¹ CaCO₃ (Andreoli, 2007). However, the mean alkalinity in the reactors ranges from 3,537.5 – 9,775 mg.L⁻¹ CaCO₃ with a mean of 8,311 mg.L⁻¹ CaCO₃ for pair 1 reactor; 4,787.5 – 8,050 mg.L⁻¹ CaCO₃ with a mean of 5,717.2 mg.L⁻¹ CaCO₃ with a mean of 3,971.9 mg.L⁻¹ CaCO₃ for pair 2 reactors, and 2,712.5 – 5,700 mg.L⁻¹ CaCO₃ with a mean of 3,972 mg.L⁻¹ CaCO₃ for pair 3 reactors. Thus, these results show that in the current study, the ammonium bicarbonate alkalinity present in all the all the AD reactors prior to their failure was close to the optimum range.

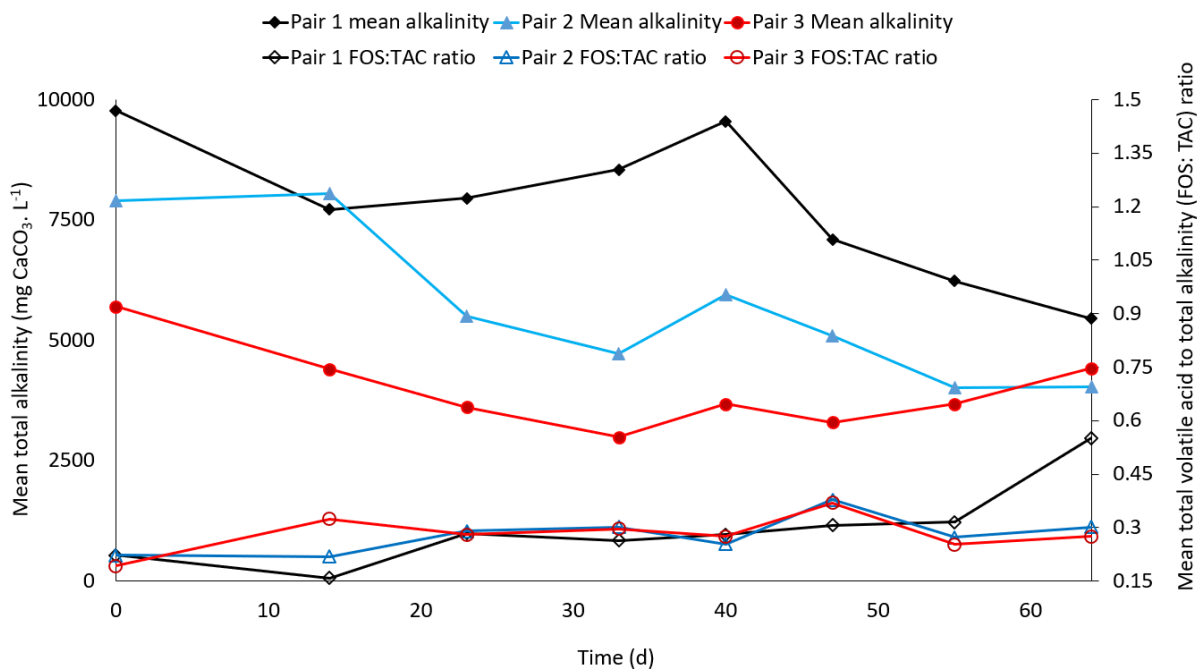


Figure 4-7 Mean concentration of alkalinity in the reactor: Pair 1 (black lines), Pair 2 (blue lines) and Pair 3 (red lines), and the mean total volatile fatty acid to total alkalinity (FOS: TAC) ratio over time

Achieving adequate alkalinity inside the reactors was further verified from the FOS:TAC ratio, based on the normal FOS:TAC ratios of AD reactors published by Lossie and Pütz (2008) using titration method (Section 3.6.1). The results in Figure 4-7 show that the mean FOS:TAC ratio in the reactors ranged from 0.2 – 0.3: 1 for the psychrophilic reactors; 0.2 - 0.4: 1 for both the mesophilic and thermophilic reactors. The information from the FOS:TAC ratio suggests that none of the reactors was overloaded between day 0 – 40. However, due to the accumulation of VFA, the FOS:TAC ratio started to increase which indicated that failure of the digesters was imminent. Statistically, there was a strong correlation ($R^2 = 0.98$) between the alkalinity within the Pair 1 (R1 and R2), the Pair 2 (R3 and R4), $R^2 = 0.82$ and the Pair 3 (R5 and R6), $R^2 = 0.84$, with no significant difference observed in the variation of alkalinity in reactors operated under the same conditions ($p > 0.05$), except for the thermophilic reactors ($p < 0.05$) which suffered temperature controller failure that led to VFA accumulation.

4.2.5 Propionate-to-acetate ratio

The propionate-to-acetate (P: A) ratio inside an AD reactor provides useful information about the condition of the digestion process. Studies have shown that AD process failure occurs at P:A ratio > 1 (Nigam & Pandey, 2009; Shah, 2014). The P:A ratio recorded in the Pair 2

(mesophilic reactors during normal discontinuous operation were effectively lower than that those of their psychrophilic and thermophilic counterpart during the period of discontinuous feeding condition (day 25 – 58) with only exception of day 47 when VFA in all the reactor (Pair 1, Pair 2 and Pair 3) increased to P:A ratios > 1:4 due power cut which led to thermal and overloading shock in all the reactors. The problem of excessive P:A ratio was resolved by suspending feeding for 3 days (day 59 – 61), while continuing bicarbonate supplementation and that effectively reduced the concentrations of VFA to zero around day 62 as shown in Figure 4-8.

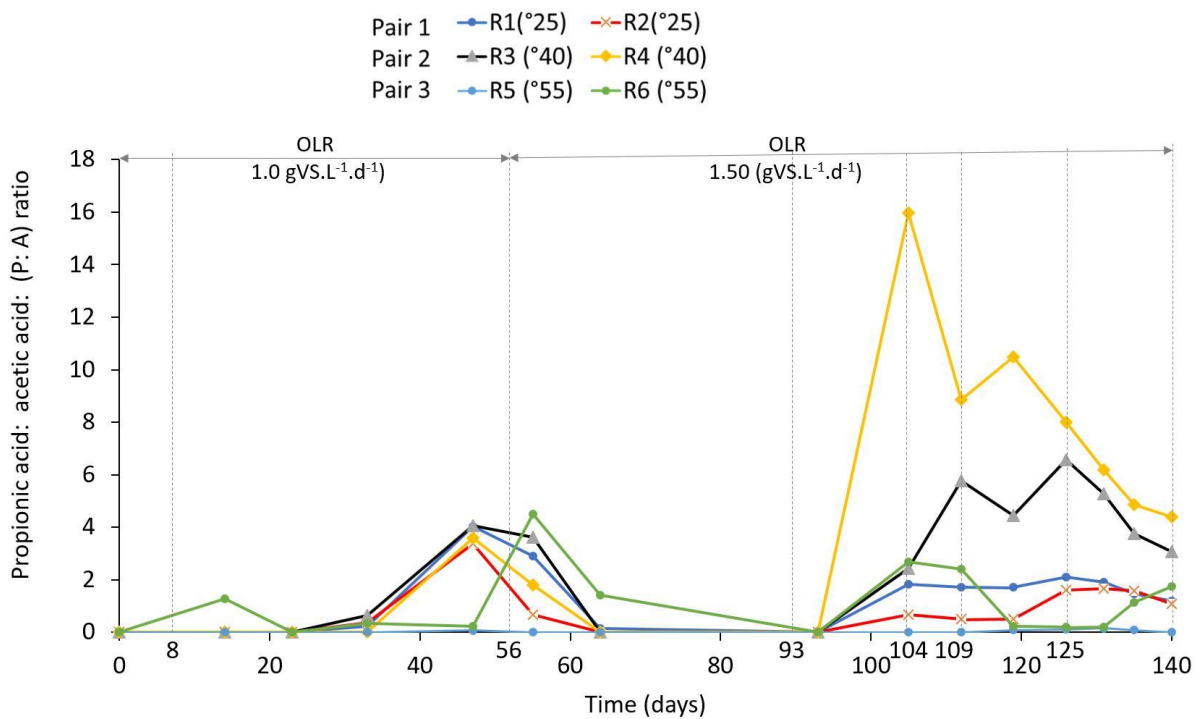


Figure 4-8 Stability check using propionate: acetate (P: A) ratios in the Pair 1, Pair 2 and Pair 3 reactors. Details of feeding regimes are presented in Table 4-1 and Figure 4-7.

However, the P:A ratio of reactor R6 in Pair 3 also increased to 1:4.5 which made it very unstable. However, with the dosing of ammonium bicarbonate, the value of P:A ratio in the reactor reduced to 1:1.4 on day 64 and < 1: 0.05 thereafter. However, after all the reactors had failed, and began to recover (day 105 - 140), due to the addition of supplement from empty palm bunch ash, only the thermophilic reactors, R5 and R6 showed a slightly better stability, based on P:A ratio, compared to Pair 1 and Pair 2 reactors. The reactor R2 was the only stable reactor between day 105 – 119, while the other reactors showed higher P: A > 1:1, especially for R3 and R4. The overall results obtained from the analysis of the reactors stability in terms of their P:A ratios, suggest that shorter feeding intervals during the irregular daily feeding practice adopted for the study enhanced acidogenesis by the acidogens due to their rapid rate

of reproduction causing pH to drop due to VFA remaining unconverted to methane by the final stage of the AD process.

4.3 Effect of temperature on biogas production

4.3.1 Overall biogas production (day 1 - 140)

The mean specific biogas production (SBP) in the Pair 1, Pair 2 and Pair 3 CSTR from day 1 - 140 were 345.5, 619.1 and 599.8 N mL biogas $g^{-1}VS$ added. d^{-1} respectively, while the mean volumetric biogas production (VBP) was 164.7, 267.2 L and 216 mL $CH_4.g^{-1}VS$ added. d^{-1} , respectively as shown in Figure 4-9. Overall, the cumulative SBP from the Pair 1, Pair 2 and Pair 3 reactors were 26,605.1, 47,672.0 and 46,187.7 mL biogas respectively, while the cumulative volumetric biogas production from the reactors were also 32,512.9; 59,634.0 and 59,411.1 mL biogas, respectively (Figure 4-9).

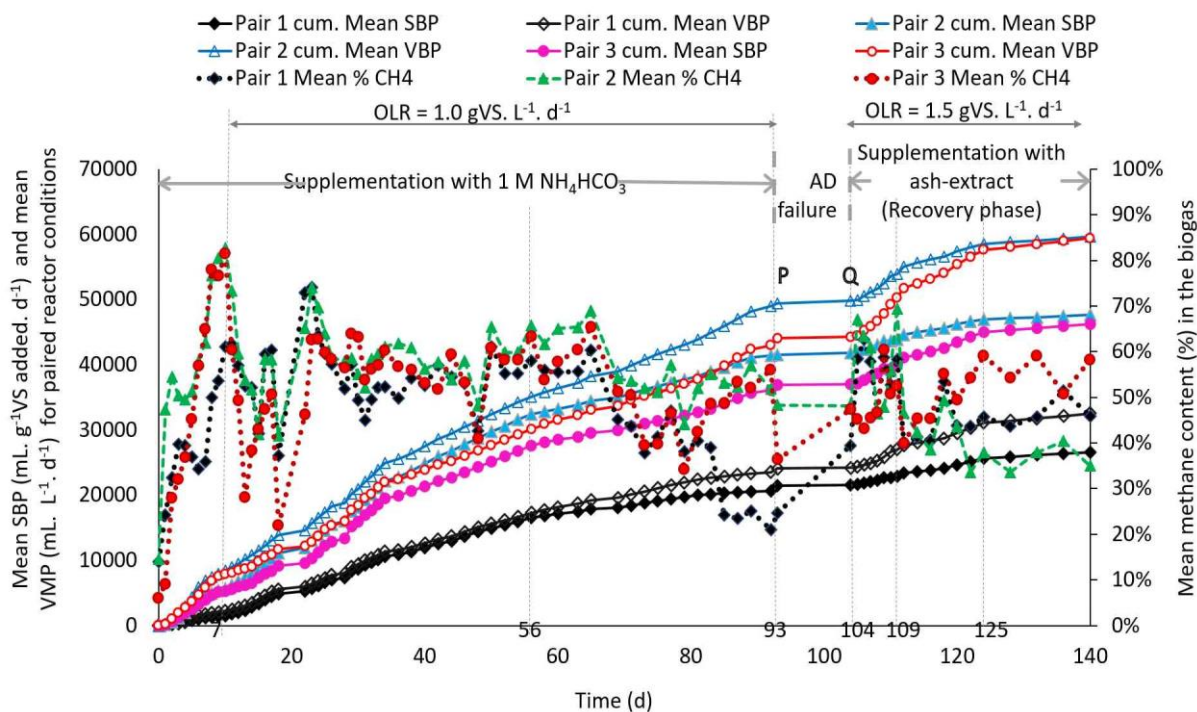


Figure 4-9 Cumulative mean specific biogas production (SBP), cumulative mean volumetric biogas production (VBP) and mean methane contents (%) in biogas from the Pair 1, Pair 2 and Pair 3 reactors. The composition of the Pair 1, Pair 2 and Pair 3 reactors defined in Table 4-3. Point P and Q (day 93 – 103) represents a period of break in the feeding due to the failure of the AD reactors.

These results show that overall, the SBP from each of the Pair 2 (mesophilic) and Pair 3 (thermophilic) reactors were 45% higher than that of the Pair 1 (psychrophilic reactors). However, the SBP from the Pair 2 and Pair 3 reactors were almost the same (Figure 4-9). The results also show that the mean VBP of the Pair 2 and Pair 3 reactors were 44 and 42% respectively, higher than that of the Pair 1 reactors. However, the cumulative mean VBP from the Pair 2 reactor was 3% higher than that of the Pair 3 reactors, which shows that overall, the performance of the mesophilic and thermophilic reactors in the current study were nearly the same in their biogas productivity (SBP and VBP), and these were nearly double that of the psychrophilic reactors. Similarly, overall, the average methane contents (%) in the wet biogas from the Pair 1, Pair 2 and Pair 3 reactors as shown in Figure 4-9 were 48, 56 and 51%, respectively.

Furthermore, the overall mean specific methane production (SMP) from the Pair 1, Pair 2 and Pair 3 reactors shown in Figure 4-10 were 221.1, 313.3 and 295.7 N mL CH₄.g⁻¹VS added.d⁻¹; and these corresponded with overall mean volumetric methane production (VMP) of 192.8, 381.2 and 366.6 N mL CH₄.d⁻¹, respectively.

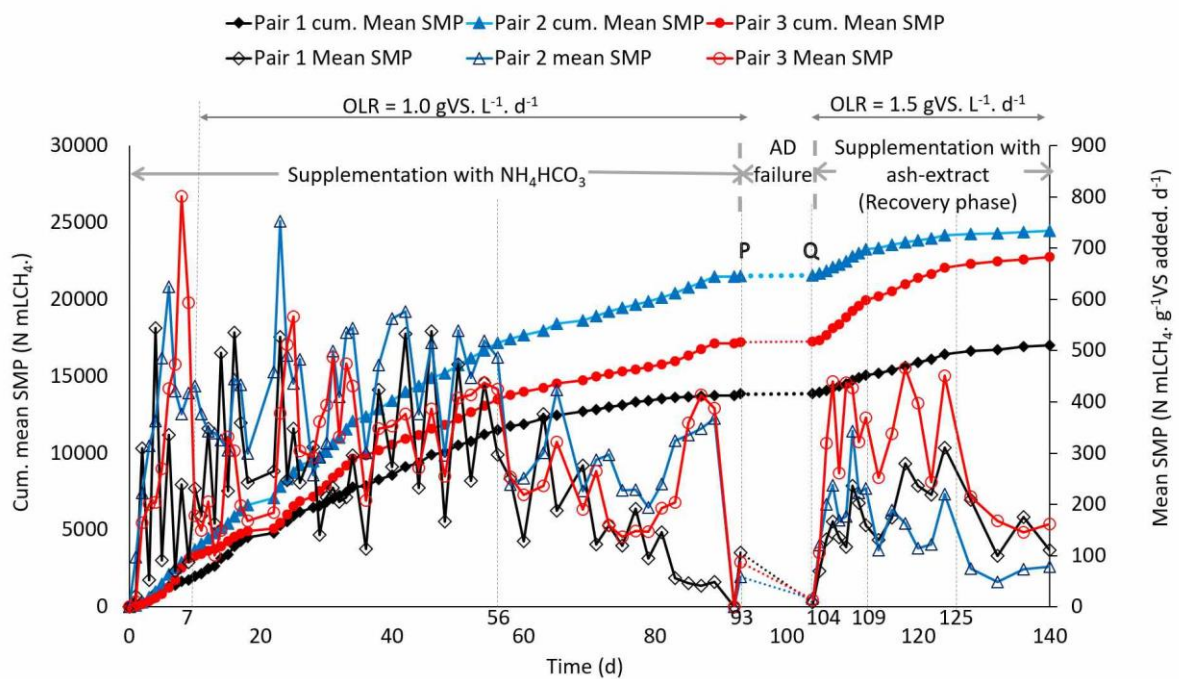


Figure 4-10 Cumulative mean specific methane production (cum SMP), specific methane production (SMP). Cum. means indicate the average of the cumulative volumes of methane produced in the Pair 1, Pair 2 and Pair 3 reactors. Other parameters are as defined in Figure 4-9.

Statistically, a paired sample t-tests between the mean SBP of the paired reactors, gave a p-value < 0.05 for (Pair 1 and Pair 2; and Pair 1 and Pair 2) respectively, while a comparison

between Pair 2 and Pair 3 reactors gave a p-value > 0.05 . These results suggest that overall, the difference between the temperatures of the mesophilic and thermophilic AD reactors did not have any significant effect on the volume of biogas production, whereas such difference had an enormous negative effect on the biogas production of the psychrophilic reactors. The higher performances of the mesophilic and thermophilic reactors can be explained by thermal advantage, because heating enhances the rate of microbial growth, and therefore increases the rate of the digestion processes and biogas production (Turovskiy, 2006).

4.3.2 Irregular daily feeding practice and a steady-state conditions

Figure 4-10 and Figure 4-11 signify that none of the reactor conditions was able to achieve steady-state conditions despite being operated at fixed temperatures and under controlled pH conditions. Table 4-7 also contains a summary of the results from a comparison of the specific methane production (SMP) in the Pair 1, Pair 2 and Pair 3 AD reactors from day 40 – 65, which represents the period of normal operation before the reactors started to fail and day 107 – 140, which represents the methane production from the reactors during the periods of recovery from failure.

Table 4-7 Minimum, maximum, mean and standard deviation of the SMP from Paired CSTR.

Paired reactors	Time (days)	Mean specific methane production for paired conditions			
		Minimum CH ₄	Maximum CH ₄	Mean	Std. Deviation
Psychrophilic (Pair 1)	25 – 58	112.9	537.9	294.5	122
	60 – 93	41.8	376.5	140	91.6
	107 - 140	99.7	296.1	185.1	61
Mesophilic (Pair 2)	25 - 58	238.7	576.4	433.5	109
	60 - 93	58.3	423.2	273.8	86.7
	107 - 140	48.5	343.2	160.8	78.7
Thermophilic (Pair 3)	25 - 58	207.6	566.5	370.2	87
	60 - 93	86.9	413.5	231.1	98.7
	107 - 140	146.0	465.7	318.2	112.6

Note: specific methane production is expressed in mL CH₄.g⁻¹VS added.d⁻¹. Refer to Table 4-3 for feeding conditions.

The results presented in Table 4-7 and Figure 4-11, signify that from day 25 – 58, the SMP from the Pair 2 and Pair 3 reactors increased by 32 and 20%, respectively compared to the Pair 1 reactors. It also indicates that the SMP from the Pair 2 reactors was 15% higher than that of the Pair 3 reactors. Similarly, the volumetric methane production (VMP) which is also presented Figure 4-11 shows that volume of methane produced by the Pair 2 and Pair 3 reactors were 50 and 41%, respectively, higher than that of the Pair 1 reactors. This means that the mesophilic reactors were more stable under the irregular daily feeding condition (with no outliers see Figure 4-5), compared to the thermophilic and mesophilic reactors. This suggests that the unequal intervals between daily feeding times could be responsible for process instability as it may have resulted in short-term changes to the actual OLR, giving irregular hydrolysis patterns and subsequent formation of varying concentrations of intermediate products inside the reactors. These results agree with Turovskiy (2006), that feeding of anaerobic digesters at regular intervals, and short intervals of 1 hour rather than 24

hours help to maintain steady-state conditions in the digester because methanogens are sensitive to sudden changes in volatile solids concentration in the AD reactors. Equally, a more uniform feeding pattern, perhaps every 8 hours, could reduce shock loadings which can lead to a reduction in alkalinity, and helps to provide more stable buffering against pH change in the reactor. It also important to note that the SMP values achieved in Table 4-7 are within the ranges of BMP values of some of the grass silages that constituted the CSTR feedstock, such as elephant grass or Napier grass (190 – 340 mL CH₄.g⁻¹VS added. d⁻¹, Timothy (333 – 385 N mL CH₄.g⁻¹VS added.d⁻¹), ensiled grass (128 – 392 N mL CH₄.g⁻¹VS added. d⁻¹), clover (290 -390 N mL CH₄.g⁻¹VS added.d⁻¹) and mixed grasses (298 – 315 N mL CH₄.g⁻¹VS added.d⁻¹) (Frigon & Guiot, 2010). Interestingly, the current study, only the mean methane produced in the thermophilic CSTR (Table 4-7) were comparable to the BMP value of 399.4 N mLCH₄.g⁻¹VS added which was obtained from the batch tests (see Annex A, Table 9-3).

Between day 60 - 93, the mean SMP from the Pair 1, Pair 2 reactors were higher than that from the Pair 1 reactors by 49 and 39%, respectively, and that shows that methane production from the mesophilic reactors within this period was almost double that from the psychrophilic reactors. Also, the SMP from the Pair 2 reactors exceeded that from Pair 3 reactors by 16%. Similarly, the VMP from the Pair 1, Pair 2 and Pair 3 reactors within this period were higher by 63 and 55% respectively, compared to the Pair 1 reactors, and that the Pair 2 reactors achieved a VMP which was 17% higher than that of the Pair 3 reactors. Also, between period A (day 25 - 58) and period B (day 60 - 93), the mean SMP from Pair 1, Pair 2 and Pair 3 reactors decreased by 52, 37 and 38%, respectively. It is also evident from the Table 4-7 that as the failing of the AD reactors progressed, the methane production in the Pair 1, Pair 2 and Pair 3 reactors further decreased gradually from the maximum values shown in Table 4-7 to lowest minimum values of 41.8, 58.3 and 86.9 N mL CH₄.g⁻¹VS added.d⁻¹, respectively. Correspondingly, the VMP for the Pair 1, Pair 2 and Pair 3 reactors also decreased to their lowest values of 62.8, 164.2 and 130.4 N mL CH₄.L⁻¹. d⁻¹. These decrease shows that the mean volumes of methane (SMP) lost in Pair 1, Pair 2 and Pair 3 reactors due to failure were 89, 86 and 79%, respectively. The period of regular decrease in daily biogas/methane production (Figure 4-9 and Figure 4-10) coincides with the period of rapid decrease in the pH of the digesters (Figure 4-1), and according to Holland (2013) as a sudden decrease of the pH of AD reactors below the neutral value can inhibit the gas production or lead to digester failure. This period of AD failure (phase B in Figure 4-12) also corresponds to the period of high concentration of VFA in the reactors (Figure 4-6). Due to the failure of all the CSTR and the pungent smell emanating from them, they were shut down from day 94 – 103 represented by

period PQ in Figure 4-10 and Figure 4-11. However, prior to and during the failure phase, the Pair 2 reactors were least affected by the process upset suffered by the reactors compared to Pair 1 and Pair 3 reactors. Such observation is in agreement with several published literature which reported that the mesophilic AD process is less sensitive to toxicants compared to the thermophilic AD processes (Gerardi, 2003; Jha & Schmidt, 2017). Also, Jha and Schmidt (2017) reported that gradual increase in ammonia concentrations resulted in substantial decrease in the maximum growth rates of thermophilic microbes, and that final cessation of growth occurred at a total ammonia nitrogen concentration of 7.0 g.L^{-1} , whereas the same concentration did not have any noticeable effect on the mesophilic reactors. Kim *et al.* (2002) also found that thermophilic single-stage CSTR produced much higher VFA than the mesophilic reactors under the same condition of operation which agrees with the results obtained on the current study.

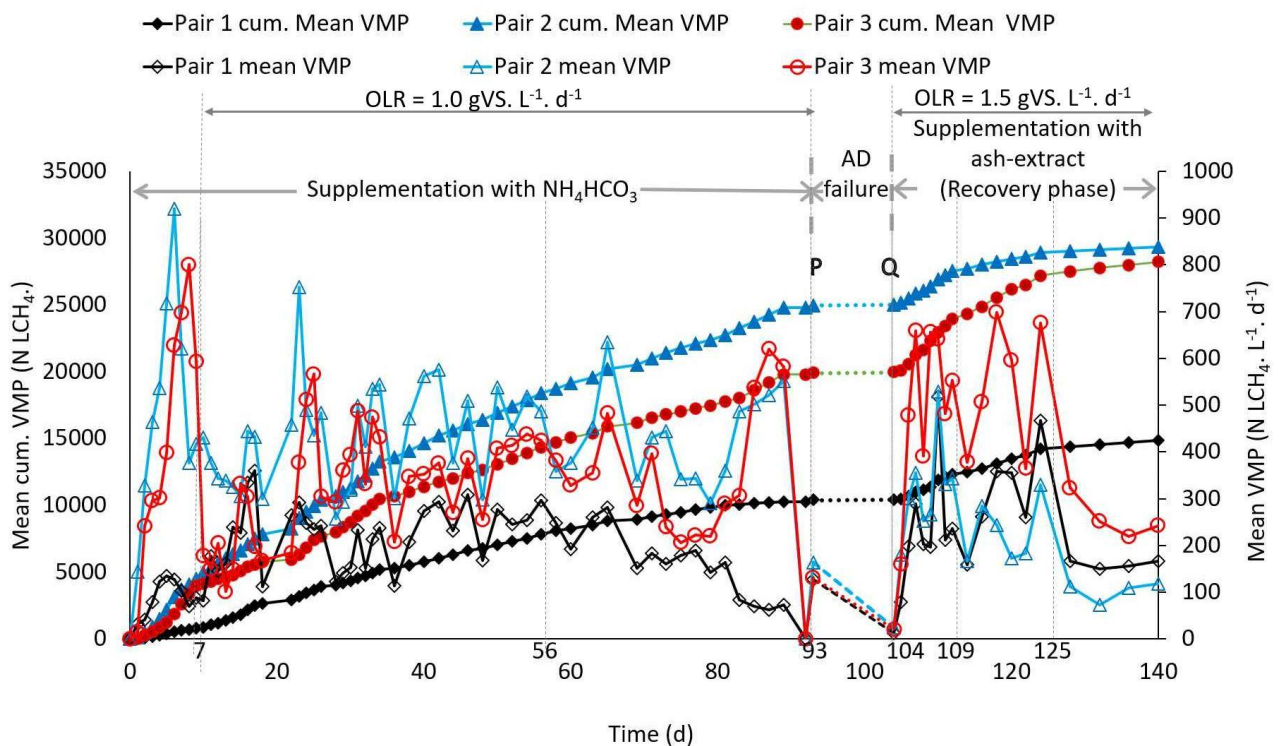


Figure 4-11 Mean cumulative volumetric methane production (cum. Mean VMP) and mean specific methane production (Mean VMP) in the Pair 1, Pair 2 and Pair 3 reactors over HRT. Other parameters are as defined in Figure 4-9.

Feeding of the reactors commenced again on day 104 (point Q in Figure 4-11), but now on regular daily (24 hourly) feeding intervals. This regular daily feeding was carried out for the 5 days without supplementation, but this did not improve the reactors conditions until supplementation of all the reactors with ash-extracts commenced on day 109, which together with the regular daily feeding, enhanced the recovery of the reactors. As evident in Figure

4-11 and Figure 4-12, the reactors, especially Pair 1 and Pair 3 started to recover gradually, but the mesophilic reactors (Pair 2) were very slow to recover. Also, the data contained in Table 4-7 implies that from day 109- 120, the SMP produced by Pair 3 reactors was 42% higher than the SMP from Pair 1 and 49% higher than that from Pair 2 reactors. Thus, during recovery (phase C), the Pair 1 (psychrophilic) and Pair 3 (thermophilic) reactors recovered faster than the Pair 2 (mesophilic) reactors. A comparison of the results obtained from the Pair 1, Pair 2 and Pair 3 reactors between the failing state (phase B) and recovery phase (phase C) also shows that during the recovery phase, the SMP improved by 24 and 27% respectively, compared to the SMP recorded during the AD process failing phase. However, the SMP from Pair 2 reactors further decreased by 41% during this recovery period suggesting that the mesophilic methanogens were much affected during the period of failure, which implies that the reactors would require a longer period to recover compared to the psychrophilic and thermophilic reactors as defined in Table 4-3. Similarly, within the same period (phase C), the VMP from the Pair 1 and Pair 3 reactors presented in Figure 4-11 were 7 and 49% respectively, higher than the VMP from the Pair 2 reactors, while the SMP from the Pair 3 reactors exceeded that of the Pair 1 reactors by 46%. The lag in the recovery of the mesophilic reactors (Pair 2) as obtained in the current study suggests that the reactors would require a much longer time to recover. This suggestion is in line with Bajpai (2017) who reported that slow-growing mesophilic methanogens require up to 130 h or 5 days for its regeneration. Also, because methanogens are slow-growing microbes, their ability remove VFA is the rate-limiting step in the AD process (Sykes & Skinner, 2015).

Further comparison between the irregular daily feeding phase (A) (day 25 - 58) and the process recovery phase (C) (day 107 - 140) also reveals that the SMP from the Pair 1, Pair 2 and Pair 3 reactors obtained during phase A were 37, 63, and 40%, respectively, higher than the SMP obtained from same reactors during recovery (phase C). The better performance of the Pair 2 (mesophilic reactors) compared to the Pair 3 (thermophilic reactors) may be due to the irregular daily feeding because thermophilic methanogens have been reported to be very sensitive to changes in operational conditions, and could easily suffer VFA or ammonia inhibition compared to the Pair 2 (mesophilic reactors)(Sani & Rathinam, 2018). However, during this same period, the VMP from the Pair 1 and Pair 3 reactors in phase C were 17 and 27% higher than the VMP obtained during phase A, which shows that feeding the AD reactors at regular feeding intervals were better than irregular feeding intervals. However, the VMP from the Pair 2 reactors during phase A was 63% higher than that of phase C probably because the mesophiles required more time either to grow or to adjust to the new feeding

mode. In the same way, a comparison between the VMP achieved in the Pair 1, Pair 2 and Pair 3 reactors during Phase B (failing phase) and phase C (recovery phase) also reveals that during the recovery phase, the VMP from the Pair 1 and pair 3 reactors increased by 40 and 27% respectively, compared to the VMP from the mesophilic reactors during the same period, which further decreased by 42%. The better performance of the Pair 3 (thermophilic reactors) over Pair 1 and Pair 2 reactors agrees with Gerardi (2003) who stated that biomethane production from the thermophilic AD reactors was considerably faster than in mesophilic reactors. It is also possible that the higher OLR in the reactor from day 57 – 140 (Table 4-1) favoured the thermophilic over the mesophilic reactors over that period, although this was more obvious during the recovery phase (Figure 4-10 and Figure 4-12). This possibly explains the results since thermophilic AD reactors are generally known to operate at a faster rate at shorter HRT and higher OLR compared to the mesophilic and psychrophilic AD reactors (Sani & Rathinam, 2018). Table 4-8 summarizes the results from correlation test and pair samples t-tests which were carried out to determine the effects of the different operating conditions and supplementation on the performances of the CSTR during phase A, B and C as defined in Figure 4-12

Table 4-8 Correlation tests and t-test statistics of paired mean SMP of the Pair 1, Pair 2 and Pair 3 CSTR at 95% confidence interval and significances of p-value (2-tailed)

Methane production	Paired CSTR	Paired Samples Test (23 - 58)		Paired samples test (Day 60 - 93)		Paired Samples Test (107 - 140)	
		R ²	p-value	R ²	p-value	R ²	p-value
Mean SMP	Pair 1 and Pair 2	0.59	0.000	-0.08	0.001	0.37	0.243
	Pair 1 and Pair 3	0.34	0.011	-0.30	0.037	0.54	0.000
	Pair 2 and Pair 3	0.59	0.005	0.81	0.014	0.75	0.000
Mean VMP	Pair 1 and Pair 2	0.82	0.000	0.01	0.000	0.71	0.431
	Pair 1 and Pair 3	0.47	0.000	-0.30	0.001	0.74	0.000
	Pair 2 and Pair 3	0.53	0.005	0.81	0.006	0.74	0.000

The results in Table 4-8 clearly shows that there were positive correlations between the all Pairs CSTR conditions compared during irregular daily feeding regime, phase A (day 23 – 58), and during the period of recovery phase C (day 109 – 120), and the period during which regular daily feeding was applied. However, Table 4-8 also reveals that during phase A and phase B, that the difference in the mean of the SMP or VMP between Pair 1 and Pair 2

reactors was statistically significant (p -value < 0.05), whereas during phase C, it was not statistically significant (p -value > 0.05). This was because during phase A and B, the all the reactors responded differently during the irregular daily feeding regime, and each pair of reactors maintained its pattern of response until the AD processes failed during phase B (Figure 4-12). However, during the recovering phase, due to the lag experienced by the Pair 2 (mesophilic) reactors, the mean values of their SMP and VMP were comparable to that of the Pair 1 (psychrophilic) reactors because the Pair 2 reactors suffered serious shock due to failure. However, for comparisons between Pair 1 and Pair 3, or Pair 2 and Pair 3, the difference between either the mean values of their SMP or VMP were statistically significant as expected. Also, during recovery (phase C), apart from a comparison between the SMP from Pair 1 and Pair 2 reactors, all other reactor paired compared (Table 4-8) showed stronger positive correlation compared to phase A and B. From these results, it is also obvious that due to the switch from irregular to regular feeding intervals, and the supplementation of ash-extracts, Pair 1 and Pair 3 reactors recovered faster and started functioning maximally, even better than their performances prior to their failure, whereas Pair 2 reactors only produced their best during phase A and B. These results suggest that the mesophilic reactors are more stable under irregular daily feeding interval condition compared to psychrophilic and

thermophilic.

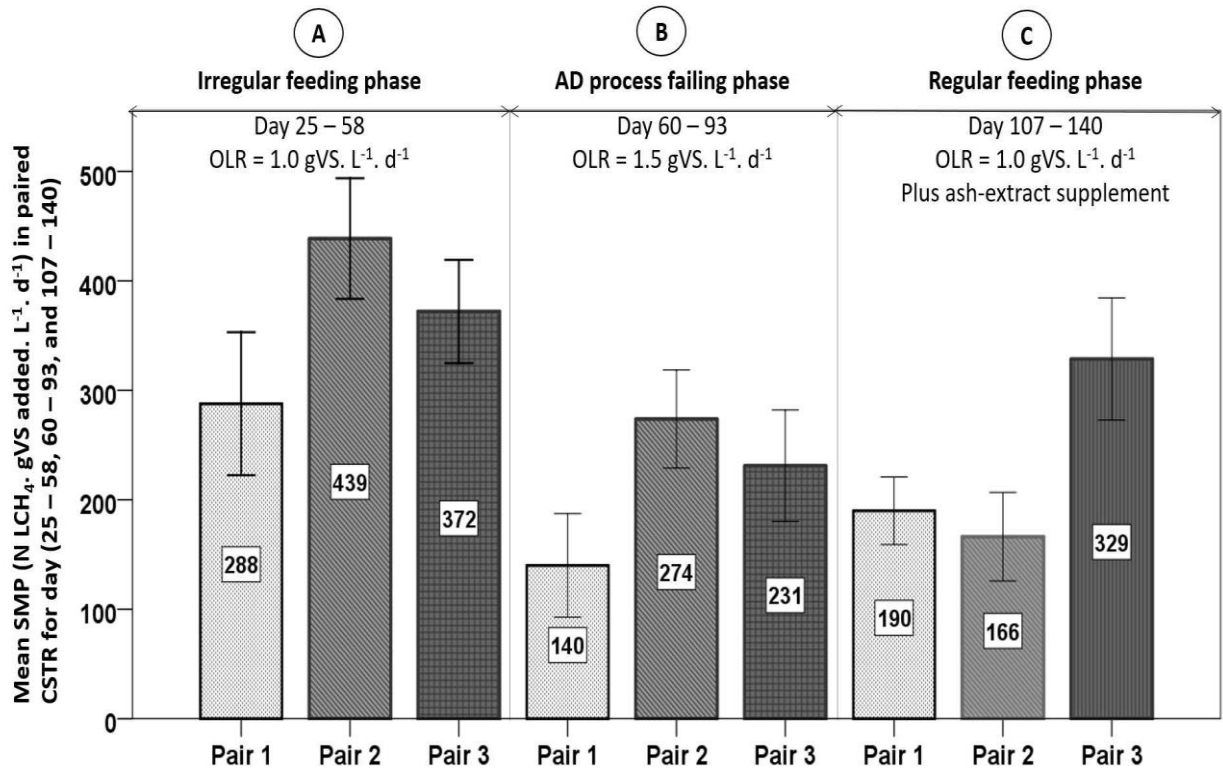


Figure 4-12 Comparison of the mean specific methane production (SMP) of CSTR operating at different temperatures, before, during and after the AD process failure. Error bars represent +/- 2 standard error (SE) of the mean. Other parameters as defined in Figure 4-9.

The poor performance of the Pair 2 (mesophilic) reactors in terms biomethane production during the recovery period (phase C) (Figure 4-12) suggests the toxicity of the reactors caused by their acidification due to high VFA concentration (Figure 4-6), which led to their failure may have led to substantial washing-out of the microbes, especially the methanogenic archaea. It may also be that the daily supplementation of the all the reactors with ammonium bicarbonate during phase A, reached a concentration which resulted to severe ammonia inhibition of the growth rate of the slow-growing methanogens and acetogens, and such might have limited methanogenesis leading to the accumulation of VFA in the first instance. This assumption could be true because according to Gerardi (2003), even though ammonium bicarbonate is the preferred bacterial nutrient source for nitrogen, and provides buffering capacity in the anaerobic digester, a high concentration of ammonium carbonate may cause free ammonia toxicity which is a cause of digester failure.

4.4 Conclusion

To compare the effects feeding interval on the specific methane production (SMP) and volumetric methane production (VMP) of CSTR during the anaerobic digestion of grass silage

Discontinuous feeding enhanced SMP in the mesophilic reactors more than the thermophilic and psychrophilic reactors. The mesophilic reactors were also more stable during irregular feeding intervals than the psychrophilic and thermophilic reactors. Prolonged operation with irregular feeding caused all the reactors to fail and although changing to a regular feeding interval improved VFA accumulation, the reactors did not recover fully. However, following the supplementation of all the reactors with EPB ash-extracts, recovery was observed, with a greater increase in methane production in the thermophilic and psychrophilic reactors compared to the mesophilic reactors. This suggests that the mesophiles in the mesophilic reactors showed a lower recovery rate after inhibition compared to the psychrophiles and thermophiles. Thus, the mesophilic reactors would require more time to recover completely.

To investigate psychrophilic anaerobic digestion of grass silage as a sustainable and affordable process in developing countries

The relatively good performance and rapid recovery of the psychrophilic reactors suggests that they could be utilised in low-income countries like Nigeria, but these reactors would require the addition of chemical supplements, such as biomass ash-extracts to counter the effects of high VFA formation and reactor instability.

To assess the effects of organic loading rate (OLR) on the SMP from grass silage at psychrophilic, mesophilic and thermophilic temperatures

Increasing the OLR of digesters during the period of irregular feeding reduced the SMP, and increased ammonia inhibition, VFA accumulation and odour (souring) of the AD reactors at all temperatures, and this increased instability caused the onset of process failure to occur despite daily supplementation of ammonium bicarbonate alkalinity.

To compare the recovery rates of psychrophilic, thermophilic and mesophilic CSTR after process failure following supplementation with biomass ash-extracts

After CSTR failure due to the increased instability caused by elevated OLR, supplementation of the reactors with EBP ash-extracts brought about a strong recovery of the psychrophilic

and thermophilic reactors by providing both adequate alkalinity and essential trace nutrients which presumably helped support bacterial growth and increased reactor performance.

The mesophilic reactors also started to recover, but at a slower rate compared to the other reactors. Therefore, low-cost alkaline-rich ash-extracts produced from agricultural biomass wastes were considered to be useful sources of alkalinity and trace nutrients for AD systems digesting lignocellulosic biomass as a mono-substrate.

Chapter 5 Effect of low-cost biomass extracts on the performance of thermophilic and mesophilic AD reactors during the co-digestion of tropical grass silage and cassava processing waste

Abstract

The current study involved the co-digestion of seven tropical grass silages and cassava processing wastes in four (4) pairs of 1 L continuously stirred tank reactors (CSTR) operating at upper mesophilic (40 °C) and lower thermophilic (55 °C) temperature conditions. The mesophilic reactors consisted of Pair 1 control reactors (unsupplemented) and Pair 2 reactors (supplemented with ash-extracts), whereas the thermophilic reactors were made up of Pair 3 control reactors (unsupplemented) and Pair 4 (supplemented with ash-extracts). All the reactors (Pair 1, 2, 3 and 4) were fed at the same organic loading rate of 2 gVS.L⁻¹.d⁻¹ and were operated at a 20 d hydraulic residence time (HRT). The ash-extract supplement was prepared by extracting the alkaline-rich soluble component of empty palm bunch ash (EPB), which also contained essential trace nutrients. The results showed that from day 35 – 60 (period of pseudo-steady-state operation), that the specific methane production from the Pair 1, Pair 2, Pair 3 and Pair 4 reactors were: 249.1, 316.6, 255.8 and 334.9 N mLCH₄.g⁻¹VS added. d⁻¹, respectively. These results signify that methane production increase by 21% in the Pair 2 (supplemented mesophilic reactors) and 24% in the Pair 4 (supplemented thermophilic reactors) compared to their un-supplemented control reactors, Pair 1 and Pair 3, respectively. The results also showed that an increase in temperature from mesophilic (40 °C) to thermophilic (55 °C) only increased the volume of methane produced by 5 %. Based on the results from the current study, overall, the performances of the upper mesophilic AD reactors and the thermophilic AD reactors were comparable. Therefore, the upper mesophilic temperature may be preferable to thermophilic temperature during the digestion of mixed lignocellulosic biomass feedstock and cassava process waste, especially due to the higher cost and instability associated with the operation of thermophilic AD reactors.

Keywords: *Anaerobic digestion, co-digestion of grass silages and cassava waste, upper mesophilic and lower thermophilic temperature, low-cost ash-extract, low-income countries*

Objectives

The objectives of the current study were:

- determine the specific methane production (SMP) from a biomass feedstock consisting of seven types of grass silage and cassava processing waste under upper mesophilic (40 °C) and optimum thermophilic (55 °C) temperatures conditions both with and without EPB ash-extract supplementation.

5.1 Materials and methods

All the biomass feedstocks and supplements used in the current study had been previously discussed in Section 2.4. Their preparation and storage have also been presented in Section 3.1. Details of the elemental composition of the feedstock and supplements have also been presented in Sections 3.2 and Table 3-2. The characteristics of the biomass feedstock and inoculum are presented in Table 5-2.

Table 5-1 Feedstock composition

Description	Composition
(a) Panicum and Pennisetum (50/50)	28.7%
(b) Speargrass	1.4%
(c) Guinea grass	1.3%
(d) Gamba grass	0.1%
(e) Panicum Max (early)	12.6%
(f) Pennisetum purpureum (late)	6.1%
(h) Ryegrass	1.4%
(i) Cassava peels	24.2%
(j) Cassava mill waste	24.2%
	100.0%

Table 5-2 Characteristics o the feedstock and inoculum

Analysis	Abbreviation	Inoculum	Feedstock
Moisture content (%)	MC	98%	10
Total solids (%)	TS	2%	90
Volatile solids (% in TS)	VS	60%	74
pH value	pH	7.91	x
Chemical oxygen demand (mg L ⁻¹)	COD	15,400	x
Ammonium nitrogen (mg L ⁻¹)	NH ₄ ⁺ - N	2,562.5	x

The physicochemical and monitoring parameters during the operation of the AD reactors included temperature, pH, alkalinity, volatile fatty acids, volatile solids removal and COD removal. These parameters were measured according to the relevant procedures in the Standard methods for the examination of water and wastewater (Section 3.1). The composition of methane gas in the biogas was determined by GC as outlined in Section 3.4.2.

5.1.1 Experimental set-up

The four (4) pairs of 1-L reactors used for this study were set-up as shown in Figure 5-1. Other details on how the components were fitted including the heating and temperature control are described in Section 3.5.



Figure 5-1 Mesophilic and thermophilic CSTRs showing overhead stirrers, a shaft with water-seal and gas-bags. Reactor vessels are obscured by gas bags. The working volume of each reactor was 1 L.

The reactors shown in Figure 5-1 were classified either as supplemented (with ash-extracts) or unsupplemented (no ash-extracts) reactors as summarised in Table 5-3. The details of the ash-extract supplement used, its preparation, analysis and chemical compositions are detailed in Section 3.2.1.

Table 5-3 Names and operating conditions of the CSTR

Reactors names	Mesophilic reactors (40 °C)	Thermophilic reactors (55 °C)
No supplement	Pair 1 Control (R1 and R2)	Pair 3 Control (R5 and R6)
Ash- extract supplementation	Pair 2 (R3 and R4)	Pair 4 (R7 and R8)

All the AD reactors (Pair 1, 2, 3 and 4) were acclimatized from day 1- 6 with daily feeding at an organic loading rate of $2.0 \text{ gVS.L}^{-1} \cdot \text{d}^{-1}$ without sampling. After this period of acclimatization, all the reactors were fed uniformly at that same OLR from day 7 – 60. Thus, at an HRT of 20 d, it means that the rate of volatile solids (VS_{in}) in the inflow (Q_{in}) was $2 \text{ g.L}^{-1} \cdot \text{d}^{-1}$, implying that inflow (during feeding) was $50 \text{ mL} \cdot \text{d}^{-1}$, which was equal to the volume of samples removed from each reactor daily or outflow (O_{out}).

5.1.2 Data analysis

Descriptive statistics were carried out on all the data obtained in the current study using Microsoft Excel and IBM Statistical Package for Social Sciences (SPSS) version 24. The correlation and statistical significances (paired samples t-tests) between selected sets of reactors pairs such as: control mesophilic (Pair 1) and control thermophilic (Pair 3) reactors; control mesophilic (Pair 1) and supplemented mesophilic (Pair 2), supplemented mesophilic (Pair 2) and supplemented thermophilic (Pair 4), and control thermophilic (Pair 3) and supplemented thermophilic (Pair 4) reactors. More details on the data analysis are given in Section 3.7.

5.2 Results and discussion

5.2.1 Solids composition, destruction and organic loading rate

A sample from the mixed biomass feedstock used for the current study was made up of 90% total solids (TS), 74% of volatile solids as %TS and 10% moisture content (MC). Results from the elemental analysis carried out using 1 g dried sample from the feedstock have been described in Section 3.2.1. Some of these results including the carbon-to-nitrogen (C: N) ratio in each feedstock and are summarised in Table 5-2 and Table 5-4.

Table 5-4 Elemental composition of the biomass feedstock components used to feed AD reactors

Sample ID	C (%)	H (%)	O (%)	N (%)	S (%)	C:N ratio
Spear grass	43.47	6.57	35.72	1.92	0.17	23:1
Gamba grass	44.46	6.79	37.90	2.39	0.19	19:1
Elephant grass	37.92	6.23	33.67	2.53	0.15	15:1
Rice straw	34.01	5.24	31.22	2.35	0.11	15:1
Guinea grass	41.58	6.95	36.58	1.79	0.19	23:1
Cassava waste	41.54	6.60	49.73	0.187	0.137	223:1

Among the nutrients contained within the biomass feedstock, carbon provides the energy needed by the microbes for metabolic activity and growth, while nitrogen is utilized for building their cell structure (Khoiyangbam *et al.*, 2011). Microbes also require small quantities of phosphorus, sulphur, sodium, calcium, potassium, magnesium, chlorine and

several trace nutrients such as iron, zinc, molybdenum, nickel, cobalt, selenium, vanadium, manganese, copper for their metabolism (Khoiyangbam *et al.*, 2011; Malik *et al.*, 2013; Wellinger, 2013). Details of the composition of some of these biomass feedstocks, including their nutrients, metals and trace nutrient contents were earlier presented in Table 3-3. In the current study, the phosphorus (P) contained in each of the biomass feedstocks was not determined. However, P content and requirement has been determined by other researchers and the empirical relationship C:N:P:S ratio of 600:15:5:3 is reported as being the adequate nutrient ratio for enhancing methane production (Khoiyangbam *et al.*, 2011; Malik *et al.*, 2013). Some of the grass silage components in Table 5-4 have C:N ratios within the optimum range, whereas others like cassava have a very high carbon content compared to nitrogen, which implies that co-digestion improves the nutrient balance of the AD biomass feedstocks (Section 2.10). Thus, why the mono-digestion of some grass silage fails when digested anaerobically as a sole substrate, could be because of insufficient trace nutrient contents in the grass in concentrations required to support anaerobic process. It could also be as a result of the starvation of anaerobic microbes of nitrogen required for their protein formation, energy synthesis and metabolism due to early exhaustion of the small contents of nitrogen in the grass by microbes or by volatilization.

Figure 5-2 shows the mean percentage reduction in volatile solids in the Pair 1 (Control), Pair 2, Pair 3 (Control) and Pair 4 reactors. Between day 1 – 33, the VS reduction in the mesophilic reactors Pair1 (Control) and Pair 2 (supplemented) varied between 49 to 67 %, and 50 – 69 % respectively, while for the thermophilic Pairs 3 (Control) and Pair 4 (supplemented), it varied between 53 – 66%, and 52 – 69%, respectively. However, from day 34 – 60, Pair 1 (Control), Pair 2, Pair 3 (Control) and Pair 4 reactors achieved a mean of VS removal of 61, 67, 64 and 69% respectively.

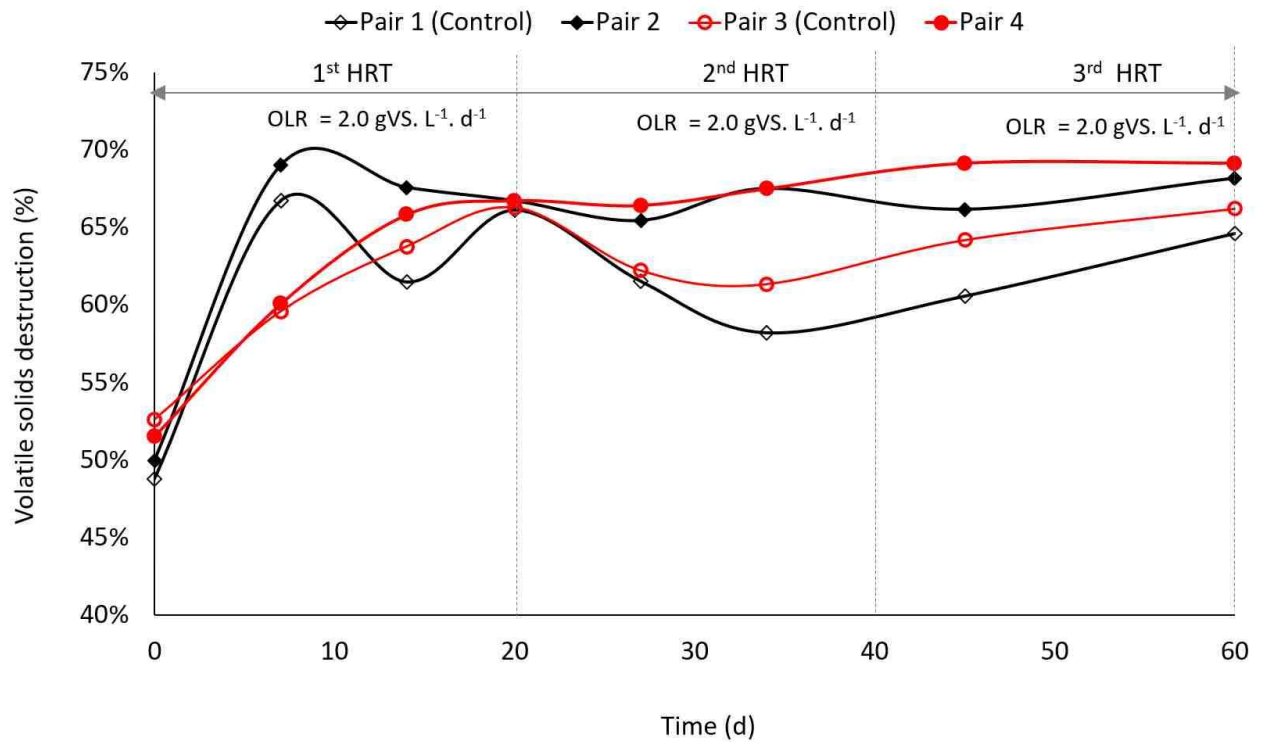


Figure 5-2 Volatile solid reduction in the Pair 1 (Control), Pair 2 (supplemented), Pair 3 (Control), and Pair 4 (supplemented) CSTR over time. Table 5-3 contains more details on CSTR classification and supplementation

The periods of low VS removal in the thermophilic reactors, Pair 3 between day 1 – 10 as shown in Figure 5-2, coincided with the lag phase in the reactors, and may represent when the thermophiles were becoming acclimatized to their new operating temperature because the inoculum was previously incubated at the upper mesophilic temperature due to equipment constraints. The better performance of the mesophilic reactors during the same initial start-up period clearly demonstrates the importance of acclimatizing inoculum at the actual operating temperature before the startup of anaerobic digestion. From Figure 5-2, it is also evident that from day 34 – 60, after all the reactors had become more stable, that the thermophilic reactors achieved higher volatile solids (VS) removal than the mesophilic reactors. This period of higher VS removal in the thermophilic reactors also corresponds with the period of higher methane production in these reactors, compared to the mesophilic reactors, as shown in Figure 5-5. This was expected because thermophilic AD processes have been reported to achieve better volatile solids removal than mesophilic processes because the rates of biological activities are faster at the higher temperatures (Sani & Rathinam, 2018; Turovskiy, 2006). However, the difference between the % VS destroyed in the mesophilic and thermophilic reactors was comparable possibly due to the closeness of their operating temperatures.

5.2.2 pH of pilot scale CSTR

The pH is a pivotal parameter which affects the performance of the anaerobic digestion process significantly due to its influence on the solubility of the substrate as well as the microbial community (Bajpai, 2016). According to Korres (2013), the pH inside the AD plant depends on the concentrations of VFAs, bicarbonate, alkalinity, retention time, loading rate and the fraction of CO₂ in the digester. The mean of daily pH of Pair 1 (Control), Pair 2 (supplemented), Pair 3 (Control), and Pair 4, reactors, from day 1 – 60 is shown in Figure 5-3.

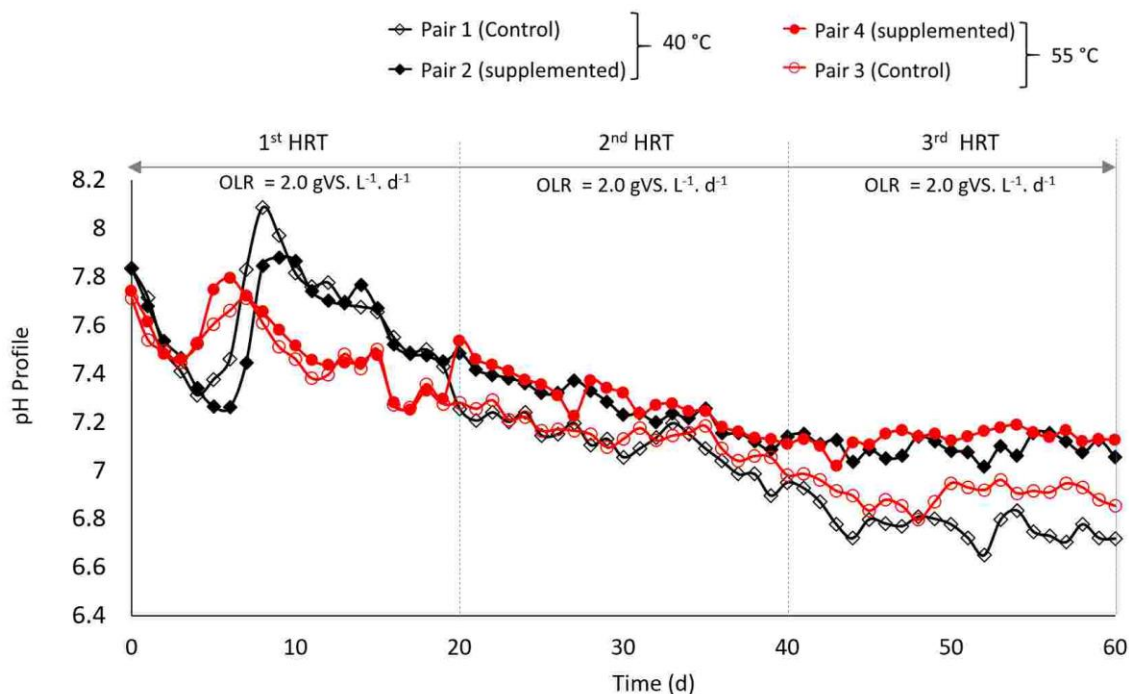


Figure 5-3 Mean pH in the Pair 1 (Control) unsupplemented and Pair 2 (supplemented) mesophilic, and Pair 3 (Control) unsupplemented and Pair 4 (supplemented) thermophilic CSTR over time. Supplementation involved the addition of ash-extract to CSTR.

From Figure 5-3, both the Pair 1 (Control) and Pair 2 (supplemented) mesophilic AD reactors had a starting pH value of 7.8, while the thermophilic AD reactors Pair 3 (Control) and Pair 4 (supplemented) had a starting pH of 7.7. The pH inside both Pair 1 (Control) and Pair 2 reactors dropped to an initial minimum value of 7.3 on day 4 and day 6 respectively.

Similarly, for the thermophilic AD reactors, on day 3, the starting pH inside both the Pair 3 (Control) and Pair 4 thermophilic reactors dropped to an initial minimum value of 7.4 and 7.3, respectively. These periods of pH reduction coincided with the period of acclimatization during which the feedstock, which was slightly acidic, was added consistently at an OLR of 2.0 g VS. L⁻¹.d⁻¹ without sampling or dilution. However, on the commencement of feeding from day 5 onwards, the pH increased to peak values of 8.1 on day 8 for Pair 1 (Control) and

to pH value of 7.9 on day 9 for the Pair 2 reactors, due to the dilution of acids inside the reactors as the new feed displaced excess acids inside the reactor by simple dilution. Similarly, peak pH values of 7.7 and 7.8 were recorded on day 7 and day 6 for the thermophilic Pair 3 (Control) and Pair 4 reactors. Figure 5-3 also shows that the pH in the thermophilic reactors were closer to the optimum for AD (pH 7) than in the mesophilic reactors, apart from day 1 – 9 when the pH of the mesophilic reactors was higher, probably because the thermophilic bacteria were acclimatizing to their new temperature as the inoculum was previously acclimatized at the mesophilic temperature prior to start-up. The pH reduction in the thermophilic digesters may have also been caused by rapid acidogenesis due to faster feedstock degradation rate at the high temperature, which may have caused an increase in VFA concentration, especially as there was no removal of digestate (giving dilution) during day 1 – 5 (section 5.1.1). However, after day 9, the pH in the Pair 1 (Control), Pair 3 (Control), Pair 2 and Pair 4 reactors started to decrease gradually over the time and became relatively stable on day 37. From day 37 – 60, the mean pH in the Pair 1 (Control), Pair 2, Pair 3 (Control) and Pair 4 reactors were 6.8, 7.1, 6.9 and 7.1 respectively.

Figure 5-3 also shows that the pH of the Pair 3 (Control) (non-supplemented thermophilic) was slightly better than that of the Pair 1 (Control), which is the unsupplemented mesophilic, while pH of Pair 3 (supplemented thermophilic) was the same as Pair 2 (supplemented mesophilic) reactors. These results suggest that the thermophilic AD reactors performed better in terms of pH stability within the optimum range compared to the mesophilic reactors, under identical operating conditions. The pH in the supplemented reactors (Pair 2 and Pair 4) was also more favourable than the pH in the non-supplemented reactors, which suggest that the addition of ash-extracts provided substantial amounts of alkalinity to the reactors. This maintenance of a favourable range of pH 7.0 – 7.2 in Pair 2 and Pair 4 reactors, coincided with higher and steadier volumetric methane production in these reactors compared to their corresponding Pair 1 (Control) mesophilic and Pair 3 (Control) thermophilic reactors (Figure 5-3). This improvement and steady volumetric methane production achieved in the current study supports the results from other researchers who have reported that operating AD reactors at pH range 7.0 – 7.2 enhances the performance of the methanogenic archaea responsible for methane production (Bitton, 2005; Schön, 2010).

5.2.3 Variation in COD and ammonium-Nitrogen of pilot scale CSTRs

Figure 5-4 shows variations in the concentrations of total chemical oxygen demand (COD_T) and concentration of ammonium nitrogen (NH₄⁺-N) in all reactor pairs from day 1 – 60. The mean COD_T in the Pair 1 (Control) unsupplemented and Pair 2 (supplemented) mesophilic reactors were 15,082 and 12,832.3 mg.L⁻¹, respectively, and for the unsupplemented Pair 3 (Control) and supplemented (Pair 4) thermophilic AD reactors, the mean COD_T was 14,291.9 and 12,729.4 mg.L⁻¹, respectively. It is also apparent that the COD_T content in the thermophilic reactors was slightly lower than their corresponding mesophilic reactors, which implies that thermophilic reactors were slightly more efficient in terms of COD_T removal. Results from the statistical correlation analysis showed that there was no correlation between the COD_T content in the Pair 1 (Control) and Pair 2 reactors ($R^2 = 0.041$). However, the COD_T of Pair 4 and Pair 3 (Control) was positively correlated ($R^2 = 0.88$). However, in all comparisons, a paired sample t-test showed that there was no statistically significant difference ($P > 0.05$) in the mean COD_T between each pair of reactors compared.

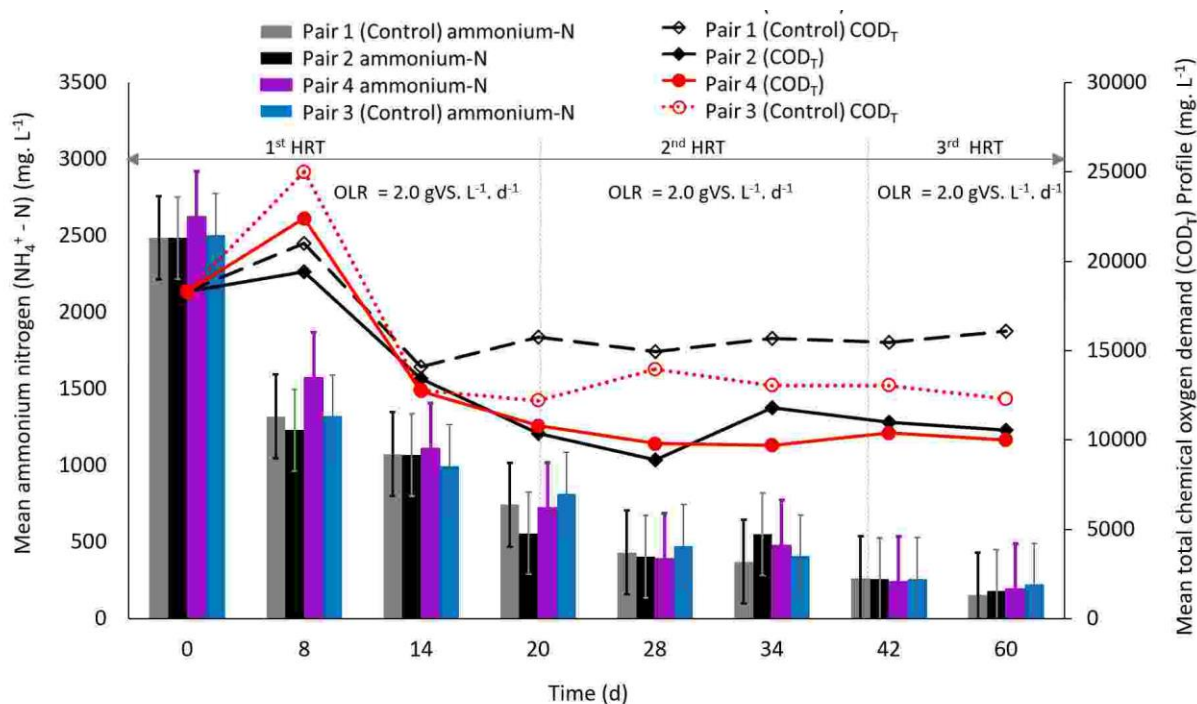


Figure 5-4 Mean of Total Chemical Oxygen Demand (COD_T) and Ammonium-Nitrogen (NH₄-N) concentration inside the (Pair 1 (Control) unsupplemented and Pair 2 (supplemented) mesophilic and (Pair 3 (Control) unsupplemented and Pair 4 (supplemented) thermophilic CSTR over time. Values are the means from duplicate reactors within a pair.

There were also relationships between the COD_T contents in the reactors and volatile solids removal such that the amount of COD_T in each reactor varied depending on the percentage of

volatile solids destroyed (Figure 5-2). The rapid increase in the concentration of COD_T recorded in the current study between day 1 - 7 coincided with the period of VS accumulation during acclimatization which was previously discussed in Section 5.2.1. The thermophilic AD reactors which achieved slightly higher volatile solids destruction were found to have correspondingly lower COD_T contents inside the reactors which shows that COD_T was converted more effectively to biogas by the anaerobes. Similarly, reactors with high COD_T contents also coincided with low VS destruction and lower biogas production (Figure 5-2). These results suggest that the value of the COD_T could be used to predict the rate of VS destruction during the anaerobic digestion process, especially where the soluble COD was not estimated.

The concentration of ammonia-N (day 0 - 60) in the reactors decreased gradually over time (Figure 5-4). In the mesophilic reactors, the concentration of NH₄⁺-N in the Pair 1 (Control) and Pair 2 reactors decreased from 2,487.5 - 156.3 mg. L⁻¹ and 2,486.3 - 182.5 mg. L⁻¹, respectively. Similarly, during the same period, the concentration of NH₄⁺-N in the thermophilic Pair 3 (Control) and Pair 4 (supplemented) reactors decreased from 2,506.3 - 223.8 mg. L⁻¹ and 2,625.0 - 195 mg. L⁻¹, respectively. The overall (day 1 - 60), the mean of the methane produced by the Pair 1 (Control), Pair 3 (Control), Pair 2 (supplemented mesophilic) and Pair 4 (supplemented thermophilic) reactors were 856.1, 843, 876.1 and 918 mg.L⁻¹, respectively. The summary statistics for the t-test and correlation values used to analyze the relationship between the ammonium-N profile between different pairs of reactors are presented in Table 5-5.

Table 5-5 Variations in mean ammonium-N concentration in AD reactors using Paired Sample Statistical Correlations and T-tests at 95% confidence interval

Reactors/Ammonium -N	Paired Correlation		Paired samples T-test
	R ²	Sig.	Sig. (2-tailed)
Pair 1 (Control) mesophilic and Pair 3 (Control) thermophilic	0.998	0.00	0.27
Pair 2 (supplemented mesophilic) and Pair 4 (supplemented thermophilic)	0.990	0.00	0.16
Pair 1 (Control) unsupplemented and Pair 2 (supplemented) mesophilic	0.991	0.00	0.73
Pair 3 (Control) unsupplemented and Pair 4 (supplemented thermophilic)	0.993	0.00	0.35

Data from Table 5-5 shows that there was a high correlation ($R^2 > 0.99$) between the ammonium-N contents in pairs of reactors, and that any small differences observed between the individual reactors were not statistically significant ($p > 0.05$). However, despite the comparable performances between the mesophilic and thermophilic reactors, it is obvious from Figure 5-4 that the thermophilic AD reactors contained slightly higher ammonium-N concentration than the mesophilic AD reactors. These higher concentrations of ammonium-N found in the current study are consistent with the observations of Ping and Tong (2015), who reported that thermophilic AD processes produce higher molecular NH_3 . However, according to these authors, mesophilic reactors are preferable to thermophilic reactors because the mesophilic reactors give greater process stability and are also more tolerant to a higher concentration of ammonia.

5.2.4 Specific methane production and cumulative methane production in CSTR under pseudo-steady-state conditions

In the current study, comparing the rate of methane productivity between two reactors was one of the key indicators used to establish improvements arising from ash-extract supplementation. The specific methane production and the cumulative methane production

from the Pair 1 (Control), Pair 2 (supplemented) mesophilic and the Pair 3 (Control) and Pair 4 (supplemented) thermophilic reactors from day 1 – 60 are presented in Figure 5-5.

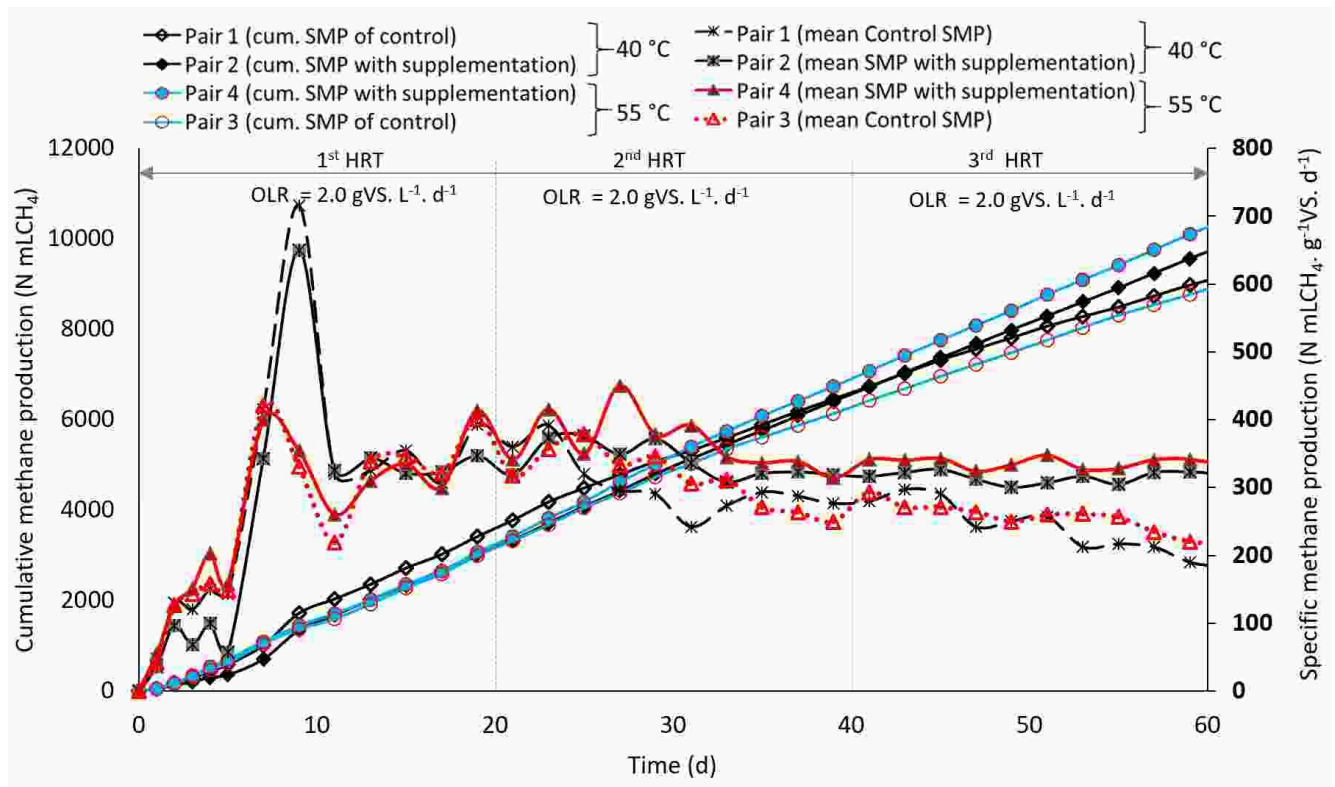


Figure 5-5 Mean specific methane production from mesophilic Control 1, Pair 1(supplemented) and the thermophilic Control 2 and Pair 2 (supplemented) CSTR over time

Figure 5-5 shows that the mean specific methane production (SMP) from the Pair 1 (Control) and Pair 2 (supplemented) mesophilic reactors from day 35 – 60, when the reactors achieved relatively stable operation, were 249.1 and 316.6 N mL CH₄.g⁻¹VS added.d⁻¹, respectively. Similarly, during this same period, the thermophilic Pair 3 (Control) and Pair 4 (supplemented) thermophilic reactors produced cumulative methane volume that was 24% higher than the unsupplemented Pair 3 (Control) thermophilic reactors. Another comparison between the Pair 2 (supplemented mesophilic) and Pair 4 (supplemented thermophilic) reactors from day 35 – 60 also showed that the cumulative SMP from the thermophilic reactors was only 5% higher than that of the mesophilic reactors. A comparison between the Pair 1 (Control) mesophilic and Pair 3 (Control) thermophilic reactors showed that the SMP from the thermophilic reactors was also 3% higher compared to than the SMP from the mesophilic reactors. These SMP

results corresponded with the variation in pH, VS and COD_T removal discussed in Sections 5.2.1 - 5.2.3). Even at a wider temperature range of 35 °C for mesophilic and 55 °C for thermophilic AD process, a recent study by Capson-Tojo *et al.* (2017) found that despite achieving higher hydrolysis rates in the thermophilic reactors in terms of high concentration of soluble COD, that such did not improve the methane yield of thermophilic reactors over the mesophilic conditions. Therefore, it possible that the improvement in the biomethane production observed in the current study in both the mesophilic and thermophilic reactors was influenced by the addition of the EPB ash-extracts. Singh *et al.* (2015) have reported that thermophilic AD process can achieve 50 – 100 % higher SMP rate than a mesophilic AD, however, in the current study, a paired sample t-test comparison between the thermophilic and mesophilic reactors showed that the effect of temperature on the cumulative methane production was not statistically significant ($p > 0.05$). The slight improvement of the thermophilic reactors over the mesophilic as found in the current study confirms the findings of Streitwieser (2017) which compared the effects of co-digesting fruit wastes and manure under thermophilic and mesophilic temperatures, which found that thermophilic AD reactors produced more biogas/methane than the mesophilic reactor under a constant organic loading rate of 1.5 kg COD. m⁻³. d⁻¹ at an HRT of 16 days. In another study involving the co-digestion of winery wastewater sludge and wine lees Da Ros *et al.* (2017) found that trace nutrients, especially iron, cobalt and nickel supplements improved the stability of the thermophilic AD reactors at 55 °C. Thus, since thermophilic AD reactors are well known for instability (Gerardi, 2003; Korres, 2013), the current study has gone a way forward to enhance our understanding that these trace nutrients needed to optimize the thermophilic process, including material for providing adequate alkalinity for the process, can be sourced from low-cost ash-extracts.

5.3 Conclusion and recommendation

To determine the specific methane production (SMP) from a biomass feedstock consisting of seven types of grass silage and cassava processing waste under upper mesophilic (40 °C) and optimum thermophilic (55 °C) temperatures conditions both with and without EPB ash-extract supplementation.

The unsupplemented thermophilic reactors showed only a slightly higher (5%) SMP than the unsupplemented mesophilic reactors, but the difference was not statistically significant ($p >$

0.05), and this therefore implies that it may be not be economically viable to operate AD reactors on a mixed grass silage feedstock at thermophilic temperatures.

The SMP of the ash-extract supplemented mesophilic and thermophilic reactors was found to be 21 and 24% greater, respectively, than the equivalent unsupplemented reactors, showing the efficacy of ash-extract supplements in enhancing methane production from grass silage feedstocks. Furthermore, this suggests that biomass ash-extracts could serve as an alternative low-cost source of alkalinity and trace nutrients that can improve the AD processes.

Chapter 6 Effect of 10 °C steps in operating temperature and increasing OLR on Specific Methane Production (SMP) during the AD of a mixed lignocellulosic feedstock

Abstract

Three pairs of 5 L CSTR were used to investigate the effects of 10 °C steps in operating temperature and increasing organic loading rate (OLR) on the specific methane potential (SMP) and volumetric methane production (VMP) from mixed lignocellulosic biomass feedstock. The reactors, Pair 1 (27 °C), Pair 2 (37 °C) and Pair 3 (47 °C) were acclimatized for 6 days with an OLR of 1.0 gVS.L⁻¹.d⁻¹, and then operated for three consecutive HRT cycles (1 HRT cycle = 20 d), with daily feeding at an OLR of 1.0, 1.25 and 1.5 gVS L⁻¹.d⁻¹ during the 1st, 2nd and 3rd HRT cycles, respectively. A mixture of ash-extract supplements prepared from empty palm bunch and empty plantain peels (EPP) was used to maintain the pH inside all the reactors within the optimum range pH 6.94 - 7.07 between day 31 and day 58, and this supplementation was only carried out whenever there was a decrease in any of the reactors below the set pH range. All the reactors were able to attain a pseudo-steady-state condition of operation during the 2nd HRT cycle (day 26 – 46), and during this period, the mean SMP for Pair 1, Pair 2 and Pair 3 reactors were 261.6, 323.7 and 303 N mL CH₄.g⁻¹VS added. d⁻¹, respectively. Similarly, the mean volumetric methane production (VMP) for the Pair 1, Pair 2 and Pair 3 reactors were 331.4, 367.9 and 385.5 N mL CH₄.L⁻¹. d⁻¹, respectively. These results signify a 24% and 16% increase in the SMP from the Pair 2 (mesophilic) and Pair 3 (thermophilic) reactors, respectively, compared to the Pair 1 (psychrophilic) of reactors, and a 6% increase of SMP of Pair 2 reactors compared to the Pair 3 reactors. Conversely, during this same 2nd HRT, the VMP from the Pair 3 reactors was higher than that of Pair 2 by 5%, which shows that increase in OLR from 1.0 to 1.25 gVS.L⁻¹.d⁻¹ favoured the VMP in the Pair 3 reactors compared to Pair 1 and Pair 2 reactors. Also, the methane contents in biogas produced in Pair 1, Pair 2 and Pair 3 reactors during the 2nd HRT were 57.7%, 57.2% and 56.0%, respectively. During the 3rd HRT cycle (day 47 – 66), increase in OLR from 1.25 to 1.5 gVS.L⁻¹.d⁻¹ resulted to the production of methane gas (SMP) from Pair 1, Pair 2 and Pair 3 reactors with mean of 204.4, 315.0, 312.2 N mL CH₄.g⁻¹VS added.d⁻¹, while the mean VMP were 306.7, 392.2 and 468.3 N mL CH₄.L⁻¹.d⁻¹, respectively. These results show that the SMP from the Pair 2 reactors were only 1% higher than that of Pair 3 reactors, whereas the SMP from each of Pair 2 and Pair 3 reactors was 35% higher than the SMP from the Pair 1 reactors.

Similarly, the mean VMP from Pair 2 and Pair 3 reactors were 22% and 35% respectively, higher than Pair 1 reactors, while the VMP from the thermophilic reactors were 16% higher than that of the Pair 2 reactors. Also, the methane contents in the biogas produced in the Pair 1, Pair 2 and Pair 3 reactors during the 3rd HRT cycle were 50.8%, 55.7% and 56.6% CH₄ content, respectively. Overall, these results show that increase in OLR in the Pair 1, Pair 2 and Pair 3 reactors, favoured volumetric methane production in the Pair 3 (thermophilic reactors) compared to the Pair 1 (psychrophilic) and Pair 2 (mesophilic reactors). It also shows that both Pair 2 and Pair 3 reactors achieved comparable SMP under each HRT cycle. The decrease in the methane contents in the biogas and SMP during HRT shows that stoppage of supplementation from day 59 – 60 during the 3rd HRT led to a decrease in the stability and efficiency of all the CSTR. Furthermore, the 10 °C difference in temperature between Pair 1 and Pair 2, or between Pair 2 and Pair 3 reactors did not double either the process rate or volume of methane produced. Finally, a mixture of ash-extract supplements from ashes from empty palm bunch and empty plantain peel (EPP) can be used effectively as AD supplements to improve both SMP and VMP, as well as to optimize the methane content of the biogas.

Keywords: *Anaerobic digestion, mixed lignocellulosic feedstock, specific methane production (SMP), volumetric methane production (VMP), 10 °C difference in temperature, ash-extract supplement.*

OBJECTIVES

The objectives of the current study were:

- To determine the effect of 10 °C degree differences in operating temperature of psychrophilic, mesophilic and thermophilic reactors on the specific methane production (SMP) and volumetric methane production (VMP) during the AD of a mixed lignocellulosic biomass feedstock.
- To determine the effect of increasing the organic loading rate on the SMP, VMP and reactor stability of psychrophilic, mesophilic and thermophilic reactors during the AD of a mixed lignocellulosic biomass feedstock.
- To investigate the effect of adding ash-extract supplements produced from empty palm fruit bunch (EPB) and empty plantain peels (EPP) on maintaining AD process stability and efficiency of reactors during the AD of a mixed lignocellulosic biomass feedstock.

6.1 Materials and methods

6.1.1 Materials

The biomass feedstock used in the current study has been described in

Table 5-1. The characteristics of the biomass feedstock are presented in Table 6-1. The source of the inoculum has been described in Section 3.3. The empty palm bunch and empty plantain peels (EPP) which were used to prepare the ash-extract supplement have also been described in Section 3.1. The properties and methods of preparation of these ash extracts are presented in Section 3.2.

Table 6-1 Characteristics of the mixed biomass feedstock

Analysis	Abbreviation	Inoculum	Feedstock
Moisture content (%)	MC	89%	10
Total solids (%)	TS	1%	90
Volatile solids (% in TS)	VS	61%	74
pH value	pH	7.74	x
Chemical oxygen demand (mg L ⁻¹)	COD	18,752	x
Ammonium nitrogen (mg L ⁻¹)	NH ₄ ⁺ - N	1,617.5	x

The letter x means that the parameter was not determined.

6.1.2 Methods

In the current study, six continuously stirred tank reactors (CSTR), each with capacity of 5 L, were used to study the effects of different operating temperatures (at 10 °C intervals) on the anaerobic digestion of a mixed lignocellulosic feedstock (prepared from selected tropical grass silages and cassava waste) at 20 d HRT. The inoculum was acclimatized to the biomass feedstock by feeding 1.0 gVS.L⁻¹. d⁻¹ for 6 days without removing any sample from the reactors. The CSTRs were set up in duplicates as described in Section 3.5. The Pair 1 reactors (R1 and R2) were operated at 27 °C; Pair 2 (R3 and R4) were operated at 37 °C; while the Pair 3 (R5 and R6) were operated at 47 °C, representing upper psychrophilic, upper

mesophilic and lower thermophilic temperatures, respectively. All the reactors were fed at an organic loading rate of 1.0, 1.25 and 1.5 gVS.L⁻¹. d⁻¹ during 1st, 2nd and 3rd HRT cycles, respectively. Due to pH decrease to pH value < 7 in the Pair 1, Pair 2 and Pair 3 reactors on day 30, a mixture of ash-extracts from empty palm fruit bunch and empty plantain peels (EPP) was used to provide buffering for the reactors from day 31 – 58. No buffer or ash-extract supplements were added between day 59 – 66 of the 3rd HRT cycle. Physical and chemical characteristics of the reactors and their contents including temperature, pH, solids (VS and TS), total chemical oxygen demand (COD_T), ammoniacal nitrogen (NH₄⁺-N), total Kjeldahl nitrogen (TKN), volatile fatty acids (VFAs) as described in the standard methods for the examination of water and wastewater (APHA., 2005) (Table 3-8 in Section 3.5). The biogas volume and composition were monitored and measured following the methods described the German Standard Protocol (VDI. 4630, 2006) (Section 3.4.2).

Table 6-2 Operating conditions, Organic loading rates, hydraulic retention time (HRT) and dosing days

Reactor	Common name	Temperature (°C)	Acclima- tization	1 st HRT	2 nd HRT	3 rd HRT
			(day 0 - 6)	(day 7 - 26)	(day 27 - 46)	(day 47 - 66)
			Organic Loading rate (kgVS. L ⁻¹ . d ⁻¹)			
R1 and R2	Pair 1	27	1.0	1.0	1.25	1.5
R3 and R4	Pair 2	37	1.0	1.0	1.25	1.5
R5 and R6	Pair 3	47	1.0	1.0	1.25	1.5

Note: Supplementation of Pair 1, Pair 2 and Pair 3 reactors with ash-extract were carried out from day 31 – 58 only.

6.2 Results and discussion

6.2.1 Temperature and pH

Pair 1, Pair 2 and Pair 3 reactors were operated at 27, 37 and 47 °C (Section 6.1.2), respectively, and temperatures fluctuated within ± 0.5 °C of the setpoint. A previous study by Drogg (2013) has reported that the recommended temperature variation during the AD process should be < 1 °C for thermophilic reactors and within 2 – 3 °C for mesophilic reactors.

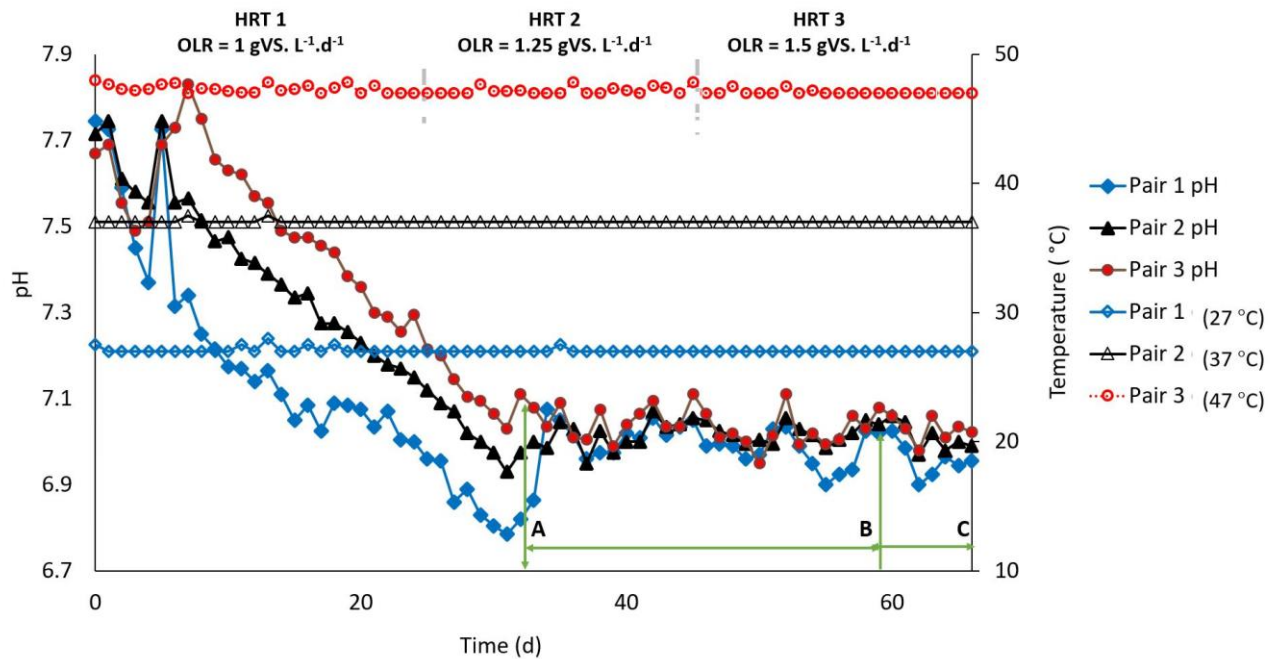


Figure 6-1 Variation of pH in the Pair 1, Pair 2 and Pair 3 reactors under psychrophilic (27°C), mesophilic (37°C) and thermophilic (47°C) temperature conditions and organic loading rate over time. Values are the means from duplicate reactors within a reactor pair, green arrows indicate periods of supplementation with ash-extract (A - B), and no supplementation (O - A and B - C)

However, no noticeable effect was observed due to these small temperature fluctuations.

From day 1 – 30, the pH recorded inside the Pair 1 reactors varied between 6.85 – 7.74, with a mean pH 7.16, Pair 2 reactors varied between pH 6.72 - 7.75 with a mean pH 7.34, while Pair 3 reactors varied between pH 6.91 - 7.79 with a mean pH 7.44 (Figure 6-1). The standard deviation of pH values in all reactors ranged between 0.22 – 0.26. Within the 2nd HRT (day 31 – 46), the mean pH recorded in all reactors became much more constant with values of pH 6.98, 7.01 and 7.05 in Pair 1, Pair 2 and Pair 3 reactors, respectively. This was achieved due to the addition of biomass extracts which provided enough alkalinity to maintain the pH within the optimum (near neutral) range from point A to B (Figure 6-1). The ash-extract supplement was only dosed into of the Pair 1, Pair 2 and Pair 3 reactors whenever the pH in any of the reactors starts decreasing towards a pH value < 7, between day 31 – 58 (Figure 6-1). According to de Lemos Chernicharo (2007), maintaining pH within the range of pH 6 – 8 is necessary for providing stability to the AD process, and maintaining pH range between pH 6.6 and 7.4 enables methanogenic archaea to achieve their optimum growth. However, due to the stability of the all the reactors because of supplementation with the ash-extracts, dosing of ash-extract was stopped from day 59 – 66 which is represented by point BC in Figure 6-1.

During the 3rd HRT (day 47 – 66), the mean pH recorded in the Pair 1, Pair 2 and Pair 3 reactors were pH 6.98, 7.00 and 7.02, respectively, all being within the optimum pH range. Statistical correlational analysis showed that the pH of the reactors within each of Pair 1 (R1 and R2), Pair 2 (R3 and R4), and Pair 3 (R5 and R6) had a strong R^2 value > 0.97 . However, between the pH in reactor Pairs (Pair 1 and Pair 2; Pair 1 and Pair 3; Pair 2 and Pair 3), a Paired samples T-tests showed that the difference between the mean pH of Pair 2 and Pair 3 reactors was not statistically significant ($p > 0.05$), whereas, the same test indicated that the differences between the mean of the pH between Pair 1 and Pair 2 or between Pair 1 and Pair 3 reactors were statistically significant ($p < 0.05$). These results suggest that temperature significantly influences the pH in the AD reactors, especially for the psychrophilic AD processes, relative to the mesophilic and thermophilic conditions. Although, no previous study known to the author exists on the effects of temperature on pH (Figure 6-1), however, Stolp (1988) reported that psychrophiles have a large content of unsaturated low-melting point fatty acids. Similarly, Hai *et al.* (2013) stated that during the psychrophilic process, long chain acids and alkanes become recalcitrant. Therefore, the large content of unsaturated acids, the formation of long-chain acids and alkanes could be the responsible for the low pH observed in Pair 1 (psychrophilic) reactors in the current study.

6.2.2 Effect of organic loading rate on volatile solids destruction in CSTR

Figure 6-2 shows the variation in the organic loading rate, OLR ($\text{gVS.L}^{-1}.\text{d}^{-1}$) and the percentage destruction of volatile solids, VS (%) in the Pair 1, Pair 2 and Pair 3 reactors from day 1 – 66). With the organic loading rate increasing in the Pair 1, Pair 2 and Pair 3 reactors from 1.0, 1.25 and 1.50 $\text{gVS.L}^{-1}.\text{d}^{-1}$ corresponding to 1st, 2nd and 3rd HRT cycles (Table 6-2), the VS destruction in the reactors ranged from 47 – 59%, 55 – 68% and 53 – 71% respectively.

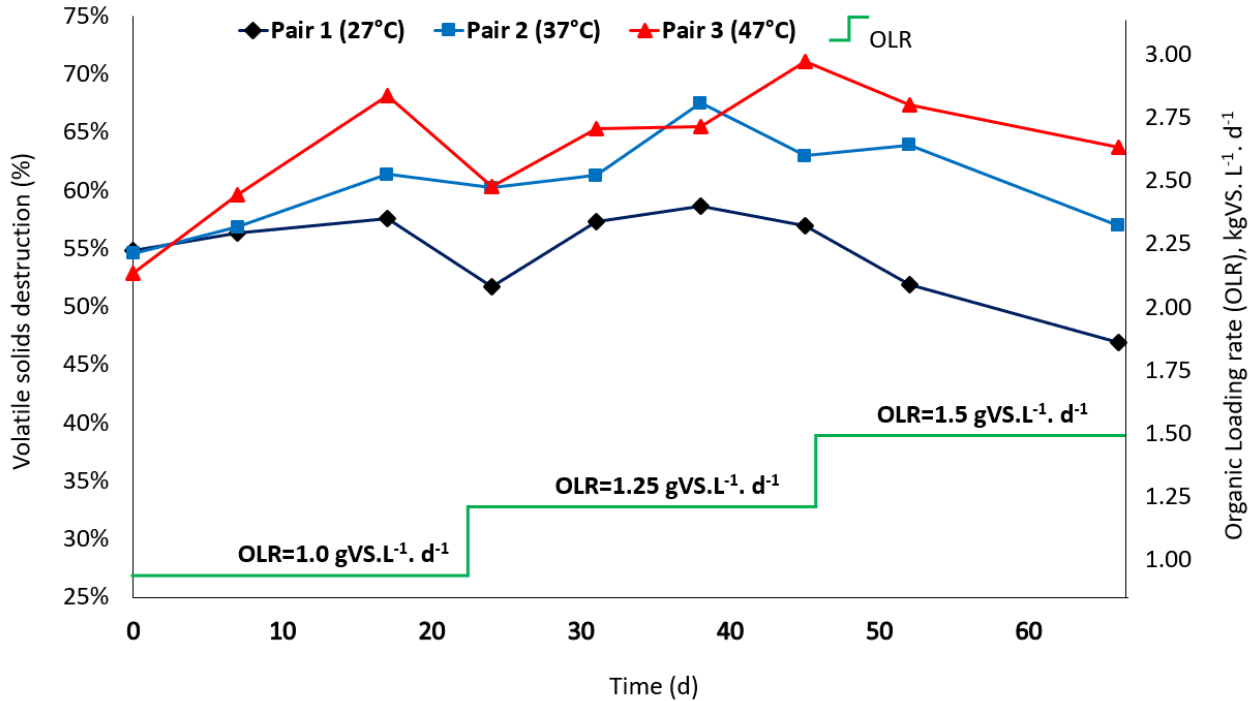


Figure 6-2 Variations in the organic loading rate and the percentage destruction volatiles solids (VS) (%) in the Pair 1, Pair 2 and Pair 3 reactors from day 1 – 66. Values are the means from duplicate reactors within a pair, OLR is the organic loading rate as stated in Table 6-2.

Furthermore, the overall mean VS destruction in the reactors from day 1- 66 in the Pair 1, Pair 2 and Pair 3 reactors was 55, 61 and 64%, respectively (Figure 6-2). These results also agree with previous results in the current study where it was shown that the VS destruction in the thermophilic reactors was higher than that of the mesophilic reactors (Sections 4.2.2). The reasons for the better VS destruction in the thermophilic reactors compared to the mesophilic reactors has also been discussed in detail in Section 2.7.1. However, it was found that the increase in the rate of VS destruction in the Pair 2 and Pair 3 reactors, coincided with the periods of increased SMP and VMP in those reactors, compared to the Pair 1 reactors (Figure 6-7). The lower VS destruction in the Pair 1 reactors also corresponded with the higher VFA concentration in the reactors (Figure 6-4) and higher COD_T . These results suggest that most of the hydrolyzed biomass feedstocks (measured as COD_T), in Pair 1 reactors were not efficiently being converted to biogas due to the accumulation of VFA, which would explain why the reactors produced lower volumes of methane and biogas compared to Pair 2 and Pair 3 reactors. As suggested in Section 2.7.6, increase in OLR at lower temperatures would require longer retention time to achieve higher methane productivity, and based on the results from the current study, it is evident that the solubilization of the substrates and the activities of the microbes which convert the solubilized materials to intermediate products and biogas,

are slower at low temperatures. This conclusion agrees with that of Hai *et al.* (2013) who reported that, despite the presence of long chain acids and alkanes in their psychrophilic reactors, they still achieved satisfactory AD process by using a high solid retention time (SRT), which compensated the low activity of the microbes at low temperature. The higher VS destruction in the Pair 3 (thermophilic) reactors also agrees with several researchers who have reported that thermophilic AD processes achieve high organic matter removal rate compared to the mesophilic reactors due to the increase in reaction rate with temperatures (Ferreira, 2013; Micolucci *et al.*, 2018).

6.2.3 Effect of HRT on the chemical oxygen demand (COD_T), total Kjeldahl N (TKN), and ammoniacal-N in the CSTR

The original COD_T in the seeding sludge (inoculum) was 18,752 mg. L⁻¹ during start-up. On day 7, this COD had increased to 21,800, 23,500 and 23,462.5 mg.L⁻¹ for Pair 1, Pair 2 and Pair 3 reactors respectively, due to the daily feeding (in fed-batch mode rather than continuous mode) of the reactors with biomass feedstock at OLR of 1.0 gVS.L⁻¹.d⁻¹ (Figure 6-3). However, during the 2nd HRT (day 26 - 46), when operated in a continuous mode, increasing OLR from 1.0 to 1.25 g.L⁻¹.d⁻¹ caused the mean COD_T in the Pair 1, Pair 2 and Pair 3 reactors to increase from 10,054 to 12,779 mg.L⁻¹, 10,454 to 11,808 mg.L⁻¹, and 9,754 to 11,052 mg.L⁻¹, respectively.

Figure 6-3 shows the variation of mean total chemical oxygen demand, total Kjeldahl Nitrogen (TKN) and ammoniacal nitrogen in the Pair 1, Pair 2 and Pair 3 reactors from day 1 – 66.

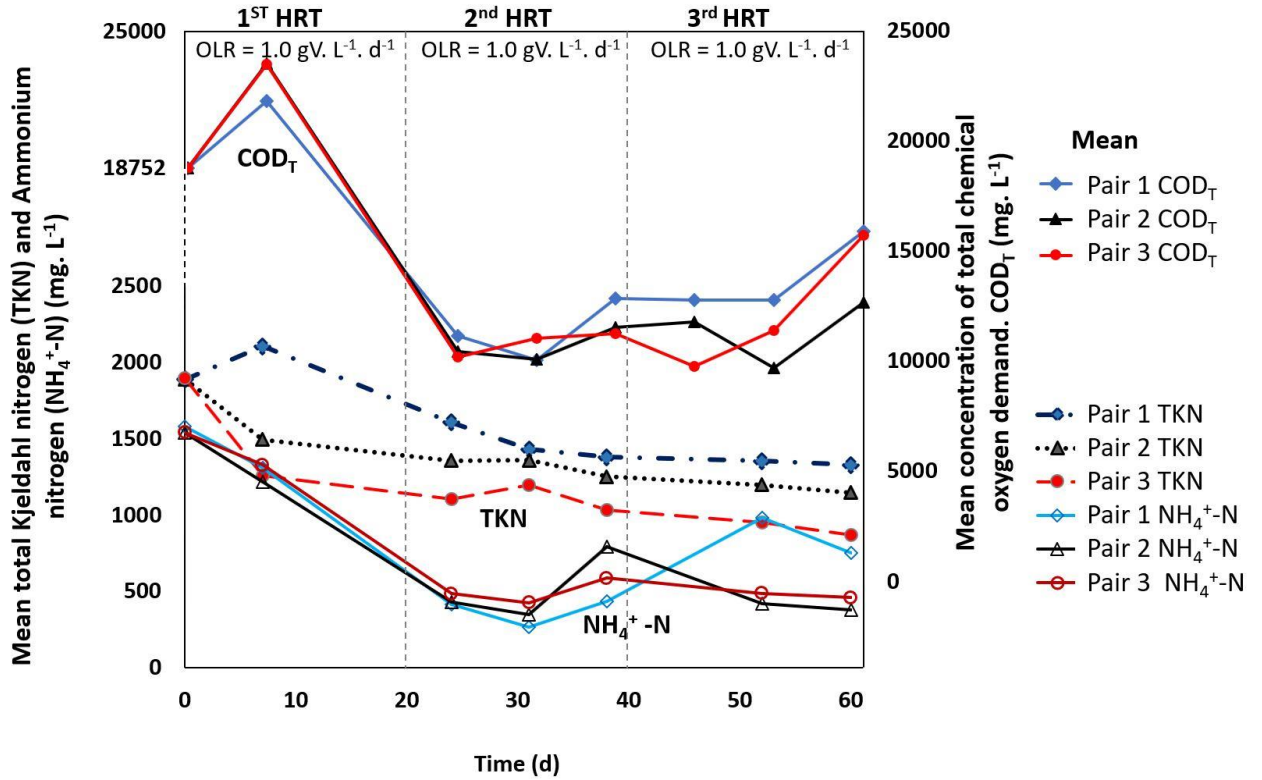


Figure 6-3 Variation of mean total chemical oxygen demand(COD_T), total Kjeldahl Nitrogen (TKN) and ammoniacal nitrogen (NH_4^+-N) in the Pair 1, Pair 2 and Pair 3 reactors with time. Values are the means from duplicate reactors within a pair (Table 6-2).

However, at the 3rd HRT cycle, a further increase in OLR to $1.5 \text{ gVS.L}^{-1} \cdot \text{d}^{-1}$ had a higher impact on the COD_T contents in the Pair 1 and Pair 3 reactors, compared to the Pair 2 reactors (Figure 6-3). For instance, from day 45 to 60, the COD_T in Pair 1, Pair 2 and Pair 3 reactors increased from 12,779 to 15,902 mg.L^{-1} ; 11,804 to 12,677 mg.L^{-1} , and 9754 to 15,727 mg.L^{-1} , respectively. It was also found that on day 60, that increase in OLR resulted to higher concentrations of COD_T , up to 7% in the psychrophilic and 3% in thermophilic reactors, compared to the mesophilic reactors. These observations coincided with periods during which there was a decrease in VS destruction (Figure 6.2), a decrease in biogas/methane production (Figure 6-6), and an increase in VFA accumulation (Figure 6-4). The accumulation of VFA was more evident in the psychrophilic reactors during the 3rd HRT cycle when the OLR was increased to $1.5 \text{ gVS.L}^{-1} \cdot \text{d}^{-1}$. These changes in the psychrophilic and thermophilic reactors suggest that these reactors were affected substantially by the increasing OLR condition at certain periods during the digestion of lignocellulosic biomass. The high percentage of COD_T found in the psychrophilic reactors also suggests that the rate of conversion of the COD_T to

biogas was slower at the low temperature, and that this was responsible for the lower rate of biogas production, compared to the mesophilic and thermophilic reactors.

From Figure 6-3, after starting-up the reactors, the mean concentration of $\text{NH}_4^+\text{-N}$ in the Pair 1, Pair 2 and Pair 3 reactors, from HRT 1 and HRT 2 (day 7 – 46), decreased from 1,580 to 266 mg.L^{-1} ; 1,542.5 to 350 mg.L^{-1} , and 1,542.5 to 427 mg.L^{-1} , respectively. Thus, from HRT 1 to the end of HRT 2, the initial ammonium-N contents in Pair 1, Pair 2 and Pair 3 reactors which were lost/washed-out, were 83%, 77% and 72%, respectively. However, during the 3rd HRT cycle (day 47 – 66), an increase in the OLR from 1.25 to 1.5 $\text{gVS.L}^{-1}.\text{d}^{-1}$, caused the concentration of $\text{NH}_4^+\text{-N}$ to gradually increase in the Pair 1, Pair 2 and Pair 3 reactors from of 266 – 756, 350 - 380 and 427 – 462 mg.L^{-1} , respectively, on day 66 (Figure 6-3). Ammonium ions in addition to providing buffering capacity in AD reactors, also serve as a vital source of nitrogen for bacterial cells (Gerardi, 2003). A number of researchers have also reported that ammonia nitrogen is beneficial to anaerobic microbes when it present at concentrations of 50 to 200 mg.L^{-1} when at neutral pH (Drosg, 2013; Gerardi, 2003; Lue-Hing, 1998). In the current study, the mean ammonium nitrogen contents in Pair 1, Pair 2 and Pair 3 reactors for both 2nd and 3rd HRTs were 571.78, 476.46 and 491.2 mg.L^{-1} , respectively, all values being above the beneficial ranges. However, the reactors did not experience ammonia inhibition, probably because the ash-extract supplementation in the reactors provided an adequate amount of alkalinity to maintain a neutral pH, and this would have prevented the release of free ammonia (NH_3) from the ammonium-N from the reactors.

The mean concentration of the total Kjeldahl nitrogen (TKN) in the AD reactors from 1st HRT to the end of 2nd HRT decreased from 1,890 to 1,381 mg.L^{-1} in the Pair 1, 1,894 to 1,255 mg.L^{-1} Pair 2 and 1,897 to 1,033 mg.L^{-1} Pair 3 reactors, respectively (Figure 6-3). This means that only 27%, 34% and 46% of the original TKN concentration was lost over these two HRT periods. The loss in TKN was less than the loss of ammoniacal-N because TKN consists of both the organic and the inorganic forms of nitrogen, and therefore some of the nitrogen may have been bound within the recalcitrant structures of the lignocellulosic biomass. Throughout the 3rd HRT cycle, the values of the TKN for each pair of reactor's conditions remained relatively constant until the end of the experiment.

6.2.4 Effects of volatile fatty acids (VFA) concentration on the CSTR

It was observed that all the reactors had their highest VFA concentrations between day 1 and day 7, possibly due to the initial concentration of VFA in the inoculum, and the further VFA

built-up during the initial fed-batch operating mode (Figure 6-4). Although for each condition tested, the reactors were operated in pairs, however, the results from the analysis of samples from the reactors showed that each individual reactor has its unique VFA content. For the pair 1 reactors, in reactor R1, the four types of VFA detected were propionate, acetate, isobutyrate and butyrate. Specifically, in R1 between day 7 and day 45, the initial concentrations propionate ranged between 356 – 457 mg.L⁻¹, and this increased substantially to 918 mg.L⁻¹ on day 60 (Figure 6-4). Similarly, for the isobutyrate, the highest concentrations detected were on days 0 and day 60, with concentrations of 420 and 229 mg. L⁻¹, respectively. In the case of acetate, the maximum concentrations were recorded on day 7 and day 60 at 842.9 and 330. 6 mg. L⁻¹, respectively. The second CSTR reactor (R2) also produced acetate, butyrate, isovalerate, propionate and valerate, with maximum concentrations of acetate produced on day 7 and day 60 being 968 mg. L⁻¹, and 10, 25.6 mg.L⁻¹, respectively (Figure 6-4).

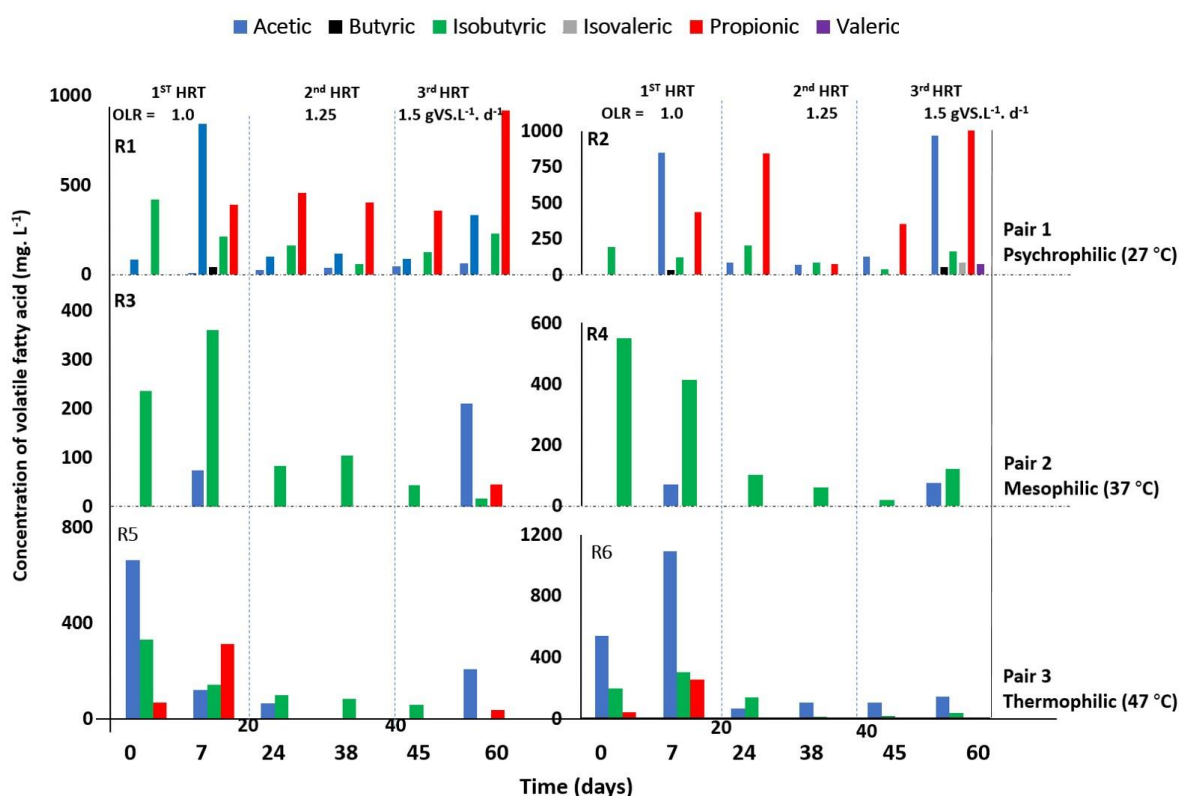


Figure 6-4 Volatile fatty acids concentration in Pair 1 psychrophilic (27 °C), Pair 2 mesophilic (37 °C) and Pair 3 thermophilic (47 °C) CSTRs. Values are the means from duplicate reactors within a pair (Table 6-2)

The VFA concentration decreased over time following the addition of ash-extract supplements but started to accumulate during 3rd HRT due to the high OLR. Higher propionate-to-acetate ratio (P:A) ratios were detected in R2 on days 7, 38, 45 and 60 were

1:1.9, 1:1, 1:0.4 and 1:0.9 mg.L⁻¹ respectively, whereas for the reactor, R1, the highest values were only recorded on day 7 and day 60, and these were 1:2.2 and 1:0.4, respectively. According to Ferreira (2013), a high concentration of acetate inhibits propionate acetogenesis, butyrate acetogenesis and acetoclastic methanogenesis, while propionate accumulation inhibits methanogenesis. Felchner-Zwirello (2014) also reported that acetic acid inhibits propionate degradation in AD reactors. as shown in Figure 6-5 Inhibiting effects of acetic acid on propionate degradation rates mM = mmol. L⁻¹. Figure 6-5,

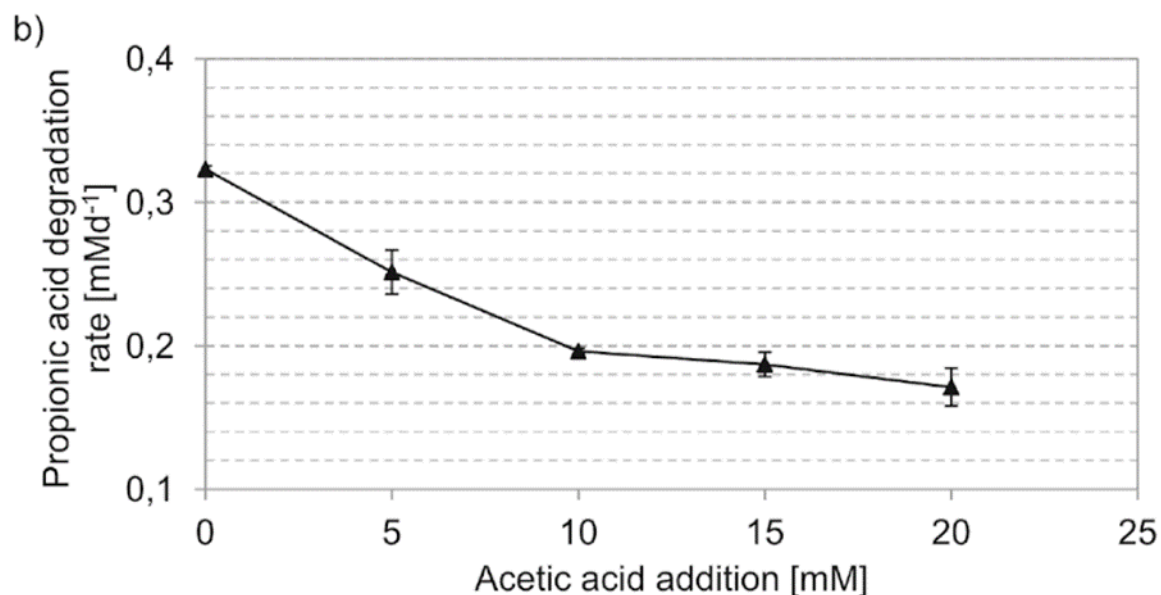


Figure 6-5 Inhibiting effects of acetic acid on propionate degradation rates mM = mmol. L⁻¹. Adapted from Felchner-Zwirello (2014).

Thus, the high P:A ratios in Pair 1 reactors suggest that the high concentration of acetate in the reactors and the low propionate degradation rate were the key rate-limiting steps in those reactors. Consequently, this led to a lower volume of biogas being produced by the R1 and R2 reactors compared to the reactors in Pair 2 and Pair 3 (Figure 6-8), because the accumulation of VFA caused a significant drop of pH in reactors R1 and R2. A drop in pH leads to the accumulation of acetate due to the inhibition of methanogenesis and that explains why Kosseva (2013) reported that acetogenesis plays an important role in AD process. According to Hill *et al.* (1987), P: A ratio of 1:1.4 or propionate concentration above 800 mg. L⁻¹ indicate impending digester failure. However, since the Pair 1 reactors in the current study had peak P:A values of 1:1.9 and 1:2.2 which exceeded the P:A ratio of 1:1.4, and yet did not fail, it implies that the addition of ash-extracts as supplement to these reactors was responsible for their sustenance.

For the Pair 2 reactors (R3 and R4) at 37 °C, the VFA that was detected throughout the experiment was isobutyrate, and its concentration decreased gradually across all the 3 HRTs (day 1 – 66). For instance, the concentration of isobutyrate decreased from 235.9 - 16 mg. L⁻¹ in R3 and 550.5 to 17.8 mg. L⁻¹ in R4, respectively. Acetate and propionate were also detected but only on the day 7 and day 60 at concentrations of 73.6 and 210 mg. L⁻¹ in R3; and 69.8 and 73.8 mg. L⁻¹ in R4. These results suggest that the mesophilic reactors were very efficient in maintaining a good balance between the acidogenic and acetogenic stages during the AD process. In addition, these pair 2 reactors had a P:A ratio <1:0.01 which is a strong indicator of the process stability and performance. The process stability and performance achieved in the Pair 2 reactors agree with several researchers who have reported that mesophilic reactors achieve higher process stability and require lower energy input compared to thermophilic reactors (Ferreira, 2013; Sani & Rathinam, 2018). However, the last P:A ratio recorded in R3, which had a value of 1:4.9 was due to the sudden VFA build-up caused by the failure of the PID temperature controller. Figure 6-6 shows the distribution of the total VFA concentrations in the Pair 1, Pair 2 and Pair 3 AD reactors at the different temperature conditions.

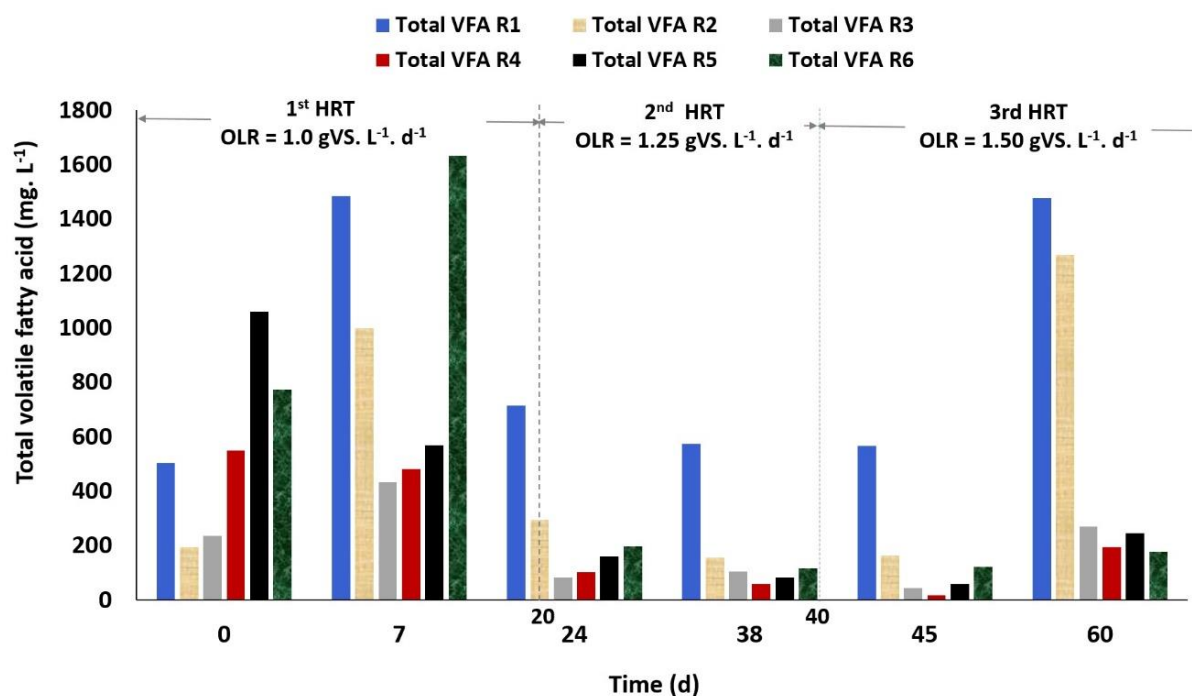


Figure 6-6 Total VFA concentrations in the Pair 1, Pair 2 and Pair 3 AD reactors at the different temperature conditions. Values are the means values of the VFA from individual reactors within a pair. (Reactor temperatures as defined in Table 6-2).

In the Pair 3 reactors (R5 and R6), the three VFA's detected inside the reactors were acetate, isobutyrate and propionate (Figure 6-6). In reactor R5, the highest concentrations of acetate

were detected on day 0, day 7 and day 60 and the values were 663.4, 118.7 and 208.0 mg.L⁻¹, respectively (Figure 6-4). Similarly, in R6, the concentrations of acetate detected on day 0, day 7 and day 60 were 538.3, 1,091.9 and 142.4 mg. L⁻¹, respectively. For days 0, 7 and 60, the P:A ratios were R5 (1:10, 1:0.38 and 1:5.8) and R6 (1:13, 1:4.3 and 1:5.7), respectively. Lee *et al.* (2016) reported that propionate and isobutyrate acids exhibit inhibitory effects on methanogenic microorganisms, and therefore should be kept at a very low concentration to increase the stability of an AD process. Thus, the high concentrations of VFAs and the high P:A ratios recorded in the pair 3 reactors strongly suggest that just like the psychrophilic reactors, that the unstable periods in the thermophilic reactors coincided with the time when there was accumulation of VFA during the start-up stage and during the HRT 3 cycle as result of increasing the OLR from 1.25 to 1.5 gVS.L⁻¹.d⁻¹. These results agree with previous research which stated that thermophilic processes have a higher risk of process instability, compared to the mesophilic AD processes (Ferreira, 2013). In addition to the benefits of thermophilic reactors describe in Section 6.2.2, the thermophilic process has also been reported to be better than the mesophilic process in terms of higher pathogen removal, faster process rates and higher substrates solubilisation (Ferreira, 2013; Sani & Rathinam, 2018; Schön, 2010; Tilak *et al.*, 2010).

6.3 Specific and volumetric specific methane production

6.3.1 Overall methane content, specific methane production and volumetric methane production in the CSTR

The mean concentration of methane gas produced by Pair 1, Pair 2 and Pair 3 reactors from day 1 – 66 were 51.8%, 54.7% and 52.7%, respectively. This clearly shows that overall, the Pair 2 (mesophilic) reactors produced biogas with the highest methane contents compared to Pair 1 and Pair 3 reactors. The mean and cumulative values of the daily specific methane production in the Pair 1, Pair 2 and Pair 3 reactors from day 1 - 66 are plotted in Figure 6-7.

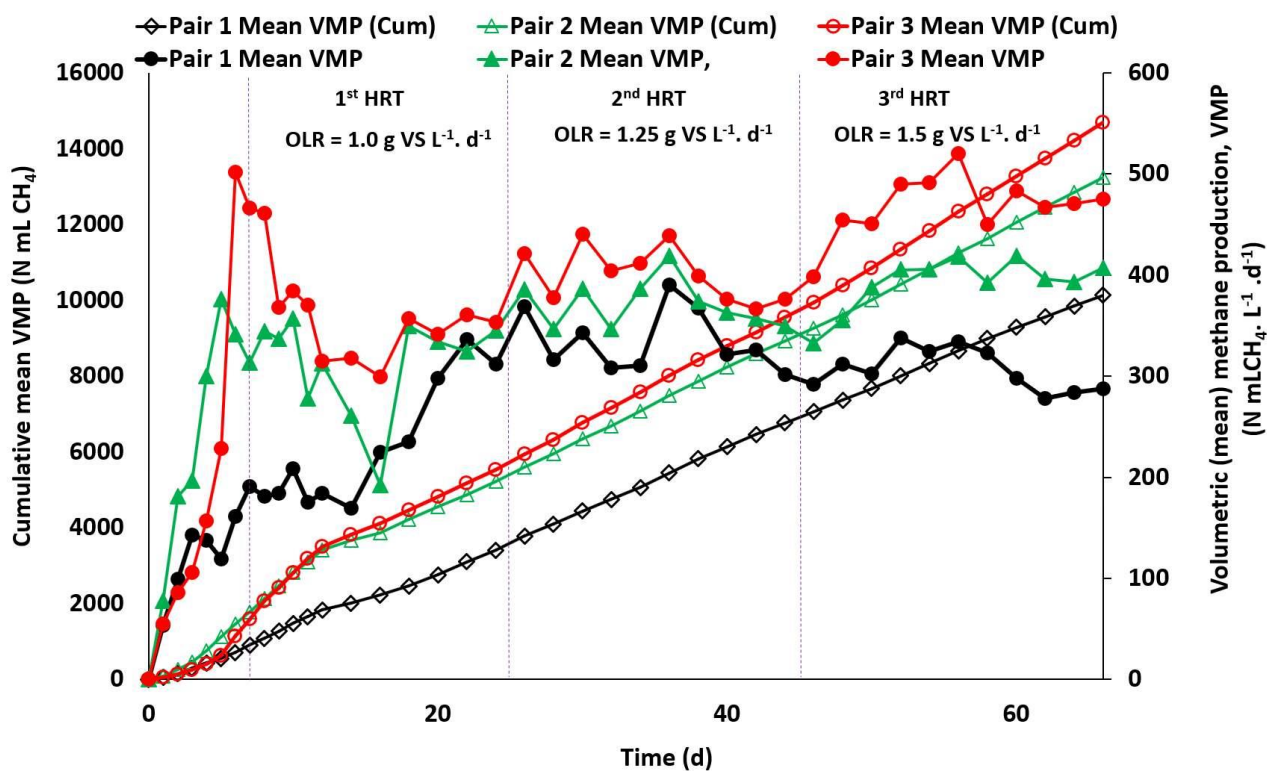


Figure 6-7 Mean specific methane production (SMP) and cumulative specific methane potential (SMP) for Pair 1, Pair 2 and Pair 3 reactors over time. Values are the means from duplicate reactors within a pair as defined in Table 6-2. The organic loading rate is presented in Figure 6-2.

Statistically, there was a strong correlation between the mean SMP from reactors under each pair of temperature conditions, as in, Pair 1 (between R1 and R2), Pair 2 (between R3 and R4) and Pair 3 (between R5 and R6) ($R^2 > 0.86$). From day 1 – 66 in Figure 6-7, in the Pair 1, Pair 2 and Pair 3 reactors, on the average, the specific methane production (SMP) were 214.0, 307.2 and 308.6 N mL CH₄·g⁻¹VS added·d⁻¹; while the volumetric methane production (VMP) was 260.0, 339.8 and 372.4 N mL CH₄·L⁻¹·d⁻¹, respectively. These results show that the specific methane production from the Pair 2 (37 °C) and Pair 3 (47 °C) reactors were 30 and 31% higher than that of the Pair 1 (27 °C) reactors. Furthermore, a paired sample t-test also showed a p-value <0.05 between the mean SMP from Pair 1 and Pair 2, and also between Pair 1 and Pair 3 reactors, which means that the difference between their mean SMP were statistically significant at a 95% confidence interval; whereas a comparison between Pair 2 and Pair 3 showed a p-value >0.05, which indicates that the difference between their mean SMP was not statistically significant.

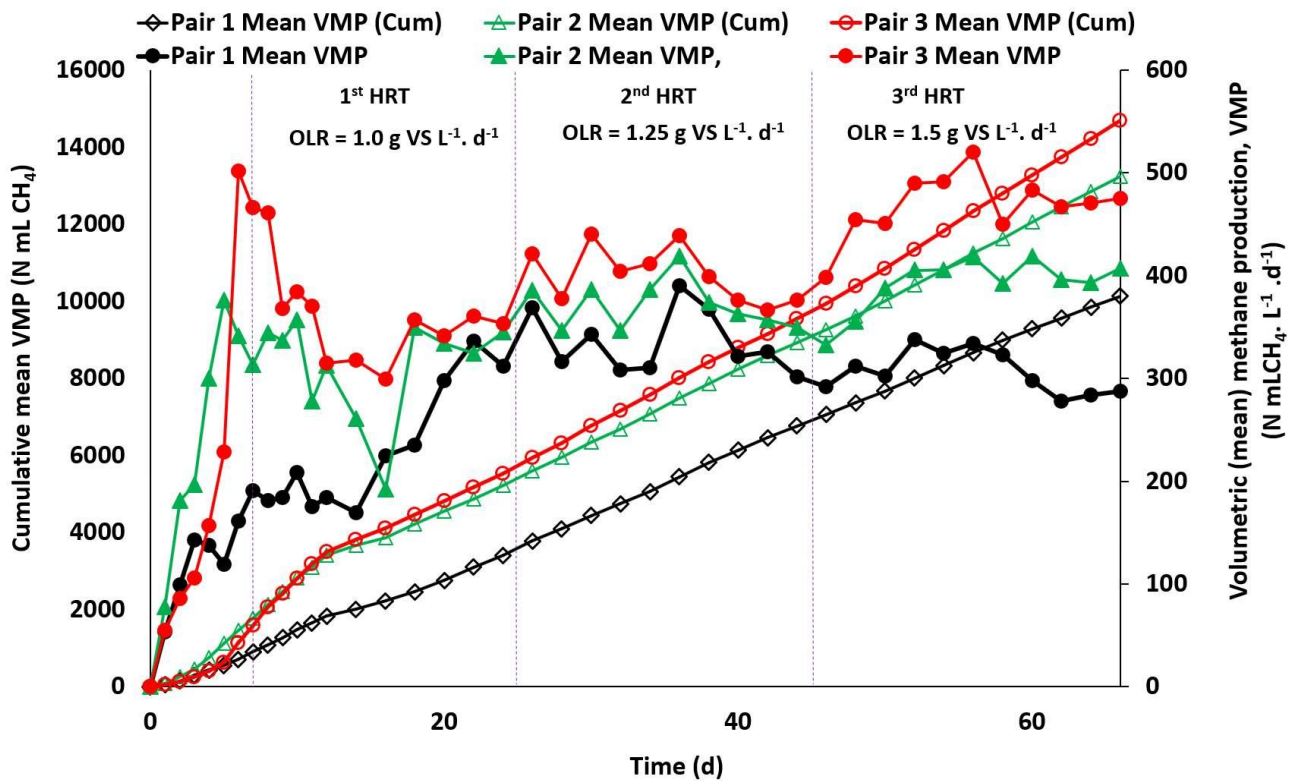


Figure 6-8 Mean volumetric methane production (VMP) and cumulative volumetric methane production (VMP) for Pair 1, Pair 2 and Pair 3 reactors over time. Values are the means from duplicate reactors within a pair as referenced in Figure 6-4.

Similarly, the volumetric methane production (VMP) from the Pair 2 and Pair 3 reactors were 23 and 30% higher than that of the Pair 1 reactors (Figure 6-8). The correlation between Pair 1 and Pair 2; Pair 1 and Pair 3 and Pair 2 and Pair 3 were all strong and positive with an R^2 value of 0.73, 0.65 and 0.81 respectively. Surprisingly, statistically analysis using paired samples t-test showed that the difference between the mean VMP when comparing between Pair 1 and Pair 2; Pair 1 and Pair 3, and Pair 2 and Pair 3 reactors, were all statistically significant ($p < 0.05$). These results probably suggest that the volumetric methane production (VMP) from the individual pair of reactors were influenced at different rates because of the increase in organic loading rates.

6.3.2 Effect of increase in organic loading rate from 1.0 to 1.25 gVS. L⁻¹. d⁻¹ on the specific and volumetric methane potential during 2nd HRT in the CSTR

During the 2nd HRT (day 26 – 46), when OLR was increased from 1.0 to 1.25 gVS.L⁻¹. d⁻¹, the mean percentage concentrations of methane across for the Pair 1, Pair 2 and Pair 3 reactors were 57.7%, 57.2% and 56.0% respectively. Figure 6-9 shows the mean specific methane

production (SMP) and volumetric methane production (VMP) during the 2nd HRT cycle (day 26 – 46).

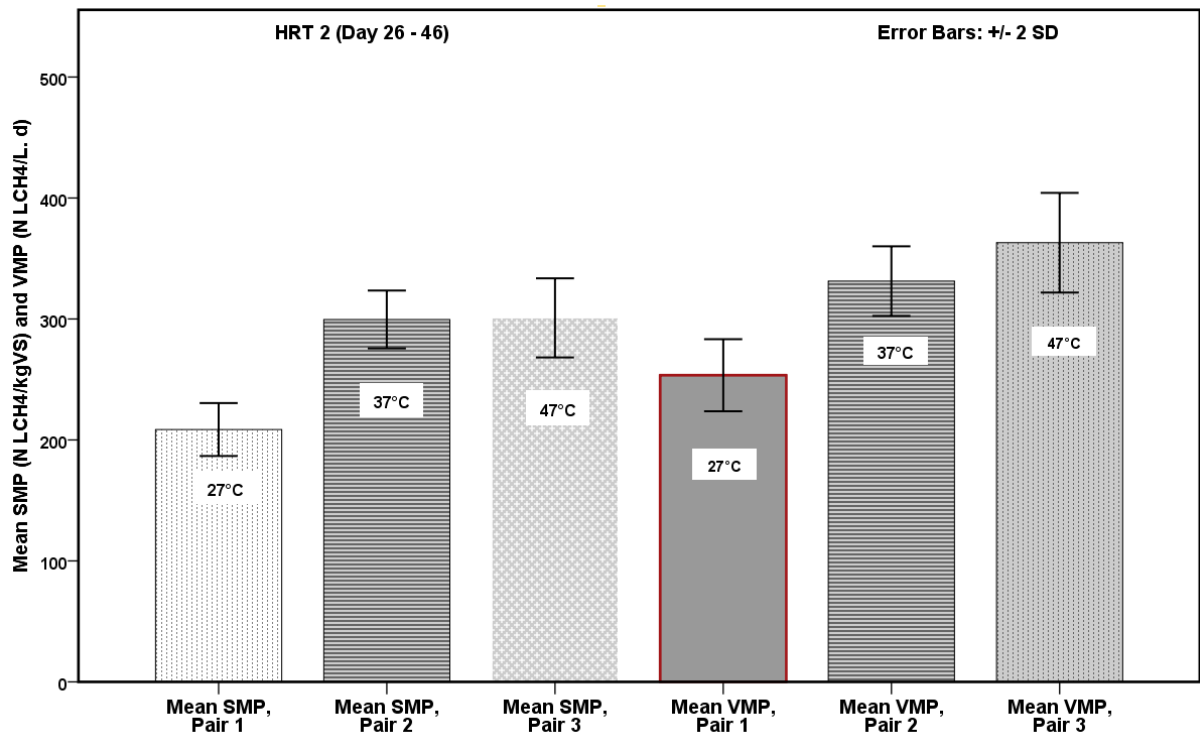


Figure 6-9 Mean of specific methane production (SMP) and mean of volumetric methane production (VMP) for the Pair 1, Pair 2 and Pair 3 reactors from day 26 – 46 (2nd HRT). Values are the means from duplicate reactors within a pair as defined in Table 6-2 and Figure 6-7.

Within this 2nd HRT period, the SMP from the Pair 1, Pair 2 and Pair 3 reactors were 261.6, 323.7 and 303.6 mL CH₄.g⁻¹VS added .d⁻¹ while the VMP from the reactors were 331.4, 367.9 and 385.5 N mL CH₄.L⁻¹.d⁻¹, respectively. These results indicate that the SMP of Pair 2 and Pair 3 reactors were 24 and 16% higher than the Pair 1 reactors, whilst their volumetric methane production was also 11 and 16%, respectively, higher than the Pair 1 reactors. A paired samples correlation analysis of the mean SMP between the paired reactors (Pair 1 and Pair 2; Pair 1 and Pair 3, and Pair 2 and Pair 3) showed a positive correlation with R² values of 0.90, 0.58 and 0.69 respectively. A similar comparison of the VMP also showed a positive correlation with R² values of 0.83, 0.48 and 0.59 respectively. However, further analysis of the mean SMP or VMP between Pair 1 and Pair 2 reactors, or Pair 1 and Pair 3 reactors using paired sample t-test showed a p-value < 0.05 in each case; while a similar comparison between Pair 2 and Pair 3 showed a p-value > 0.05. These results imply that whereas the mean SMP or VMP between the Pair 2 (mesophilic) and Pair 3 (thermophilic) reactors are comparable, the difference between these mean SMP and that of the psychrophilic AD

processes differ in terms of their statistical significance. The results also indicate that the 10 °C difference in temperature between the Pair 2 and the Pair 3 reactors had no significant impact on the methane productivity, whereas it had a serious impact when comparing the methane productivity between the psychrophilic and mesophilic reactors. These results agree with a previous report about AD plant in India where it was found that lower mesophilic temperature or psychrophilic temperature range adversely affected methane production in the AD plants during winter months (Tilak *et al.*, 2010).

6.3.3 Effect of increase organic loading rate from 1.25 to 1.5 gVS. L⁻¹.d⁻¹ on the specific and volumetric methane production during 3rd HRT in the CSTR

During the 3rd HRT cycle (Table 6-2), with an increase in OLR from 1.25 to 1.5 gVS.L⁻¹.d⁻¹, (day 48 – 66), the mean values of the methane composition (%) in the biogas from the reactors at the three temperatures for the Pair 1, Pair 2 and Pair 3 reactors were 50.8%, 55.7% and 56.6% respectively. The SMP produced by the Pair 1, Pair 2 and Pair 3 reactors were 205.4, 320.0 and 316.9 mL CH₄.g⁻¹VS added.d⁻¹; while the mean VMP from the reactors were also 308.1, 398.2 and 475.3 N mL CH₄.L⁻¹.d⁻¹, respectively (Figure 6-10). These results show that the specific methane production (SMP) from the Pair 2 and Pair 3 reactors were 36 and 35% respectively, higher than that of the Pair 1 reactors; while that from Pair 2 reactors were only 1% higher than Pair 3 reactors. Similarly, the volumetric methane production (VMP) from the Pair 2 and Pair 3 reactors were also 22 and 35% respectively, higher than that of the Pair 1 reactors; while conversely, the VMP from Pair 3 reactors exceeded that from Pair 2 reactors by 16%. These higher SMP and VMP from Pair 2 and Pair 3 reactors compared to Pair 1 reactors used in the current study followed the same trends observed in Sections 6.3.1 and 6.3.2 respectively. Research has shown that thermophilic AD reactors can achieve high degradation of organic waste to produce high volume of biogas even at high OLR and short HRT compared to mesophilic AD reactors (Schön, 2010; Tilak *et al.*, 2010). This might be why the thermophilic AD reactors used in the current study had better performance compared to their mesophilic counterpart under increased OLR condition. The instability of the thermophilic reactors at higher loading may have also been reduced by supplementation of the reactors with ash-extracts A statistical paired samples correlation between the mean SMP of Pair 1 and Pair 2 reactors showed that there was no correlation ($R^2 = 0.03$) between the specific methane production in the two reactors. However, there was a positively moderate correlation between the mean SMP between Pair 1 and 3 ($R^2 = 0.44$) and positive strong correlation ($R^2 = 0.70$) between the mean SMP from Pair 2 and Pair 3 reactors.

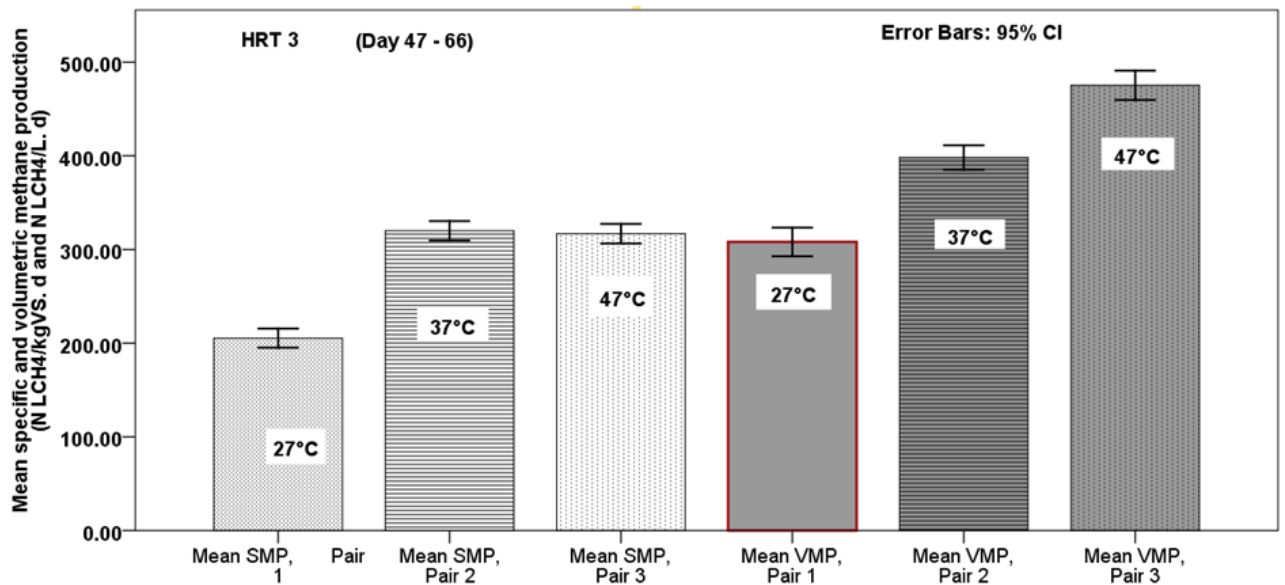


Figure 6-10 Mean of specific methane production (SMP) and mean of volumetric methane production (VMP) for the Pair 1, Pair 2 and Pair 3 reactors from day 47 – 66 (3rd HRT). Values are the means from duplicate reactors within a pair as defined in Table 6-2.

Similarly, a comparison between the VMP of Pair 1 and Pair 2 reactors showed that a very weak correlation exists between the two pairs of reactors; whereas the VMP of Pair 1 and Pair 3 showed were positive moderately correlated ($R^2 = 0.44$). However, there was a strong and positive correlation between the mean VMP of Pair 2 and Pair 3 reactors. These results also show that the SMP from the Pair 2 and Pair 3 reactors were very comparable but was much different from the SMP from the Pair 1 reactors. A possible explanation for these results could be that the anaerobic microbes were probably more active at the mesophilic and thermophilic temperature ranges compared to the upper psychrophilic temperature range (27 °C) at which Pair 1 reactors were operated, that also supports the reason given in Section 6.3.2. However, the only difference between the correlation between the Pair 1, Pair 2 and Pair 3 reactors was that, in terms of VMP, the R^2 values for the correlation between Pair 1 and Pair 2; Pair 1 and Pair 3 and Pair 2 and Pair 3 reactors were 0.12, 0.44 and 0.72 respectively. As expected, the results from the paired samples t-tests showed that the difference between the mean SMP from the Pair 1 and Pair 2; and between Pair 1 and Pair 3 reactors were both statistically significant ($p < 0.05$); while the difference between the mean SMP from Pair 2 and Pair 3 reactors was not statistically significant ($p > 0.05$). However, the paired samples t-test showed that the difference between the VMP from Pair 1 and Pair 2; Pair 1 and Pair 3, and Pair 2 and Pair 3 were all statistically significant ($p < 0.05$); which further

signifies that in terms of volumetric methane production (VMP), each pair of reactors responded distinctly and differently to increase the OLR based on its operational temperature. In the current study, the thermophilic reactors (Pair 3) were expected to produce higher SMP and VMP compared to the mesophilic and psychrophilic. However, the difference between the SMP from the thermophilic and mesophilic was nearly the same across the three consecutive HRTs. One possible explanation of the results could be related to the rapid decrease in the growth rate of microbes when AD process temperature approaches 45 °C as reported by Gray (2004). According to Kim *et al.* (2002), the yield of thermophilic microorganisms per unit amount of substrate is lower due to their increase decay rate and because the cells under thermophilic are liable to undergo lysis, or due to the higher energy required to maintain specific molecular properties of the enzymes. However, the performance of the thermophilic reactors over the mesophilic reactors in terms of VMP could be attributed to their higher substrate utilization rate and higher microbial growth rate at higher temperatures. Based on the temperature coefficient, Q_{10} which assumes that the rate of biogas production will double at a temperature difference of 10 °C (Nijaguna, 2006), however, such doubled rate was not achieved in the current study possibly because the activities of the AD microbes are restricted within certain temperature ranges.

6.4 Conclusion

To determine the effect of 10 °C degree differences in operating temperature of psychrophilic, mesophilic and thermophilic reactors on the specific methane production (SMP) and volumetric methane production (VMP) during the AD of a mixed lignocellulosic biomass feedstock

Results showed that the SMP and VMP of the mesophilic and thermophilic reactors were comparable and were considerably higher than those of the psychrophilic reactor. This was considered to reflect the lower activity of the methanogenic archaea in the psychrophilic reactor. Although the methane productivity in the mesophilic and thermophilic reactors was comparable, the thermophilic CSTR had a slightly higher VMP than the mesophilic reactors, which showed that methane production was temperature dependent to some degree but did not produce major differences in methane productivity at the higher temperatures.

Chapter 7 Assessing biomass ash extracts as sources of buffer and trace nutrients supplements for improved CH₄ production during the anaerobic co-digestion of cassava wastes and cattle slurry

Abstract

The current study involved the co-digestion of cassava processing wastes and cattle slurry in the ratio of 4:1 (in terms of VS) in six 5 L CSTR operated at a hydraulic retention time (HRT) of 20 d, an organic loading rate (OLR) of 1.0 gVS.L⁻¹.d⁻¹, and a temperature of 37 ± 0.5 °C. All six reactors were operated identically, in terms of HRT and OLR from day 1 – 64. During this period, the pH in all the CSTR decrease gradually from pH 7.67 – 7.0 without the need for ash supplementation (no alkali source), except for day 43 – 50 when ash supplements were added as a source of alkalinity to control the pH in all CSTR which had decreased slightly below pH 7 due to a power cut. On day 65, the six reactors were operated separately as three different pairs. Pair 1 (Control) reactors continued operation without supplementation, Pair 2 reactors continued running but with the addition of empty palm bunch ash-extracts supplement, while Pair 3 reactors were supplemented with ash-extract from the empty cocoa pod (ECP). The results showed that from day 25 – 65, the Pair 1, 2 and 3 CSTR achieved a mean VS destruction of 83, 86 and 85% VS; a mean specific methane production (SMP) of 284.0, 258.3 and 284.7 N mL CH₄.g⁻¹VS added.d⁻¹, and methane content of 55.8%, 55.7% and 56.4% respectively, indicating all reactors performed very similarly. However, from day 65 – 85, the Pair 1, 2, 3 reactors achieved a mean SMP of 79.3, 258.1 and 297.3 N mL CH₄.g⁻¹VS added. d⁻¹ respectively, and correspond to methane contents of 24.6%, 56.7% and 57.0%, respectively. This means that from day 65 – 85, the efficiency of methane production by the Pair 3 reactors was 73 and 13% respectively, higher than of the Pair 1(unsupplemented) and Pair 2 (ECP supplemented) CSTR. The Pair 1 reactors finally failed around day 78 due to VFA accumulation. The difference in the performance between Pair 2 and Pair 3 reactors was only due to an electrical fault in the temperature controller in the reactor, R4 which is one of the Pair 2 reactors. The propionate-to-acetate (P:A) ratio in the unsupplemented Pair 1 reactors also varied from 1:2.1 – 1:3.2, with acetic acid concentrations ranging between 2,262 – 8,917 mg.L⁻¹, while its FOS:TAC ratio ranged from 0.2 – 1.4 when the reactors were failing. However, the addition of EPB ash-extract to Pair 1 reactors from day 78 – 85 improved the pH and the performance of the reactors, and this change, together with the stability achieved in the supplemented Pair 2 and Pair 3 reactors, strongly suggests that ash-extracts can serve as

a sustainable source of low-cost alkalinity and trace elements for the maintenance of CSTR stability and enhancement of methane yields.

Keywords: *Anaerobic digestion, continuously stirred tank reactors (CSTR), cassava wastes, cattle slurry co-digestion, low-cost supplementation specific methane production (SMP)*

Objectives

The objectives of the current study were:

- To determine the effectiveness of empty palm fruit bunch (EPB) and empty cocoa pod (ECP) ash-extracts in providing alkalinity and buffering for the maintenance of pH within the optimum range for AD processes.
- To determine whether EPB and ECP ash-extract supplements can maintain steady-state conditions in continuous AD reactors over extended operating periods.
- To determine whether ash-extract supplements can restore the activity of AD reactors that are exhibiting a declining or failing performance.

7.1 Materials and methods

7.1.1 Materials

The source of the cassava wastes, and the inoculum used for the current study, including the methods used in preparing and preserving them prior to this experiment has been described in Section 3.1. The final co-digestion feed comprising of the cassava processing waste and cattle slurry was prepared by mixing both wastes (cassava: cattle slurry) in the ratio of 4:1 (in terms volatile solids) based on their equivalent dry weights. A summary of the composition of the biomass feedstock and the inoculum are presented in Table 7-1. The biomass composition was determined using methods presented in Section 3.4.2.

Table 7-1 Composition and properties of inoculum and cassava waste used for the study

Analysis	Abbreviation	Inoculum	Cassava waste (2:1)
Moisture content (%)	MC	87%	12%
Total solids (%)	TS	13%	88%
Volatile solids (% in TS)	VS	85%	95%
Ash content (%)	Ash	15%	5%
pH value	pH	7.67	x
Chemical oxygen demand (mg L ⁻¹)	COD	14,333.3	x
Total Kjeldahl Nitrogen (mg L ⁻¹)	TKN	2,415	345.8
Ammonium nitrogen (mg L ⁻¹)	NH ₄ ⁺ - N	2,016	0.84
Alkalinity (mg CaCO ₃ L ⁻¹)	TAC	19,550	x
Total volatile fatty acid (mg HAc L ⁻¹)	FOS	7275.7	x
Carbon (%)	C	41.89	41.5
Hydrogen (%)	H	x	6.57
Nitrogen (%)	N	2.58	0.187
Oxygen (%)	O	x	49.73
Sulphur (%)	S	0.35	0.137

x denotes that the parameter was not measured

7.1.2 Methods

The six continuously stirred tank reactors (CSTR) used for this study were set up following the procedure described in Session 3.5. All the reactors were operated at a mesophilic temperature (37 ± 0.5 °C) and at an HRT of 20 d. The reactors were first acclimatized from day 1 – 5 using an organic loading rate (OLR) of $1.0 \text{ gVS.L}^{-1} \cdot \text{d}^{-1}$. After acclimatization, all the reactors were daily fed at same OLR from day 6 – 64 without the addition of ash-extract supplements to any of the reactors. The aim was to identify the point from which all the reactors showed declining performance and required supplements to enable them to maintain their stability and steady-state conditions. This would establish whether the use of ash-extract supplements could be used as potential low-cost alternatives to commercial additives and maintain the performance of anaerobic digesters. From day 65, all the reactors had lost over 85% of their ammonium–nitrogen (contributed by the inoculum) leading to a pH drop in all the six reactors to $\text{pH} < 7$. On the same day, the six (6) reactors were grouped into three (3) pairs. Pair 1 (R1 and R2) were the control and continued operating without supplementation, except for short period day 43 – 50, when ash-extracts were added to all the reactors in order to restore their pH to the same level before their categorization. From day 65 – 85, Pair 2 (R3 and R4) were supplemented with Cocoa pod ash-extract (ECP) at a dosing rate 20 ml per day, while Pair 3 (R5 and R6) were supplemented with Empty palm bunch ash-extracts also at a dosing rate of 20 mL per day, and these ash-extracts were prepared as described in Section 3.2. The ash-extract supplements were added to the reactors to restore pH to the range of 6.8 – 7.2, whenever pH drop was observed. These alkaline ash-extracts were prepared as previously described in Section 3.2 and were used as potential low-cost supplements to provide buffering and trace nutrients for these reactors. The variations in pH, volatile solids destruction (%), alkalinity, COD, TKN, ammonium-N, volatile fatty acid concentrations and biogas volumes and compositions were measured as summarized in Table 3-8.

7.2 Results and discussion

7.2.1 Characterization of the biomass feedstock and the carbon-to-nitrogen ratio

The characterization of the biomass feedstocks used for the present study and the elemental composition of the biomass ash-extracts are presented in Section 3.2 (Table 3-1 and Table 3-2), respectively. Data from elemental analysis and X-ray diffraction (

Figure 3-1, 3-2, 3-3 and Table 3-4) also showed that these biomass ash-extracts were very high in potassium (K_2CO_3 and $KHCO_3$), and that they also contained essential trace nutrients, which implies that they might serve as good sources of bicarbonate alkalinity and trace elements for the maintenance of reactor stability and for the optimization of the AD process. According to Gerardi (2003), supplements that release bicarbonate alkalinity directly into the AD process mixture are desirable because methanogenic archaea require bicarbonate alkalinity for their optimum function. Korres (2013) also reported that trace nutrients act as co-factors in enzymes, and thus are essential for the microbial metabolism. The same author reported that lack of adequate trace elements during AD process can lead to malfunction of key enzymes of methanogenic archaea, which could result in complete cessation of methanogenesis, a decline in biogas formation and acidification of the reactor contents due to VFA accumulation. Thus, the high bicarbonate and trace element content in biomass ash-extracts (Table 3-4), suggests that they could potentially substitute commercial reagents for the optimization of the AD process.

An important factor in selecting suitable feedstocks was the carbon-to-nitrogen (C:N) ratio of the materials. This was important because carbon is the main component of organic waste which bacteria digest to release CH_4 and CO_2 , however, the microbes also require nitrogen for their metabolic activities, especially for the synthesis of new biomass (Korres, 2013; Mital, 1997). The C:N ratio in the cassava wastes and the cattle slurry were 86: 1 and 8: 1, respectively. These values are not compatible individually for mono-digestion which needs a C:N ratio of 20 – 30: 1 for stable biogas production (Demirbas, 2008; Soni, 2007). The high C:N ratio of cassava waste indicates its nitrogen content is very low, which implies that the nitrogen will be exhausted before the carbon is completely digested. Similarly, the low C:N ratio in the cattle slurry means that it has a high concentration of nitrogen, which suggests that an AD reactor utilizing cattle slurry as a mono-substrate could fail due to ammonia inhibition. From the information obtained after compositional analysis, a mixture of cassava waste and cattle slurry in the ratio of 4:1 (in terms of VS) produced a co-digestion feedstock with a C:N ratio of 32:1, which contributed to the stability of all the reactors from day 5 – 65 without any supplementation. The reactor stability (Figure 7-8) achieved from the mixed cassava wastes and cattle slurry feedstock shows that co-digestion can improve both the nutritional balance and the stability of AD reactors. The result agrees with Khairuddin *et al.* (2015), who reported achieving 78% improvement and good process stability in methane production during the co-digestion of household wastes and cow manure in AD reactors. Cook *et al.* (2017), also reported that co-digestion increased operational stability and resources recovery

during anaerobic digestion compared to mono-digestion. However, they pointed out that co-digestion can lead to operational complexity, and that it can also suffer nutrient imbalance and ammonia inhibition in the same way as mono-digestion.

7.2.2 Organic loading rate and volatile solids destruction

Figure 7-1 shows the mean values mean of the concentration and mean destruction (%) of volatile solids. Pair 1, Pair 2 and Pair 3 reactors respectively.

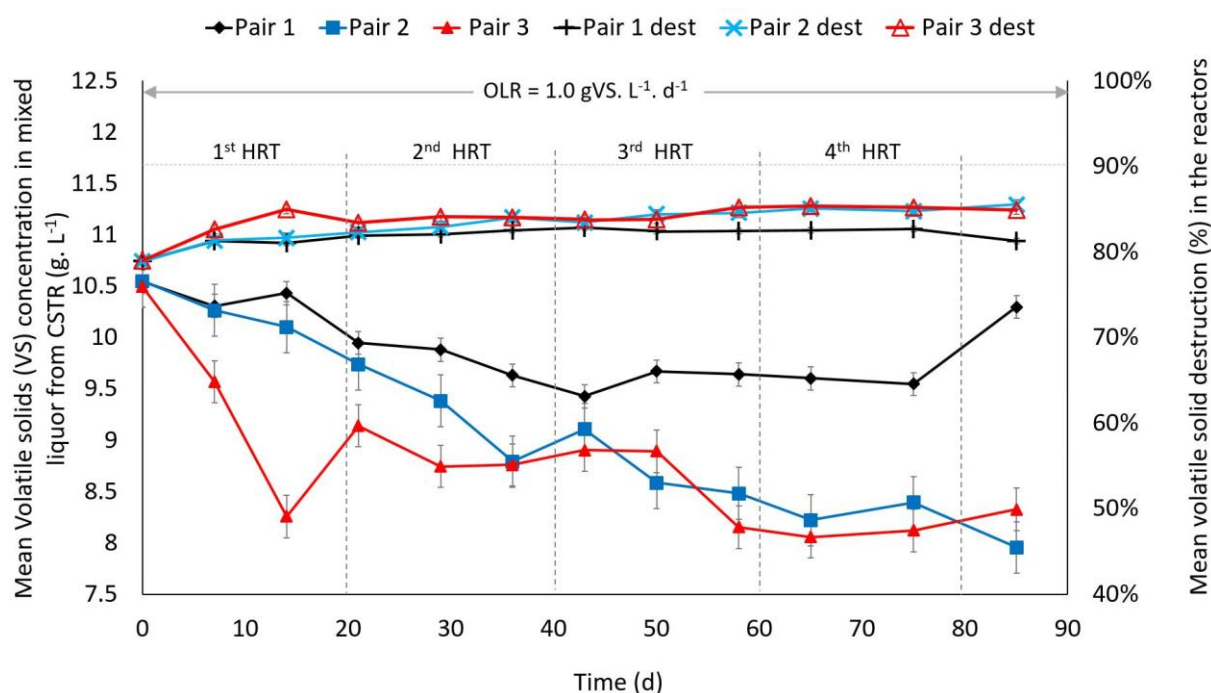


Figure 7-1 Mean volatile solids concentration, and mean volatile solids destruction (%), of Pair 1, Pair 2 and Pair 3 reactors over time. Dest. refers to the destruction of volatile solids

From day 7 – 64, each of Pair 1, Pair 2 and Pair 3 reactors achieved a mean VS destruction of 83, 86 and 85%, respectively. This was very high and comparable to the VS destruction of $88.25 \pm 0.03\%$ achieved by previous studies by Glanpracha and Annachatre (2016) by co-digesting cassava pulp with pig manure. However, the high level of VS destruction for the co-digested cassava waste and cattle slurry in the Pair 1, Pair 2 and Pair 3 reactors from day 7 – 64 in the current study was almost certainly due to the easy biodegradability of cassava, as discussed in Section 2.4.2, and that of cattle slurry, as well as the low organic loading rate. However, from day 65 – 85, Pair 1 reactors (control) had a higher VS accumulation (Figure 7-1), and lower VS destruction compared to Pair 2 and Pair 3 reactors (both supplemented with ash-extracts). The increase in VS accumulation in the Pair 1 (control) reactors was linked

to a decrease in pH (Figure 7-4), alkalinity (Figure 7-6), biogas production and methane content (Figure 7-7 and Figure 7-8) and to an increase in VFA accumulation (Figure 7-6), which were the direct opposite of observations in Pair 2 and Pair 3 reactors. Evidence from Figure 7-1 suggests that there was VS accumulation in the Pair 1 reactors from day 65 – 85, probably due to the inhibition of the hydrolytic bacteria caused by the acidification of the reactors caused by the increasing VFA concentrations (Figure 7-5), and that caused Pair 1 reactors to be overloaded (FOS:TAC ratio > 1.4: 1 (Figure 7-6), leading to a decrease in biogas production (Figure 7-7). A study by Li *et al.* (2017) on the instability mechanism and early warning indicator for mesophilic AD reactors treating vegetable waste at OLR of 0.5, 1.0 and 1.5 gVS.L⁻¹.d⁻¹ showed that process inhibition occurred at an OLR of 1.5 gVS.L⁻¹.d⁻¹. Thus, in addition to the benefits of co-digestion described earlier, the low OLR used in the current study may have also contributed to the stability observed in the operation of all reactors from day 7 – 64, including those without ash-extract supplementation.

7.2.3 Reactor concentrations of ammoniacal nitrogen (NH₄⁺-N), free ammonia (NH₃), chemical oxygen demand (COD_T), total Kjeldahl nitrogen (TKN) and pH

The ammoniacal-N which was present in the AD reactors during start-up at a concentration of 2,030 mg.L⁻¹, came from the digested cattle slurry inoculum, most likely from the urea originally present in the undigested slurry. However, due continuous wash-out and volatilization, the concentrations of the original ammoniacal-N in Pair 1, Pair 2 and Pair 3 reactors by day 36 had reduced by 79.7, 77.6 and 79.7%, respectively. Figure 7-2 shows the variation in the mean concentrations of ammoniacal-N, total Kjeldahl nitrogen and organic nitrogen in the Pair 1, Pair 2 and Pair 3 reactors from day 1 – 84.

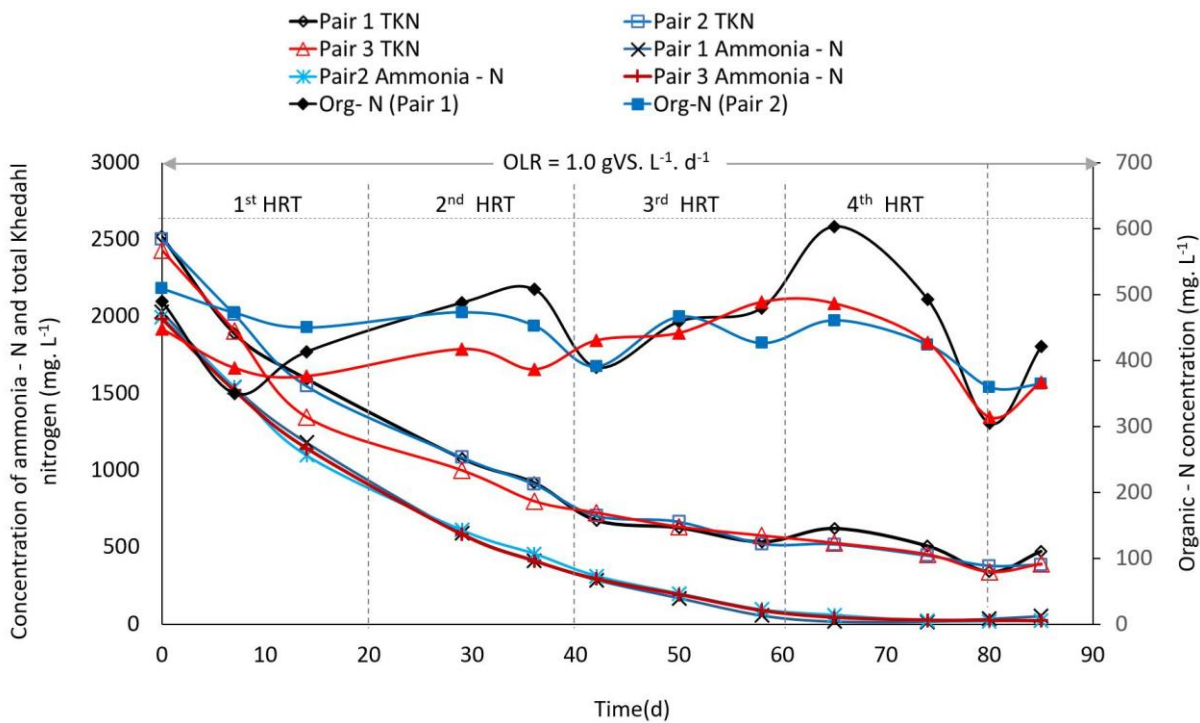


Figure 7-2 Mean concentration of ammoniacal nitrogen ($\text{NH}_4^+\text{-N}$), total Kjeldahl nitrogen (TKN) and total organic nitrogen (Organic-N) in the Pair 1, Pair 2 and Pair 3 reactors against time.

The large reduction in ammoniacal-N concentration in the reactors shown in Figure 7-2 resulted to a continual decrease in the pH inside reactors until the pH in the six reactors dropped to a value < 6.75 on day 65 (Figure 7-4), leading to a sharp decline in methane production in all the six reactors (Figure 7-7). The response of the AD CSTR used in the current study to pH change agrees with Holland (2013), who reported that a sudden fluctuation in pH can inhibit gas production and precipitate failure of an AD digester. However, between day 62 – 65, the concentration of $\text{NH}_4^+\text{-N}$ in Pair 1, 2 and 3 reactors ranged from 16.1 – 51.8, 22.4 – 57.4 and 25.2 – 42 mg.L^{-1} , respectively, is still within the acceptable range (i.e. 50 - 200 mg.L^{-1}) reported by Gerardi (2006) as being beneficial to methanogens. However, between day 65 – 85, the Pair 1, 2 and 3 had lost 97, 99 and 99% of their original $\text{NH}_4^+\text{-N}$ content, respectively. Interestingly, Pair 2 and Pair 3 reactors did not show signs of acidification because of the supplementation with biomass ash-extracts that commenced from day 65 onwards. However, within the same period (day 65 – 85), the non-supplemented control reactors (Pair 1) failed completely (Figure 7-3) due to rapid acidification.

The concentration of free ammonia inside the reactors (Figure 7-3) appeared to decrease in line with the pH of the reactors (Figure 7-4). From day 1 – 42, the concentration of free NH_3

varied from $88.7 - 2.7 \text{ mg.L}^{-1}$ in Pair 1; $80.4 - 2.7 \text{ mg.L}^{-1}$ in Pair 2 and $78.6 - 3.3 \text{ mg.L}^{-1}$ in Pair 3 reactors, indicating the reactors lost 97%, 96% and 96%, respectively, of the initial free ammonia concentration inside the reactors at day 42.

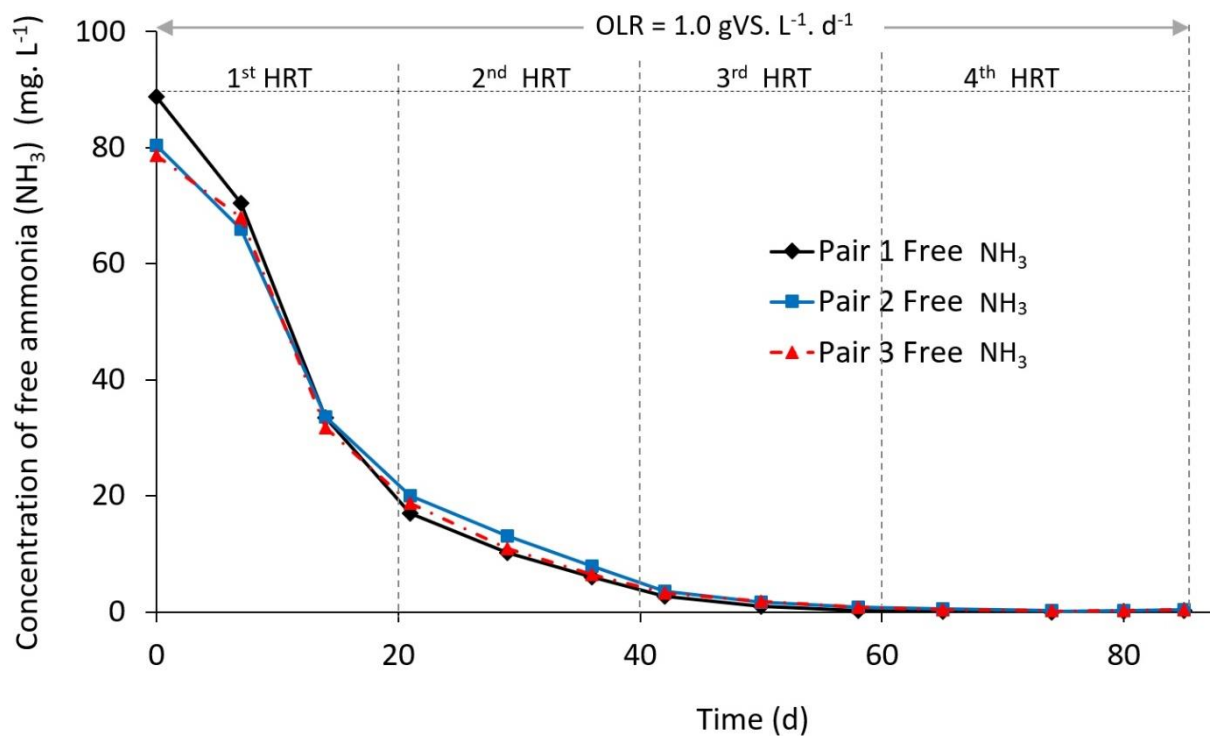


Figure 7-3 Free ammonia (NH₃) in the Pair 1, Pair 2 and Pair 3 reactors with pH over time (See Equation 2-12)

From day 43 – 85, the concentration of free ammonia remained relatively stable but at a value below 1.0 mg.L^{-1} in all the reactors, indicating nearly 100% of the original ammonia present during start-up had been washed out, corresponding to the near total loss of ammoniacal-N (Figure 7-2). However, this loss in ammonia only resulted to a slight decrease in pH for Pair 2 and 3 reactors (Figure 7-4), compared to the Pair 1 reactors, where the pH had decreased substantially to $\text{pH} < 7$. The large reduction in pH seen in Pair 1 (unsupplemented CSTR) with Varjani *et al.* (2018), who reported that total loss of ammonia/ammonium-N during the AD process signifies the loss of the primary source of the bicarbonate-ammonia buffering (alkalinity), which helps to control the pH and maintain process stability. Inasmuch as ammonia-N is beneficial nutritionally to microbes when present at the right concentration, on the contrary, free ammonia is toxic to the AD process microbes and can cause serious instability problems leading to process failure when present at high concentrations (Khedim *et al.*, 2018; Nijaguna, 2006), particularly for free ammonia concentration above 80 mg.L^{-1}

(Shah, 2014). In the current study, however, there was no evidence of possible free ammonia inhibition in any of the reactors at any time (Figure 7-3), since all the concentrations measured were below the inhibition threshold, except the high concentration of ammonia-N recorded only during start-up (Figure 7-2).

The total chemical oxygen demand (COD_T) concentration in the reactors (Figure 7-4) indicates that the total COD content in the reactors decreased steadily from day 1 - 30, and then stabilized from day 31 – 62. This period of stability in the COD_T concentration corresponds to the period during which all the reactors attained their pseudo-steady-state conditions, and when all the AD reactors had steady and similar biogas production rates, and the biogas had similar methane content (Figure 7-7 and Figure 7-8).

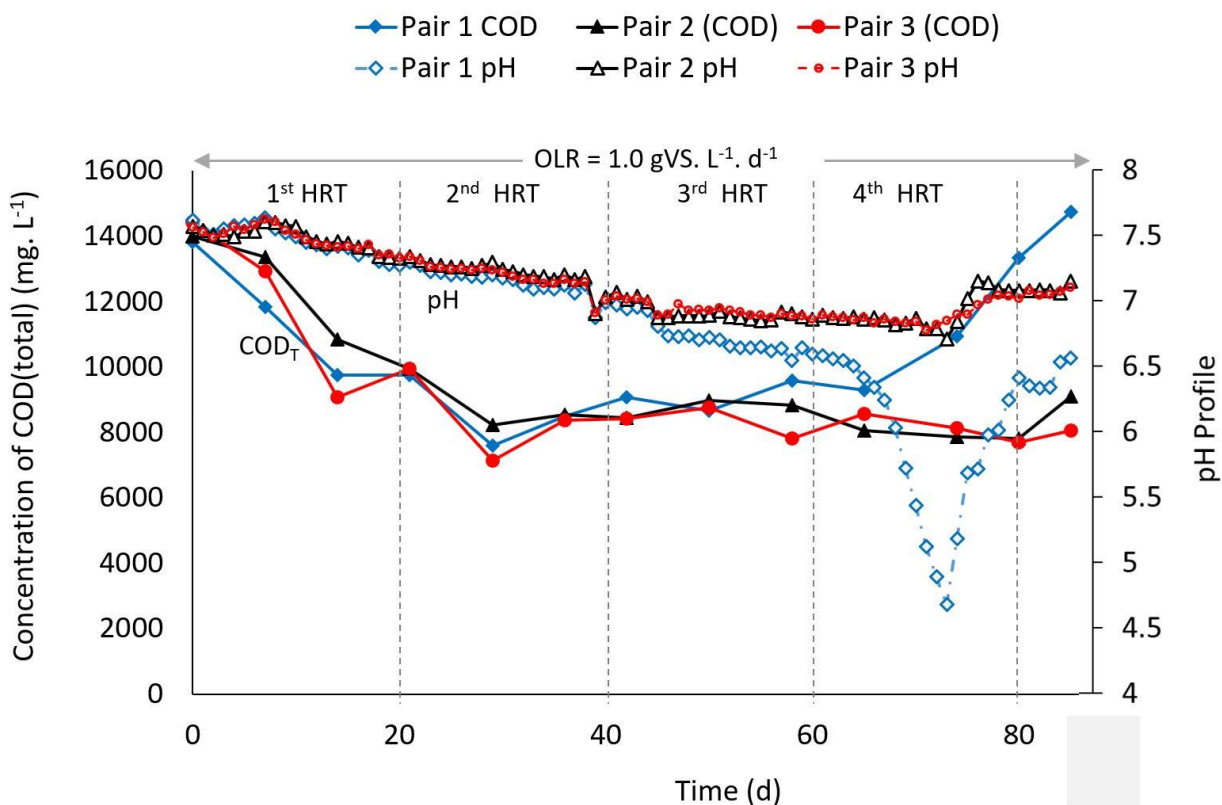


Figure 7-4 Total chemical oxygen demand (COD_T) and pH in the Pair 1, Pair 2 and Pair 3 reactors over time

Between day 1 – 64 (prior to the pH drop in Pair 1), it was observed that an increase COD_T removal resulted to a corresponding increase in biogas production (Figure 7-7), and a decrease in VFA production (Figure 7-5) in all the reactors. However, from day 65 – 85, the COD_T in the Pair 1 reactors increased substantially, due to the observed accumulation of volatile solids (Figure 7-1) which probably resulted from inhibition of the hydrolytic bacteria caused by unfavourable pH in the reactors ($pH < 5$) (Figure 7-4). These changes may be

responsible for the continual decrease in the SMP observed in the Pair 1 reactors over time (Figure 7-7), until they failed almost completely.

7.3 Volatile fatty acid profile

Figure 7-5 shows the concentration of volatile fatty acids (VFA) in the individual Pair 1, Pair 2 and Pair 3 reactors from day 1 – 85. As discussed in Session 2.7.9, VFA which are the main precursors of methanogenesis can cause inhibition to the acetoclastic and hydrogenotrophic methanogens, as well as acetogenic microbes at pH below 7 (Schön, 2010). In the current study, the VFA content of the inoculum was high (Table 7-1), which possibly led to high VFA concentrations during start-up (Figure 7-5). The main VFAs detected in the reactors in decreasing order of abundance were acetate, propionate, butyrate, valerate, isovalerate, isobutyrate, and formate. However, the concentration of these VFA decreased gradually in all reactors over the first 50 days. This period was when all the reactors maintained stable operation. However, due to slight fluctuations in pH, some traces of VFA were detected in the reactors on day 58, but these were present at concentrations which were below the typical inhibition range (Table 7-2), and they disappeared over time.

7.3.1 Volatile fatty acid (VFA) profile for Pair 1 Reactors

Figure 7-5 and Table 7-2 provide insight into variations in the concentration of VFA in the individual reactors over time. In the Pair 1 reactors (R1 and R2), the VFA started to accumulate from day 58, due to no additions of ash-extract supplements, and that caused an initial decrease in biogas production around day 60 (Figure 7-7). From day 76 – 85, these reactors showed clear signs of instability due to increasing acidification, and pH value decreasing below 6 (Figure 7-4). During this period, the concentration of acetate in reactor R1 increased from 2,262.2 – 5,934.4 mg. L⁻¹, while the propionate also increased from 920.9 – 1,897.0 mg L⁻¹. The concentration of butyrate and isobutyrate also increased from 410.9 – 677.3 mg. L⁻¹ and 54.1 – 109 mg. L⁻¹, respectively. Similarly, the concentrations of valerate and isovalerate ranged from 47.0 – 194.3 mg. L⁻¹ and 55.0 – 123.0 mg. L⁻¹, respectively. Prior to the process failure in the Pair 1 reactors, (day 65 - 75), acetate content in reactor R2 increased from 228.2 – 5,503.6 mg. L⁻¹, while the propionate also increased from 168.2 – 1,847.6 mg. L⁻¹. The concentration of butyrate and isobutyrate also increased from 408.4 – 761.9 mg. L⁻¹ and 66.1 – 101.9 mg. L⁻¹ respectively. Similarly, the concentrations of valerate and isovalerate during this time ranged from 62.6 – 289.8 mg. L⁻¹ and 63.2 – 113.4 mg. L⁻¹

respectively. The above results indicate that the individual reactors in Pair 1 had very close agreement in VFA accumulation, and all the VFA accumulation measured from day 65 – 85 in the Pair 1 reactors, corresponded with a progressive decrease in the digesters pH (Figure 7-4) and reduction in biogas and methane production (Figure 7-7 and Figure 7-8). According to Schön (2010), AD processes fail at low pH values due to the disruption of homeostasis inside the cells of the methanogens when VFAs in their unionized form penetrate the cell membrane.

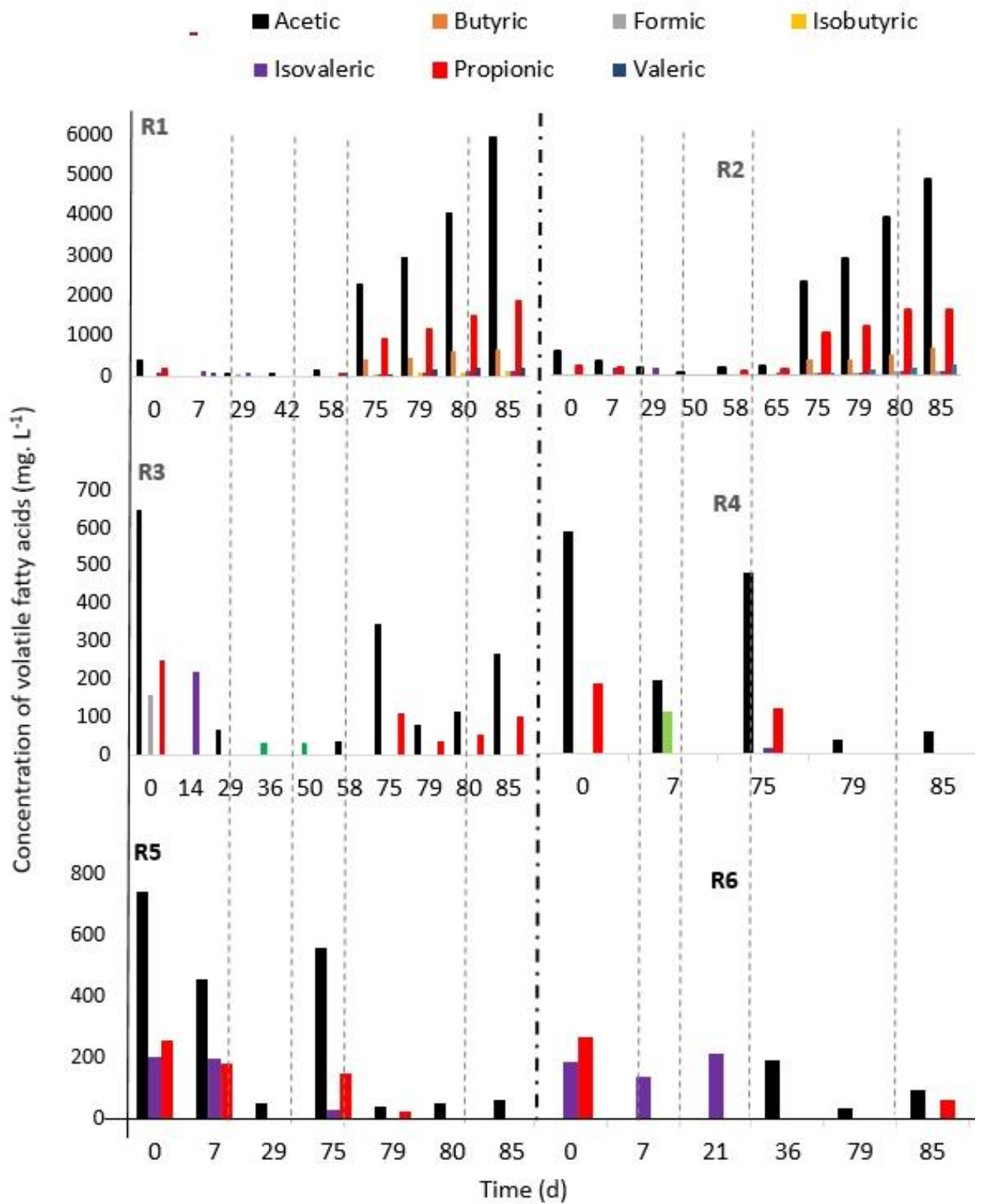


Figure 7-5 Concentration of volatile fatty acids (VFA) in the individual reactors in Pair 1 (R1 and R2), Pair 2 (R3 and R4) and Pair 3 (R5 and R6) reactors with time. The initial VFA or Pair 1 reactors was similar to Pair 2 & 3. Values in the graph represent mean values of the respective VFA from the CSTR.

Apart from the high concentration of VFA recorded during start-up, and day 75 when pH dropped briefly below 7 (Figure 7-4), a favourable pH was observed in the Pair 2 and Pair 3 reactors despite ammonia/ammonium-N washout. The most dominant VFAs detected in the Pair 2 and Pair 3 reactors from day 76 - 85 were acetate and propionate. These VFAs were mostly present at concentrations either slightly above or slightly below the inhibition threshold ($< 200 \text{ mg.L}^{-1}$) (Andreoli *et al.*, 2007; Gerardi, 2006). For instance, in the Pair 2 reactors, the concentration of acetate and propionate in R3 ranged from $79.7 - 267.5 \text{ mg.L}^{-1}$ and $98.8 - 110.1 \text{ mg.L}^{-1}$ respectively, whereas in R4 acetate and propionate ranged from $36.6 - 60.3 \text{ mg.L}^{-1}$ and $0 - 126 \text{ mg.L}^{-1}$, respectively. For the Pair 3 reactors, from day 76 - 85, the concentration of acetate in R5 and R6 varied from $42.4 - 61.3 \text{ mg.L}^{-1}$ and $0 - 26.2 \text{ mg.L}^{-1}$. Within this same period, the concentration of propionate in the same reactors (R5 and R6) were $35 - 103.9 \text{ mg.L}^{-1}$ and $0 - 70.2 \text{ mg.L}^{-1}$ respectively. At these levels of VFA, the Pair 2 and Pair 3 reactors remained stable throughout the experiment, due to the addition of ECP and EPB ash-extract supplements respectively, unlike the Pair 1 which failed because of pH and VFA concentration resulting from the absence of ash-extract supplementation.

The major difference observed between the types of VFA present in the Pair 1 (failed reactors) and the Pair 2 and 3 (stable) reactors were that the failed reactors had high concentrations of butyrate, isobutyrate, valerate and isovalerate (Figure 7-5), but these were not detected in the stable Pair 2 and Pair 3 reactors. Thus, these findings suggest that the presence of butyrate, isobutyrate, valerate and isovalerate were strong indicators of AD process failure. This observation agrees with the work of Mechichi and Sayadi (2005) and Andreoli (2007), who reported that increases in the concentration of long-chain VFA such as butyrate, isobutyrate, valerate and short-chain VFA such as propionate were indicators of AD process imbalance or instability. However, the addition of EPB ash-extract to Pair 1 reactors from day 78 - 85 started to have positive effects on the pH (Figure 7-4), and the reactor performance (Figure 7-7), and with time might eventually have led to a full recovery, despite the VFA still being very high when the reactor run was terminated (Table 7-2). From these results, it is evident that the addition of ash-extracts to the AD reactors helped to maintain a favourable pH range between $6.8 - 7.2$ inside the reactors, which enabled Pair 2 and Pair 3 to maintain their stability and to produce a steady volume of methane from day 65 - 85 (Figure 7-8). Similarly, the introduction of ash-extracts to the failed reactors (Pair 1) from day 78 - 85 started to improve their pH from 4.7 to 6.5, probably because the ash provided alkalinity and trace elements that enabled the methanogenic population to begin growing again and consume acetate.

7.3.2 Total volatile fatty acid (TVFA) from IC analysis

Total volatile fatty acid (TVFA) concentrations in the AD reactors were determined using both ion chromatographic methods (IC) and titrimetric methods as described in Section 3.8.1. Table 7-2 shows the results obtained from TVFA analysis using IC. The variation in TVFA concentration in the individual reactors generally followed the same trend. For instance, all the reactors had high concentration during start-up (day 0) due to the presence in the inoculum, as discussed above. However, from day 7 onwards, the TVFA concentration decreased until day 29, from which point it stabilized at levels below detection limits in most of the reactors.

Table 7-2 Total volatile fatty acid (TVFA) concentration in reactors R1 to R6.

Days (d)	Concentrations of total volatile fatty acids (mg. HAc. L ⁻¹)					
	Pair 1		Pair 2		Pair 3	
	R1	R2	R3	R4	R5	R6
0	768.9	895.7	1,051.0	817.0	1,203.0	503.2
7	428.4	750.9	n.d	325.3	838.3	149.4
14	n.d	n.d	217.7	n.d	n.d	n.d
21	n.d	n.d	n.d	n.d	n.d	236.9
29	268.3	391.4	66.6	n.d	53.2	n.d
36	n.d	n.d	29.0	n.d	n.d	211.7
42	71.5	n.d	n.d	n.d	n.d	n.d
50	n.d	51.6	29.1	n.d	n.d	n.d
58	280.7	278.0	35.5	n.d	n.d	n.d
65	n.d	421.6	n.d	n.d	n.d	n.d
75	3,750.2	4,361.1	458.0	646.4	737.2	n.d
79	4,904.5	5,315.5	112.8	36.7	68.5	35.0
80	6,496.7	7,183.0	162.4	n.d	51.8	n.d
85	8,917.0	8,618.0	366.3	60.4	61.3	174.2

From day 65 – 85, no supplement was added to the Pair 1 reactors. However, Pair 2 and Pair 3 were supplemented with ash extracts from the empty cocoa pod (ECP) and empty palm bunch (EPB) respectively. The information from Table 7-2, clearly shows that the TVFA concentration in the Pair 1 reactors was different from Pair 2 & 3 reactors and that is

presumed to be a result of having no additions of ash-extracts. Previous studies have shown that concentration of total TVFA in AD reactors operating normally should be below 200 mg.L⁻¹ (Andreoli, 2007). The high TVFA found in Pair 1 suggests that its failure was mainly due to acidification of the digester caused by the accumulation of volatile fatty acids.

7.3.3 Stability checks for AD reactors

7.3.3.1 Propionate to acetate ratio (P: A)

Table 7-3 shows the propionate-to-acetate (P: A) ratio in Pair 1, Pair 2 and Pair 3 reactors. According to Hill *et al.* (1987), acetic acid levels greater than 800 mg.L⁻¹, and propionate-to-acetate (P:A) ratios greater than 1:1.4 indicate an impending failure during the anaerobic digestion of cow manure. In the current study, the P:A ratio recorded in the reactors during start-up period (day 0 – 7) in reactors, R1, 2, 3, 4,5 and 6 were 1:2.1, 1:2.9, 1:2.6, 1:3.2, 1:2.9 and <1:0.005, respectively. These ratios decreased further between day 8 – 57, during which time the reactors worked normally.

Table 7-3 Propionate-to-acetate (P:A) ratio in Pair 1, 2 and 3 reactors (day 1 – 85)

Days (d)	Propionate-to-acetate ratio (P:A)					
	Pair 1		Pair 2		Pair 3	
	R1	R2	R3	R4	R5	R6
0	1:2.1	1:2.9	1:2.6	1:3.2	1:2.9	x
7	x	1:2.0	x	x	1:2.5	x
14	x	x	x	x	x	x
21	x	x	x	x	x	x
29	x	x	x	x	x	x
36	x	x	x	x	x	x
42	x	x	x	x	x	x
50	x	x	x	x	x	x
58	1:2.1	1:2.2	x	x	x	x
65	x	1:1.4	x	x	x	x
75	x	1:2.2	1:3.2	1:1.4	1:3.8	x
79	1:2.5	1:2.4	1:2.4	x	1:1.6	x
80	1:2.7	1:2.5	1:2.2	x	x	x
85	1:3.2	1:3.0	1:2.7	x	x	1:1.5

However, due to no alkaline supplementation in Pair 1 reactors, from day 58 – 85, their P:A ratios increased continuously (Table 7-3) due to the accumulation of VFA, which led to a fall in alkalinity and corresponding pH drop to below the preferred range. Thus, the evidence from this study suggests that the Pair 1 reactors suffered inhibition which led to their complete failure, when P:A ratio was between 1:2.1 – 1:3.2, and an acetic acid concentration between 2,262 – 8,917 mg.L⁻¹ in the digester. This contrasts with the findings reported by Hill *et al.* (1987) which suggested that acetic acid concentration of 800 mg.L⁻¹, or propionate to acetate ratio above 1: 1.4 is a sign of impending process failure.

The P:A ratios of reactor R4 in Pair 2 was also increased due to due to the temperature controller failure (Table 7-3), which also resulted to substantial decrease its specific methane

production (SMP) (Figure 7-7). However, the reactor did not fail due to supplementation with EPB ash-extract. In contrast, with the exception of the start-up period, the P:A ratio in reactor R3 (Pair 2) and the P:A ratio Pair 3 reactors were below the value published by (Hill *et al.*, 1987) except for few occasional values corresponding to periods of pH drop. However, increase in the P:A in those times (Table 7-3) were restored immediately by the addition of EPB ash-extract which suggests that the ash-extract shifts the equilibrium from the protonated acid to the less toxic ionized form (propionate anion). This evidence suggests that ash-extracts effectively create a good environment for the utilization of acetate and propionate, as found in Pair 2 and Pair 3 reactors. Conversely, the Pair 1 reactors experienced lack of alkalinity supplements which led to the accumulation of propionate. Comparing the performance of Pair 1 (unsupplemented) and Pair 2 and 3 (supplemented) CSTR, it is likely that the accumulation of propionate in Pair (R1 and R2) and R4 in Pair 2 AD reactors (Table 7-2 and Table 7-3) imposed changes in the thermodynamics of substrate utilization for the microbial community, making methane production unfavourable. These changes in substrate (intermediate) concentrations could lead to the inhibition of the methanogenic archaea which are the terminal electron acceptors, resulting in the accumulation of hydrogen and a rise in the free energy (ΔG) threshold for substrate utilization (Penning & Conrad, 2006). Therefore, with these assumptions, from the results obtained in the current study, it can be stated that propionate and acetate concentrations are good indicators of process instability during the AD process.

7.3.3.2 Alkalinity, TVFA and FOS:TAC ratio determined by the titrimetric method

Figure 7-6 shows the variation of total volatile fatty acid (TVFA), alkalinity and FOS:TAC ratio (all measured by simple titration; Section 3.6.1) in the Pair 1, Pair 2 and Pair 3 AD reactors over time. In a study which used alkali ratios to identify imbalances in anaerobic digesters, Martín-González *et al.* (2013) reported that the digester was able to achieve stable performance when a TVFA between 2,500 and 3,500 mg.L⁻¹ was maintained in the reactor with total alkalinity (TA) ranging between 13,000 and 15,000 mg.L⁻¹ CaCO₃. However, in the current study, the alkalinity in the reactors decreasing in line with pH over time until they became relatively stable on day 36 (Figure 7-6). The alkalinity recorded around this period in Pair 1, Pair 2 and Pair 3 reactors was 5,130; 5775 and 5,385 mg. L⁻¹ CaCO₃, respectively. However, a drop in the alkalinity was noticed in all reactors between day 43 – 50, which caused the pH to drop. This was rectified by the addition of ash-extract supplements to Pair 2 and Pair 3 reactors over this period (Figure 7-3 shows the effects of the addition of ash-

extract). However, from day 68, the alkalinity in Pair 1 reactors reduced to $< 3000 \text{ mg. L}^{-1} \text{ CaCO}_3$, while the alkalinity of Pair 2 and Pair 3 reactors, which were supplemented with biomass ash-extracts ranged between $4000 - 5000 \text{ mg. L}^{-1} \text{ CaCO}_3$. According to Andreoli (2007), a normal working AD reactor has alkalinity between $4000 - 5000 \text{ mg.L}^{-1} \text{ CaCO}_3$ and that confirms why Pair 2 and Pair 3 reactors which maintained that range of alkalinity was more stable and efficient than Pair 1 reactors (Figure 7-6 and Figure 7-7).

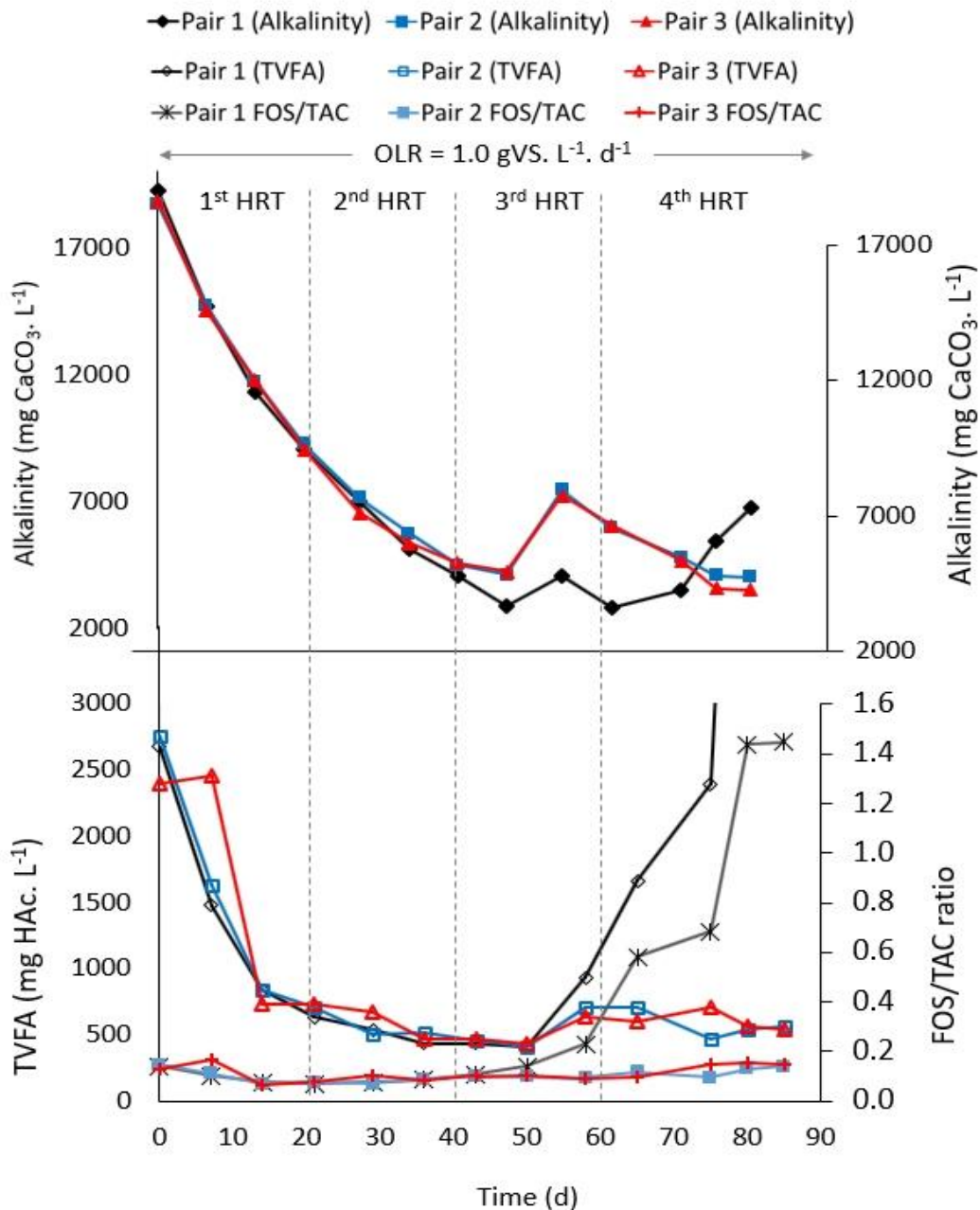


Figure 7-6 Total volatile fatty acid (TVFA), alkalinity and FOS:TAC ratio in the Pair 1, Pair 2 and Pair 3 AD reactors over time.

The TVFA concentration recorded from day 0 – day 30 in the AD reactors decreased from $2,675 - 537.6 \text{ mg HAc.L}^{-1}$ (Pair 1), $2,762 - 504.4 \text{ mg HAc.L}^{-1}$ (Pair 2) and $2,396.8 - 537.6 \text{ mg}$

HAc.L⁻¹. However, despite the high TVFA concentration in the reactors compared to the maximum of 200 mg HAc.L⁻¹ reported for stable AD processes (Andreoli, 2007), there was no inhibition in the digesters due to sufficient alkalinity being present. This was evident from the FOS:TAC ratio of < 0.2 being recorded in all the reactors within this period; confirming the reactors were not overloaded. The TVFA concentration became stable from day 30 - 58, with similar concentrations of 420 ± 16 mg HAc.L⁻¹, 430 ± 24 mg HAc. L⁻¹ and 430 ± 20 mg HAc. L⁻¹ in Pair 1, Pair 2 and Pair 3, respectively. However, around the time of a sudden pH drop < 7 (day 64), the TVFA increased to 936, 703.6 and 604 mg HAc.L⁻¹, respectively. However, the addition of biomass ash-extracts to Pair 2 and Pair 3 reactors provided alkalinity which brought about a reduction in the VFA and maintained the reactors in stable condition throughout the remainder of the study. In contrast, when no supplements were added, after day 58, Pair 1 reactors continued to accumulate TVFA which ranged from 1,666.4 – 9,800 mg HAc.L⁻¹ and explains why biogas production ceased almost completely due to reactor failure.

Figure 7-6 also presents the FOS:TAC ratio inside the reactors, which is an important indicator of the condition of AD reactors. Due to the addition of the ash-extract supplements, the maximum FOS:TAC ratio recorded in Pair 2 and Pair 3 reactors during the study ranged from 0.1 – 0.2: 1, which indicates an efficient AD process (de Lemos Chernicharo, 2007; Khanal, 2011a; Lossie & Pütz, 2008). On the contrary, the FOS:TAC ratio recorded in the Pair 1 reactors between day 58 – 85 ranged from 0.2 – 1.4: 1, indicating failure, and parallels the decrease in methane production and the high VFA (Figure 7-5) recorded at this time. The FOS:TAC ratio > 0.8 in the Pair 1 reactors indicates that the TVFA exceeded the alkalinity from day 65 – 73, which was also evident from the drop in pH to values < 5 (Figure 7-4). Conversely, a FOS:TAC ratio < 0.3: 1 was recorded in Pair 2 and Pair 3 reactors over the same period suggesting that ash-extract supplementation provided a suitable environment in the reactors for the methanogenic archaea and was considered to be the main reason for the improved efficiency and stability of the supplemented reactors throughout the study.

7.4 Methane production and composition

7.4.1 Performance of the reactors during pseudo-steady-state conditions

Anaerobic digestion process produces renewable biogas which can serve as an alternative source to fossil fuel (Khedim *et al.*, 2018). Therefore, achieving a stable or steady-state

operation over a long period of time during the process could provide useful information about the sustainability, viability and cost-benefits, that might be useful for investors, economic analysts and policymakers. Thus, in the current study, a pseudo-steady-state condition was defined to be when the reactors had been operated in a stable condition over a period during which daily variations in the biogas volume and composition were typically < 10% over the period. In the current study, between day 0 – 24, the volume of methane produced in the reactors varied greatly, probably due to different rates of hydrolysis of the substrates inside the reactors, acclimatization and lag phase affecting bacterial and archaeal population composition, and the inclusion of the background methane production from the organic matter present in the inoculum into the biogas mix. In contrast, from day 25 – 85, some of the reactors achieved a relatively steady and comparable rate of methane production (Figure 7-7).

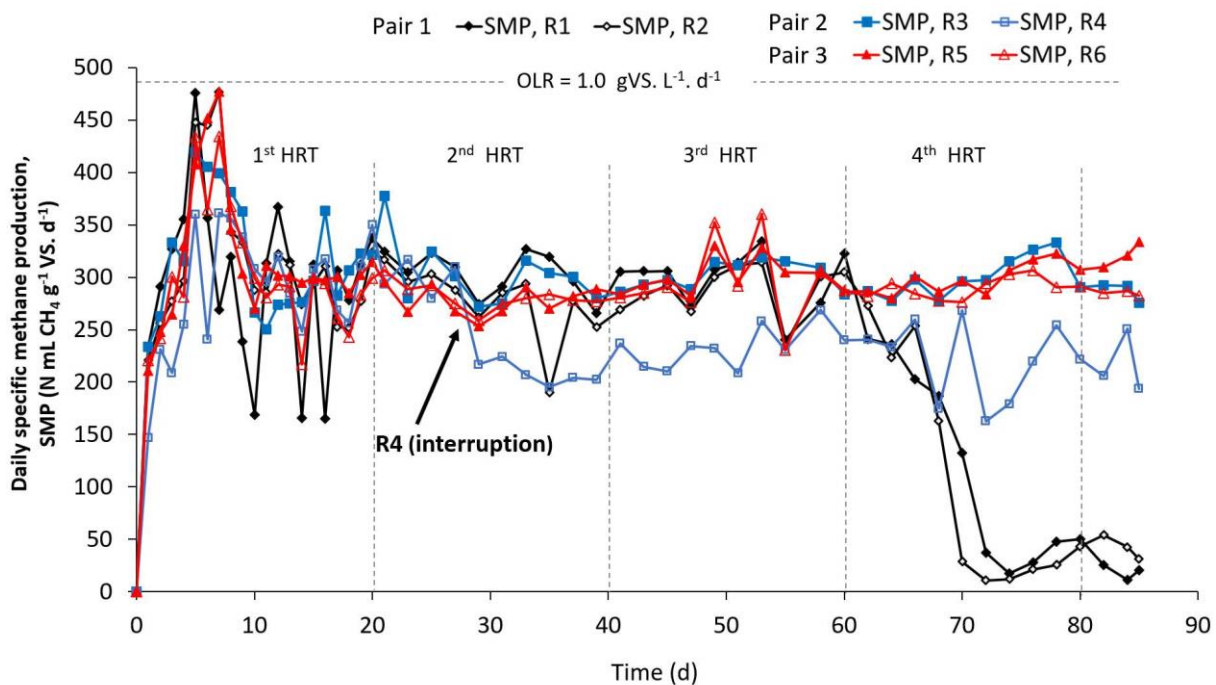


Figure 7-7 Specific methane production from individual reactors in the Pair 1, Pair 2 and Pair 3 reactors over time. The arrow shows the point from which R4 suffered interruption due to temperature controller failure.

On day 28, there was a large reduction in the daily methane production by Pair 2 reactors compared to Pair 1 and Pair 3 due to unplanned power interruptions suffered by one of the reactors in Pair 2 (i.e. reactor R4) which affected temperature control (Figure 7-8). Between day 30 – 64, during which time all the reactors attained a pseudo-steady state, the mean pH in

the Pair 1, Pair 2 and Pair 3 reactors were 6.87, 7.02 and 7.01, respectively. During this period, the cumulative methane from Pair 1, Pair 2 and Pair 3 reactors during the steady-state period were 3,407; 3,099.6 and 3,416.9 N mL CH₄ per reactor (Figure 7-8). These results show that between day 20 – 64, during which time the reactors were operating at a pseudo-steady-state, apart from Pair 2 reactors, all other reactors produced nearly equal volumes of dry methane gas at STP (Figure 7-8).

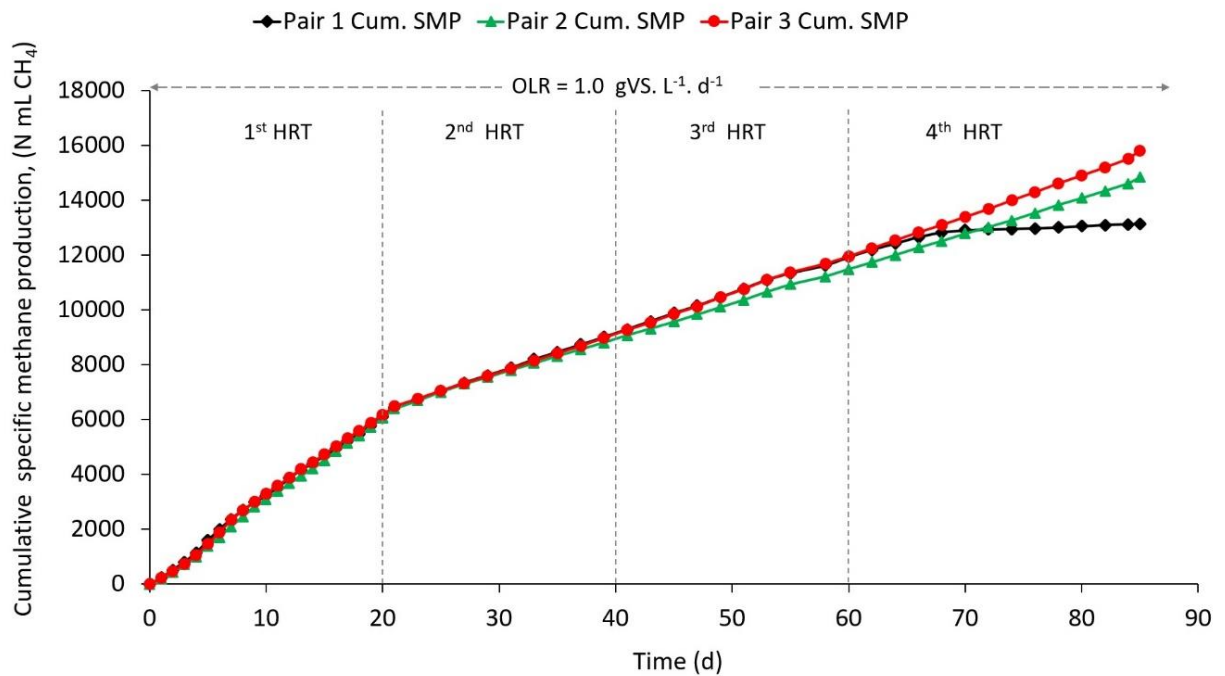


Figure 7-8 Cumulative and specific methane production (SMP) from Pair 1, Pair 2 and Pair 3 reactors over time

During the pseudo-steady-state period, the specific methane production (SMP) for Pair 1, Pair 2 and Pair 3 reactors were 284.0, 258.3 and 284.7 N mL CH₄.g⁻¹VS added.d⁻¹, respectively, and mean methane content (%) in the biogas for Pair 1, Pair 2 and Pair 3 reactors was 55.8%, 55.7% and 56.4%, respectively. This indicates that at the steady-state, all the reactors had similar methane composition in their biogas, with a difference between the mean SMP of Pair 1 and Pair 3 reactors of just 0.3%, while the difference between the mean SMP of Pair 1 reactors and Pair 2 was 9%. This large difference between the SMP from Pair 1 and Pair 2 reactors was due to a decrease in the volume of methane gas produced by the reactor R4 caused by its faulty temperature controller from day 28 – 85 (Figure 7-7). These results were analyzed further by comparing the mean of the SMP from each pair of reactors to identify any correlations between the different pairs of reactors at the 5% level of significance. A paired sample t-test (2-tailed) was also used to determine the statistical significance of the effects of

ash extract additions on the methane productivity and biogas composition. A comparison between the mean volumetric production Pair 1 and Pair 2 reactors from day 65 – 85 showed a very weak correlation ($R^2 = 0.25$), and the comparison between Pair 1 and 3 also showed a very weak correlation ($R^2 = 0.33$). However, the same comparison between Pair 2 and Pair 3 reactors, which were both supplemented with ash-extracts, showed a positive correlation ($R^2 = 0.71$). A paired sample t-test at the 95% confidence interval also showed that the difference between the mean SMP over the period day 65 – 85 from Pair 1 and Pair 2 reactors, and between the Pair 1 and Pair 3 reactors was statistically significant ($p < 0.05$), whereas there was no statistically significant difference between the mean SMP in Pair 2 and Pair 3 reactors ($p > 0.05$).

7.5 Conclusion

To determine the effectiveness of ash-extracts in providing alkalinity and buffering for the maintenance of pH within the optimum range for AD processes.

The data obtained from X-ray diffraction and elemental analysis showed that the EPB and ECP ash-extracts were very high in K_2CO_3 , NaOH and $KHCO_3$, and that they also contained trace metals, which suggests that they could serve as good sources of bicarbonate alkalinity and trace elements for the maintenance of reactor stability and optimization of the AD process.

To determine whether EPB and ECP ash-extract supplements can maintain steady-state conditions in continuous AD reactors over extended operating periods

Pair 1 (non-supplemented reactors) started to fail from day 65 – 75 as a result of VFA accumulation, which led to a decrease in alkalinity, and fall in pH from 7 to 4.6, and a decrease in the mean SMP by 73%, compared to Pair 3 (supplemented with EPB ash-extracts). Pair 2 (supplemented with ECP ash-extracts) gave approximately 60% higher methane production than Pair 1 reactors, but less than Pair 3 reactors due to an electrical fault. These findings indicate that the stability achieved in the Pair 2 and 3 reactors was due to supplementation with ash-extracts, and as a result of this investigation, there appears to be clear benefits to methane production following supplementation with ash-extracts.

To determine whether ash-extract supplements can restore the activity of AD reactors that are exhibiting a declining or failing performance

Pair 1(non-supplemented reactors) which had failed completely by day 75 began to show initial signs of recovery after commencing supplementation with EPB ash-extract from day 75 onwards. The short duration of the experiment did not provide sufficient time for full recovery; however, noticeable improvement was observed in terms of higher methane production, lower VFA concentrations and a rising pH value compared to the period before supplementation.

Chapter 8 Final remarks and recommendations for further research work

8.1 Final remarks

Extensive research has already been carried out by many investigators on the anaerobic digestion (AD) of various biomass feedstocks but has focussed on the use of expensive chemical reagents for the AD process optimization. Prior to the current study, no previous research has investigated the use of ash-extracts, produced from ash generated by the burning of agricultural wastes, an abundant and readily available material in developing countries, as an alternative low-cost trace nutrient substitute or alkaline supplement for AD process optimization. Interestingly, the current study has demonstrated successfully that the high alkalinity content of the ash-extracts enables it to maintain favourable operating pH and provide stability to the AD process. In addition to the high alkalinity, ash extracts contain beneficial levels of essential trace nutrients which were also considered to have played a supporting role in optimizing the process since failure of AD reactors with grass silage as a mono-feedstock is often linked to a deficiency of trace nutrients. Thus, the current study has made a major contribution to research on AD processes by demonstrating that value-added products in the form of nutrient-rich soluble extracts can be recovered from biomass ash and used to optimize AD processes. This implies that the AD processes could be made more efficient and ultimately, they should become cheaper, making them more accessible to people from low-income countries and developing countries, helping them to solve their energy needs. The current study also offered some important insights into the possibilities of processing these ash-extracts further into solid crystals (salts). Further studies of more efficient ways of producing these salt-extract crystals could lead to its production in commercial quantities, opening the possibility for it to be sold in different parts of the world for the optimization of AD processes, generating income for low-income countries.

8.2 Recommendations

Although ash-extracts from empty palm fruit bunch, empty cocoa pods and plantain peels used in the current study have proven to have great potential for enhancing and optimizing AD processes, there are certain limitations to the work in the sense that it has only been applied to lignocellulosic biomass feedstocks. Therefore, further research should be carried out on other feedstocks such as food wastes, municipal sewage and other industrial wastes

with greater focus on the use of low-cost ash-extract supplementation as an effective low-cost substitute to expensive commercial chemical reagents. That work may reveal other practical benefits and lead to the wider application of ash-extracts and help to advance affordable AD technologies in developing countries. To realise this potential, specific research should be conducted in the following areas:

1. Compare the physical and chemical characteristics of ash from various types of biomass, especially their alkalinity or saponification value, and their trace nutrient contents, for the estimation of the actual quantities required to optimize any AD process.
2. More research is also needed to determine standard concentrations for a range of different ash-extracts proposed for optimizing AD processes using batch assays and continuous reactors.
3. The effects of supplementation with a range of different ash-extracts should be investigated on a broad range of anaerobic digestion feedstocks, including the digestion of food wastes, animal manures, industrial effluents, wastewater sludge, etc.
4. As a result of several power cuts experienced in the current study, and their adverse effects on the process stability, more studies should investigate the effect of sudden temperature changes on the microbial community compositions with and without ash-extracts as supplements.
5. To investigate the potential of using a mixture of crude bacterial enzymes and ash-extracts as process supplements to stimulate the anaerobic digestion of different lignocellulosic feedstocks, as an alternative to supplementation with pure enzymes already used in practice.
6. To better understand the effects of the combination of ash-extracts and chemical reagents in the pretreatment of biomass feedstock to serve as potential ways of reducing the cost and quantity of commercial reagents used during pretreatment.
7. To investigate the effects of ash-extracts on the growth rate of microbes and microbial diversity through cell enumeration, cell sorting and biomarkers using biophysical technologies such as flow cytometry.
8. To establish the optimum ignition temperatures for preparing the ashes from the waste biomass material, in order to minimize the degradation or volatilization of essential trace nutrients at excessive temperatures.
9. The current study found that the addition of raw biomass ash to batch assays could lead to inhibition of methane production at certain concentrations. Although this was

not reported in the main thesis, results supporting this conclusion are annexed (See Annex 2). Therefore, further work is needed to better understand the inhibitory nature of these materials at certain concentrations.

10. Future research also needs to examine the potential of exploiting bread mould (containing hydrolytic enzymes) and ash-extracts as low-cost materials for aerobic pretreatment of lignocellulosic feedstocks. Preliminary research has identified a potential synergistic effect between these materials.
11. Further research should be conducted on the mass balance to determine the fate of the trace nutrients from the ash-extract supplements, trace nutrients in the feedstock and the trace nutrients in the seed sludge, before and after anaerobic digestion, to establish the fate of the trace nutrients, and their partitioning and adsorption by the microbial biomass. This can be studied together with recommendation 1.
12. With respect to COD analysis, organic phase analysis methods are available, for example by differential filtration and settlement. This is recommended for work which necessitates a mass balance and analysis of rate limiting steps in the AD community.

REFERENCES

- Abdel-Jawad, M. (2001). Energy options for water desalination in selected ESCWA member countries. *UN, New York*.
- Abu-Dahrieh, J., Orozco, A., Groom, E., & Rooney, D. (2011). Batch and continuous biogas production from grass silage liquor. *Bioresour Technol*, 102(23), 10922-10928. doi: 10.1016/j.biortech.2011.09.072
- Acton, Q. A. (2012). *Advances in Ethanol Research and Application: 2012 Edition*: ScholarlyEditions.
- Agbor, V. B., Cicek, N., Sparling, R., Berlin, A., & Levin, D. B. (2011). Biomass pretreatment: fundamentals toward application. *Biotechnol Adv*, 29(6), 675-685. doi: 10.1016/j.biotechadv.2011.05.005
- Akuru, U. B., Onukwube, I. E., Okoro, O. I., & Obe, E. S. (2017). Towards 100% renewable energy in Nigeria. *Renewable and Sustainable Energy Reviews*, 71, 943-953. doi: 10.1016/j.rser.2016.12.123
- Alloway, B. J. (1995). *Heavy Metals in Soils*: Blackie Academic & Professional.
- Andreoli, C. V., Von Sperling, M., Fernandes, F., & Ronteltap, M. (2007). *Sludge Treatment and Disposal*: IWA Publishing.
- Andreoli, C. V., Von Sperling, M., Fernandes, F., & Ronteltap, M. . (2007). Sludge treatment and disposal. IWA publishing.
- Angelidaki, I., Alves, M., Bolzonella, D., Borzacconi, L., Campos, J., Guwy, A., Kalyuzhnyi, S., Jenicek, P., & Van Lier, J. (2009). Defining the biomethane potential (BMP) of solid organic wastes and energy crops: a proposed protocol for batch assays. *Water science and technology*, 59(5), 927-934.
- Angelidaki, I., & Sanders, W. (2004). Assessment of the anaerobic biodegradability of macropollutants. *Reviews in Environmental Science and Biotechnology*, 3(2), 117-129.
- Apha. (2005). Standard methods for the examination of water and wastewater. *Federation, Water Environmental, American Public Health Association (APHA): Washington, DC, USA*.
- Ayoub, A. S., & Lucia, L. A. (2017). *Introduction to Renewable Biomaterials: First Principles and Concepts*: John Wiley & Sons.

- Bajpai, P. (2016). Pretreatment of lignocellulosic biomass for biofuel production. . *Springer*.
- Bajpai, P. (2017). *Anaerobic Technology in Pulp and Paper Industry*: Springer Singapore.
- Barnett, J., & Jeronimidis, G. (2009). *Wood Quality and its Biological Basis*: Wiley.
- Bassam, N. (2013). *Energy plant species: their use and impact on environment and development*: Routledge.
- Bassam, N. E. (2010). *Handbook of Bioenergy Crops: A Complete Reference to Species, Development and Applications*: Earthscan.
- Basu, P. (2013). *Biomass Gasification, Pyrolysis and Torrefaction: Practical Design and Theory*: Elsevier Science.
- Beline, F., Rodriguez-Mendez, R., Girault, R., Bihan, Y. L., & Lessard, P. (2017). Comparison of existing models to simulate anaerobic digestion of lipid-rich waste. *Bioresour Technol*, 226, 99-107. doi: 10.1016/j.biortech.2016.12.007
- Bergin, B. (2004). *Loyal to the Land: The Legendary Parker Ranch. 1950-1970, the senior stewards*: University of Hawai'i Press.
- Bharathiraja, B., Sudharsana, T., Jayamuthunagai, J., Praveenkumar, R., Chozhavendhan, S., & Iyyappan, J. (2018). Biogas production – A review on composition, fuel properties, feed stock and principles of anaerobic digestion. *Renewable and Sustainable Energy Reviews*, 90, 570-582. doi: 10.1016/j.rser.2018.03.093
- Bitton, G. (2005). *Wastewater Microbiology*: Wiley.
- Boe, K., Batstone, D. J., Steyer, J.-P., & Angelidaki, I. (2010). State indicators for monitoring the anaerobic digestion process. *Water Res*, 44(20), 5973-5980.
- Boller, B., Posselt, U. K., & Veronesi, F. (2010). *Fodder Crops and Amenity Grasses*: Springer New York.
- Boonman, G. (2013). *East Africa's grasses and fodders: Their ecology and husbandry*: Springer Netherlands.
- Brink, M. a. D. E. G. (2012). *Fibres*: PROTA Foundation.

- Brodeur, G., Yau, E., Badal, K., Collier, J., Ramachandran, K., & Ramakrishnan, S. (2011). Chemical and physicochemical pretreatment of lignocellulosic biomass: a review. *Enzyme research*, 2011.
- Brown, H., & Stigge, B. (2017). *Infrastructural Ecologies: Alternative Development Models for Emerging Economies*: MIT Press.
- Bureau, U. S. C. (2017). U.S. Census Bureau Current Population (<https://www.census.gov/popclock/print.php?component=counter>(Accesed 28/11/2017)).
- Buswell, A., & Mueller, H. (1952). Mechanism of methane fermentation. *Industrial & Engineering Chemistry*, 44(3), 550-552.
- Cai, Y., Hua, B., Gao, L., Hu, Y., Yuan, X., Cui, Z., Zhu, W., & Wang, X. (2017). Effects of adding trace elements on rice straw anaerobic mono-digestion: Focus on changes in microbial communities using high-throughput sequencing. *Bioresour Technol*, 239, 454-463. doi: 10.1016/j.biortech.2017.04.071
- Capson-Tojo, G., Torres, A., Muñoz, R., Bartacek, J., & Jeison, D. (2017). Mesophilic and thermophilic anaerobic digestion of lipid-extracted microalgae *N. gaditana* for methane production. *Renewable Energy*, 105, 539-546. doi: 10.1016/j.renene.2016.12.052
- Casler, M. D., & Duncan, R. R. (2003). *Turfgrass Biology, Genetics, and Breeding*: Wiley.
- Charrier, A. (2001). *Tropical Plant Breeding*: Quae.
- Chen, B., Li, J. S., Wu, X. F., Han, M. Y., Zeng, L., Li, Z., Chen, G. Q. . (2018). Global energy flows embodied in international trade: A combination of environmentally extended input–output analysis and complex network analysis. *Applied Energy*, 210, 98–107. doi: 10.1016/j.apenergy.2017.10.113
- Chen, L., Jian, S., Bi, J., Li, Y., Chang, Z., He, J., & Ye, X. (2016). Anaerobic digestion in mesophilic and room temperature conditions: Digestion performance and soil-borne pathogen survival. *J Environ Sci (China)*, 43, 224-233. doi: 10.1016/j.jes.2015.11.013
- Chen, Y., Cheng, J. J., & Creamer, K. S. (2008). Inhibition of anaerobic digestion process: a review. *Bioresour Technol*, 99(10), 4044-4064. doi: 10.1016/j.biortech.2007.01.057
- Cheng, J. (2009). *Biomass to renewable energy processes*: CRC press.

- Cheng, Y., Engling, G., Moosmüller, H., Arnott, W. P., Chen, L. W. A., Wold, C. E., Hao, W. M., & He, K.-B. (2016). Light absorption by biomass burning source emissions. *Atmospheric Environment*, *127*, 347-354. doi: 10.1016/j.atmosenv.2015.12.045
- Chikoye, D., Ellis-Jones, J., Alum, A., Tarawali, G., & Avav, T. (2005). *Reducing poverty through improved Imperata control*. Paper presented at the Proceedings of the second Imperata management stakeholders' conference, held in Makurdi, Benue State, Nigeria. IITA, Ibadan, Nigeria. 119pp.
- Chojnacka, K., & Saeid, A. (2018). *Recent Advances in Trace Elements*: Wiley.
- Choong, Y. Y., Norli, I., Abdullah, A. Z., & Yhaya, M. F. (2016). Impacts of trace element supplementation on the performance of anaerobic digestion process: A critical review. *Bioresour Technol*, *209*, 369-379. doi: 10.1016/j.biortech.2016.03.028
- Chynoweth, D. P., Turick, C. E., Owens, J. M., Jerger, D. E., & Peck, M. W. . (1993). Biochemical methane potential of biomass and waste feedstocks. *Biomass and bioenergy*, *5(1)*, 95-111.
- Clark, J. H., & Deswarte, F. (2014). *Introduction to Chemicals from Biomass*: Wiley.
- Cochrane, M. (2010). *Tropical Fire Ecology: Climate Change, Land Use and Ecosystem Dynamics*: Springer Berlin Heidelberg.
- Cook, S. M., Skerlos, S. J., Raskin, L., & Love, N. G. (2017). A stability assessment tool for anaerobic codigestion. *Water Res*, *112*, 19-28. doi: 10.1016/j.watres.2017.01.027
- Cushion, E., Whiteman, A., & Dieterle, G. (2009). *Bioenergy Development: Issues and Impacts for Poverty and Natural Resource Management*: World Bank Publications.
- Da Ros, C., Cavinato, C., Pavan, P., & Bolzonella, D. (2017). Mesophilic and thermophilic anaerobic co-digestion of winery wastewater sludge and wine lees: An integrated approach for sustainable wine production. *J Environ Manage*, *203(Pt 2)*, 745-752. doi: 10.1016/j.jenvman.2016.03.029
- Dahlquist, E. E. (2013). Technologies for converting biomass to useful energy: combustion, gasification, pyrolysis, torrefaction and fermentation. *CRC Press*.
- De Lemos Chernicharo, C. A. (2007). *Anaerobic Reactors*: IWA Publishing.
- De Mes, T., Stams, A., Reith, J., & Zeeman, G. (2003). Methane production by anaerobic digestion of wastewater and solid wastes. *Bio-methane & Bio-hydrogen*, 58-102.

- De Souza, W. R. (2013). Microbial degradation of lignocellulosic biomass *Sustainable Degradation of Lignocellulosic Biomass-Techniques, Applications and Commercialization*: InTech.
- Demirbas, A. (2008). *Biofuels: Securing the Planet's Future Energy Needs*: Springer London.
- Demirbas, F. M., Balat, M., & Balat, H. (2011). Biowastes-to-biofuels. *Energy Conversion and Management*, 52(4), 1815-1828. doi: 10.1016/j.enconman.2010.10.041
- Demirbas, M. F., Balat, M., & Balat, H. (2009). Potential contribution of biomass to the sustainable energy development. *Energy Conversion and Management*, 50(7), 1746-1760.
- Drosg, B. (2013). Process monitoring in biogas plants. In IEA Bioenergy Task (Vol. 37).
- Eia. (2016). U.S. Energy Information Administration_Nigeria.pdf.
- Eia. (2017). Biomass—renewable energy from plants and animals. U.S. Energy Information Administration. https://www.eia.gov/energyexplained/index.cfm?page=biomass_home (Assessed: 17/11/17).
- Eleri, E. O., Ugwu, O., & Onuvae, P. (2012). Expanding access to pro-poor energy services in Nigeria. *International Center for Energy, Environment and Development, Abuja, Nigeria*.
- Emodi, N. V. (2016). *Energy Policies for Sustainable Development Strategies: The Case of Nigeria*: Springer Singapore.
- Energy-Insights. (2011). Energy News: Peak Oil: a brief introduction. <http://www.energyinsights.net/cgi-script/csArticles/articles/000068/006853.htm> (Accessed 30/12/2017).
- Engineers, N. B. C. (2008). *The Complete Technology Book on Minerals & Mineral Processing*: NIIR Project Consultancy Services.
- Eu-Commission. (2003). Directive 2003/30/EC of the European Parliament and of the Council of 8 May 2003 on the promotion of the use of biofuels or other renewable fuels for transport. *Official Journal of the European Union*, 5.
- Faithfull, N. T. (2002). *Methods in agricultural chemical analysis: a practical handbook*: Cabi.
- Fao. (2013-2017). Country Programming Framework (CPF) Federal Republic of.
- Federation, W. E. (2007). Operation of Municipal Wastewater Treatment Plants: Manual of Practice 11: New York: McGraw-Hill Professional.

- Felchner-Zwirello, M. (2014). *Propionic Acid Degradation by Syntrophic Bacteria During Anaerobic Biowaste Digestion*: KIT Scientific Publishing.
- Ferreira, D. D. J., Lana, R. D. P., Zanine, A. D. M., Santos, E. M., Veloso, C. M., & Ribeiro, G. A. (2013). Silage fermentation and chemical composition of elephant grass inoculated with rumen strains of *Streptococcus bovis*. *Animal Feed Science and Technology*, 183(1-2), 22-28. doi: 10.1016/j.anifeedsci.2013.04.020
- Ferreira, G. (2013). *Alternative Energies*. Springer. *Springer Berlin Heidelberg*
- Freeman, C., Leane, E., & Watt, Y. (2011). *Considering Animals: Contemporary Studies in Human-animal Relations*: Ashgate Pub.
- Frigon, J. C., & Guiot, S. R. (2010). Biomethane production from starch and lignocellulosic crops: a comparative review. *Biofuels, Bioproducts and Biorefining*, 4(4), 447-458.
- Gerardi, M. H. (2003). *The microbiology of anaerobic digesters*: John Wiley & Sons.
- Gerardi, M. H. (2006). *Wastewater Bacteria*: Wiley.
- Ghosh, S. K. (2017). *Utilization and Management of Bioresources: Proceedings of 6th IconSWM 2016*: Springer Singapore.
- Glanpracha, N., & Annachhatre, A. P. (2016). Anaerobic co-digestion of cyanide containing cassava pulp with pig manure. *Bioresour Technol*, 214, 112-121. doi: 10.1016/j.biortech.2016.04.079
- Gnanamanickam, S. S. (2009). *Biological Control of Rice Diseases*: Springer Netherlands.
- Goel, R. (2007). *Laboratory techniques in sericulture*: APH Publishing.
- Grady Jr, C. L., Daigger, G. T., Love, N. G., & Filipe, C. D. . (2011). *Biological wastewater treatment*. CRC press.
- Gray, N. F. E. (2004). *Biology of wastewater treatment World Scientific.*, 4.
- Gübitz, G., Bauer, A., Bochmann, G., Gronauer, A., & Weiss, S. (2015). *Biogas Science and Technology*: Springer International Publishing.
- Gupa, M. K. (2012). *Power Plant Engineering*: PHI Learning.

- Gupta, V. G., Tuohy, M., Kubicek, C. P., Saddler, J., & Xu, F. (2013). *Bioenergy Research: Advances and Applications*: Elsevier Science.
- Gupta, V. K., & Tuohy, M. G. (2013). *Biofuel Technologies: Recent Developments*: Springer Berlin Heidelberg.
- Hackstein, J., & Van Alen, T. (2010). (endo) symbiotic methanogenic archaea.
- Haghighi Mood, S., Hossein Golfeshan, A., Tabatabaei, M., Salehi Jouzani, G., Najafi, G. H., Gholami, M., & Ardjmand, M. (2013). Lignocellulosic biomass to bioethanol, a comprehensive review with a focus on pretreatment. *Renewable and Sustainable Energy Reviews*, 27, 77-93. doi: <https://doi.org/10.1016/j.rser.2013.06.033>
- Hahn, S., Reynolds, L., & Egbunike, G. (1992). *Cassava as Livestock Feed in Africa: Proceedings of the IITA/ILCA/University of Ibadan Workshop on the Potential Utilization of Cassava as Livestock Feed in Africa: 14-18 November 1988, Ibadan, Nigeria*: IITA.
- Hai, F. I., Yamamoto, K., & Lee, C. H. (2013). *Membrane Biological Reactors*: IWA Publishing.
- Hakeem, K. R., Jawaid, M., & Rashid, U. (2014). *Biomass and Bioenergy: Processing and Properties*: Springer International Publishing.
- Half, A., Sovacool, B. K., & Rozhon, J. (2014). *Energy Poverty: Global Challenges and Local Solutions*: Oxford University Press.
- Hamzehkolaei, F., T., Amjady, N. (2018). A techno-economic assessment for replacement of conventional fossil fuel based technologies in animal farms with biogas fueled CHP units *Renewable Energy*, 118, 602-614.
- Han, F. X. (2007). *Biogeochemistry of Trace Elements in Arid Environments*: Springer Netherlands.
- Harmsen, P., Huijgen, W., Bermudez, L., & Bakker, R. (2010). Literature review of physical and chemical pretreatment processes for lignocellulosic biomass: Wageningen UR Food & Biobased Research.
- Harzevili, F. D., & Hiligsmann, I. S. (2017). *Microbial Fuels: Technologies and Applications*: CRC Press.
- Hatti-Kaul, R., Mamo, G., & Mattiasson, B. (2016). *Anaerobes in Biotechnology* (Vol. 156): Springer.
- Hendriks, A. T., & Zeeman, G. (2009). Pretreatments to enhance the digestibility of lignocellulosic biomass. *Bioresour Technol*, 100(1), 10-18. doi: 10.1016/j.biortech.2008.05.027

- Hill, D., Cobb, S., & Bolte, J. (1987). Using volatile fatty acid relationships to predict anaerobic digester failure. *Transactions of the ASAE*, 30(2), 496-0501.
- Hobson, P. N., Bousfield, S., & Summers, R. (1981). *Methane production from agricultural and domestic wastes*: Applied Science Publishers Ltd.
- Hohenstein, W. (2011). *U.S. Agriculture and Forestry Greenhouse Gas Inventory: 1990-2008*: DIANE Publishing Company.
- Holland, K. T. (2013). *Anaerobic bacteria*. Springer Science & Business Media.
- Jansen, R. A. (2012). *Second Generation Biofuels and Biomass: Essential Guide for Investors, Scientists and Decision Makers*: Wiley.
- Janssen, R., & Rutz, D. . (2012). Bioenergy for sustainable development in Africa. (Eds.). *Springer Science & Business Media*.
- Jawaid, M., Tahir, P. M., & Saba, N. (2017). *Lignocellulosic Fibre and Biomass-Based Composite Materials: Processing, Properties and Applications*: Elsevier Science.
- Jekayinfa, S. O., & Scholz, V. (2013). Laboratory Scale Preparation of Biogas from Cassava Tubers, Cassava Peels, and Palm Kernel Oil Residues. *Energy Sources, Part A: Recovery, Utilization, and Environmental Effects*, 35(21), 2022-2032. doi: 10.1080/15567036.2010.532190
- Jha, P., & Schmidt, S. (2017). Reappraisal of chemical interference in anaerobic digestion processes. *Renewable and Sustainable Energy Reviews*, 75, 954-971. doi: 10.1016/j.rser.2016.11.076
- Jinsheng, G. (2009). *Coal, Oil Shale, Natural Bitumen, Heavy Oil and Peat - Volume I*: EOLSS Publ.
- Jose, S., & Bhaskar, , T. (2015). Biomass and biofuels: advanced biorefineries for sustainable production and distribution. (Eds.). *CRC Press*.
- Kabata-Pendias, A. (2000). *Trace Elements in Soils and Plants, Third Edition*: CRC Press.
- Kabata-Pendias, A., & Mukherjee, A. B. (2007). *Trace Elements from Soil to Human*: Springer.
- Karimi, K. (2015). *Lignocellulose-Based Bioproducts*: Springer International Publishing.
- Karthikeyan, O. P., Heimann, K., & Muthu, S. S. (2016). *Recycling of Solid Waste for Biofuels and Bio-chemicals*: Springer Singapore.

- Kaur, K., & Phutela, U. G. (2016). Enhancement of paddy straw digestibility and biogas production by sodium hydroxide-microwave pretreatment. *Renewable Energy*, *92*, 178-184.
- Khairuddin, N., Manaf, L. A., Halimoon, N., Ghani, W. a. W. a. K., & Hassan, M. A. (2015). High Solid Anaerobic Co-digestion of Household Organic Waste with Cow Manure. *Procedia Environmental Sciences*, *30*, 174-179. doi: 10.1016/j.proenv.2015.10.031
- Khanal, S. K. (2011a). Anaerobic biotechnology for bioenergy production: principles and applications. *John Wiley & Sons*.
- Khanal, S. K. (2011b). *Anaerobic Biotechnology for Bioenergy Production: Principles and Applications*: Wiley.
- Khanal, S. K. (2011c). Anaerobic biotechnology for bioenergy production: principles and applications. John Wiley & Sons. *Willey*.
- Khedim, Z., Benyahia, B., Cherki, B., Sari, T., & Harmand, J. (2018). Effect of control parameters on biogas production during the anaerobic digestion of protein-rich substrates. *Applied Mathematical Modelling*, *61*, 351-376. doi: 10.1016/j.apm.2018.04.020
- Khoiyangbam, R. S., Gupta, N., Kumar, S., & Institute, E. R. (2011). *Biogas Technology: towards sustainable development*: Energy and Resources Institute.
- Kim, M., Ahn, Y.-H., & Speece, R. (2002). Comparative process stability and efficiency of anaerobic digestion; mesophilic vs. thermophilic. *Water Res*, *36*(17), 4369-4385.
- Klemes, J., Smith, R., & Kim, J. K. (2008). *Handbook of Water and Energy Management in Food Processing*: Elsevier Science.
- Koch, K., Lubken, M., Gehring, T., Wichern, M., & Horn, H. (2010). Biogas from grass silage - Measurements and modeling with ADM1. *Bioresour Technol*, *101*(21), 8158-8165. doi: 10.1016/j.biortech.2010.06.009
- Korres, N. (2013). Bioenergy production by anaerobic digestion: using agricultural biomass and organic wastes. *Routledge*.
- Kosseva, M., & Webb, C. (Eds.). (2013). Food industry wastes: assessment and recuperation of commodities. . *Academic Press*.
- Kumar, P., Barrett, D. M., Delwiche, M. J., & Stroeve, P. (2009). Methods for pretreatment of lignocellulosic biomass for efficient hydrolysis and biofuel production. *Industrial & engineering chemistry research*, *48*(8), 3713-3729.

- Labrada, R., Caseley, J. C., Parker, C., Food, & Nations, A. O. O. T. U. (1994). *Weed Management for Developing Countries*: FAO.
- Lee, D. J., Hallenbeck, P. C., Ngo, H. H., Jegatheesan, V., & Pandey, A. (2016). *Current Developments in Biotechnology and Bioengineering: Biological Treatment of Industrial Effluents*: Elsevier Science.
- Lenihan, P., Orozco, A., O'neill, E., Ahmad, M. N. M., Rooney, D. W., & Walker, G. M. (2010). Dilute acid hydrolysis of lignocellulosic biomass. *Chemical Engineering Journal*, 156(2), 395-403. doi: <https://doi.org/10.1016/j.cej.2009.10.061>
- Lettinga, G., Rebac, S., & Zeeman, G. (2001). Challenge of psychrophilic anaerobic wastewater treatment. *TRENDS in Biotechnology*, 19(9), 363-370.
- Li, D., Chen, L., Liu, X., Mei, Z., Ren, H., Cao, Q., & Yan, Z. (2017). Instability mechanisms and early warning indicators for mesophilic anaerobic digestion of vegetable waste. *Bioresour Technol*, 245(Pt A), 90-97. doi: 10.1016/j.biortech.2017.07.098
- Li, Y. (2016). *Bioenergy: Principles and Applications*: John Wiley & Sons.
- Lichtfouse, E. (2011). *Genetics, Biofuels and Local Farming Systems*: Springer Netherlands.
- Lossie, U., & Pütz, P. (2008). Targeted control of biogas plants with the help of FOS/TAC. *Practice Report Hach-Lange*.
- Love, J., & Bryant, J. A. (2017). *Biofuels and Bioenergy*: John Wiley & Sons.
- Lue-Hing, C. (1998). *Municipal Sewage Sludge Management: A Reference Text on Processing, Utilization and Disposal, Second Edition*: Taylor & Francis.
- Lupoi, J., Simmons, B., & Henry, R. (2016). Biomass Modification, Characterization, and Process Monitoring Analytics to Support Biofuel and Biomaterial Production. *Frontiers in bioengineering and biotechnology*, 4.
- Luque, R., & Balu, A. M. (2013). *Producing Fuels and Fine Chemicals from Biomass Using Nanomaterials*: Taylor & Francis.
- Malik, A., Grohmann, E., & Alves, M. (2013). *Management of Microbial Resources in the Environment*: Springer Netherlands.
- Management Association, I. R. (2017). *Materials Science and Engineering: Concepts, Methodologies, Tools, and Applications: Concepts, Methodologies, Tools, and Applications*: IGI Global.

- Mancini, G., Papirio, S., Riccardelli, G., Lens, P. N. L., & Esposito, G. (2018). Trace elements dosing and alkaline pretreatment in the anaerobic digestion of rice straw. *Bioresource Technology*, 247, 897-903. doi: 10.1016/j.biortech.2017.10.001
- Martín-González, L., Font, X., & Vicent, T. (2013). Alkalinity ratios to identify process imbalances in anaerobic digesters treating source-sorted organic fraction of municipal wastes. *Biochemical Engineering Journal*, 76, 1-5. doi: 10.1016/j.bej.2013.03.016
- Mccartney, D. M., & Oleszkiewicz, J. A. . (1991). Sulfide inhibition of anaerobic degradation of lactate and acetate. *Water Research*, 25(2), 203-209.
- Mccarty, P. L. (1964). Anaerobic waste treatment fundamentals. *Public works*, 95(9), 107-112.
- Mechichi, T., & Sayadi, S. (2005). Evaluating process imbalance of anaerobic digestion of olive mill wastewaters. *Process Biochemistry*, 40(1), 139-145. doi: 10.1016/j.procbio.2003.11.050
- Meng, L. (2011). *Improved Hydrogen Sorption Kinetics in Wet Ball Milled Mg Hydrides*: Forschungszentrum, Zentralbibliothek.
- Meyer, D., & Powers, T. (2011). *Manure Treatment Technologies: Anaerobic Digesters*: University of California, Agriculture and Natural Resources.
- Micolucci, F., Gottardo, M., Pavan, P., Cavinato, C., & Bolzonella, D. (2018). Pilot scale comparison of single and double-stage thermophilic anaerobic digestion of food waste. *Journal of Cleaner Production*, 171, 1376-1385. doi: 10.1016/j.jclepro.2017.10.080
- Miller, P. A., & Clesceri, N. L. (2002). *Waste Sites as Biological Reactors: Characterization and Modeling*: CRC Press.
- Mital, K. M. (1997). *Biogas Systems: Policies, Progress and Prospects*: New Age International (P) Limited.
- Modi, V., Mcdade, S., Lallement, D., & Saghir, J. (2005). Energy services for the Millennium Development Goals. *Energy services for the Millennium Development Goals*.
- Mohee, R., & Mudhoo, A. (2012). Bioremediation and sustainability. *Environmental Engineering and Management Journal*, 11(12), 2335-2336.
- Mondal, P., & Dalai, A. K. (2017). *Sustainable Utilization of Natural Resources*: CRC Press.

- Monyei, C. G. (2017). Nigeria's energy poverty: Insights and implications for smart policies and framework towards a smart Nigeria electricity network. *Renewable and Sustainable Energy Reviews*. doi: 10.1016/j.rser.2017.05.237
- Moran, J. (2005). *Tropical Dairy Farming: Feeding Management for Small Holder Dairy Farmers in the Humid Tropics*: Land Links.
- Mosier, N., Wyman, C., Dale, B., Elander, R., Lee, Y. Y., Holtzaple, M., & Ladisch, M. (2005). Features of promising technologies for pretreatment of lignocellulosic biomass. *Bioresource Technology*, 96(6), 673-686. doi: <https://doi.org/10.1016/j.biortech.2004.06.025>
- Muchie, M., & Baskaran, A. (2012). *creating systems of innovation in Africa: country case studies*: African Books Collective.
- Mussagy, M., Sanni, L., Onadipe, O., Ilona, P., & Dixon, A. (2009). *Viability of commercializing cassava in districts covered by the Common Fund for Commodities in West Africa*: IITA.
- Mustafa, A. M., Poulsen, T. G., Xia, Y., & Sheng, K. (2017). Combinations of fungal and milling pretreatments for enhancing rice straw biogas production during solid-state anaerobic digestion. *Bioresour Technol*, 224, 174-182. doi: 10.1016/j.biortech.2016.11.028
- Naeem, M., Ansari, A. A., & Gill, S. S. (2017). *Essential Plant Nutrients: Uptake, Use Efficiency, and Management*: Springer International Publishing.
- Nayono, S. E. (2010). *Anaerobic Digestion of Organic Solid Waste for Energy Production*: KIT Scientific Publ.
- Net, T. C. (2010). *Cap and Trade: The Kyoto Protocol, Greenhouse Gas (GHG) Emissions, Carbon Tax, Emission Allowances, Acid Rain SO2 Program, Ozone Transport Commission, NOX, Carbon Markets, and Climate Change*: The Capitol Net Inc.
- Nielsen, S. S. (2017). *Food Analysis*: Springer International Publishing.
- Nigam, P. S. N., & Pandey, A. (2009). *Biotechnology for Agro-Industrial Residues Utilisation: Utilisation of Agro-Residues*: Springer Netherlands.
- Nijaguna, B. T. (2006). *Biogas Technology*: New Age International.
- Nitsos, C. K., Matis, K. A., & Triantafyllidis, K. S. (2013). Optimization of hydrothermal pretreatment of lignocellulosic biomass in the bioethanol production process. *ChemSusChem*, 6(1), 110-122.

- Nizami, A.-S., & Murphy, J. D. (2010). What type of digester configurations should be employed to produce biomethane from grass silage? *Renewable and Sustainable Energy Reviews*, *14*(6), 1558-1568.
- O'rear, C. (2012). *Biodeterioration Research 2: General Biodeterioration, Degradation, Mycotoxins, Biotoxins, and Wood Decay*: Springer US.
- Okeh, O. C., Onwosi, C. O., & Odibo, F. J. C. (2014). Biogas production from rice husks generated from various rice mills in Ebonyi State, Nigeria. *Renewable Energy*, *62*, 204-208. doi: 10.1016/j.renene.2013.07.006
- Oreopoulou, V., & Russ, W. (2006). *Utilization of By-Products and Treatment of Waste in the Food Industry*: Springer US.
- Owen, W., Stuckey, D., Healy, J., Young, L., & Mccarty, P. (1979). Bioassay for monitoring biochemical methane potential and anaerobic toxicity. *Water Res*, *13*(6), 485-492.
- Paul, S., & Dutta, A. (2018). Challenges and opportunities of lignocellulosic biomass for anaerobic digestion. *Resources, Conservation and Recycling*, *130*, 164-174. doi: 10.1016/j.resconrec.2017.12.005
- Pella, E., & Colombo, B. (1973). Study of carbon, hydrogen and nitrogen determination by combustion-gas chromatography. *Microchimica Acta*, *61*(5), 697-719.
- Pellera, F. M., & Gidarakos, E. (2018). Chemical pretreatment of lignocellulosic agroindustrial waste for methane production. *Waste Manag*, *71*, 689-703. doi: 10.1016/j.wasman.2017.04.038
- Penning, H., & Conrad, R. (2006). Effect of inhibition of acetoclastic methanogenesis on growth of archaeal populations in an anoxic model environment. *Applied and environmental microbiology*, *72*(1), 178-184.
- Poltronieri, P., & D'urso, O. F. . (2016). Biotransformation of Agricultural Waste and By-products: The Food, Feed, Fibre, Fuel (4F) Economy. (Eds.). *Elsevier*.
- Pullen, T. (2015). *Anaerobic Digestion – Making Biogas – Making Energy: The Earthscan Expert Guide*: Taylor & Francis.
- Qi, H. (2016). *Novel Functional Materials Based on Cellulose*: Springer International Publishing.
- Radu, T., Smedley, V., Wheatley, A. D., Blanchard, R. E., & Theaker, H. (2014). Operational experiences of industrial scale AD: Lessons for the future.

- Riffat, R. (2012). *Fundamentals of wastewater treatment and engineering*. CRC Press.
- Rocco, M. V., Ferrer, R. J. F., Colombo, E. (2018). Understanding the energy metabolism of World economies through the joint use of Production- and Consumption-based energy accountings. *Applied Energy*, 211, 590-603. doi: 10.1016/j.apenergy.2017.10.090
- Romero-Güiza, M. S., Vila, J., Mata-Alvarez, J., Chimenos, J. M., & Astals, S. (2016). The role of additives on anaerobic digestion: A review. *Renewable and Sustainable Energy Reviews*, 58, 1486-1499. doi: 10.1016/j.rser.2015.12.094
- Romero-Güiza, M. S., Wahid, R., Hernández, V., Møller, H., & Fernández, B. (2017). Improvement of wheat straw anaerobic digestion through alkali pre-treatment: Carbohydrates bioavailability evaluation and economic feasibility. *Science of The Total Environment*, 595, 651-659.
- Rosato, M. A. (2017). *Managing Biogas Plants: A Practical Guide*: CRC Press.
- Röser, D., Asikainen, A., Raulund-Rasmussen, K., & Stupak, I. (2008). *Sustainable Use of Forest Biomass for Energy: A Synthesis with Focus on the Baltic and Nordic Region*: Springer Netherlands.
- Rouches, E., Dignac, M.-F., Zhou, S., & Carrere, H. (2017). Pyrolysis-GC-MS to assess the fungal pretreatment efficiency for wheat straw anaerobic digestion. *Journal of Analytical and Applied Pyrolysis*, 123, 409-418.
- Russell-Smith, J., Whitehead, P., & Cooke, P. (2009). *Culture, Ecology and Economy of Fire Management in North Australian Savannas: Rekindling the Wurrk Tradition*: CSIRO PUBLISHING.
- Saha, J. K., Selladurai, R., Coumar, M. V., Dotaniya, M. L., Kundu, S., & Patra, A. K. (2017). *Soil Pollution - An Emerging Threat to Agriculture*: Springer Singapore.
- Said, Z., Alshehhi, A. A., & Mehmood, A. (2018). Predictions of UAE's renewable energy mix in 2030. *Renewable Energy*, 118, 779-789. doi: 10.1016/j.renene.2017.11.075
- Sani, R. K., & Rathinam, N. K. (2018). *Extremophilic Microbial Processing of Lignocellulosic Feedstocks to Biofuels, Value-Added Products, and Usable Power*: Springer.
- Schön, M. (2010). *Numerical Modelling of Anaerobic Digestion Processes in Agricultural Biogas Plants*: Innsbruck University Press.
- Service, U. S. N. P. (2010). *South Florida and Caribbean Parks Exotic Plant Management Plan: Environmental Impact Statement*.

- Shah, Y. T. (2014). *Water for Energy and Fuel Production*: Taylor & Francis.
- Sharma, A. (2018). *Microbial Biotechnology in Environmental Monitoring and Cleanup*: IGI Global.
- Sharma, R. (2008). *Basic techniques in biochemistry and molecular biology*: IK International Pvt Ltd.
- Shetty, D. J., Kshirsagar, P., Tapadia-Maheshwari, S., Lanjekar, V., Singh, S. K., & Dhakephalkar, P. K. (2017). Alkali pretreatment at ambient temperature: A promising method to enhance biomethanation of rice straw. *Bioresour Technol*, 226, 80-88. doi: 10.1016/j.biortech.2016.12.003
- Shi, X., Lin, J., Zuo, J., Li, P., Li, X., & Guo, X. (2017). Effects of free ammonia on volatile fatty acid accumulation and process performance in the anaerobic digestion of two typical bio-wastes. *J Environ Sci (China)*, 55, 49-57. doi: 10.1016/j.jes.2016.07.006
- Siegel, J., & Nelder, C. (2008). *Investing in Renewable Energy: Making Money on Green Chip Stocks*: Wiley.
- Singh, B., Baudh, K., & Bux, F. (2015). *Algae and Environmental Sustainability*: Springer India.
- Singh, V. P. (2014). *FLORA OF MADHYA PRADESH (WESTERN PART)*: SCIENTIFIC PUBLISHER (IND).
- Sluiter, A., Hames, B., Hyman, D., Payne, C., Ruiz, R., Scarlata, C., Sluiter, J., Templeton, D., & Wolfe, J. (2008). Determination of total solids in biomass and total dissolved solids in liquid process samples. *National Renewable Energy Laboratory, Golden, CO, NREL Technical Report No. NREL/TP-510-42621*, 1-6.
- Soni, S. K. (2007). *Microbes: A Source of Energy for 21st Century*: New India Publishing Agency.
- Srivastava, A. K. (2012). *Advances in Citrus Nutrition*: Springer Netherlands.
- Stolp, H. (1988). *Microbial Ecology: Organisms, Habitats, Activities*: Cambridge University Press.
- Stow, A., Maclean, N., & Holwell, G. I. (2014). *Austral Ark*: Cambridge University Press.
- Streitwieser, A. (2017). Comparison of the anaerobic digestion at the mesophilic and thermophilic temperature regime of organic wastes from the agribusiness. *Bioresour Technol*, 241, 985-992. doi: 10.1016/j.biortech.2017.06.006
- Stronach, S. M., Rudd, T., & Lester, J. N. (2012). *Anaerobic Digestion Processes in Industrial Wastewater Treatment*: Springer Berlin Heidelberg.

- Sun, Y., & Cheng, J. (2002). Hydrolysis of lignocellulosic materials for ethanol production: a review. *Bioresource Technology*, 83(1), 1-11.
- Sykes, G., & Skinner, F. A. (2015). *Microbial Aspects of Pollution*: Elsevier Science.
- Teymoori Hamzehkolaei, F., & Amjady, N. (2018). A techno-economic assessment for replacement of conventional fossil fuel based technologies in animal farms with biogas fueled CHP units. *Renewable Energy*, 118, 602-614. doi: 10.1016/j.renene.2017.11.054
- Tilak, K., Pal, K., & Dey, R. (2010). *Microbes for sustainable agriculture*: IK International New Delhi.
- Tong, Z., Cheng, N., & Pullammanappallil, P. (2013). Pretreatment of Ligno-cellulosic Biomass for Biofuels and Bioproducts: University of Florida.
- Tranter, R. B., Swinbank, A., Jones, P. J., Banks, C., & Salter, A. (2011). Assessing the potential for the uptake of on-farm anaerobic digestion for energy production in England. *Energy Policy*, 39(5), 2424-2430.
- Turovskiy, I. S., Mathai, P. K. (2006). Wastewater sludge processing. *John Wiley & Sons*.
- Undp. (2015). Promoting sustainable energy for all. UNDP supports rural communities in Nigeria. <http://www.ng.undp.org/content/nigeria/en/home/presscenter/articles/2015/04/01/reducing-the-energy-poverty-gap-nigeria-embarks-ambitious-plan-to-increase-power-generation.html> (Accessed:18/11/2017).
- Van Haandel, A., & Van Der Lubbe, J. (2012). Handbook of biological wastewater treatment. *Iwa Publishing*.
- Van Haandel, A., & Van Der Lubbe, J. . (2007). *Handbook Biological Waste Water Treatment - Design and Optimisation of Activated Sludge Systems*: Quist.
- Van Loo, S., & Koppejan, J. (2012). *The Handbook of Biomass Combustion and Co-firing*: Taylor & Francis Group.
- Van Soest, P. J. (1963). Use of detergents in the analysis of fibrous feeds. 2. A rapid method for the determination of fiber and lignin. *Journal of the Association of Official Agricultural Chemists*, 46, 829-835.
- Varjani, S. J., Gnansounou, E., Gurunathan, B., Pant, D., & Zakaria, Z. A. (2018). *Waste Bioremediation*: Springer Singapore.

- Vdi. 4630. (2006). Fermentation of organic materials. *Characterization of the substrate, sampling, collection of material data, fermentation tests*, 92.
- Vertes, A. A., Qureshi, N., Yukawa, H., & Blaschek, H. P. (2011). *Biomass to Biofuels: Strategies for Global Industries*: Wiley.
- Von Sperling, M., & De Lemos Chernicharo, C. A. (2005). *Biological Wastewater Treatment in Warm Climate Regions*: IWA Publishing.
- Wang, B., Nges, I. A., Nistor, M., & Liu, J. (2014). Determination of methane yield of cellulose using different experimental setups. *Water science and technology*, 70(4), 599.
- Wang, B., Strömberg, S., Li, C., Nges, I. A., Nistor, M., Deng, L., & Liu, J. (2015). Effects of substrate concentration on methane potential and degradation kinetics in batch anaerobic digestion. *Bioresource Technology*, 194, 240-246.
- Wang, L. (2014). *Sustainable Bioenergy Production*: Taylor & Francis.
- Wang, L. K., Ivanov, V., Tay, J. H., & Hung, Y. T. (2010). *Environmental Biotechnology*: Humana Press.
- Wang, Z., Danish, Zhang, B., & Wang, B. (2018). Renewable energy consumption, economic growth and human development index in Pakistan: Evidence form simultaneous equation model. *Journal of Cleaner Production*, 184, 1081-1090. doi: 10.1016/j.jclepro.2018.02.260
- Warren, G. M. (1924). *Farm Plumbing*: U.S. Department of Agriculture.
- Weber, E. (2017). *Invasive plant species of the world: a reference guide to environmental weeds*: CABI.
- Wellinger, A., Murphy, J. D., & Baxter, D. (Eds.). (2013). *The biogas handbook: science, production and applications*. Elsevier.
- Wheatley, A., Fisher, M., & Grobicki, A. (1997). Applications of anaerobic digestion for the treatment of industrial wastewaters in Europe. *Water and Environment Journal*, 11(1), 39-46.
- Wilawan, W., Pholchan, P., & Aggarangsi, P. (2014). Biogas Production from Co-digestion of Pennisetum Purpurem cv. Pakchong 1 Grass and Layer Chicken Manure Using Completely Stirred Tank. *Energy Procedia*, 52, 216-222. doi: 10.1016/j.egypro.2014.07.072
- Wong, J. W. C., Tyagi, R. D., & Pandey, A. (2016). *Current Developments in Biotechnology and Bioengineering: Solid Waste Management*: Elsevier Science.

- Worldbank. (2014). World Development Indicators: Electricity production, sources, and access. <http://databank.worldbank.org/data/reports.aspx?source=2&series=EG.ELC.ACCS.ZS&country=:> <http://wdi.worldbank.org/table/3.7> (Accessed 18/11/2017).
- Wormworth, J., & Sekercioglu, C. H. (2011). *Winged Sentinels: Birds and Climate Change*: Cambridge University Press.
- Wu, Y., Zhu, Q., Zhu, B. (2018). Comparisons of decoupling trends of global economic growth and energy consumption between developed and developing countries. *Energy Policy*, 116 30–38. doi: 10.1016/j.enpol.2018.01.047
- Xu, Z., & Zhou, G. (2017). *Identification and Control of Common Weeds*: Springer Netherlands.
- Yamada, T., & Spangenberg, G. (2010). *Molecular breeding of forage and turf: the proceedings of the 5th International Symposium on the Molecular Breeding of Forage and Turf*: Springer Science & Business Media.
- Yang, B., Dai, Z., Ding, S.-Y., & Wyman, C. E. (2011). Enzymatic hydrolysis of cellulosic biomass. *Biofuels*, 2(4), 421-449.
- Zamorano, M. (2008). *Waste Management and the Environment IV*: WIT Press.
- Zealand, A. M., Roskilly, A. P., & Graham, D. W. (2017). Effect of feeding frequency and organic loading rate on biomethane production in the anaerobic digestion of rice straw. *Applied Energy*. doi: 10.1016/j.apenergy.2017.05.170
- Zhang, Q., He, J., Tian, M., Mao, Z., Tang, L., Zhang, J., & Zhang, H. (2011). Enhancement of methane production from cassava residues by biological pretreatment using a constructed microbial consortium. *Bioresour Technol*, 102(19), 8899-8906. doi: 10.1016/j.biortech.2011.06.061
- Zhang, Q., Tang, L., Zhang, J., Mao, Z., & Jiang, L. (2011). Optimization of thermal-dilute sulfuric acid pretreatment for enhancement of methane production from cassava residues. *Bioresour Technol*, 102(4), 3958-3965. doi: 10.1016/j.biortech.2010.12.031
- Zhang, X. R., & Dincer, I. (2016). *Energy Solutions to Combat Global Warming*: Springer International Publishing.
- Zhang, Z. (2017). *Multivariate Time Series Analysis in Climate and Environmental Research*: Springer International Publishing.

Zhu, I. (2017). *Nitrification and Denitrification*: IntechOpen.

Chapter 9 Annex A

Biochemical potential of selected biomass feedstocks and the effect of biomass ash-extract supplementation on the methane yield

Objectives of the batch experiments

- To determine the biochemical methane potential (BMP) of Gamba grass, crystalline cellulose, Guinea grass, cassava waste, plantain peels and elephant grass as mono-substrates
- To determine biomethane production from mixtures of different types of biomass feedstocks with supplementation
- Investigate of the effects of using biomass-derived ash and ash-extract supplementation on methane yield from rice straw

9.1 Materials and methods

The sources, methods collection, drying and grinding of each of the biomass feedstocks are presented in Section 3.1. The chemical composition and characteristics of the materials are also presented in Section 3.2.1. The procedures used for the determination of the physiochemical characteristics of the biomass feedstocks are described in Section 3.4. The inoculum was made up of a mixture of 80% rumen fluid and 20% inoculum collected from an abattoir and an active commercial mesophilic AD plant, respectively, all located in Newcastle upon Tyne, United Kingdom. This inoculum was incubated at a temperature of 37 °C for 7 days prior to its use for the batch experiment. The experiment was setup in Duran bottles each with a working volume of 400 mL and a headspace volume of 200 mL. Table 9-1 shows a summary of the biomass feedstock used for the BMP experiment.

Table 9-1 Physiochemical characteristics of the biomass feedstocks used for BMP tests

Biomass feedstock	Characteristics			
	Moisture content (%)	%TS in dry weight	%VS in TS	%Ash
Guinea grass	8%	92%	90%	10%
Rice	7%	93%	82%	18%
Cassava	10%	90%	93%	7%
Rye	10%	90%	94%	6%
Gamba	9%	91%	95%	5%
Plantain peels	11%	89%	89%	11%
Gamba + Guinea (1:1)	8%	92%	93%	7%
Elephant + Guinea (1:1)	13%	87%	84%	16%
Rice + Yam Beans (1:1)	10%	90%	84%	16%
Rice + Cassava (1:1)	8%	92%	86%	14%
Rice + Plantain peels (1:1)	8%	92%	84%	16%
Elephant grass	8%	92%	91%	9%

The inoculum was made up of a mixture of rumen fluid and cattle slurry. The inoculum-to-substrate ratio used for the current study was 3:1 (on a VS basis). Details of the experimental methods are presented in Section 3.4. Physiochemical characteristics of the inoculum are presented in Table 9-2.

Table 9-2 Physiochemical characteristics of the inoculum

Inoculum characteristics	Abbreviation/units	Concentration
Moisture content	MC (%) in TS	96%
Total solids content	%TS in weight	4%
Volatile solids content	%VS in TS	60%
Ash content	Ash content in VS	40%
Total Kjeldahl nitrogen	TKN (mg. L ⁻¹)	1,523.0
Ammonium nitrogen	NH ₄ -N (mg. L ⁻¹)	1,133.0
Chemical oxygen demand	COD (mg. L ⁻¹)	25,000.0

Each batch condition was carried out in triplicate in accordance with the German Standard Protocol (VDI. 4630, 2006). The procedure for monitoring, biogas collection and measurement by GC of the methane content in the biogas are detailed Section 3.4.2.

9.2 Statistical analysis

The results obtained from the batch study were analysed using Microsoft Excel and SPSS data analysis software. The curved fitting tools of MATLAB R2016a were also used to fit the experimental data onto the Gompertz model to check the goodness of the fit in order to compare the predicted BMP to the experimental BMP results.

$$P = A \exp \left\{ -\exp \left[\frac{Ue}{A} (\lambda - t) + 1 \right] \right\} \quad \text{Equation 9-1}$$

where, P is the cumulative specific methane production (N mL.g⁻¹VS added); A is the methane production potential (mL); U is the maximum methane production rate (mL.g⁻¹VS.d⁻¹); λ is the duration of the lag phase (d⁻¹) and t is the cumulative time for methane production (d⁻¹). The t-test statistical analysis was also carried out to compare the means of triplicates with the mean of the control to see if any significant difference. Further details on the analysis carried out are presented in Section 3.7.

9.3 Results

9.3.1 Biochemical methane potential (BMP) of Gamba grass, crystalline cellulose, Guinea grass, cassava waste, plantain peels and elephant grass

The cumulative volumes and daily volumes of methane produced from gamba grass, guinea grass, elephant grass, crystalline cellulose, cassava waste and plantain peels are presented in Figure 9-1 and Figure 9-2, respectively. From the results, the BMP of B (Gamba grass), C (Crystalline cellulose), D(Guinea grass), F (Cassava wastes), H (Plantain peels) and M (Elephant grass) were 202.4, 341.9, 480.1, 248.8, 321.8 and 369.6 N mL CH₄.g⁻¹VS added.

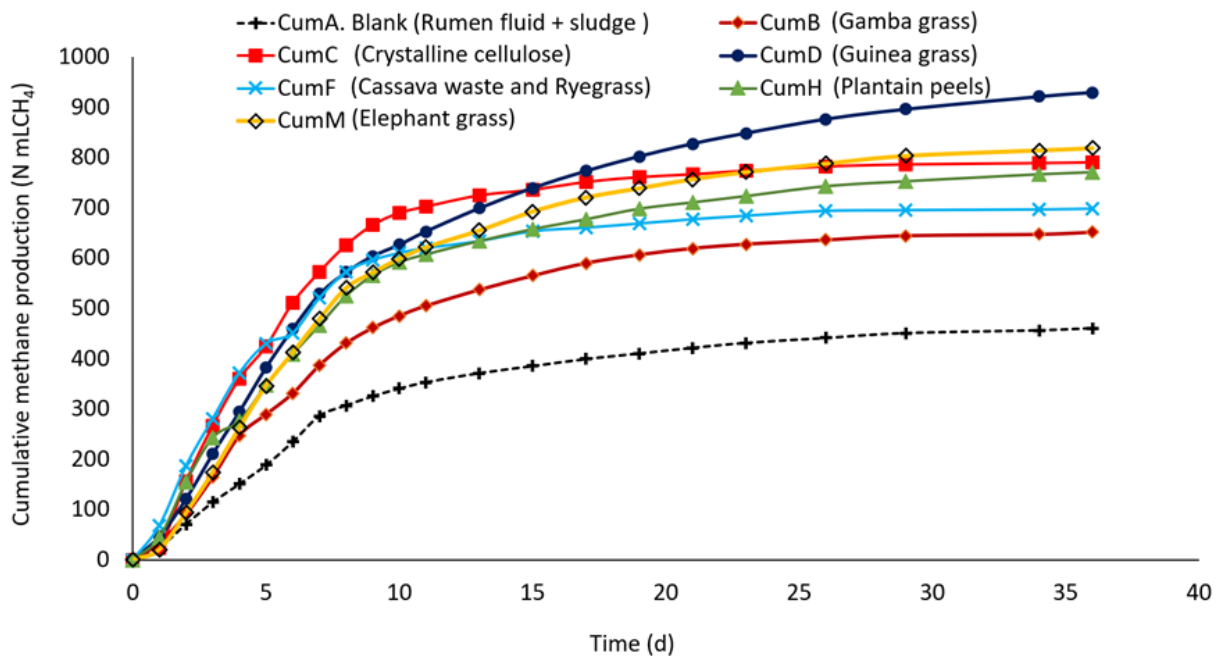


Figure 9-1 Cumulative methane production of biomass feedstocks together with methane from blank, where A is the blank, B is Gamba grass, C is crystalline cellulose, D is Guinea grass, F is cassava waste, H is plantain peels and M is elephant grass.

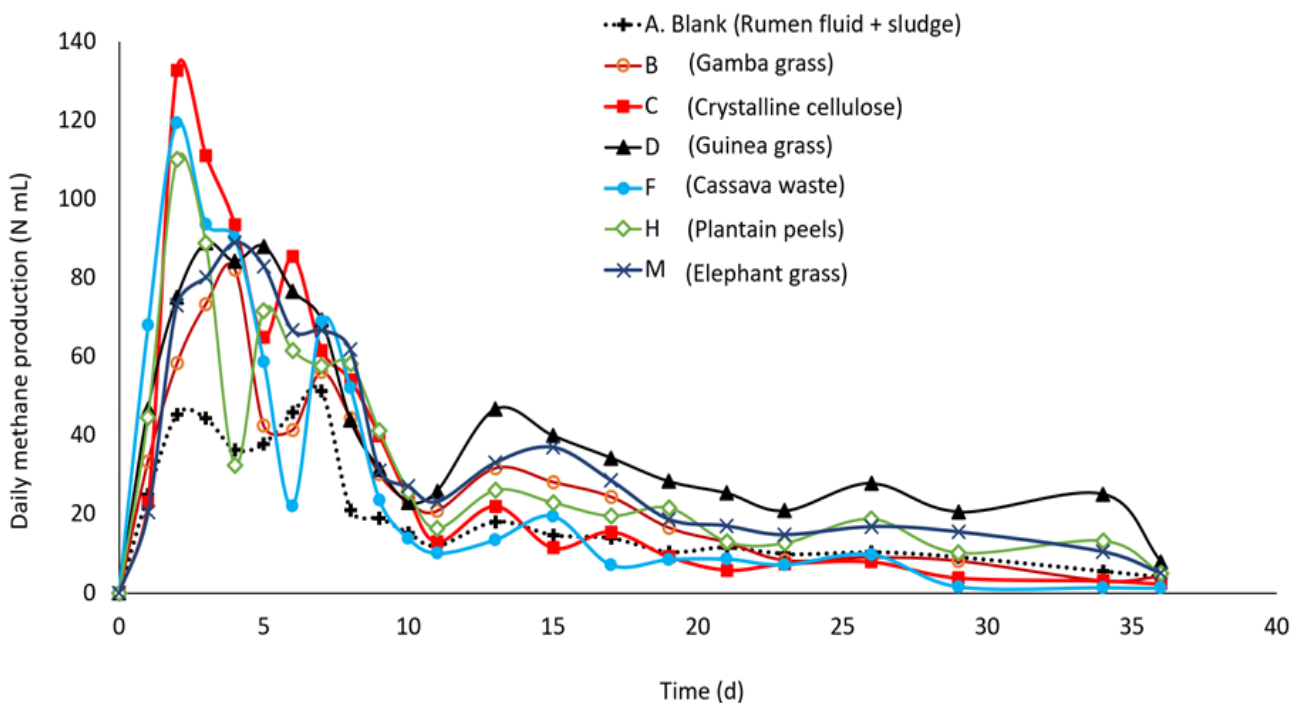


Figure 9-2 Daily methane production of the biomass feedstocks together with blank methane. Where A, B, C, D, F, H and M are as defined in the legend

From Figure 9-2, crystalline cellulose and cassava waste achieved the highest maximum methane production rate with U (max) values of 132.6 and 119.2 N mLCH₄.d⁻¹, respectively. Other biomass feedstocks, namely: Gamba grass, Guinea grass, Plantain peels, and Elephant grass were 82.1, 88.9, 110 and 88.9 N mLCH₄.d⁻¹, respectively. From these results, it is evident that the crystalline cellulose, the cassava waste and the plantain peels had the maximum methane production rate. Further details on the yields from each of the biomass feedstocks, their hydrolysis constants, experimental BMP determined using batch assays and theoretical BMP estimated using the Gompertz model are presented in Table 9-3. For Elephant (Napier) grass, the BMP value obtained in the current study agrees with the result obtained in a BMP study carried out by Chynoweth (1993) with ensiled Napier grass in which they achieved an ultimate methane yield of 0.310 ± 0.011 mL CH₄.g⁻¹VS added. In another study, Zhang, Tang, *et al.* (2011) pretreated cassava residues by thermal-dilute sulfuric acid hydrolysis using a statistically designed set of experiments and reported achieving an optimum methane yield of 248 mL CH₄.g⁻¹VS added. In another study, Jekayinfa and Scholz (2013) found that the methane production from cassava tuber and cassava peels was 310 and 280 mL CH₄.g⁻¹VS added, respectively. However, in the current study, the results obtained (Table 9-3) shows that the BMP of Cassava waste was 248.8 CH₄.g⁻¹VS added which agrees with the result obtained by Zhang, Tang, *et al.* (2011), but contrast that of Jekayinfa and Scholz (2013), which was far higher.

Similarly, in another AD experiment to determine the methane yield of cellulose using manometer, water column, gas bag and an automatic experimental setup, Wang *et al.* (2014) found that the methane yields were 340±18, 354±13, 345±15 and 366±5 mL CH₄.g⁻¹VS added, respectively. However, in the current study, the methane yield from the Crystalline cellulose was 341.9 CH₄.g⁻¹VS added which is very comparable to previous studies.

In a related BMP assay with Rice straw as feedstock but operated under thermophilic temperature (55 °C) using a constructed microbial consortium as inoculum, Zhang, He, *et al.* (2011) reported a maximum methane yield of 259.46 mL CH₄.g⁻¹VS added. Similarly, Mustafa *et al.* (2017) reported that after milling and fungal treatment, the highest methane yield achieved from Rice straw was of 258 mL CH₄.g⁻¹VS added. Despite the pretreatment carried out in that study, the BMP value they achieved for rice straw was slightly lower than the BMP value of 266.1 N mLCH₄.g⁻¹VS added obtained in the current study without treatment.

9.3.2 Determination of biomethane production from mixtures of different types of biomass feedstocks with EPB ash-extract supplementation

The cumulative biomethane yields and the specific daily biomethane production from the batch tests comprising different mixtures of biomass with EPB ash extract supplementation are presented in Figure 9-3 and Figure 9-4, respectively. From the data, the BMP of the biomass feedstocks G(Perennial Ryegrass, Clover and Timothy grass), I(Gamba and Guinea), J(Rice + Yam Beans), K(Rice straw + Cassava waste) and L(Rice + Plantain peels) were 399.4, 268.8, 410.5 and 474, 539.9 N mL CH₄.g⁻¹ VS added. The maximum methane production rates (U_x) for G, I, J, K and L were 88.6, 90.7, 92.5, 107.6 and 110.3 N mL CH₄.g⁻¹VS.d⁻¹.

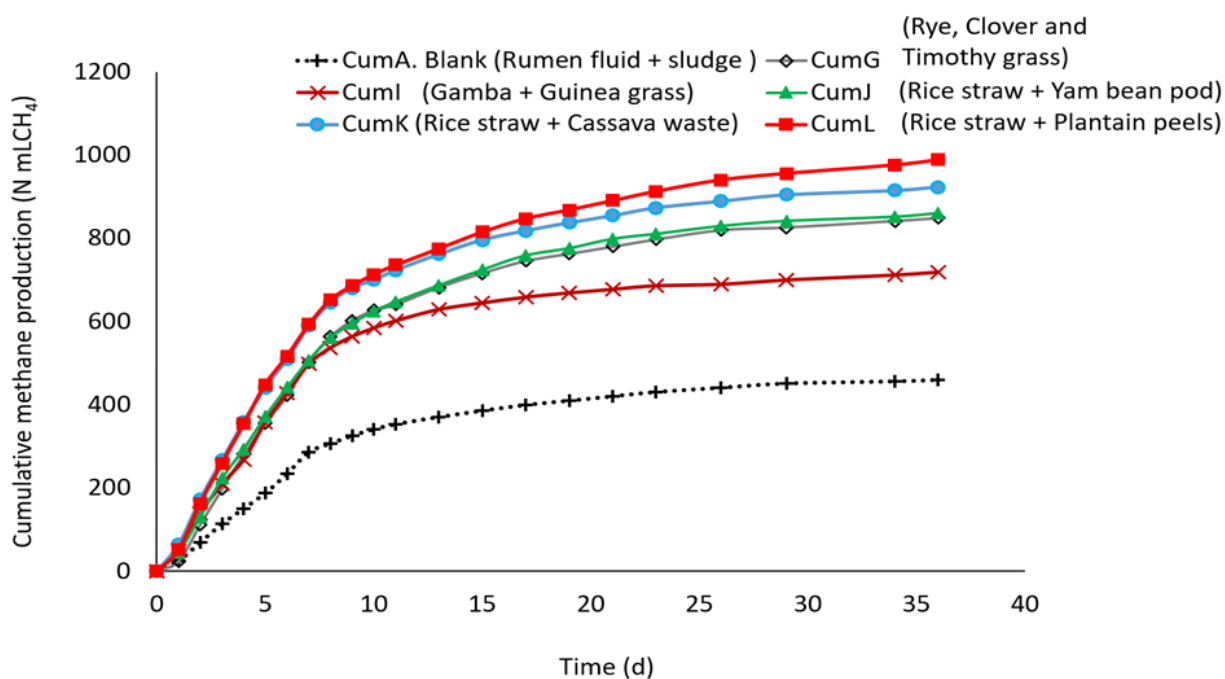


Figure 9-3 Cumulative methane production of biomass feedstocks with EBP supplementation where A is blank (inoculum), G (mixture of perennial ryegrass, clover and timothy grass), I(mixture of Gamba and Guinea grass), J(mixture of rice straw and empty yam bean pod), K(mixture of rice straw and cassava waste), and L(mixture of rice straw and plantain peels).

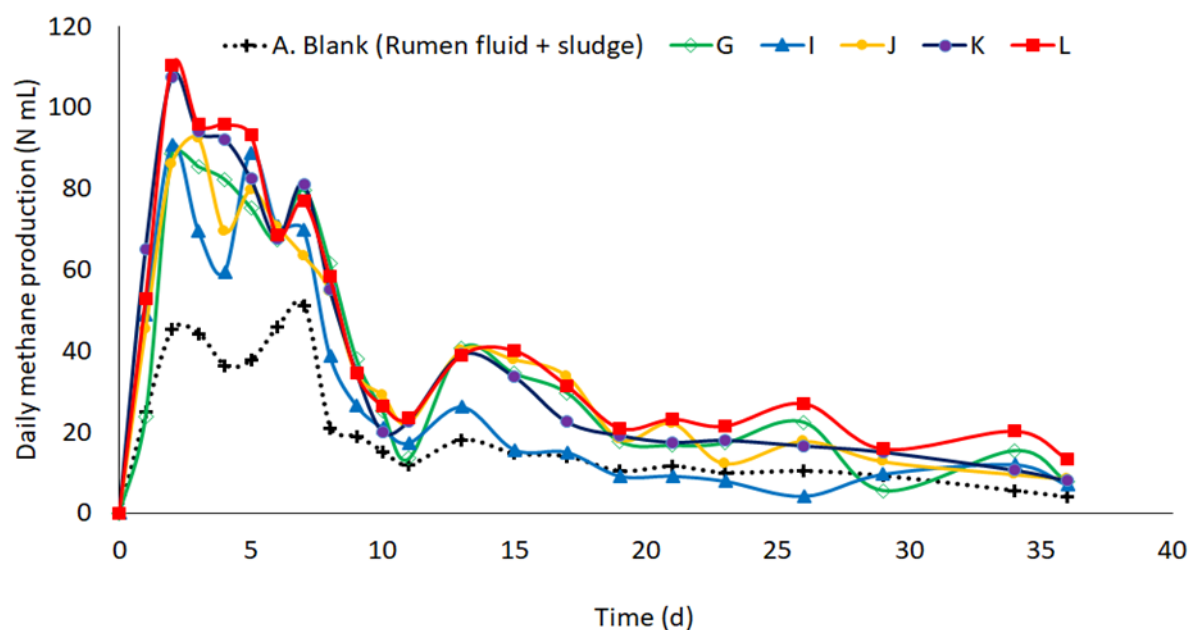


Figure 9-4 Daily methane production from biomass feedstocks G, I, J, K and L as defined in the legends where A is the inoculum

In a study involving the co-digestion of Elephant grasses, otherwise known as Napier grass (*Pennisetum Pururem Schum*) and chicken manure in CSTR, Wilawan *et al.* (2014) reported that they achieved a specific methane production (SMP) of $270 \pm 10 \text{ mL CH}_4 \cdot \text{g}^{-1} \text{VS}^{-1}$ added under steady-state operation. Similarly, during the anaerobic co-digestion of cyanide-containing cassava pulp with pig manure in laboratory scale single stage semi-continuously stirred reactor operating at ambient temperature, Glanpracha and Annachhatre (2016) reported an average VS removal and methane yield of 82% and $380 \text{ mL CH}_4 \cdot \text{g}^{-1} \text{VS} \cdot \text{d}^{-1}$ added, respectively. Although the current study neither involved pig manure or chicken manure, however, the results obtained during the co-digestion experiment showed evidence of improved methane recovery from the biomass feedstocks, and also higher ultimate methane production rate (U_x), compared to mono-fermentation (Table 9-3).

9.3.3 Determination of the effects of using biomass-derived ash and ash-extract supplementation on methane yield from rice straw

The cumulative volumes of methane produced due to the addition of biomass ash-extract supplements produced from empty palm bunch to rice straw in batch assays are presented in Figure 9-5.

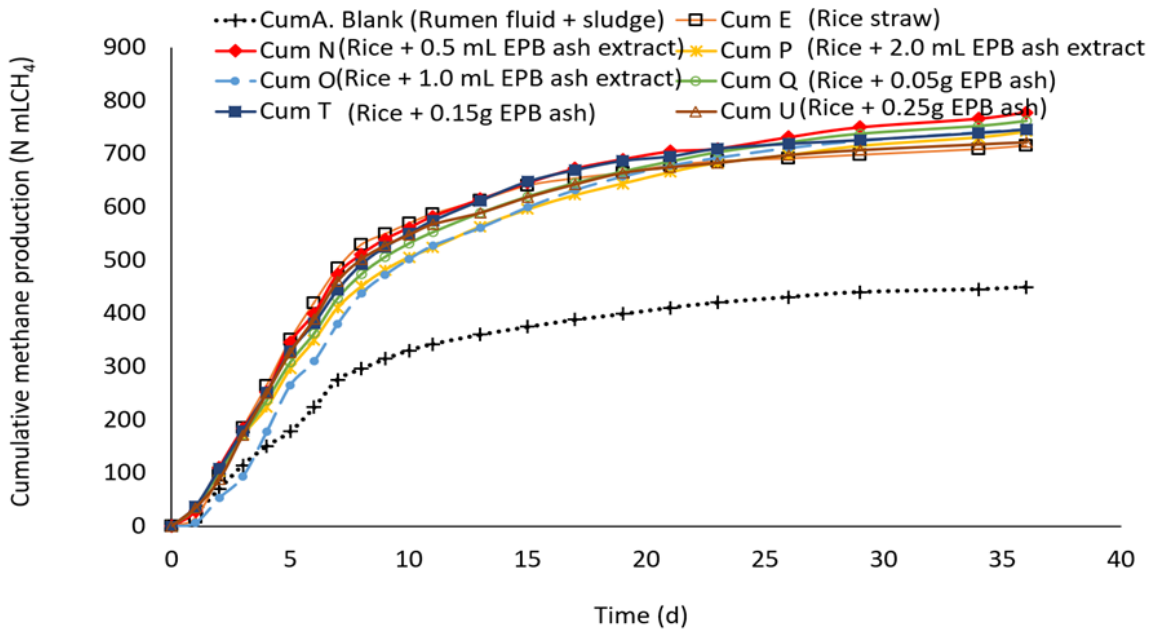


Figure 9-5 Cumulative methane production of biomass feedstocks with inoculum A. E(rice straw + A), N (rice straw with 0.05 mL EPB ash-extract supplement + A), O(rice straw supplemented with 1.0 mL EPB ash-extract supplement + A), P(rice straw supplemented with 2 mL EPB ash-extract + A), Q(rice straw supplemented with 0.05g EPB ash + A), T(rice straw + 0.15g EPB ash + A), and U(rice straw + 0.25g EPB ash + A).

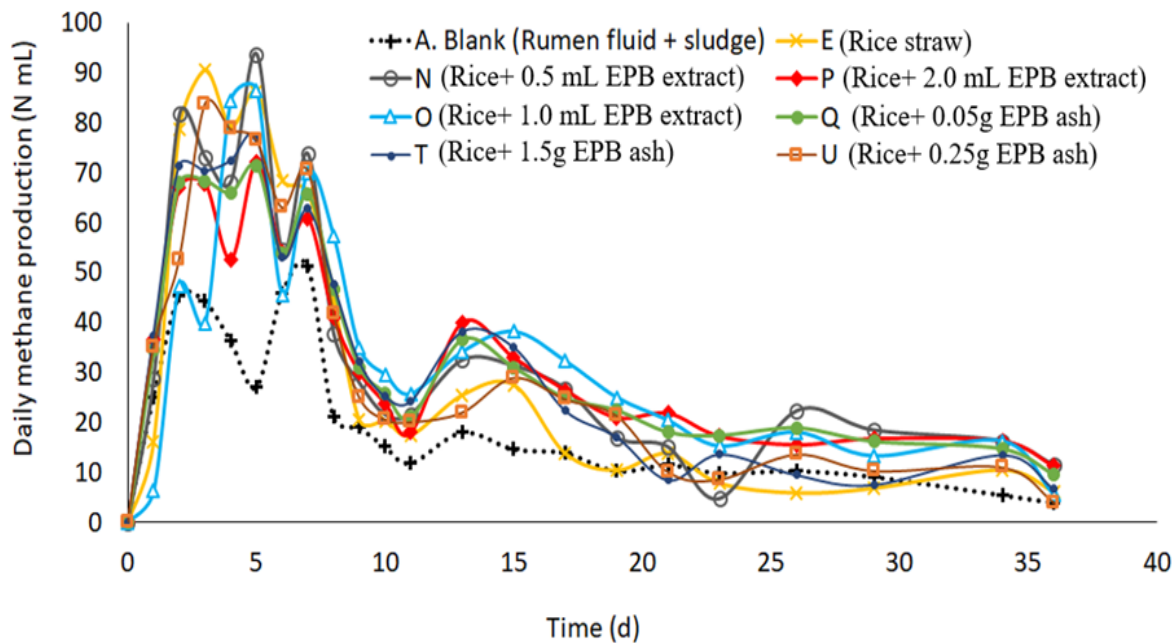


Figure 9-6 Daily methane production from biomass feedstocks where A is the blank (inoculum). The names of the biomass feedstocks E, N, O, P, Q, T and U are as defined in the legends and in Figure 9-5.

In the current study, the BMP values from rice straw, rice straw + 0.5 mL, 1.0 mL, 2.0 mL EPB ash extract were 266.1, 328.4, 296.2, 293.0 N mLCH₄.g⁻¹VS added. These results

showed a remarkable improvement in biomethane recovery from rice straw compared with results from previous study using rice straw as feedstock, indicating that the addition of ash-extract supplement from palm bunch ash improved the value of BMP from each biomass. For instance, in a recent study to investigate the effect of trace elements dosing and alkaline pretreatment during the anaerobic digestion of rice straw using granular sludge as inoculum, (Mancini *et al.*, 2018) reported that the SMP from rice straw was 259 ± 5 mL $\text{CH}_4 \cdot \text{g}^{-1} \text{VS}$ added. The same author also reported that rice straw produced SMP value of 262 ± 26 mL $\text{CH}_4 \cdot \text{g}^{-1} \text{VS}$ when buffalo manure was used as inoculum. However, with alkaline pretreatment using NaOH followed by supplementation with $9 \mu\text{g} \cdot \text{g}^{-1}$ TS straw of cobalt and nickel had SMP of 329 ± 11 and 330 ± 12 mL $\text{CH}_4 \cdot \text{g}^{-1} \text{VS}$, respectively.

Although no previous study has shown the potential use of ash-extract supplementation as a source of trace nutrients to AD process, however, compositional analysis of these ash-extracts has shown that they are very rich in soluble essential trace nutrients (Table 3-4 in Section 3.2.1). Thus, the improvement in methane production achieved in the current study could be due to factors identified by Cai *et al.* (2017) on effects of trace elements supplementation during mono-digestion of rice straw on the microbial communities. During their study, it was reported that supplementation of the AD reactors with Fe, Mo, Se and Mn led to the production of the maximum methane yields of 289.2, 289.6, 285.3, 293.0 mL $\text{CH}_4 \cdot \text{g}^{-1} \text{VS}$, respectively from rice straw. Interestingly, the maximum volumes of methane produced in their study are comparable to the values of EPB ash extract were 266.1, 328.4, 296.2, 293.0 N mL $\text{CH}_4 \cdot \text{g}^{-1} \text{VS}$ added which was achieved using extracts from EPB as supplements (Table 9-3). Furthermore, from the results obtained from this study, the addition of 0.05, 0.15 and 0.25g of raw ash from empty palm bunch (EPB) to rice straw (Q, T and U) produced 312.5, 296.9 and 273 N mL $\text{CH}_4 \cdot \text{g}^{-1} \text{VS}$ added, respectively. Thus, increasing the concentration of raw ash from EPB added to the batch experiment resulted to decrease in the amount of methane gas recovered from the rice straw.

For all the biomass feedstock tested during the batch experiments, the Buswell equation (Equation 9-1) was able to accurately predict a theoretical methane potential for each of the biomass which was very close to the experimental values (Table 9-3).

Table 9-3 Summary of the results from experimental, Buswell equation and Gompertz models for the determination of the biochemical methane potential of selected biomass feedstocks

Label	Biomass feedstocks	Experimental							Gompertz Model						
		K -value	R ²	BMP _{gross}	BMP (N mLCH ₄ . g ⁻¹ VS)	U (max)	Theoretical BMP	Degrad. rate (%)	Lag phase, λ (d)	BMP _{gross}	BMP (N mLCH ₄ . g ⁻¹ VS)	U (max)	SSE	R ²	RMSE
A	Blank (Rumen fluid + sludge)	0.27	0.94	449.4	0	51.3	x	x	0.37	435.5	0	40.9	4594	0.99	15.6
B	Gamba grass	0.33	0.95	651.8	202.4	82.1	500	40%	0.27	631	195.5	57.6	6828	1	19
C	Cellulose	0.36	0.93	791.3	341.9	132.6	x	x	0.59	770.2	334.7	99.3	7030	0.99	19.2
D	Guinea grass	0.33	0.91	929.5	480.1	88.9	510	94%	0.01	872	436.5	70.3	2.84E+04	0.98	38.7
E	Rice straw	0.33	0.91	715.5	266.1	90.5	467	57%	0.82	681.6	246.1	80.5	8338	0.99	21
F	Cassava waste	0.37	0.98	698.2	248.8	119.2	409	61%	0.01	677.7	242.2	85.9	8457	0.99	21.1
G	Perennial Ryegrass. Clover and Timothy grass	0.31	0.93	848.8	399.4	88.6	498	80%	0.54	805.1	369.6	76.3	1.50E+04	0.99	28.1
H	Plantain peels	0.34	0.94	771.2	321.8	110	x	x	0.01	733.5	298	68.5	1.28E+04	0.99	26
I	Gamba + Guinea	0.31	0.92	718.2	268.8	90.7	x	x	0.47	685.8	250.3	78.7	5.69E+03	0.99	17.3
J	Rice + Yam Beans	0.34	0.92	859.9	410.5	92.5	x	x	0.16	821.5	386	72.7	1.43E+04	1	27.4
K	Rice + Cassava waste	0.33	0.95	923.4	474	107.6	x	x	0.05	876.5	441	85.3	1.76E+04	0.99	30.4
L	Rice + Plantain peels	0.34	0.94	989.4	539.9	110.3	x	x	0.01	926	490.5	83.2	2.80E+04	0.99	38.4
M	Elephant grass	0.33	0.91	819	369.6	88.9	491	75%	0.67	778	342.5	74.2	1.42E+04	0.99	27.3
N	Rice + 0.5 mL EPB	0.31	0.92	777.8	328.4	93.7	467	70%	0.39	726.2	290.7	68.7	1.57E+04	0.99	28.8
O	Rice + 1.0 mL EPB	0.29	0.88	745.6	296.2	86.5	467	63%	1.14	707.8	272.3	61	1.31E+04	0.99	26.2
P	Rice + 2.0 mL EPB	0.31	0.93	742.4	293	72.1	467	63%	0.09	699.7	264.2	56	1.34E+04	0.99	26.5
Q	Rice + 0.05g Ash	0.31	0.93	761.9	312.5	71.4	467	67%	0.25	718.3	282.8	60.6	1.35E+04	0.99	26.6
T	Rice + 0.15g Ash	0.32	0.93	746.3	296.9	77.1	467	64%	0.4	715.1	279.6	66.6	7.53E+03	0.99	19.9
U	Rice + 0.25g Ash	0.31	0.91	722.4	273	83.7	467	58%	0.61	686.2	250.7	70.6	1.07E+04	0.99	23.7

k-value = hydrolysis constant (d^{-1}); *U*_{max} = maximum methane production rate ($N mLCH_4.d^{-1}$); *BMP* = biochemical methane potential ($N mLCH_4. g^{-1}VS$ added); *BMP*_{Theo} = theoretical biochemical methane potential estimated using the Buswell equation; *BMP*_{gross} = biochemical methane potential of feedstock and blank (rumen fluid + sludge); *RMSE* = Root Means Squared error values and a smaller *RMSE* shows that the predicted and observed values are closer; λ = lag phase (d), *R*² = correlation coefficient or coefficient of determination

9.4 Conclusion

To determine the biochemical methane potential (BMP) of Gamba grass, crystalline cellulose, Guinea grass, cassava waste, plantain peels and elephant grass as mono-substrates

The BMP of Gamba grass, crystalline cellulose, Guinea grass, cassava wastes, plantain peels and elephant grass were determined in the current study. The study has shown that substantial amount of methane can be recovered from these feedstocks and that indicates that these agricultural biomass feedstocks could serve as feedstock for sustainable bioenergy generation, especially in developing countries where they are in abundant supplies.

To determine biomethane production from mixtures of different types of biomass feedstocks with supplementation

Supplementation of batch experiments with appropriate quantities biomass ash or ash-extracts can enhance methane yield from grass biomass or agricultural residues. This suggest that ash extract supplements contain essential nutrients which favour the activities of the methanogens and other microbes which are involved in the AD process.

Investigate of the effects of using biomass-derived ash and ash-extract supplementation on methane yield from rice straw

Thus, it important to determine and use an appropriate amount of supplement that would augment nutrient deficiency and alkalinity in the AD process as such would reduce inhibition arising from the addition of excessive supplement.

REFERENCES

- Cai, Y., Hua, B., Gao, L., Hu, Y., Yuan, X., Cui, Z., Zhu, W., & Wang, X. (2017). Effects of adding trace elements on rice straw anaerobic mono-digestion: Focus on changes in microbial communities using high-throughput sequencing. *Bioresour Technol*, 239, 454-463. doi: 10.1016/j.biortech.2017.04.071
- Chynoweth, D. P., Turick, C. E., Owens, J. M., Jerger, D. E., & Peck, M. W. . (1993). Biochemical methane potential of biomass and waste feedstocks. *Biomass and bioenergy*, 5(1), 95-111.
- Glanpracha, N., & Annachhatre, A. P. (2016). Anaerobic co-digestion of cyanide containing cassava pulp with pig manure. *Bioresour Technol*, 214, 112-121. doi: 10.1016/j.biortech.2016.04.079
- Jekayinfa, S. O., & Scholz, V. (2013). Laboratory Scale Preparation of Biogas from Cassava Tubers, Cassava Peels, and Palm Kernel Oil Residues. *Energy Sources, Part A: Recovery, Utilization, and Environmental Effects*, 35(21), 2022-2032. doi: 10.1080/15567036.2010.532190
- Mancini, G., Papirio, S., Riccardelli, G., Lens, P. N. L., & Esposito, G. (2018). Trace elements dosing and alkaline pretreatment in the anaerobic digestion of rice straw. *Bioresource Technology*, 247, 897-903. doi: 10.1016/j.biortech.2017.10.001
- Mustafa, A. M., Poulsen, T. G., Xia, Y., & Sheng, K. (2017). Combinations of fungal and milling pretreatments for enhancing rice straw biogas production during solid-state anaerobic digestion. *Bioresour Technol*, 224, 174-182. doi: 10.1016/j.biortech.2016.11.028
- Vdi. 4630. (2006). Fermentation of organic materials. *Characterization of the substrate, sampling, collection of material data, fermentation tests*, 92.
- Wang, B., Nges, I. A., Nistor, M., & Liu, J. (2014). Determination of methane yield of cellulose using different experimental setups. *Water science and technology*, 70(4), 599.
- Wilawan, W., Pholchan, P., & Aggarangsi, P. (2014). Biogas Production from Co-digestion of Pennisetum Purpurem cv. Pakchong 1 Grass and Layer Chicken Manure Using Completely Stirred Tank. *Energy Procedia*, 52, 216-222. doi: 10.1016/j.egypro.2014.07.072
- Zhang, Q., He, J., Tian, M., Mao, Z., Tang, L., Zhang, J., & Zhang, H. (2011). Enhancement of methane production from cassava residues by biological pretreatment using a constructed

microbial consortium. *Bioresour Technol*, 102(19), 8899-8906. doi:
10.1016/j.biortech.2011.06.061

Zhang, Q., Tang, L., Zhang, J., Mao, Z., & Jiang, L. (2011). Optimization of thermal-dilute sulfuric acid pretreatment for enhancement of methane production from cassava residues. *Bioresour Technol*, 102(4), 3958-3965. doi: 10.1016/j.biortech.2010.12.031

Appendix A

Appendix 1 Saturation vapour pressure (mb) of air at different temperatures

°C	0.0	0.1	0.2	0.3	0.4	0.5	0.6	0.7	0.8	0.9
0	6.11	6.15	6.20	6.24	6.29	6.33	6.38	6.43	6.47	6.52
1	6.57	6.61	6.66	6.71	6.76	6.81	6.86	6.91	6.96	7.01
2	7.06	7.11	7.16	7.21	7.26	7.31	7.36	7.42	7.47	7.52
3	7.58	7.63	7.69	7.74	7.80	7.85	7.91	7.96	8.02	8.08
4	8.13	8.19	8.25	8.31	8.36	8.42	8.48	8.54	8.60	8.66
5	8.72	8.78	8.85	8.91	8.97	9.03	9.09	9.16	9.22	9.29
6	9.35	9.42	9.48	9.55	9.61	9.68	9.75	9.81	9.88	9.95
7	10.02	10.09	10.16	10.23	10.30	10.37	10.44	10.51	10.58	10.65
8	10.73	10.80	10.87	10.95	11.02	11.10	11.17	11.25	11.33	11.40
9	11.48	11.56	11.64	11.71	11.79	11.87	11.95	12.03	12.12	12.20
10	12.28	12.36	12.44	12.53	12.61	12.70	12.78	12.87	12.95	13.04
11	13.13	13.21	13.30	13.39	13.48	13.57	13.66	13.75	13.84	13.93
12	14.02	14.12	14.21	14.30	14.40	14.49	14.59	14.69	14.78	14.88
13	14.98	15.07	15.17	15.27	15.37	15.47	15.57	15.68	15.78	15.88
14	15.98	16.09	16.19	16.30	16.40	16.51	16.62	16.73	16.83	16.94
15	17.05	17.16	17.27	17.38	17.50	17.61	17.72	17.84	17.95	18.07
16	18.18	18.30	18.42	18.53	18.65	18.77	18.89	19.01	19.13	19.25
17	19.38	19.50	19.62	19.75	19.87	20.00	20.12	20.25	20.38	20.51
18	20.64	20.77	20.90	21.03	21.16	21.30	21.43	21.56	21.70	21.84
19	21.97	22.11	22.25	22.39	22.53	22.67	22.81	22.95	23.09	23.24
20	23.38	23.53	23.67	23.82	23.97	24.11	24.26	24.41	24.56	24.72
21	24.87	25.02	25.18	25.33	25.49	25.64	25.80	25.96	26.12	26.28
22	26.44	26.60	26.76	26.92	27.09	27.25	27.42	27.59	27.75	27.92
23	28.09	28.26	28.43	28.61	28.78	28.95	29.13	29.30	29.48	29.66
24	29.84	30.02	30.20	30.38	30.56	30.74	30.93	31.11	31.30	31.49
25	31.67	31.86	32.05	32.25	32.44	32.63	32.82	33.02	33.22	33.41
26	33.61	33.81	34.01	34.21	34.41	34.62	34.82	35.03	35.23	35.44
27	35.65	35.86	36.07	36.28	36.50	36.71	36.92	37.14	37.36	37.58
28	37.80	38.02	38.24	38.46	38.68	38.91	39.14	39.36	39.59	39.82
29	40.05	40.28	40.52	40.75	40.99	41.22	41.46	41.70	41.94	42.18
30	42.43	42.67	42.92	43.16	43.41	43.66	43.91	44.16	44.41	44.67
31	44.92	45.18	45.44	45.69	45.95	46.22	46.48	46.74	47.01	47.27
32	47.54	47.81	48.08	48.35	48.63	48.90	49.18	49.46	49.73	50.01
33	50.30	50.58	50.86	51.15	51.44	51.72	52.01	52.30	52.60	52.89
34	53.19	53.48	53.78	54.08	54.38	54.69	54.99	55.30	55.60	55.91
35	56.22	56.53	56.84	57.16	57.48	57.79	58.11	58.43	58.75	59.08
36	59.40	59.73	60.06	60.39	60.72	61.05	61.39	61.72	62.06	62.40
37	62.74	63.08	63.43	63.77	64.12	64.47	64.82	65.17	65.53	65.88
38	66.24	66.60	66.96	67.32	67.69	68.05	68.42	68.79	69.16	69.53
39	69.91	70.28	70.66	71.04	71.42	71.80	72.19	72.58	72.96	73.36